UNIVERSITY OF LONDON THESIS

Degree PhD Year 2006 Name of Author AL-MARZOUQI Ihsan

Recovery and Purification of Plasmid DNA Gene Therapy Vectors using Aqueous Two-Phase Systems in a J-Type Countercurrent Chromatograph

A thesis submitted to the University of London

for the degree of

Doctor of Philosophy

by

Ihsan Al-Marzouqi M.Sc, B.Eng (Hons)

Department of Biochemical Engineering, University collage London

Torrington Place, London, WC1E 7JE.

ProQuest LLC
789 East Eisenhower Parkway
P.O. Box 1346
Ann Arbor, MI 48106-1346

Abstract

The use of plasmid DNA (pDNA) as a vector for gene therapy, or DNA vaccination, has been of considerable interest during the last decade with DNA vaccines for HIV, various cancers, cystic fibrosis and influenza presently under development. The size of pDNA molecules and the limitations this imposes on conventional chromatographic matrices mean that attractive pDNA separation techniques need to be found. This work focuses on the downstream processing of naked DNA using a novel technique utilizing countercurrent chromatography (CCC) for the separation of DNA from contaminant RNA, chromosomal DNA and proteins as a primary purification technique. CCC is a liquid-liquid chromatographic technique, in which solutes are fractionated based on their selective partitioning between two immiscible phases.

Initial research addressed the need for identifying suitable operating modes for the use of aqueous two-phase systems (ATPS) in CCC in order to obtain high levels of stationary phase retention. The degree of stationary phase retention once a hydrodynamic equilibrium is achieved was shown to be a function of mobile phase flow rate, coil rotational speed, column volume, choice of mobile phase and mobile phase pumping direction with a maximum value of 73.3% v/v obtained. In addition, it was shown to be possible to predict stationary phase retention as functions of mobile phase flow rate and rotational speed.

Experiments studying the batch extraction of pDNA using ATPS, and subsequent CCC operations with ATPS, showed successful pDNA purification was possible. This pre-purification procedure was needed to act as a buffer exchange step in order to reduce the disturbance on the hydrodynamic equilibrium, in addition to reducing the amount of contamination present in the lysate. Initial studies examined the degree of pre-purification required prior to CCC separation by testing plasmid DNA partitioning in batch ATP extraction with factors such as volume ratios, plasmid sizes, pH and PEG molecular weights. The recovery yield of plasmid DNA was typically 60% w/w with a reduction in the amount of RNA and chromosomal DNA, and complete

removal of proteins. CCC studies were able to obtain overall plasmid DNA recovery yields of 97 % (w/w) with no detection of RNA and chromosomal DNA.

Further studies were aimed at optimising CCC performance with regard to larger scale operating strategies. Experiments showed how DNA fractionation at laboratory scale varied with changes in operating variables such as feed type, mobile phase flow rate, rotational speeds and solute loading. In addition, several unique operating modes were tested in order to allow continuous elution of the plasmid DNA. The success of these experiments varied with the highest overall plasmid yields of 58% (w/w) being attainable. The use of unclarified lysates showed the potential to overcome the initial separation steps (filtration and centrifugation) normally utilised in the downstream processing of plasmid DNA with recovery yields of 49% (w/w) being attainable. Overall the results of this work have established the potential of using CCC for the large scale purification of plasmid DNA.

Acknowledgements

First and foremost I would like to express my gratitude to my supervisor, Professor Gary Lye for providing me with this opportunity to read for a Ph.D in Biochemical Engineering and for his invaluable support and guidance throughout my studies.

I would like to thank Aloke Dey-Chowdary for his constant assistance in method development and familiarisation of the analytical techniques, fermentation and cell lysis procedures. My thanks also goes out to Dr. Andrew Booth for showing me initially how to operate the CCC machine, and to Professor Ian Sutherland of Dynamics Extractions for his helpful comments on the hydrodynamics of it, and allowing me to use the tensiometer. In addition, I would like to thank Dr. Philip Wood for setting up the CCC machine during my first days of research.

I would also personally like to thank Mr Abdul Razzaq of Gulf Pharamceuticals Industries (Julphar in Ras Al-Khaimah, United Arab Emirates) for his financial support and believing in me, in addition to the Ministry of Higher Education and Scientific Research, United Arab Emirates for giving me and every UAE national the chance to continue our education.

Finally, to my parents, for believing in me, and of course to my beautiful wife Sema, without her constant support I would not have reached to this stage. Thank you for being patient with me and for your love throughout the hard times.

Table of Contents

List of Figures

CHAPTER 4

CHAPTER 5

CHAPTER 6

List of Tables

CHAPTER 4

CHAPTER 5

CHAPTER 6

CHAPTER 7

List of Abbreviations

Abs	Absorbance
ATP	Aqueous two phase
ATPS	Aqueous two phase system
BCA	Bicinchonic acid
BIB	Brunel Institute of Bioengineering
CCC	Countercurrent chromatography
chrDNA	Chromosomal deoxyribonucleic acid
CPC	Coil planet centrifuge
CV	Column volume
Da	Daltons
dsDNA	Double stranded deoxyribonucleic acid
Dx	Dextran
DNA	Deoxyribonucleic acid
EDTA	Ethylenediaminetetraacetic acid
EU	Endotoxin units
FDA	Food and drug administration
H	Head end
HIV	Human immunodeficiency virus
HPLC	High performance liquid chromatography
IT	Interfacial tension
kb	kilo base pairs
LAL	Lymulus amebocyte
MW	Molecular weight
OC	Open circular
pH	Hydrogen ion concentration
pK_a	$-\log_{10}$ (acid dissociation constant)
pDNA	Plasmid deoxyribonucleic acid
PEG	Polyethylene glycol
PTFE	Polytetrafluoroethylene
RNA	Ribonucleic acid
rpm	Revolution per minute
SC	Supercoiled
SDS	Sodium dodecyl sulphate
SS	Stainless steel
ssDNA	Single stranded deoxyribonucleic acid
T	Tail end
UV	Ultra violet

Nomenclature

A	Cross-sectional area of CCC coil
c_t	Concentration of pDNA in the top phase (ug.mL^{-1})
c_b	Concentration of pDNA in the top phase (ug.mL^{-1})
d	Internal tubing (coil) diameter (mm)
D	Diameter of drop in tensiometer (mm)
F	Mobile phase flow rate (mL.min^{-1})
i.d	Internal coil (tubing) diameter (mm)
K	Partition coefficient
L	Coil length (cm)
L	Length of droplet in tensiometer (mm)
o.d	Outer coil (tubing) diameter (mm)
PF	Purification factor
r_i	Inner coil radius (mm)
r_o	Outer coil radius (mm)
R	Rotor radius (mm)
R_s	Resolution
S_f	Stationary phase retention within the CCC coil (% v/v)
V_B	Volume of the lower phase (mL)
V_c	System volume (mL)
V_e	Volume of eluted stationary phase volume originally in the coil that has been displaced by the mobile phase during phase equilibrium (mL)
$V_{e\text{-corrected}}$	Corrected volume of eluted stationary phase obtained by subtracting the volumes of the inlet (V_{in}) and outlet (V_{out}) flying leads (mL)
V_{in}	Volume of the inlet flying lead (mL)
V_m	Volume of the mobile phase within the coil (mL)
V_{out}	Volume of the outlet flying lead (mL)
V_R	Volume ratio – Ratio of the volume of the upper phase (V_T) to the volume of the lower phase (V_H)
V_T	Volume of the upper phase (mL)
u	Linear mobile phase velocity (mL.min^{-1})
z_b	Charge of biomolecule

Greek symbols

β	Ration of the inner (r_i) or outer (r_o) coil radius to the rotor (R) radius
γ	Interfacial tension (N.m^{-1})
ρ_1, ρ_2	Density of the upper and lower phases (kg.m^{-3})
η_1, η_2	Viscosity of the upper and lower phases (mPa.s)
$\Delta\sigma$	Density difference of phases in tensiometer
$\Delta\psi$	Electrostatic potential difference
ω_N	Rotational speed of column

Chapter 1
Introduction

1.1 Gene therapy

The use of plasmid DNA as a vector for gene therapy, or especially vaccination, has been given considerable interest during the last decade [Prather *et al.*, 2003]. The principle behind gene therapy relies on introducing a gene into the genetic component of a cell, with its subsequent expression achieving a therapeutic function. Hence, if adequately administered, it could effectively pose a curative approach to inborn metabolic errors or other conditions induced by presence of a defective copy of a specific gene. Several investigators [Prather *et al.*, 2003] have demonstrated that injection of plasmid DNA containing selected genes from pathogens can elicit a protective immune response and, thereby, be developed into vaccines. To date, encouraging results have been yielded in the fights against malaria and AIDS. Thus far, over 400 clinical gene therapy protocols have been or are being undertaken involving *circa* 6000 patients worldwide [Walsh, 2003] many of which are currently in early stage clinical trials [Mhashilkar *et al.*, 2001; Mountain, 2000; Hasan *et al.*, 1999]. At this time, DNA vaccines against such conditions as HIV, various cancers and influenza are presently under development [Mhashilkar *et al.*, 2001; Koide *et al.*, 2000; Shroff *et al.*, 1999; Hasan *et al.*, 1999]. Table 1.1 lists the major disease types for which gene therapy treatment is under current assessment through clinical trials. Despite the initial focus of gene therapy for treatment of genetic diseases, the field has expanded, with well over half of all gene therapy trials conducted to date aiming at treating cancer [Walsh, 2003].

1.1.1 Non-viral vectors versus viral vectors

The transport of therapeutic genes to the target recipient cells can be carried out either by viral or non-viral DNA-based vectors. To date, the majority of clinical trials undertaken have utilized retroviral vector systems, while non-viral systems have been employed less often [Walsh, 2003]. These are efficient with regard to gene transfer and effective at reproducing themselves, but may cause an immunogenic response within the patient which is undesirable [Crystal, 1995].

Cancer –various forms	AIDS
Cystic fibrosis	Haemophilia
Familial hypercholesterolemia	α_1-Antitrypsin deficiency
Gaucher's disease	Chronic granulomatous disease
Rheumatoid arthritis	Peripheral vascular disease
Purine nucleoside phosphorylase deficiency	Severe combined immunodeficiency diseases (SCID)

Table 1.1: Possible applications for gene therapy as appraised in clinical trials [Walsh, 2003].

The recent deaths of patients involved in clinical trials using such vectors has caused concern [Fox, 1999]. The use of genetically modified retroviruses, adenoviruses and other viral systems present some problems and raise safety concerns, whereas synthetic formulations of genes inserted into non-viral systems are expected to overcome these drawbacks and as such, research under this area is experiencing an exponential growth [Prazeres *et al.*, 1999]. It is anticipated that other methods such as calcium phosphate precipitation, electroporation and particle acceleration will unlikely be employed to any great extent at an industrial-scale [Walsh, 2003].

In order to circumvent the problems associated with viral vectors, other researchers are designing new methods for introducing DNA into cells. Plasmid DNA-liposome complexes are under development [Crystal, 1995], and in many cases naked plasmid DNA may be used [Hasan *et al.*, 1999; Mahvi *et al.*, 1997; Robinson *et al.*, 1997; Horn *et al.*, 1995]. Two major advantages of non-viral gene vectors are low/non-immunogenicity, and non-occurrence of integration of the therapeutic gene into the host chromosome [Prather *et al.*, 2003; Walsh, 2003]. The former avoids rejection of the gene once encountered in the body of the patient; whereas, the latter eliminates the potential to disrupt any essential host genes or to, otherwise, activate host encogenes.

1.1.2 DNA-Based Vectors

Modern DNA-based systems generally entail complexing, or packaging, the gene to be transferred (along with appropriate promoters, vegetative origin of replication, etc.)

into a circular plasmid. This is, essentially, an extrachromosomal double-stranded DNA element found in microorganisms. As explained by Prazeres *et al.* [1999], plasmids for gene therapy can either carry human or non-human genes and are characterised as being very large molecules when compared to proteins, usually being between 5 and 20 kb in length ($3.3x10^6$-$13.2x10^6$ Da respectively). Furthermore, the plasmid can be coated with phospholipids or conjugated with polycations to stabilise the DNA, protect it (e.g. from serum nucleases), and/or to improve its uptake into the host cell [Walsh, 2003].

The genetic material to be transferred is packaged into a vector, which is exogenously up-taken by the target cell. Target cells such as the patient's liver or lung cells are infected with the vector. The vector is mobilised into the nucleus and unloads its genetic material containing the therapeutic human gene into the target cell. The gene is expressed resulting in the synthesis of the desired functional peptide or protein product. The generation of a functional protein product from the therapeutic gene restores the target cell to a normal state.

Regulatory elements of the nucleic acid transferred may be designed to ensure the peptide/protein product is retained within the cell or exported to the extracellular environment as necessary.

The principles behind the use of plasmids in gene therapy techniques are presented in Figure 1.1.

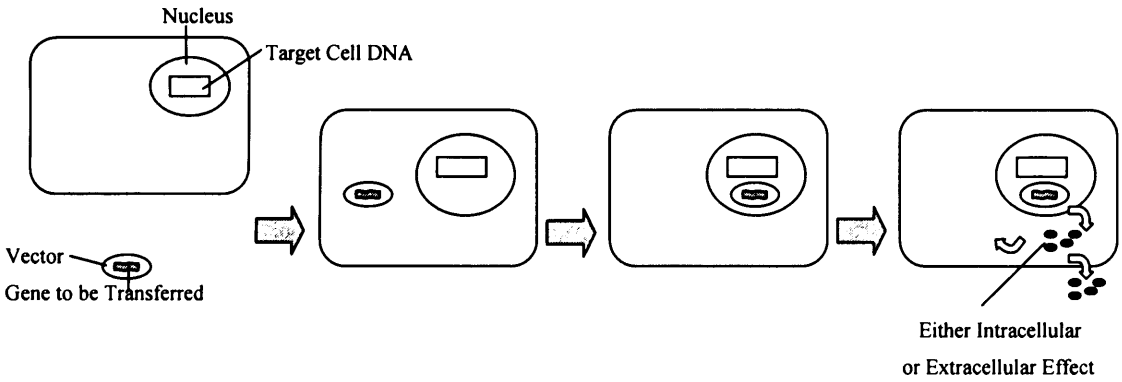

Figure 1.1: Simplified schematic representation of the basis of gene therapy.

It is estimated that only one in 10^4-10^5 plasmids taken up by the cell will enter the nucleus intact and be successfully expressed [Walsh, 2003], thereby enhancing the need for large quantities of plasmid that would theoretically be required in treatments.

1.1.3 Administration

Gene therapy can theoretically modify specific genes resulting in a cure following a single administration [Mhashilkar *et al.*, 2001]. A typical dose size (for instance, as used in trials involving patients with melanoma) is 0.3 μg but full treatments could require milligram quantities of plasmid DNA [Prather *et al.*, 2003; Ferreira *et al.*, 2000; Prazeres *et al.*, 1999]. At a practical level, there are three different administration strategies for gene therapy protocols. The *in vitro* approach entails initial removal of the target cells from the body. These are then cultured *in vitro* and incubated with a vector containing the nucleic acid to be delivered. The genetically modified cells are then re-introduced into the patient's body. In order to succeed, target cells must be relatively easy to remove and re-introduce into the body. To date, this approach has been the most commonly adopted and results have proven satisfactory with various cell types, including blood, stem, epithelial, and muscle cells, as well as hepatocytes [Walsh, 2003].

A less complex method involves direct injection/administration of the nucleic acid-containing vector to the target cell, *in situ* in the body. Examples have included the direct injection of vectors into a tumour mass, as well as aerosol administration of vectors –for instance, containing the cystic fibrosis gene- to respiratory tract epithelial cells [Walsh, 2003]. However, the feasibility of such an approach requires the target cells to be localised to one specific area of the body. Alternatively, the development of vectors capable of recognising and subsequently binding to specific, pre-defined cell types is being studied. These could be easily administered by intravenous injection with the specificity in the design being advantageous to deliver the nucleic acid exclusively to the target cells.

1.2 Molecular structure of DNA and other cellular constituents

1.2.1 DNA structure

DNA can be thought of as a polymer (multiple chemical units) composed of monomers (single chemical units), called nucleotides. All nucleotides have a common structure: a *phosphate* group linked by a phosphoester bond to a *pentose* (a five carbon sugar molecule) that is in turn linked to an organic base. The pentose is deoxyribose, while the bases are adenine, guanine, cytosine and thymidine. The order in which the bases appear along the DNA strand forms the basis of the genetic code. DNA consists of two associated polynucleotide strands that wind together through space to form a structure often described as a double helix [Watson and Crick, 1953].

DNA can undergo reversible strand separation. The unwinding and separation of DNA strands (denaturation) can be induced by heating or exposure to high pH [Birnboim, 1983]. Denaturation yields two single strands of DNA (ssDNA) that form random coils without a regular structure. Lowering the temperature or increasing the ion concentration causes the two complimentary strands to reassociate into a perfect double helix .

Plasmid DNA occurs in different topological structures, and is influenced by nucleotide sequence and its environment. The three most common isoforms of DNA are linear, open circular and supercoiled (Figure 1.2) [Sinden, 1994]. When the two ends of a DNA molecule are fixed, the molecule exhibits a superstructure. This forms due to interruption of the base pairing and unwinding of a local region.

The stress that results from unwinding is relieved by twisting of the helix forming supercoils. The extra twists assume the DNA to form the supercoiled (SC) structure. Enzymes called topoisomerases are responsible for introducing the extra twists in vivo [Lodish *et al.*, 2001].

During DNA replications, shear and chemical degradation may cause nicks in one of the DNA strands. In this case, one of the separated strands is circular and the other is linear. The plasmid will relax from the supercoiled to open circular (OC) form. If both DNA strands are nicked in the same place, then the SC plasmid will form into linear double stranded DNA. Heating of this linear double stranded DNA will separate the strands and form single stranded DNA. Generally, the shear sensitivity of DNA molecules increases with size [Levy *et al.*, 1999]. Shearing of large DNA molecules

will also result in increased shearing of the large contaminant chromosomal DNA (chrDNA) molecules, which becomes exceeding difficult to separate due to their similar properties. Plasmids exist predominantly in the supercoiled form, and the major impurities due to degradation are linearized and nicked open circular forms [Mao *et al.*, 1998]. It is essential for the final product to be > 95 % SC to ensure potency and stability [Levy *et al.*, 2000]. Thus the design of downstream process will require the shear forces to be kept below a critical level, especially during the early stages of the process [Levy *et al.*, 2000] (see Section 1.3).

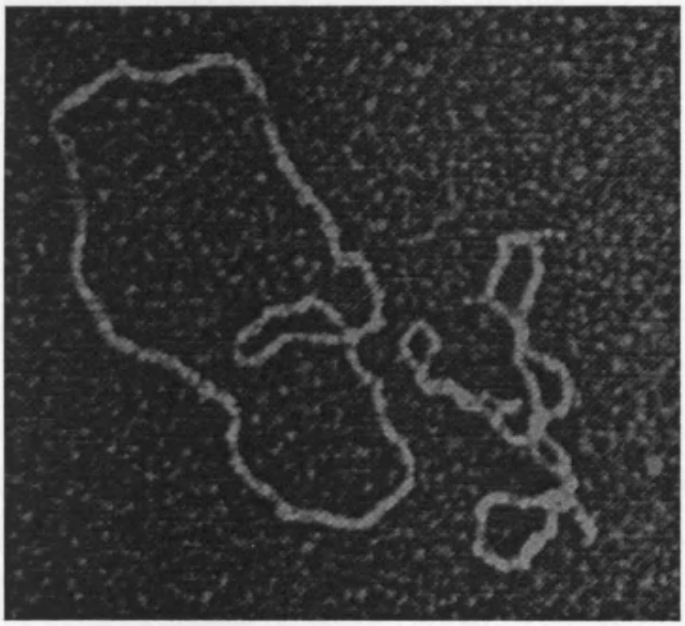

Figure 1.2: Electron micrograph showing the open circular (left) and supercoiled (right) isoforms of plasmid DNA [Kendall, 2002].

1.2.2 RNA structure

The structure of RNA is similar to DNA except that the pentose sugar is ribose and the base Uracil replaces Thymidine. RNA is a long polynucleotide that can be double-stranded but is a generally a single stranded molecule. RNA is considered a major contaminant in plasmid purification process mainly because it is present at high concentrations in addition to structural similarities to plasmid DNA.

1.2.3 Protein structure

Proteins are un-branched chains of amino acids monomers. The shape of proteins arises from non-covalent interactions between the regions in the linear sequence of amino acids. A total of 20 different amino acids can be incorporated into proteins. The size of proteins is much smaller than for a plasmid DNA molecule. Proteins exist in different structures. The primary structure is a linear arrangement of amino acids that constitute the polypeptide chain. The secondary structure is due to localized parts of the polypeptide chain, resulting in α helix (spiral structure) or β sheet (planar structure) stretches. Following the in-vivo synthesis of the amino acid sequence, the protein is folded into the tertiary globular structure, the shape being fixed by di-sulphide bonds. The association of folded protein sub-units with other protein sub-units results in the quaternary structure for some proteins.

1.2.4 Endotoxins

Endotoxins are very stable molecules, their biologically active part surviving extremes in temperature and pH [Petsch *et al.*, 2000]. They are essentially lipopolysaccharides which form micelle-like structures. These have similar sizes and densities compared to large DNA molecules, and have similar interaction properties, making them difficult to remove. Bacterial endotoxins show strong biological effects at very low concentrations in humans when entering the blood stream [Petsch *et al.*, 2000], thus it is essential for the plasmid DNA to be endotoxin free for future gene therapy vaccinations.

1.3 Plasmid DNA manufacture

On a small scale, plasmids are relatively easy to produce and purify from a wide variety of microbial cells [Prather *et al.*, 2003, Walsh, 2003]. However, plasmid production under non-optimised laboratory conditions invariably leads to very low (5-40 $mg.L^{-1}$) titres; whereas, the utilisation of laboratory-scale purification methods at larger scales leads to poor yields [Prather *et al.*, 2003]. Thus, assuming dosages ranging from one to a few milligrams, it is readily apparent that these un-optimised, low productivity processes are inadequate at the industrial scale. The acceptable cellular DNA contamination has been set at 100pg per dose [Marquet *et al.*, 1997]. Maintaining such levels will be very challenging when quantities of plasmid in the order of 100 μg are to be injected [Marquet *et al.*, 1995].

In addition, commercial scale processes will have to support not only the economics but also the regulatory standards required to commercialise DNA plasmids in gene therapy protocols and vaccines. These are regarded by the Food and Drug Administration (FDA) as biological products. It is a requirement of the FDA that these large-scale processes be designed to produce a certain amount of plasmid within certain specifications of purity, potency, identity, efficacy and safety that are inherent in the intended therapeutic use [Prazeres *et al.*, 1999]. The major approval specifications for contaminants, as dictated by the FDA, are listed in Table 1.2; this also includes the recommended assays for their assessment.

Although the removal of all contaminants must be considered, the greatest challenge at this stage is the removal of chromosomal DNA (chrDNA) and RNA, given the similarities of these to the product molecules. The SC plasmid form is the form required for the final product. Hence it is desirable to remove if possible OC and linear forms of plasmid from the SC plasmid product to ensure the potency and stability of the final dosage form [Bergan *et al.*, 2000; Middaugh *et al.*, 1998; Bonilla *et al.*, 1991].

1.3.1 Upstream processing and fermentation

The DNA manufacturing process is characterised by three major stages: upstream processing, fermentation and downstream processing. These three stages are integrated and must therefore not be approached on an individual basis as the downstream processing of biologicals is greatly affected by any impurities and/or contaminants present in the process streams, which in turn, are strongly influenced by upstream processing and fermentation conditions.

The upstream processing operations involve the construction and selection of appropriate expression vectors and production microorganisms. These should consider the demand for high yields that results from large-scale production and anticipate some of the recurrent problems during fermentation and downstream processing (Table 1.3). In fact, the judicious selection of plasmid vector and host strain, combined with growth-condition optimisation (media and conditions), can

result in plasmid yields as high as 220 $mg.L^{-1}$ and in a 40% reduction in the RNA content during cell lysis [Ferreira *et al.*, 2000].

Impurity	Recommended Assay	Approval Specification
Proteins	BCA protein assay	Undetectable
RNA	Agarose-gel electrophoresis	Undetectable
chrDNA	Agarose-gel electrophoresis Southern blot	Undetectable <0.01 μg (μg plasmid)$^{-1}$
Endotoxins	LAL assay	<0.1 EU (μg plasmid)$^{-1}$
Plasmid isoforms (linear, relaxed, denatured)	Restriction endonucleases	<5%
Biological activity and identity	Restriction endonucleases Agarose-gel electrophoresis Transformation efficiency	Coherent fragments with the plasmid restriction map Expected migration from size and supercoiling Comparable with plasmid standards

Table 1.2: Principal approval specifications and recommended assays for assessing the purity, safety and potency of DNA preparations for gene therapy and DNA vaccines reproduced from Ferreira *et al.* [2000]. Abbreviations: BCA, bicinchonic acid; LAL, *Lymulus amebocyte* lysate; EU, endotoxin units.

Fermentation	Primary Isolation	Purification
▪ Low yield ▪ Plasmid instability ▪ High cell density	▪ High cell density ▪ Shear thickening ▪ High viscosity ▪ Mixing ▪ Denaturation ▪ Nuclease action ▪ Shear sensitivity ▪ Handling of lysates ▪ Fragmentation of chrDNA	▪ Low capacity of sorbents ▪ Co-purification of endotoxins and chrDNA with plasmid DNA in ion-exchange chromatography ▪ Endotoxin and chrDNA clearance ▪ Column cleaning and regeneration

Table 1.3: Identified problems during the large-scale production and purification of plasmids reproduced from Prazeres *et al.* [1999].

At the commercial scale, only plasmid production from *Escherichia coli* is yet feasible [Prather *et al.*, 2003; Levy *et al.*, 2000]. This is typically performed in either large shake flasks or small laboratory fermentors [Prather *et al.*, 2003]. The organism is well characterized and there exist a multitude of strains with various characteristics that may be desirable. *E. coli* grows quickly and is amenable to industrial scale

fermentation. Due to the large amount of information that may be necessary to include in a gene therapy vector, it may ultimately be necessary to use a vector other than plasmid, such as Human Artificial Chromosome [Brown *et al.*, 2000; Willard, 1998]. However, plasmid DNA produced using *E. coli* as host is a good starting point at the present time.

The cultivation medium composition directly dictates the amount of biomass produced and, hence, plasmid volumetric yield. In addition, medium composition directly bears on the physiology of the microorganisms by influencing their intricate regulatory systems, and, hence, controls plasmid copy number or specific yield. By optimizing the combination of host strain, vector and growth conditions (fed batch versus batch fermentation and the use of defined as opposed to complex culture media are two examples) plasmid yields can be enhanced. Yields as high as 220 $\mu g.mL^{-1}$ plasmid DNA fermentation broth have been reported [Lahijani *et al.*, 1996]. A high titre of plasmid from the fermentation has the effect of decreasing the overall level of contaminants. It is therefore essential that reproducibly high plasmid titres be achieved during fermentation for the success of the downstream processes, both in terms of the purification achieved and for the maximum quantity of end product.

1.3.2 Downstream processing

The majority of problems in the production of plasmids are encountered during the downstream processing operations, which aim to eliminating cellular components of the host strain. An illustrative flow sheet, showing some of the common unit operations employed, is presented in Figure 1.3. The first critical step in downstream processing of plasmid DNA is cell lysis. Here, all intracellular components, including pDNA, RNA, chrDNA, endotoxins and proteins, are released. Although mechanical methods such as sonication, bead milling and homogenization [Ferreira *et al.*, 2000; Prazeres *et al.*, 1999] have been tested, the process of choice has most often been a variation of the alkaline-lysis procedure originally described by Birnboim and Doly [1979]. The lysis reaction is initiated by the addition of an equal volume 0.2 M sodium hydroxide (NaOH) containing 1% w/v sodium dodecyl sulphate (SDS) to the harvested cells, suspended in 10 mM Tris-HCl, 1 mM EDTA pH 8 (TE) buffer. The SDS interacts with the protein and lipid in the cell wall to render them soluble causing

the cells to lyse. The pH of the solution is such that proteins and chrDNA, once released are irreversibly denatured, while the denaturation of pDNA is reversible [Sambrook *et al.*, 1989]. A high pH is necessary to ensure complete conversion of chrDNA to single-stranded form [Meacle *et al.*, 2004]. Typically, five minutes is allowed for the completion of the lysis reaction and denaturation of DNA and protein [Ciccolini *et al.*, 1998]. The solution is then neutralized by the addition of one volume 3 M chilled potassium acetate. The solubility of SDS decreases with temperature, so that SDS-protein complexes precipitate at this point. RNA, cell debris, high molecular weight chromosomal DNA and other impurities also precipitate with the salt-detergent complexes to form an insoluble floc. However pDNA will re-nature and remains in solution as the pH is reduced upon potassium acetate addition.

At large scale the mixing of the lysis reaction mixture after the addition of the alkaline detergent and potassium acetate presents a challenge. It is important to ensure thorough mixing of the cell suspension and alkaline detergent to avoid localized extremes of pH, since irreversible plasmid denaturation will occur at pH values over 12.5 [Prazeres *et al.*, 1998]. Recently there has been evidence that depending on NaOH concentration, moderate to high mixing rates in stirred vessels are needed to maximize plasmid yields [Meacle *et al.*, 2004]. However, levels of shear must be kept to a minimum during mixing for the neutralization step to avoid damaging the delicate floc and releasing contaminants back into the plasmid-containing liquor [Levy *et al.*, 2000]. RNase or high temperatures can be used to reduce the RNA content but the use of RNase raises considerable difficulties for process validation [Ferreira *et al.*, 2000]. Ideally, no enzymes should be used during plasmid DNA manufacture.

For large plasmids (>100kb), there is an apparent loss of the desired plasmid product when the above alkaline lysis procedure is performed using potassium acetate for the neutralization step [Sinnett *et al.*, 1998]. This may be because larger plasmids have insufficient time to reanneal during the reaction. The procedure can be modified to utilize sodium acetate instead of potassium acetate. The higher plasmid yield in this case is offset by higher levels of contaminants such as RNA and protein. In the adapted protocol suggested by Sinnett and co-workers, sodium N-lauroylsarcosine (SLS) was employed instead of SDS, and in this case no loss of large plasmids was observed when the lysis was performed using potassium acetate.

Following the alkaline-lysis step, a precipitate is formed that contains cell debris, denatured proteins and nucleic acids. Plasmid DNA normally represents only 2% w/w of the total nucleic acids in *E. coli* lysates [Ferreira *et al.*, 2000]. The clarification and concentration steps are entitled to remove these and to reduce further the volume of the process stream prior to chromatography. At the laboratory and pre-preparative scales, centrifugation is the most common operation. However, centrifugation is not suitable for large-scale production as these machines usually operate with continuous feed flow that could shear and consequently break the precipitated material and chrDNA molecules. Filtration is thus regarded [Ferreira *et al.*, 2000] as the best operation to use in large-scale plasmid production processes.

At the final stage, the majority of impurities in the process stream are RNA, chrDNA fragments, endotoxins and plasmid variants. The similarity of these molecules to pDNA, as described in Section 1.2, and their wide molecular range makes purification a difficult task [Prazeres *et al.*, 1999].

1.3.3 Chromatographic methods for plasmid purification

Size exclusion and ion-exchange column chromatography have played a central role in the purification of plasmids, whereas reversed-phase and affinity chromatography have been restricted to small-scale production [Prazeres *et al.*, 1999]. Among the different chromatography modes available for plasmid purification, anion-exchange chromatography [Gustavsson *et al.*, 2004; Varley *et al.*, 2000; Prazeres *et al.*, 1999; Ferreira *et al.*, 1998; Prazeres *et al.*, 1998] and size-exclusion chromatography [Prazeres *et al.*, 1999; Edwardson *et al.*, 1986; Bywater *et al.*, 1983] are probably the most utilised methods. A complete review on chromatographic methods for the purification of plasmid DNA has recently been published [Diogo *et al.*, 2005]. Our laboratory has recently been able to use the liquid-liquid nature systems utilized in countercurrent chromatography for the separation of the different isoforms of pDNA from a pure sample [Kendall *et al.*, 2001]. Due to the absence of a solid phase, this method has the potential to circumvent many of the problems associated with conventional purification techniques such as high cost of matrix and low capacity for pDNA. In addition, the viscosity of alkaline lysates may reach 15-60 mPa. For chromatography carried out in conventional backed bed columns, high viscosity may

translate into high pressure drops and consequently limit the range of linear flow rates available and throughput. There has so far been limited research on pDNA purifications using different designs of countercurrent chromatographs and these are shown later in Section 1.11.

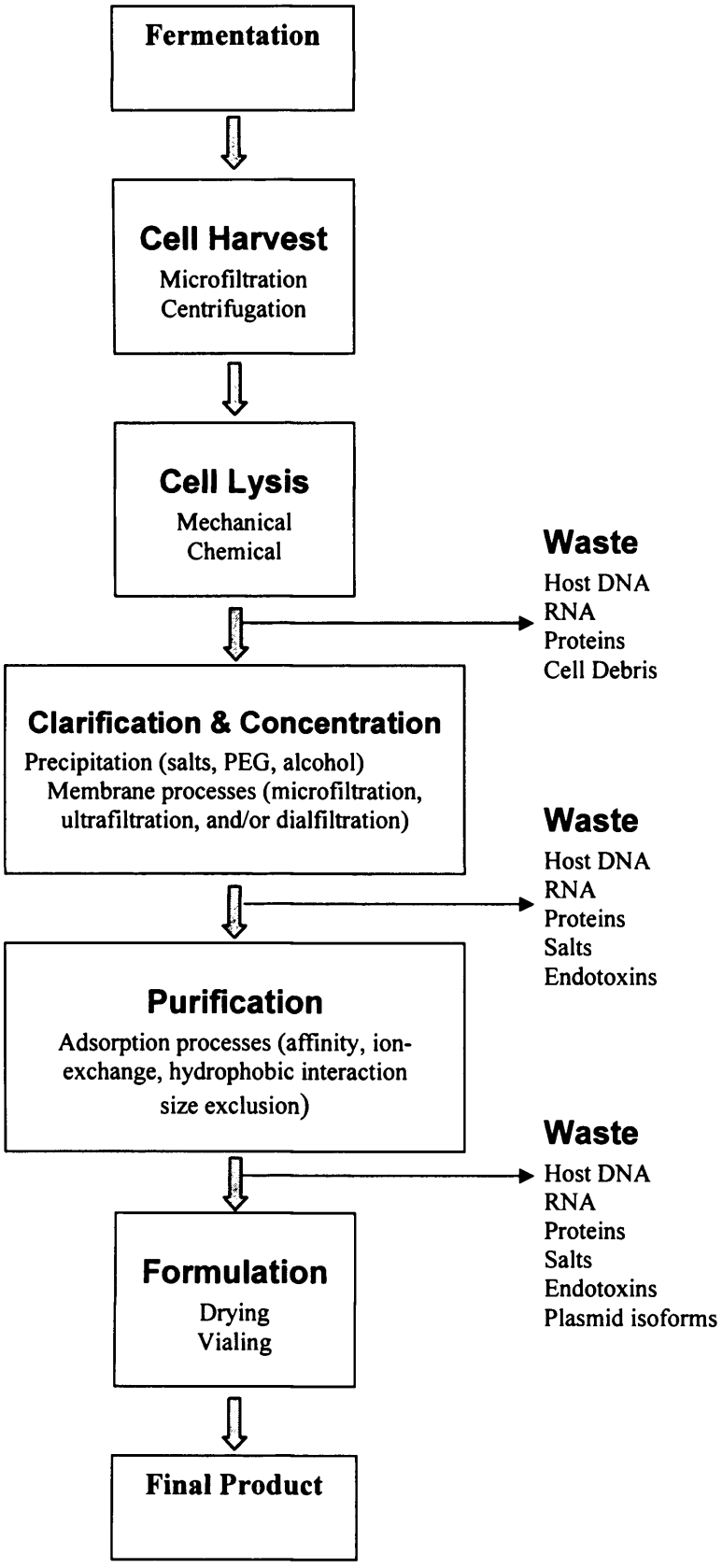

Figure 1.3: Process flow sheet for the large-scale recovery and purification of supercoiled plasmid DNA. Unit operations to be considered during process development are indicated together with the eliminated impurities. Abbreviations: PEG, polyethylene glycol.

1.4 Introduction to aqueous two-phase systems

The immiscible nature of aqueous and organic liquids, such as water and oil, is a well-known phenomenon. Combinations of specific polymers, or a polymer and salt, in aqueous solutions can also result in the formation of two immiscible phases. The pioneering works of Albertsson [1956] in aqueous two-phase systems (ATPS) are finding increasing use in extractive separations and high-sensitivity assays of biomaterials [Albertsson, 1986]. These can be used to effect separations of biological solutes through preferential partitioning between the two phases. Several experiments describing the partition behaviour of bio-molecules such as nucleic acids and proteins, and bio-nanoparticulates such as viruses have been published [Hatti-Kaul, 2000; Zaslavsky, 1995; Albertsson, 1986; Walter *et al.*, 1985]. ATPS has the potential to produce a concentrated and purified product in one step when compared to a number of steps involved in conventional downstream processing such as clarification, filtration, concentration and purification. The use of ATPS is a straightforward separation process, and it offers gentle non-toxic environments for bio-molecules.

The bulk of publications in this field have dealt mostly with polymer-polymer systems. The present work deals with polymer-salt ATPS. Polymer-salt systems have several advantages over polymer-polymer systems, such as higher interfacial tension (although still low enough to allow effective partitioning between the two phases) [Mishima *et al.*, 1998], which shortens phase separation times and facilitates continuous phase separation. They also have lower viscosities than polymer-polymer systems [Hustedt *et al.*, 1985] which makes them easier to handle on a large scale [Kaul and Asenjo, 1994]. Finally, phase-forming chemicals are less expensive for polymer-salt than polymer-polymer systems. Among many two-phase systems studied, polyethylene glycol (PEG)-dextran-water and PEG-salt-water systems are most commonly used for bio-molecule separation. These systems generally contain 80 % (w/w) to 95 % (w/w) water. This high water content, combined with low interfacial tension of the two-phase system, allows for non-destructive partitioning of sensitive biomaterials [Diamond and Hsu, 1992; Albertsson, 1986]. PEG-salt systems, as used here, has added advantages over PEG-dextran-water systems such as lower viscosity and lower cost [Salabat, 2001; Diamond and Hsu, 1992]

The affinity for a given macromolecule for each phase is dependent on a large number of factors (Table 1.4). There is also a considerable dependence on the macromolecule properties itself. The distribution of a solute between the two phases is expressed using a partition coefficient K which is a simple ratio between the concentrations of the solute in the top phase (c_t) to the bottom phase (c_b):

$$K = \frac{c_t}{c_b} \qquad \text{(Equation 1.1)}$$

Phase system properties	Biomolecule properties
Ionic strength	Molecular weight
Molecular weight of polymer	Isoelectric point or pK
pH	Size, shape
Viscosity	Conformation
Interfacial tension	Chirality
Electrochemical potential	Biospecific affinity
Hydrophobicity	Concentration of contaminants
Density	Type of contaminant

Table 1.4: Summary of phase system and macromolecule properties that affect partitioning of bio-molecules in two-phase systems [Kendall, 2002].

1.4.1 Phase diagrams

Phase diagrams indicate the concentrations of phase forming chemicals required for the formation of two immiscible phases. They are created by adding two polymers or one polymer and a salt to water, provided that the concentrations of both components exceed their solubility limit in water. Due to density differences, a lighter phase (termed top phase) and a heavier phase (termed bottom phase) forms within an interface between the phases. For PEG-salt system (S), the PEG-rich phase is the top phase (T) and the salt-rich phase is the bottom phase (B). A typical phase diagram is shown (Figure 1.4). The curve is called the binodial curve, which separates the bi-

phasic and mono-phasic areas. The areas to the left of the binodial curve indicate compositions for which two phases will not form (mono-phasic). The line through S, T and B is called the tie line. An increase in tie line length increases the property difference between the two phases. Phase diagrams are constructed by careful dilution of a phase forming mixture of known composition until the cloud point has been reached. The cloud point signifies that the solutes in the phase system had been diluted to the critical concentration at which two phases are no longer formed in the system [Bamberger *et al.*, 1985]. From this, the chemical compositions of the two phases can be estimated, and hence a point on the binodial curve constructed. The points on the binodial cure are compositions of phase forming chemicals at the cloud point for different volume ratio systems. The volume ratio is simply the ratio of the volume of the top to the bottom phase ($V_R = V_T/V_B$). Point C indicates the critical composition of the system in which the compositions of the two phases are identical and the volume ratio is one. With regards to biological macromolecule partitioning, the phase forming chemicals have to be carefully selected, as moving further into the bi-phasic area begins to increase the difference in the rheological properties of the two phases (interfacial tension, density and viscosity), thus affecting the partitioning of the macromolecules.

It has been noted that the addition of other components to an ATPS could disturb the equilibrium conditions along the binodial curve [Zaslavsky, 1995]. The addition of biological macromolecules shifted the binodial curve to the left (Figure 1.4), thus resulting in smaller amounts of phase chemicals [Lebreton *et al.*, 2002; Rito-Palomares and Cueto, 2000; Köhler *et al.*, 1989]. This trend was also observed for temperature increases [Saeki *et al.*, 1970], addition of salts [Mistry *et al.*, 1996] and pH increases [Lei *et al.*, 1990].

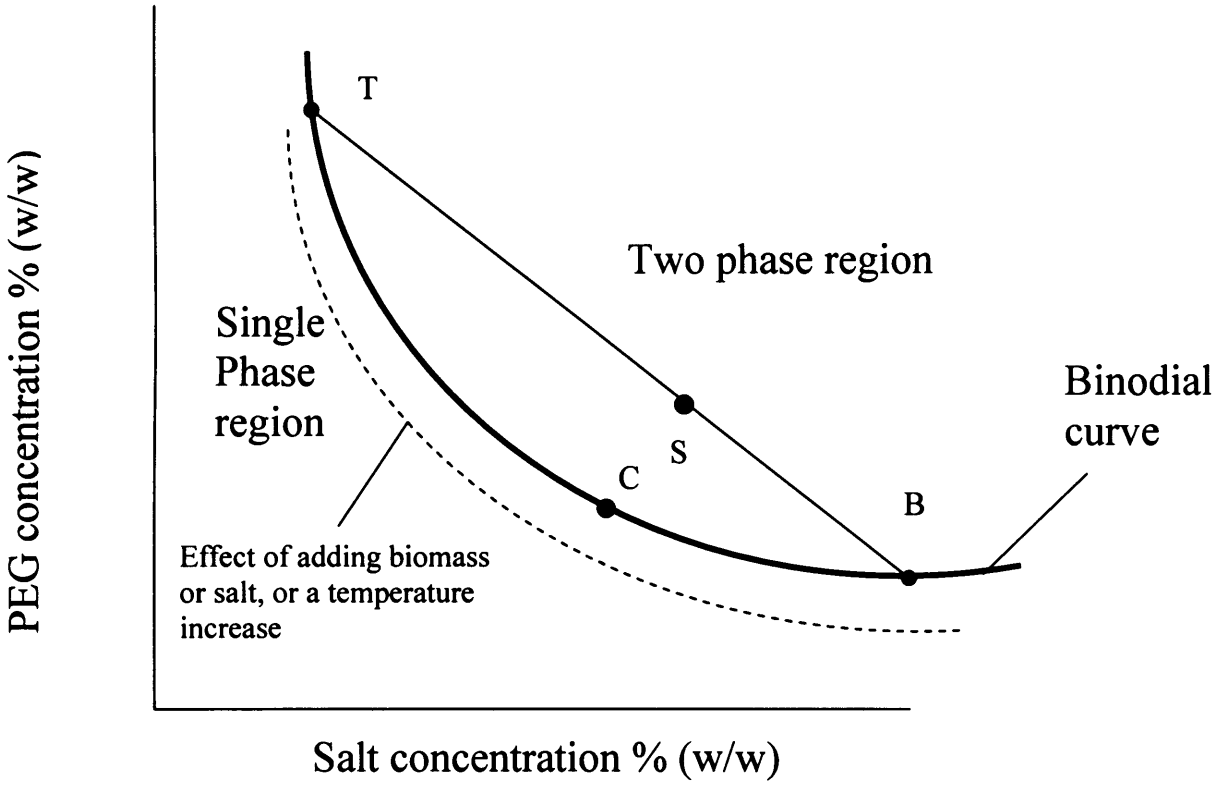

Figure 1.4: Binodial curve for a typical polymer-salt system, representing compositions required for two phases to form. A system of given compositions S separates into top (T) and bottom (B) phases. The line through T, B and S is called a tie line. The critical point C indicates that the system properties of the two phases are identical. When biomass or salt is added to the ATPS, or the temperature of the system is increased, the binodial curve is shifted to the left, as indicated by the dashed binodial curve.

1.5 Pervious work of pDNA/biomolecule separation using ATPS

1.5.1 DNA separations

1.5.1.1 PEG-Dextran systems

Rudin and Albertsson [1967] and then Favre and Pettijohn [1976] described a method for purifying DNA, RNA and DNA-protein complexes from bacterial feedstock using PEG-dextran systems at different ionic strengths. Rudin and Albertsson [1967] were able to partition proteins and low molecular weight RNA to the top PEG phase, while DNA and high molecular weight RNA were partitioned to the bottom dextran phase. A fresh upper phase PEG was then used to reduce the ionic strength of the system, resulting in DNA partitioning to the upper PEG phase while high molecular weight RNA preferred to stay in the bottom dextran phase. Favre and Pettijohn [1976] used similar methods, but partitioned the DNA from the upper phase to the lower phase in the final step. Most of the high and low molecular weight RNA, and denatured DNA partitioned to the upper phase. Generally, the phase compositions used were between 10-20 % (w/w).

Later Ohlsson [Ohlsson *et al.*, 1978] reported a method for isolating circular pDNA from cleared lysate of E. *coli* based on different configurational shapes of pDNA. The lysate was subjected to a heating step at 100 °C for two minutes to denature chromosomal DNA and pDNA, and then rapidly cooled to renature double stranded DNA. During the cooling step, the pDNA re-annealed much quicker than chrDNA leading to distinct partition behaviour for both. PEG and Dextran were added to form a two-phase system and pDNA partitioned to the PEG-rich top phase. Most of the RNA and cDNA could be removed. The yield of the pDNA in the PEG-phase was 79 % (w/w).

1.5.1.2 PEG-Salt systems

The partitioning of pDNA in PEG-salt systems was initially illustrated by Cole [1991], where nucleic acids remain in the lower (salt) phase, while proteins, cellular debris and other constituents are in the upper (polymer) phase, or are precipitated at

the interface region. The use of lower molecular weight PEG resulted in higher protein partitioning and less precipitation of proteins and DNA at the interface. Lower concentrations of PEG also resulted in less precipitation of DNA and proteins. Cole also stressed on the importance of pH, and reported much higher protein extraction to the top phase at pH values above 7.

Ribeiro *et al.* [2002] recently investigated the partitioning of pDNA (8.5 kb) in PEG-K_2HPO_4 systems (Figure 1.5) using different PEG molecular weights (200 to 8000 Da) and lysate loads (20-60 % w/w) in ATPS. The experiments tested only one composition of PEG and salt for each PEG molecular weight. Nucleic acids were seen to prefer the top phase for lower PEG molecular weights (PEG 200 and 300), while higher MW PEG systems showed the nucleic acids to partition to the lower salt phase (PEG 600-8000). An intermediate PEG MW (PEG 400) showed nucleic acids to partition preferentially to the interface. It was also seen that the open-circular form of the plasmid increased when it was present in the bottom salt-phase as a result of conformational changes that occur in the presence of salt and that the majority of RNA co-partitioned with the pDNA (Figure 1.5). The amount of lysate loaded to the systems also affected the partitioning. As stated before in Section 1.4, the addition of biomass shifts the binodial curve towards the origin, which implies that the PEG and salt concentrations in the top and bottom phases are higher. The difference in composition of the top and bottom phases increases with the lysate load, providing an increased driving force for the unequal partition of the macromolecules [Zaslavsky, 1995]. This was observed for PEG 600 and 1000, where the recovery yield increased with the plasmid load. PEG 300 showed the opposite trend due to lack of free volume left in the PEG-phase. The maximum recovery yield obtained for PEG 300, 600 and 1000 systems were 30, 62 and 146 % (w/w) respectively.

Trindade *et al.* [2005] also tested the partitioning of pDNA (6.1 kb) in PEG-ammonium sulphate systems using different PEG MW (300, 400 and 600), tie-line length and lysate load. The best results were obtained with PEG 600 using compositions close to the binodial curve and low lysate loading (20% w/w), with almost 100% of pDNA recovered in the bottom phase. Further increases in the lysate load up to 40% (w/w) resulted in an eight-fold increase in pDNA concentration but with a yield loss of 15%. However unlike PEG-potassium phosphate systems used by

Ribeiro *et al.* [2002], protein co-partitioning with pDNA was seen for all experiments regardless of PEG molecular weight, lysate loading or tie-line length used.

1.5.1.3 Thermoseparating aqueous systems

Kepka *et al.* [2004a] recently used a system comprised of thermoseparating polymer $EO_{50}PO_{50}$ and bottom phase forming polymer Dextran T 500 for plasmid DNA separations from a desalted alkaline lysate solution. The EO-PO copolymer consists of 50% (w/w) propylene oxide groups and 50% (w/w) ethylene oxide groups that are randomly distributed within the polymer chain. The EO-PO copolymer has thermoseparating properties, i.e. when heated over its cloud point temperature the solution becomes cloudy and separates into one water phase and one polymer phase. Plasmid DNA was completely recovered in the top phase while 80% of the total RNA and 58% of the total protein was discarded to the bottom phase. Moreover, a 3.8-fold reduction of the plasmid DNA solution was achieved and performing a final thermoseparating step resulted in the plasmid solution containing less than 1% polymer. An integrated process for purification of plasmid DNA using these thermoseparating two-phase systems combined with membrane filtration and lid bead chromatography also produced RNA and protein-free plasmid solution with an overall recovery yield of 69% (w/w) [Kepka *et al.*, 2004b].

1.5.2 RNA separation

Kimura and Kobayashi [1996] first reported a detailed analytical study on how RNA partitions in aqueous two phase systems. Using PEG-potassium phosphate systems, it was seen that low-molecular weight RNA (comprising of 5.8S, 5S and lower) showed partition behaviour of a typical soluble substance, retaining a constant partition coefficient between the two phases and consequently changing the partition coefficient with phase volume ratio. The low molecular weight RNA partitioned between the two phases with no retention at the interface. For high MW RNA (comprising of 26S and 17S), more than 95 % was absorbed at the interface. It was thought that ribosomal high-molecular mass RNA in water has a much wider surface area than the RNA in ribosomes that have a folded compact structure together with

ribosomal proteins meaning that a significant proportion of it accumulates at the interface.

Kimura [2000] also reported that low-molecular weight RNA was caught at the interface to a significant extent if partitioned with high-molecular weight RNA. The degree of accumulation of low MW RNA increased with an increase in the content of the high MW RNA. The reason for simultaneous accumulation of the RNAs was due to the affinity between RNA molecular surfaces, which is general for RNA in spite of their molecular mass. This affinity, which will be exposed under the partitioning condition where the high molecular weight RNA is accumulated at the interface, but common among RNA molecules, will act as a main driving force for the simultaneous accumulation. This situation of the dynamic partitioning process ruled-out pervious suggestions that the accumulation at the interface was due to precipitation in the top phase or salting-out effect in the bottom phase. Kimura also tested the influence of system composition using a range of molecular weight PEGs (PEG 300-20000) and found that although all results were similar, the PEG 1000-1500 systems exhibited a significant accumulation of high and low molecular weight RNA at the interface. Also for systems chosen away from the binodial curve of their respected PEG-salt systems, the accumulated amount of low-molecular mass RNA linearly increased with that of high-molecular mass RNA. The RNA accumulation depending on the PEG molecular weight was not based on specific interactions between certain molecules mass PEGs and RNA but as a result of the dynamic partitioning described earlier.

It was seen in Figure 1.5 that RNA and DNA usually partition to the same phase, however, the effect of changing molecular weight of PEG was more profound for RNA partitioning. This is because RNA is more easily accumulated at the interface than the DNA. The presence of RNA in the phase where DNA partitions is undesirable. Thus the choice of PEG molecular weight needs to be carefully selected to allow maximum DNA recovery in one of the bulk phases with the majority of the RNA partitioning to the interface.

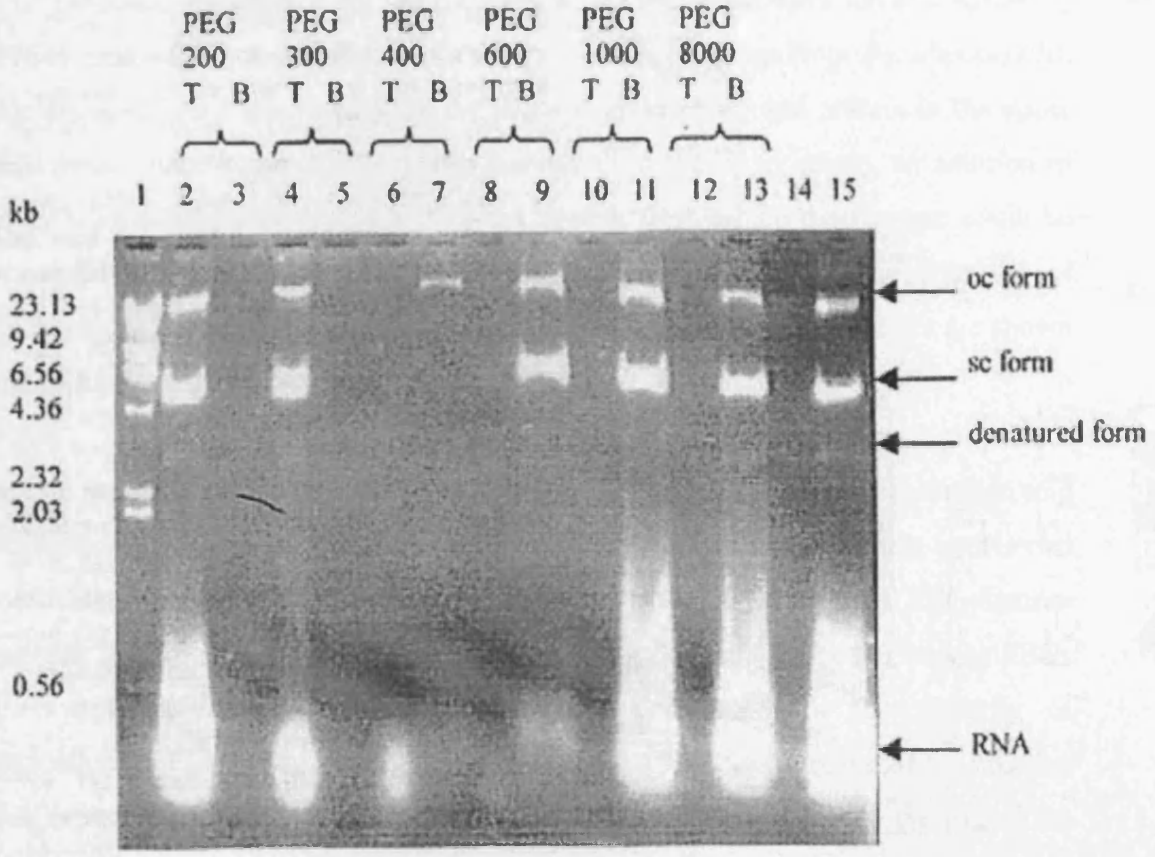

Figure 1.5: Results from Ribeiro *et al.* [2002] showing nucleic acid partition in PEG-salt systems for a range of molecular weight PEG with 40 % (w/w) lysate loading. For low molecular weight PEG's (lanes 2-7), pDNA and RNA partitioned to the top (PEG) phase. For high molecular weights (lanes 8-13), the pDNA and RNA partitioned to the bottom (salt) phase. All lanes are loaded with 15 µL of the indicated phase with no dilution. Lane 15 shows the lysate used. Lane 1: Lambda DNA/*Hind*III marker. OC pDNA was higher when the pDNA partitioned to the bottom phase. RNA partitioned to the same phase as the pDNA, with most partitioning to the interface when PEG 600 was selected.

1.5.3 Protein partitioning

Protein purification and recovery using ATPS have been extensively studied [Kaul, 2000; Albertsson, 1986]. The importance of nucleic acid partitioning free of proteins is of particular importance for the recovery of nucleic acids. Okazaki and Kornberg [1964] used a PEG-dextran system to purify DNA polymerase from *Bacillus subtilis*. Nucleic acids were concentrated in the lower dextran phase and protein in the upper PEG phase. After removal of salts by dialysis from the upper phase, an addition of ammonium sulphate generated a PEG-salt system from which the enzyme could be recovered (together with other proteins) in the salt-rich phase. Some examples of aqueous systems for the separations of nucleic acids from proteins/peptides are shown in Table 1.5.

Protein partitioning depends on many of the same parameters that affect nucleic acid partitioning (Table 1.4). Albertsson *et al.* [1987] determined that protein partitioned coefficients increased with increasing molecular mass of dextran in PEG-dextran systems. In addition, PEG-phosphate systems using different molecular weight PEGs (PEG 1000-2000) showed changes in phase preference for the majority of intracellular proteins from yeast [Huddleston *et al.*, 1990]. Partitioning of the proteins also depend on whether their isoelectric points are higher/lower than the pH of the system [Huddleston *et al.*, 1990]. Proteins (from *Escherichia coli*) were shown to partition to the top phase using PEG 200-600, but some partitioned to the bottom using PEG 1000 [Ribeiro *et al.*, 2002] as shown in Figure 1.6. For higher molecular weight PEG (PEG 8000), protein was almost completely found in the bottom phase and interface. The results were promising using PEG 600, were plasmids partitioned to the bottom phase, while proteins partitioned to the top phase. Systems using PEG 1000 showed around 80 % of the proteins partitioned to the top and interface.

Protein/Peptide	Source	Reference
RNA polymerase	*Escherichia coli*	Bibilashvili and Savochkina (1971) Alberts (1967)
DNA polymerase	*Escherichia coli* *Bacillus subtilis* Yeast	Ribeiro *et al.* (2002) Okazaki and Kornberg (1964) Falasch and Kornberg (1966) Huddleston *et al.* (1991)
DNA ligase	Rabbit bone marrow cells	Gaziev and Kuzin (1973)
RNA polymerase α peptide	*Escherichia coli* *bacteriophage*	Goff (1974)
DNase	*Diplococcus pneumoniae*	Vovis and Buttin (1970)
Λ-Exonuclease	Bacteriophage γ	Radding (1966)

Table 1.5: Examples of aqueous systems for separation of nucleic acids from protein/peptides reproduced from Walter *et al.* [1985]

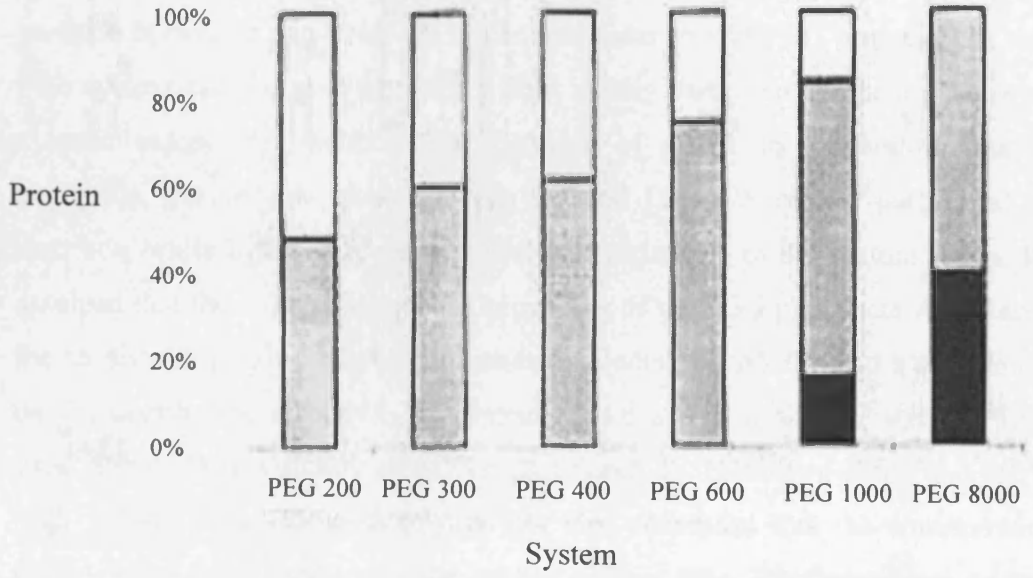

Figure 1.6: Protein partitioning in PEG-phosphate ATPS using 40 % w/w lysate for the following PEG/salt systems: PEG 200 (20/20% w/w), PEG 300 (20/20% w/w), PEG 400 (20/20% w/w), PEG 600 (20/20% w/w), PEG 1000 (15/13% w/w) and PEG 8000 (10/10% w/w). The percentage of protein in the top phase (white bars), interface (grey bars) and bottom phase (black bars) are shown for different MW PEG systems reproduced from Ribeiro *et al.* [2002].

1.6 Summary of factors affecting plasmid DNA partitioning in ATPS

As mentioned in Section 1.5, the partitioning of plasmid DNA in PEG-Phosphate systems is affected by the molecular weight of PEG. Previous research has shown the partitioning of pDNA seems to be one-sided when ATPS were composed of higher molecular weight PEG (>300 Daltons) [Kune, 2002; Cole *et al.*, 1991]. For lower molecular weight PEG systems, the partitioning behaviour of pDNA was seen to be selective and was shown to depend on (i) Phase system composition and volume ratios (ii) System temperature (iii) pDNA loaded in ATPS (iv) pDNA concentration in ATPS. The effect of each of these on pDNA partitioning is discussed below.

1.6.1 Phase system composition and volume ratios

Recently, Kune [2002] has studied the effect of phase composition (and hence volume ratios) on a PEG 300-Potassium phosphate system using lysate containing the pTX0161 plasmid (7.8 kb). The lysate was treated with Ribonuclease A to remove the contaminant RNA. It was found that interfacial partition had a large influence on the partition behaviour of pDNA when low molecular weight PEG was used. In systems with volume ratios higher than one, pDNA mainly partitioned to the top phase and to a lesser extent the interface. The partition of pDNA to the bottom phase was negligible. For volume ratios between 0.5 and 1, pDNA mainly partitioned to the interface, while below 0.5, most pDNA was recovered in the bottom phase. It was assumed that the solute changes the properties of the PEG-phosphate ATPS and that the co-distribution of crude contaminants (excluding RNA) also had a notable impact on the distribution of pDNA. In contrast, when a high molecular weight PEG was used (PEG 1450), virtually all pDNA partitioned to the bottom phase and increased with volume ratio [Kune, 2002]. It was also concluded that the concentration of pDNA was a linear function of the applied volume ratio. The dependence on volume ratios was also seen when proteins were used [Huddleston *et al.*, 1994; Flanagan *et al.*, 1991].

1.6.2 System temperature

Temperature effects in polymer-polymer systems have been described by Johansson and Andersson [1984]. It has been suggested that temperature influences the partition of solutes indirectly by changing the chemical compositions of the two bulk phases [Albertsson, 1986]. In polymer-salt systems, the partition mechanism is probably different [Zaslavsky, 1995]. PEG 300-Phosphate systems using temperatures between 4 and 25^{0}C have shown the pDNA to partition to the interface with increasing temperatures [Kune, 2002]. At 25^{0}C, over 80 % of pDNA was recovered in the interface. From a temperature of 25^{0}C upwards, the top phase did not seem to play a role as the target phase for pDNA. Instead, partitioning to the bottom phase increased with increasing temperatures up to 40^{0}C while partitioning to the interface decreased. This result is shown in Figure 1.7. The volume ratio also decreased with increasing temperature (from 0.97 to 0.79 for a temperature range from 4 to 40^{0}C). From the previous section, it was mentioned that the preference for the top phase changed to the bottom phase with decreasing volume ratios. However, the change in volume ratio was small and was not thought to have caused this. Kune [2002] explained the temperature effect by suggesting that the two phase area widened and the binodial curve shifts to the left hand side for temperature increases (Figure 1.7). This changes the chemical compositions of the top and bottom phases and the properties of the ATPS [Kune 2002]. The resulting ATPS will increase the concentration of PEG 300 in the top phase and decreases the phosphate concentration in the bottom phase. The partition of pDNA can be described in terms of excluded volume effects in the top phase caused by the steric exclusion of pDNA by PEG molecules. If increasing the temperature means increasing the concentration of PEG 300 in the top phase, the pDNA is increasingly excluded from that phase. In contrast, the concentration of salt in the bottom phase decreases thus pDNA can be solubilized in the salt phase. It is not known whether higher molecular PEG (>300 Daltons) systems will also show a change of partitioning preference with temperature.

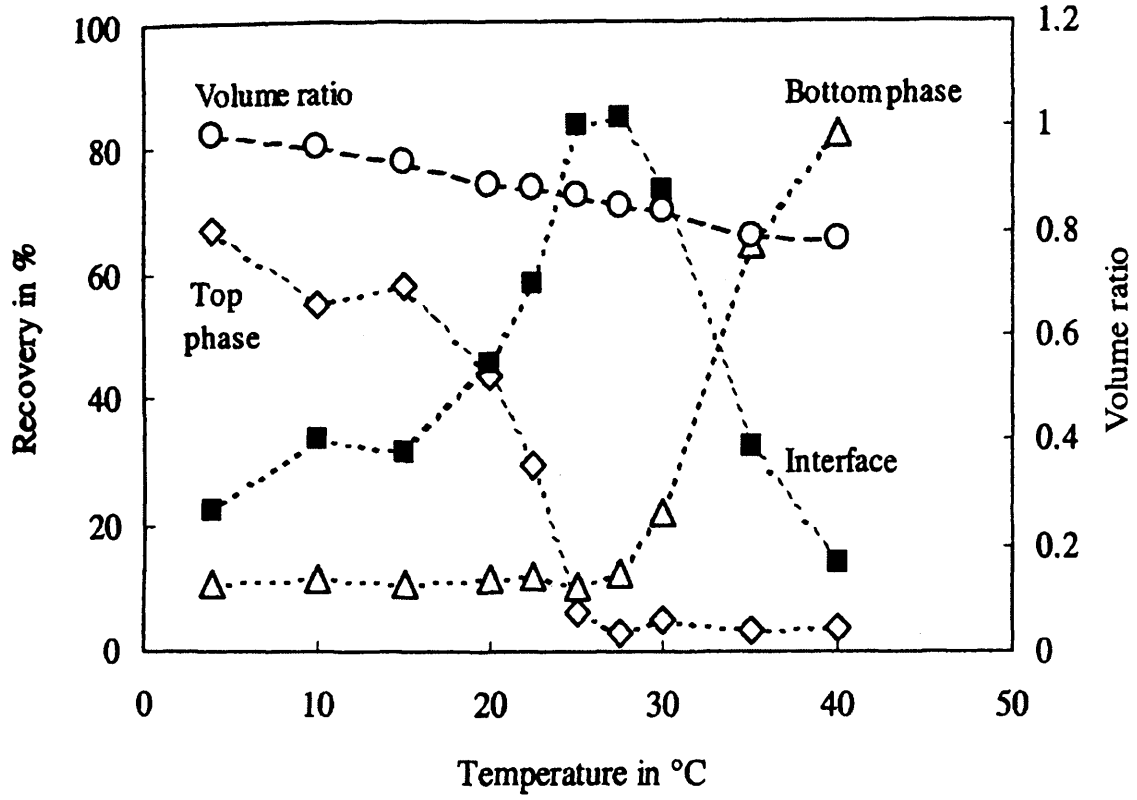

Figure 1.7: Partition effect of pDNA as a function of system temperature. The system used was PEG 300-K_2HPO_4 (15-22 % w/w) with 40 % (w/w) lysate loading. Temperature controlled between 4 to 40 ^{0}C in a water bath. Phase separation was accelerated by centrifugation at 1000 g for 3 minutes and the concentration of pDNA was estimated by PicoGreen™ analysis. Reproduced from Kune [2002].

1.6.3 Lysate composition loaded

The effect of pDNA partitioning on the amount of lysate loaded to ATPS has been studied [Ribeiro *et al.*, 2002] for PEG 300-K_2HPO_4 (20-20% w/w), PEG 600-K_2HPO_4 (20-20% w/w) and PEG 1000-K_2HPO_4 (15-13% w/w) systems. Increasing the amount of lysate loaded increased the pDNA partitioning for PEG 600 and PEG 1000 systems where the plasmid partitions to the lower salt phase. The lysate used by Ribeiro includes contaminants such as RNA, proteins, cell debris, chrDNA and detergents from the alkaline lysis steps. The addition of higher volumes of cell debris and components changes the position of the binodial curve in phase diagrams by displacing it towards the origin [Alstine and Veidi, 1999; Huddleston *et al.*, 1991]. This shift implies that the PEG and salt concentration in the top and bottom phases is

higher and increases the differences in the compositions of the top and bottom phases, and hence increases the driving force for the partitioning of solutes [Zaslavzky, 1995].

For PEG 300-K_2HPO_4 systems, where the pDNA partitions to the top phase, recovery decreased with increasing lysate loadings. This is because the polymer concentration in the top phase increases with lysate loading thus reducing the amount of free volume left in the PEG-rich phase. This enhanced the exclusion of pDNA from the top phase [Ribeiro *et al.*, 2002; Kune 2002]. Protein partitioning for this system increased with lysate loaded due to the fact of its much smaller size thus allowing it to penetrate inside the PEG molecules. Figure 1.8 shows the pDNA partitioning with respect to lysate concentration at 20^0C. The effect of temperature together with lysate loading has shown that at low lysate concentrations, pDNA partitioned to the top phase regardless of the temperature for low molecular weight PEG systems [Kune 2002]. With increasing lysate concentrations, the recovery of pDNA in the top phase decreased and this occurred more rapidly at higher temperatures. Interfacial partitioning was seen to dominate at higher temperatures.

1.6.4 Initial pDNA concentration

Results from Kune [2002] and Ribeiro *et al.* [2002] on the effect of plasmid concentration and partitioning show conflicting results. Ribeiro showed that a decrease in the plasmid concentration in the lysate decreased the recovery yield in all the systems (PEG 300/600/1000-K_2HPO_4) used for a range of lysate loading amounts (20-60%). Plasmid concentrations of 89 and 44.5 $\mu g.mL^{-1}$ were used. Recovery yield decreased by at least 20% when the concentrations were halved. Similar results on protein partitioning were also seen to depend on overall protein concentration [Schmidt *et al.*, 1996; Schmidt *et al.*, 1994]. On the other hand, Kune [2002] used lysate concentrations from 20 -180 $\mu g.mL^{-1}$ at constant loading amount of 40% (w/w) and different system temperature (15-35 ^{0}C). The partition behaviour did not change at elevated pDNA concentrations. It was concluded that the maximum capacity of pDNA in each phase has not been reached and that each phase could easily accommodate a much larger amount of pDNA present in the original feedstock. Similar results were obtained when low and high molecular weight RNA from bakers yeast was used [Kimura, 2000; Kimura and Kobayashi, 1996].

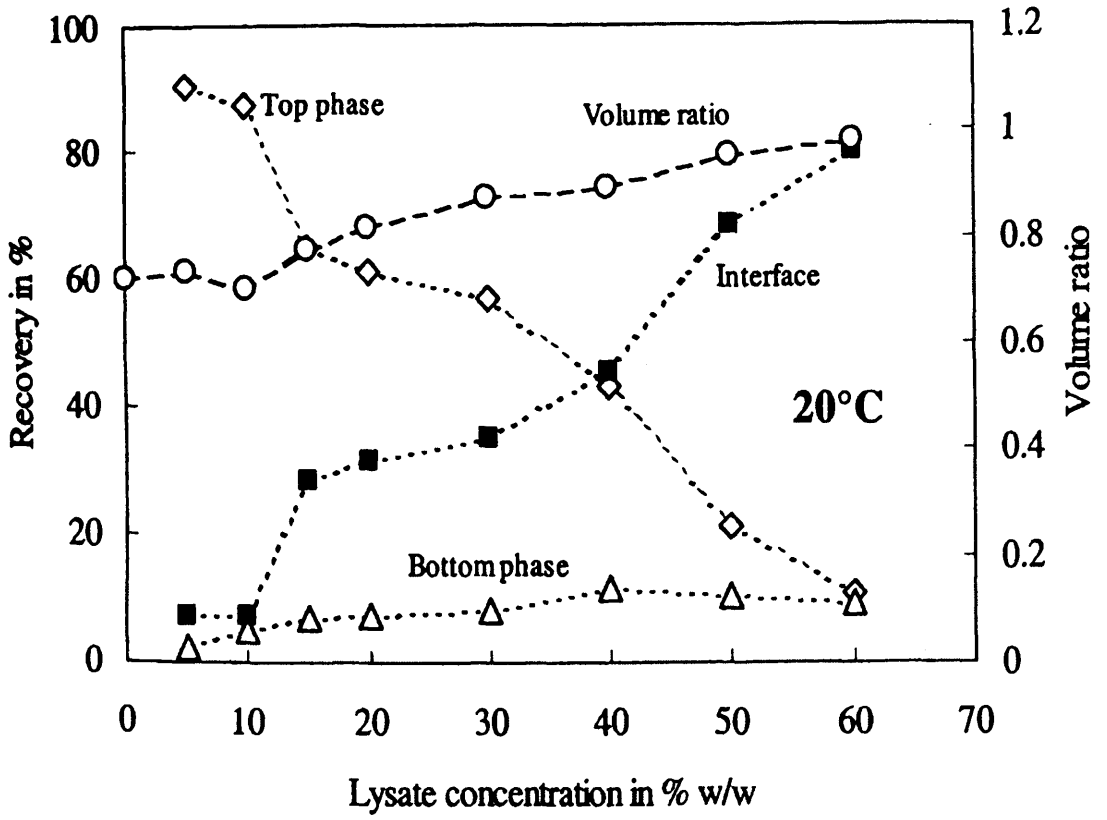

Figure 1.8: Partition effect of pDNA with respect to lysate concentration. PEG 300-K_2HPO_4 (15-22 % w/w) lysate loading ranging from 10 to 60 % (w/w). Temperature controlled at 20^{0}C in a water bath. pH was adjusted to 8.0. Phase separation was accelerated by centrifugation at 1000 g for 3 minutes and the concentration of pDNA was estimated by PicoGreen^{TM} analysis reproduced from Kune [2002].

1.7 Countercurrent chromatography

1.7.1 Introduction

Countercurrent chromatography (CCC) has a characteristic feature among all chromatographic systems in that the method utilizes no solid matrix [Ito, 1985]. It is essentially a form of liquid-liquid partition chromatography in which the stationary phase is retained in the apparatus without use of a porous or adsorption matrix. CCC may be considered as a hybrid of two classical partition methods, counter-current distribution (CCD) and liquid partition chromatography, and inherits all the merits from both parents methods. CCC eliminates all the complications arising from the use of solid supports, such as absorptive sample loss and deactivation, tailing of solute

peaks, and contamination. It is an emerging low pressure chromatographic technique, which separates molecules on the basis of different partition coefficients between two immiscible liquid phases.

Within the CCC column, one liquid phase (the stationary phase) is held in place by centrifugal forces created as a result of spinning a spirally wound tubing i.e. the CCC column. A second liquid phase (mobile phase) is then continuously pumped through the column and is subjected to multiple stages of mixing (during which solute mass transfer occurs) and settling with the stationary phase. The retention of the stationary phase in the open column can be accomplished by a combination of column geometry and the applied force field, either gravitational or centrifugal in nature. Those components having a higher affinity for the mobile phase are eluted first. For detailed reviews of countercurrent chromatography, refer to books by Conway [1990], Ito [1996] and Menet and Thiebaut [1999].

Some advantages of CCC over conventional chromatographic methods are listed below [Conway, 1990]:

- Economical: Column is indestructible, dirty samples accepted
- Predictable: Retention predictable from partition coefficients K
- Reproducible: Very reproducible in instruments and columns of different style and size
- Good resolution: Standard column provides 350 to 1000 plates
- Versatility: Choice of either phase as mobile phase, eliminates containments leached from adsorbents, many two-phase systems available to choose from

1.7.2 J-type multi-layer coil planet centrifuge

1.7.2.1 Design of J-type CCC

The design of the CCC device used consists of two gears, the central 'sun' gear being interlocked with the planetary gear. Numerous CCC designs described in Section 1.10 exist. The J-type centrifuge has a bobbin that rotates in planetary gear motion. A coil of tubing is wound on this bobbin to form the column. This arrangement produces a particular type of planetary motion whereby the column holder is rotated around the central sun gear axis, while the planetary gear causes simultaneous rotation of the

column holder around its own axis (Figure 1.9). As a result of the gear mechanism and the 1:1 gear ratio between the sun and planet gears, the rotational speed of the bobbin is equal to that of the rotor. Due to this motion, the coil is subjected to a varying centripetal acceleration. Originally a counterweight was used to balance the system. However this proved awkward, as the weight would have to be adjusted to account for different densities of the solvent systems used. This problem has been overcome by placing multiple column holders symmetrically around the rotary frame.

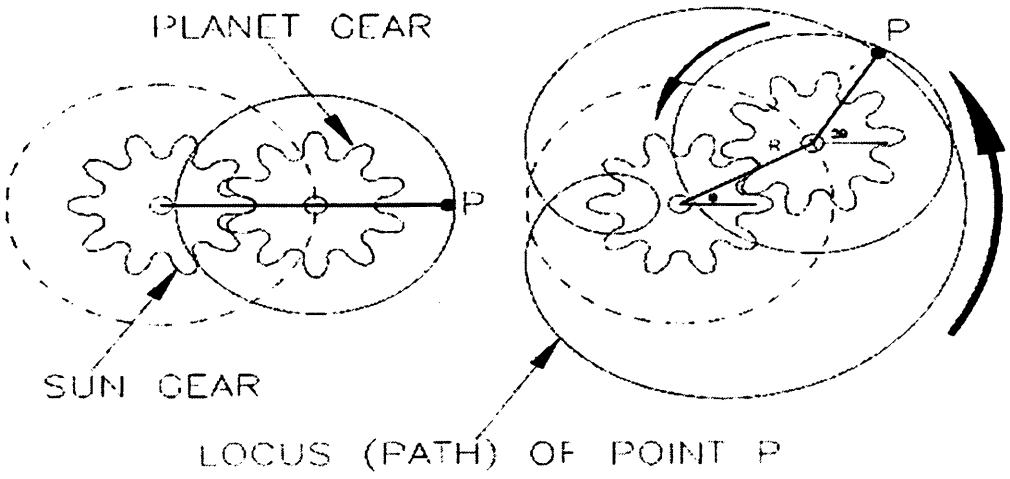

Figure 1.9: Planetary gear motion of a J-type centrifuge. r is the radial distance between the centre of the coil and the R is the radial between the centre of the sun gear and the planet gear. Taken from Brunel J-type CCC manual, Brunel Institute of Bioengineering.

1.7.2.2 β Values

The β value is a dimensionless term that helps describe the motion of point P (Figure 1.9). The β value is the radial distance (r) between the centre of the coil and the point P divided by the radial distance (R) between the centre of the sun gear and the planet gear. In this figure, the β value equals 1, which means r is equal to R and the locus of the point P is a cardioid. When the β value equals 0, r equals 0, and the locus of the point P is a circle.

The influence of the β ratio was proved to be important for the force field created by the J-type motion [Conway, 1990]. Menet and Ito [1993] described the motion induced by J-type coil planet centrifuge. For $\beta = 0.1$, the shape of the path is quite circular, and the corresponding force field is similar to that obtained with a

completely circular motion. As the β value increase, an inward loop develops as the increase in the radius of the holder begins to impact on the path that the coil follows. For β = 0.25, the centrifugal force fields from the two gears cancel out around the modification in the path. At higher β values ($0.7 \geq \beta \geq 0.4$) the centrifugal fields reverses during the inwards loop, the relative magnitude and direction of the centrifugal forces at the various points along the path being important for the vigorous mixing achieved with high β values. The value of β was also found to affect the retention of the stationary phase [Fedetov *et al.*, 2003; Bhatnagar *et al.*, 1989] and explained in more detail in Section 1.9.

1.7.2.3 Two-bobbin machine

The CCC machine used here was a Brunel Labprep, "J" type design (Dynamic Extractions, Uxbridge, UK). Full details of the design and operation are given in Section 2.4. This machine has two flying leads for filling with liquid, one for each bobbin (Figure 1.10). These flying leads do not need to be counter rotated to stop them from twisting. An advantage of the design is the ability to achieve a maximum β value of 1. The 2-bobbin machine can achieve higher β values compared to other configurations. The radial acceleration increases with higher β values which improves stationary phase retention S_f (the amount of initial stationary phase retained after displacement which occurs due to the pumping of the mobile phase) [Bhatnagar *et al.*, 1989]. This is possible since the main drive shaft does not pass between the rotor plates (Figure 1.11). Therefore the maximum β value is not limited by the diameter of the main drive shaft but by the outer diameter of the other bobbin. The outer diameters of the bobbins will touch when each has a β value of 1. Currently the β value range of this machine is 0.7- 0.91; however this can be expanded to 0.5-0.95.

The machine has an active temperature control allowing the chromatography to experience an identical temperature from one separation to the next. This increases the repeatability of separations when compared to other machines.

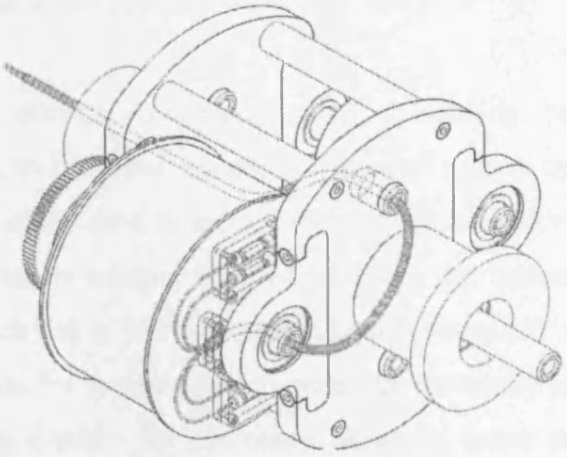

Figure 1.10: Brunel two bobbin J-type CCC machine showing the route of a flying lead (only one bobbin shown) taken from Brunel J-type CCC manual, Brunel Institute of Bioengineering.

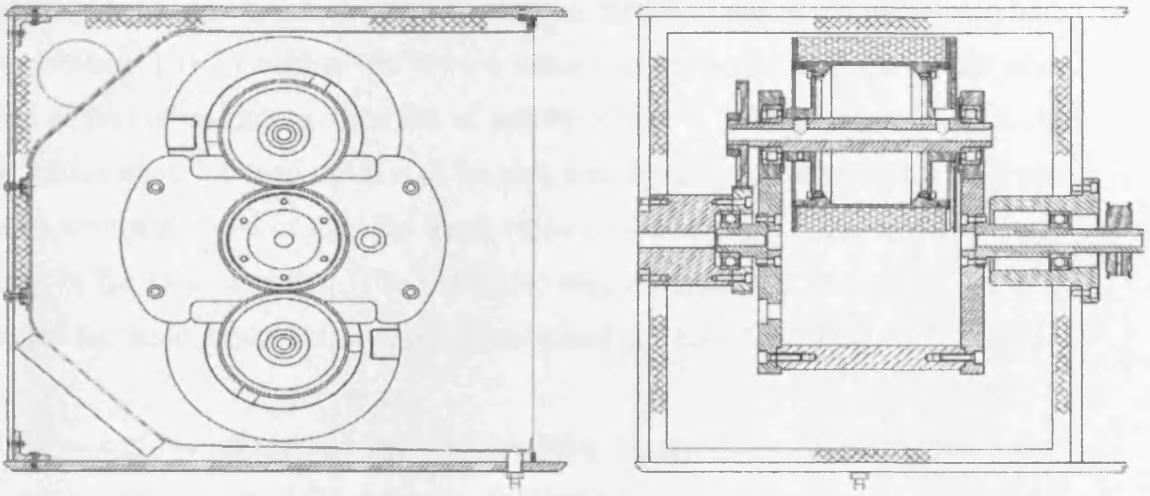

Figure 1.11: 2 Bobbin machine with drive shaft replaced by two half shafts [Wood, 2002].

1.7.3 Forces involved in countercurrent chromatography

To understand hydrodynamics of CCC, an understanding of the forces involved must be outlined. There are three principle forces that affect the performance of the CCC: Archimedean, hydrostatic and external pumping forces. The addition and negation of each of these forces primarily determine whether reasonable stationary phase retention can be achieved.

1.7.3.1 Archimedean screw force

The Greek mathematician Archimedes used a rotating helical structure, the Archimedean screw, to lift water against the force of gravity up onto the riverbank. This principle can also be used to move two immiscible liquids past each other in a countercurrent manner by rotating a coiled tube in a gravitational field. This is also the principle by which one of two immiscible liquid phases can be retained within the rotating CCC column. For a separation to occur the externally pumped mobile phase must not completely displace the stationary phase i.e. some stationary phase must remain in the coil. This is achievable because of the Archimedean screw effect. This screw effect is an internal pumping effect that redistributes the upper and lower phases to opposite ends of the coil when no externally pumped mobile phase is present. This effect occurs in all coils and can be visualised using a glass bead and air bubble place somewhere in a coil, representing the lower phase and the upper phase respectively. The air bubble will always remain at the top of the coil and the glass bead at the bottom due to the effect of gravity. Figure 1.12 illustrates this effect. As the tube is rotated around the axis of the coil, both the air bubbles and glass bead will move toward one end of the tube. Both objects, whether light or heavier than water move in the same direction. The end of the tube toward which the objects move is termed the 'head' of the coil, and the opposite end the 'tail' [Ito, 1996].

In the case of two immiscible liquid phases being present in the coil, the lighter phase moves toward the top of the coil with each helical turn, and the heavier drops to the bottom. Given time the two phases will establish a hydrodynamic equilibrium, with each phase occupying roughly equal space at the head of the coil with excess of either phase being pushed back to the tail. Further rotation of the two phases simply results in the mixing of the two phases with each turn of the coil with no change in the overall volumetric distribution of the phases [Ito, 1996]. Ito generalised his experimental observations into two categories to describe phase distribution patterns [Ito, 1992]:

1) Unilateral hydrodynamic distribution equilibrium - both phases are distributed along the length of the coil, so that one phase occupies the head and the other the tail in an approximately 50:50 ratio.

2) Uniform radial distribution – both phases are uniformly distributed along the length of the coil occupying at each helical turn equal volumes.

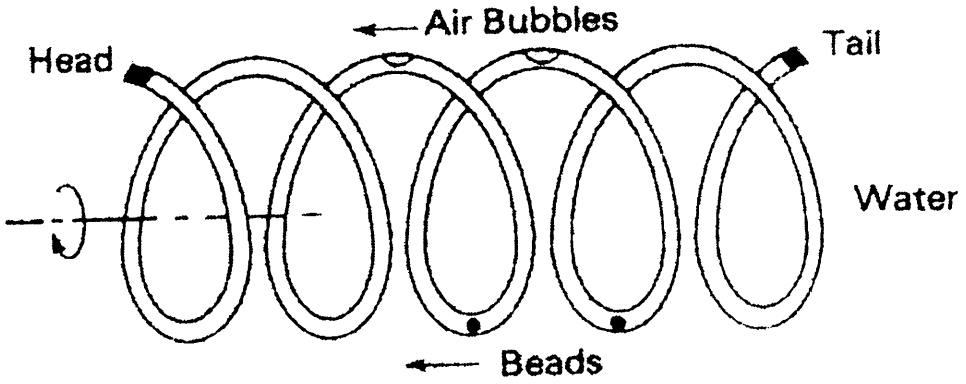

Figure 1.12: Illustration of the Archimedean screw principle in a helical coil. Light and heavy phases are depicted by air bubbles and beads respectively. Both solvent phases have a tendency to move in the same direction towards the 'head' of the coil. Reproduced from Ito [1996].

1.7.3.2 Hydrostatic/centrifugal force

The application of a simple CCC system described in Section 1.7.3.1, had the disadvantage, due to the low Archimedean screw forces generated under gravity, of a low degree of stationary phase retention. As a result, long processing times and lack of sufficient resolution rendered these devices unsuitable for use. Ito [1992] postulated that by applying a centrifugal force to a helically wound coil, the tangential force component, responsible for generating the Archimedean screw effect, would act against the radial forces to generate a hydrostatic phase distribution. This finding led to the development of a series of synchronous devices, which can achieve a high degree of stationary phase retention.

The speed of revolution of the coil has been found to have a profound effect on the phase distribution in the coil [Ito, 1996]. At a slow rotation (10-20 rpm) the two solvent phases are quite evenly distributed (Figure 1.13-A). Under these conditions the centrifugal force generated by the rotation of the coil is negligible, and the Archimedean screw effect acts evenly on the two phases, both phases moving toward the head in the upper and lower portions of the coil dependent of the respective density. As the rotational speed increases the centrifugal force generated begins to

negate the gravitational effect, thus the progression of the lighter phase toward the head is retarded as the net effect of the centrifugal force and the downwards gravitational force accelerate the progress of the heavier phase toward the head end of the coil preferentially. At a critical speed range between 60 and 100 rpm the two phases are completely separated, with the heavier phase at the head, and the lighter at the tail (Figure 1.13-B). Berthod [1991] also studied the effects of increased rotational speed on phase volume distribution, finding a critical rotational speed (60-100 rpm) where the immiscible solvents are completely separated along the coil length. After this critical speed further increases in the speed of rotation of the coil introduces a stronger radial force field which negates the gravitational effect and the phases become redistributed so that the heavier phase occupies the outer part of the coil, and vice versa, resulting in the phases gradually returning to an even distribution through the coil (Figure 1.13-C). It was found to be essential for the Archimedean and hydrostatic forces to be additive for a reasonable stationary phase retention [Sutherland *et al.*, 2000a]. This will be further explained in Section 1.7.3.4.

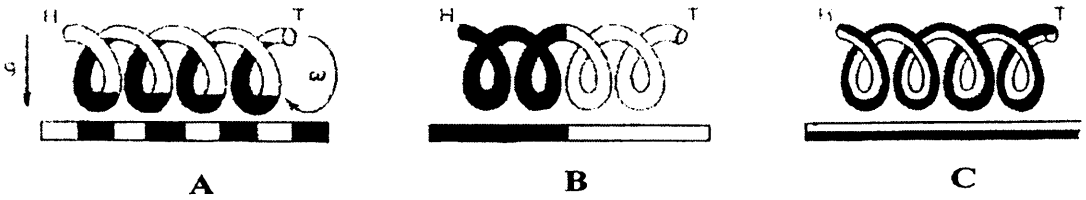

Figure 1.13: Representation of the variation in the distribution of the heavy (■) and light (□) solvent phases within a helically wound coil. (A) slow rotation (10 rpm) illustrating Archimedean distribution. (B) Intermediate rotation (10-160 rpm) illustrating unilateral distribution. (C) High rotation (~300 rpm) where uniform, radial distribution is achieved. H = 'Head' of coil; T = 'Tail' of coil. Reproduced from Conway [1990].

1.7.3.3 External pumping force

At the critical speed (60-100 rpm) when the two phases are completely separated in the coil, the hydrodynamic equilibrium condition present enables a large degree of retention of stationary phase if the chosen mobile phase is introduced from the end that the chosen stationary phase would occupy (i.e. if mobile phase is lighter, elute head to tail, and if mobile phase is heavier, elute tail to head) [Ito, 1996]. To retain a stationary phase, the mobile phase must be externally pumped throughout the coil in the opposite direction to which the Archimedean screw effect is pumping the

stationary phase. This means that the mobile and stationary phases are being pumped in opposite directions and hence have the potential for countercurrent flow. It also means that the mobile phase is being externally pumped in the same direction as the internal Archimedean screw effect. Thus the direction of pumping the mobile phase needs to be known in order to achieve satisfactory stationary phase retention.

1.7.3.4 Considerations in pumping directions

Knowing which phase moves towards the head or tail tells the experimenter in which direction to pump the selected mobile phase in order to retain the stationary phase. Ito [1992, 1984a, 1984b] and Sutherland *et al.* [2000a] have studied the pumping orientations on a range of organic-aqueous systems.

a) Ito's Observations

According to Ito [1992, 1984a, 1984b], the behaviour of a phase system, i.e. whether the heavy or light phase moves towards the head end of the coil, depends upon the system's hydrophobicity. Ito [1992] classified the retention profile findings into three groups dependent on the phase systems used and operating conditions:

1. *Hydrophobic system (Hexane-Water , 1:1)*

   A hydrophobic phase system (settling time < 15 seconds) has high values of interfacial tension and low values of viscosity. With such systems, the upper phase will go towards the head while the lower phase will move towards the tail. If the upper phase is the mobile phase, the pumping direction of the mobile phase has to be from tail to head. If the lower phase is the mobile phase, the pumping direction has to from head to tail.

2. *Hydrophilic system (Butanol-Water, 1:1)*

   A hydrophilic system (settling time > 30 seconds) has low values of interfacial tension and high values of viscosity. With a hydrophilic solvent system, the lower phase will go to the head and therefore the upper phase will go to the tail. If the

upper phase is the mobile phase, the pumping direction has to be from head to tail. If the lower phase is the mobile phase, the pumping direction has to be from tail to head.

3. Intermediate system (nButanol-Water, 1:1)

For these systems, the head and tail preference is sensitive to the centrifugal conditions. For small β-values, the hydrodynamics of the intermediate system approaches that of a hydrophilic system with lower phase going to the head and the upper phase to the tail. For larger β-values, the hydrodynamics approaches that of a hydrophobic system with the upper phase going to the head and the lower phase going to the tail.

b) Observations of Sutherland and co-workers

Sutherland *et al.* [2000a] recently reported on the relative actions of the hydrostatic and Archimedean forces present during CCC runs. Sutherland felt that phase systems should not be characterised by hydrophobicity but by physical properties of the phase systems such as: density difference between the upper and lower phases, viscosities and interfacial tension. As discussed before, in Archimedean screw helical spirals operating under unit gravity, the heavy phase goes to the 'head' end of the coil and the light phase to the 'tail'. In gravitational systems like the J-type centrifuge, the distribution is reversed, with the light phase moving toward the 'head' and the heavy phase being displaced toward the 'tail' [Sutherland *et al.*, 2000a; Ito, 1996; Conway, 1990].

If the Archimedean screw effect is neglected and only the hydrostatic centrifugal forces are considered, it is known that in a simple centrifuge, the heaviest phase is driven to the furthest point away from the centre of rotation and the lightest phase is displaced towards the centre. In a spirally wound coil, the heavier lower phase will try to move to the radially outer edge of the coil, called the periphery. This action displaces the lighter phase towards the centre of the coil. For multi-layer coils, it would be sensible to place the end of the coil to which the Archimedean screw effect was pushing the lower phase to the periphery. When the 'tail' is at the periphery of the coil (coil is rotated in the same direction as coil has been wound) hydrostatic

forces can also be expected to force the heavier phase to the 'tail'. This means that the two pumping effects would push the lower phase to the periphery increasing the unilateral distribution. However knowledge of which end of a coil that the lower phase is pushed under the Archimedean screw effect is needed without the interference of the centrifuge effect. Examination of unilateral distribution in helically wound coils is due purely to the Archimedean screw effect because no centrifuge effect is present. Sutherland *et al.* [2000a] hypothesised that the Archimedean screw effect pumps the upper phase to the head and the lower phase to the tail. Therefore to combine the centrifuge and Archimedean screw effects in spirally wound coils the head should be at the centre and the tail at the periphery. Orientating the coil in this way will give the greatest unilateral distribution achievable and hence give the best stationary phase retention.

During operation of the CCC machine, it is desirable to pump the mobile phase against the stationary phase. Thus if the chosen stationary phase is the heavier one (for normal phase chromatography) the mobile phase should be pumped from 'tail' to 'head', when the column is rotated in the forward direction. Conversely if the chosen stationary phase is the lighter one (for reverse phase chromatography) the mobile phase should be pumped from 'head' to 'tail'.

When choosing the direction for the external pumping of the mobile phase, the density difference of the phases needs to be considered. Sutherland reported when using different organic-aqueous solvent systems that when the 'tail' is at the periphery, the heavy phase always goes to the tail, supporting the hypothesis that the Archimedean and hydrostatic forces are additive and that this is accentuated when the density difference is large. However when the 'head' is at the periphery, then whether the forces are additive is dependent on the density difference of the system. For high density difference phase systems, the heavy phase goes to the tail, as before, but for low density difference systems, the heavier phase moves to the head. Low interfacial tension systems was also seen to show this effect.
Sutherland concluded that the best retention would be achieved when pumping a mobile phase in the direction that the coil would naturally pump the mobile phase:

1. When rotating in the clockwise direction, the Archimedean and hydrostatic forces are additive, placing the coil 'Head' at the centre, and the 'Tail' at the periphery. In this operating mode, the denser (lower) phase always travels towards the 'Tail' of the coil.
2. When rotating in the counter-clockwise direction, i.e. the opposite direction to which the coils are wound onto the bobbin, the Archimedean and hydrostatic forces oppose each other, placing the coil head at the periphery and the tail at the centre. When the phase density ratio is > 1.15, the denser phase moves towards the 'Tail'. For a phase density ratio < 1.15, the denser phase moves towards the 'Head'.
3. Under counter-clockwise rotation, for high density ratio phase systems the Archimedean forces dictates the movement of the phases. For low density ratio phase systems, the hydrostatic forces dictate the movement of the phases.

A summary of the forces are shown in Table 1.6 for reverse direction of the J-type CCC.

1.8 Mixing and settling in CCC

The hydrodynamic motion and distribution of two immiscible phases in a rotating CCC coil was first reported by Conway and Ito [1984], who observed distinct zones of rapid phase mixing and settling. The generation of these mixing and settling zones is the result of cardiodial motion which every location on the column follows. Ito's [1992] experimental observations concluded that for each helical turn of the coil, there are two key points, termed nodes, where the Archimedean force reverses its direction with respect to the coil. These are the proximal and distal key nodes, and are positioned at the centre of revolution and the point furthest from the centre of rotation respectively. Upon coil rotation, at the proximal key node, the lighter phase moves towards the coil 'Head', and at the distal key node, the heavier phase moves towards the coil 'Head'.

Each loop of a coil contains a mixing zone and a settling zone. As the coil rotates these zones travel towards the head end of the coil (Figure 1.14). During a single rotation of a centrifuge, a mixing zone and a settling zone will have travelled through a single loop. Therefore, the rate of mixing and settling zones passing a certain point

is equal to the rotational speed of the centrifuge. This must not be confused with the rate at which the mobile phase is travelling through the coil, which is dependent on the flow rate and the amount of stationary phase present in the coil.

The hydrodynamic motion and phase distribution within a J-type column has been observed by Conway [1990] using a J-type centrifugal precipitation chromatograph (CPC) equipped with a spiral column and a transparent plastic cover. A two-phase solvent system comprising chloroform and water, each stained with a dye to facilitate stroboscopic observation was utilized in the experiment. After steady state hydrodynamic equilibrium was established two distinct zones could be observed; approximately one fourth of the area closest to the centre showed violent mixing of the two phases (the mixing zone), while in the remainder of the coil the phases were separated into two layers forming a linear interface (settling zone). The mixing zone is always in the section of the loop of the coil nearest to the centre of rotation, while the coil itself rotates around its own axis, thus the mixing zone is travelling through the spiral column toward the head at a rate equal to the column rotation. In any part of the column the two phases are subjected to repeated mixing and settling stages at a frequency of over 13 times per second for a rotational speed of 800 rpm [Ito, 1996] hence a high partition efficiency can be achieved by high speed CCC. Sutherland *et al.* [2000a] also observed that phase mixing occurs at the proximal node, where the centrifugal forces are low. Phase settling, i.e. the formation of two distinct immiscible phase, occurs at the distal key node.

Direction	Reverse rotation (anticlockwise)
Alignment of ends	Tail – periphery Head - centre
Hydrostatic force	Lower – periphery Upper – centre
Archimedean force	Lower – tail Upper - head
External mobile pumping	Head to tail if lower phase pumped Tail to head if upper phase pumped

Table 1.6: Summary of hydrostatic, Archimedean and external mobile pumping forces for reverse rotational direction of J-type CCC and recommended directions of pumping as proposed by Sutherland *et al.* [2000a].

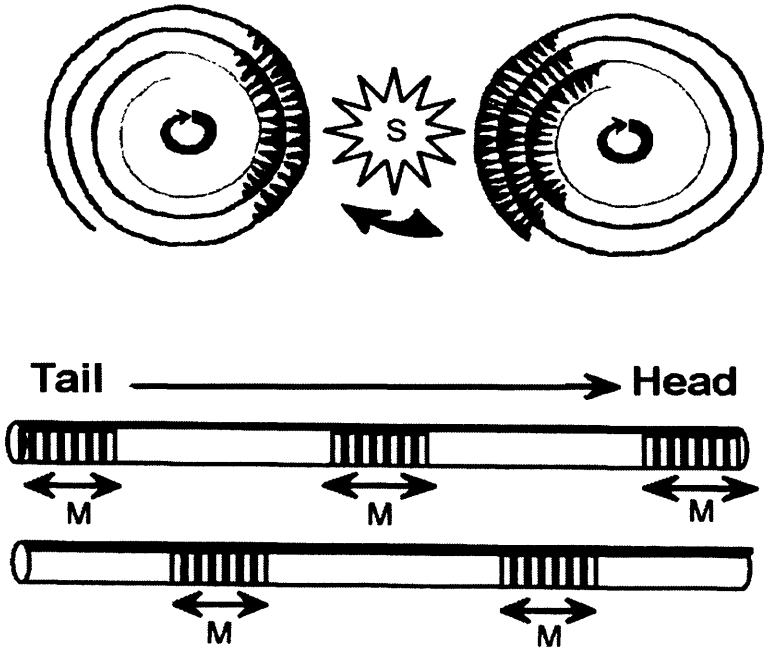

Figure 1.14: Illustration of the distribution of the mixing and settling zones present during rotation of CCC column on a twin bobbin machine. Top diagram indicates location of the mixing zones (black bars) in the coil created due to the planetary motion created as it orbits the sun gear (S). The lower diagram shows straightened sections of the coil and illustrates the progression of the mixing zones (M) from the 'tail' to the 'head' reproduced from Conway and Ito [1984].

The J-type centrifuge mainly uses a form of wave mixing. The motion of the J-type causes two thin layers; each layer formed by one of the immiscible phases. Zones of mixing and settling travel along the coiled tubing coincident with the low and high accelerations caused by the epicyclic motion of the coils [Sutherland *et al.*, 1987]. The mixing zones are coincident to the low accelerations and take the form of waves [Sutherland *et al.*, 1986]. The settling zones are coincident with the high accelerations and take the form of a smooth interfacial area [Conway, 1990]. Wood *et al.* [2001] recently described wave mixing as the primary method of mass transfer between mobile and stationary phases when using organic-aqueous two phase systems. He described the interfacial movement as a relative pumping action between the phases. During mixing, the interfacial area increases and each phase form droplets in the other phase. These droplets have a high surface area to volume ratio and promote the mass transfer of a sample between the two phases. The settling stage ensures that the mobile phase moves past the stationary phase, while no significant mass transfer occurs. This settling stage also ensures that the mixing stages are discrete from each other. Wood hypothesized that it is a combination of pumping of the mobile phase and the internal pumping of the phases within a loop that causes the relative velocity between the phases to exceed a certain velocity termed Kelvin-Helmholtz threshold velocity. When this velocity is exceeded, mixing occurs. This threshold velocity was also mentioned earlier by Sutherland [Sutherland *et al.*, 1986]. Wood *et al.* [2003a] also hypothesized that the total pressure drop across a coil is independent of the mobile phase flow. The pressure drop across a coil is constant because the mobile flow rate proportionally increases the cross-sectional area occupied by the mobile phase, and remains constant for a given coil, phase system and rotational speed. With the basis of this assumption, Wood [2002] was able to show linear relationships between the mobile phase volume in the coil and rotational speed of the column.

The importance of wave mixing was further studied by König and Sutherland [2003] where they have recently used numerical modelling of liquid-liquid flow to show the mass transfer and the movement of the interface. Although the hydrodynamics are complex and not yet fully understood, the result of this motion is the formation of waves and a wave mixing effect, and good agreement between the numerical and experimental models were seen for the straight model tube (Figure 1.15) for

Heptane/Ethyl acetate/Methanol/Water phase systems with the exception of systems that have very high interfacial tension.

Figure 1.15: Simulation for the straight tube model for a Heptane/Ethyl acetate/Methanol/Water phase system, density difference = 98 $kg.m^{-3}$, Viscosity difference = 9.3 x 10^{-4} $kg.m^{-1}.s^{-1}$, Interfacial tension = 1.1 x 10^{-3} $N.m^{-1}$ reproduced from König and Sutherland [2003].

1.9 Variables that affect the stationary phase retention and the chromatographic process

A large number of variables affect the efficiency that can be obtained in countercurrent chromatography. These variables can be listed in five main groups below [Wood, 2002]:

1. Phase system:
   - Settling times
   - Densities of upper and lower phases
   - Viscosities of upper and lower phases
   - Surface tension of the upper and lower phases and hence interfacial tension

2. Operating variables:
   - Mobile phase flow rate
   - Rotational speed
   - Choice of mobile phase (upper or lower phase)
   - Mobile phase direction of pumped flow (head to tail or tail to head)
   - Direction of rotation (clockwise or anticlockwise)
   - Process temperature

3. Coil/Column parameters

- Coil/column tubing length (number of loops)
- Coil/column tubing internal diameter (bore)
- Coil/column tubing material
- Tube geometry
- Coil/column type: spiral wound, axial wound or multi-layer
- Coil radius (r) and hence β value (r/R)

4. Rotor Parameter:
   - Planetary radius (R)
   - Maximum axial length of bobbin
   - Maximum rotational speed of rotor

5. Chromatographical variables
   - Coil volume
   - Sample volume
   - Partition coefficients
   - Sample concentration

1.9.1 Phase systems

The most important group of variables is the choice of phase system. The choice of phase system will depend upon the sample and the components of the sample to be separated. Most of the work done testing phase system parameters on retention and resolution have involved organic-aqueous phase systems. Authors seem to be in conflict upon which of the parameters (density difference, viscosity or interfacial tension) seems to primarily affect stationary phase retention. The choice of two phase systems and hence their settling time (the time it takes for two phases to form) directly affects retention of the stationary phase. The close correlation found between the settling time, the stationary phase retention profile and hydrodynamic behaviour provides useful guidance in developing applications for CCC [Ito and Conway, 1984]. In a standard multilayer coiled column, a solvent system with a settling time less that 30 seconds would display normal hydrodynamic behaviour which distributes the upper phase towards the head and lower phase towards the tail. If the settling time

considerably exceeds 30 seconds, it is most likely that the hydrodynamic behaviour of the two phases is reversed. Ito and Conway [1984] showed that viscosity of the phase system strongly affected the level of stationary phase retention. The less viscous the solvent system, the higher the level of retention, due to a decrease in settling times. The density difference and interfacial tension showed less influence on retention, as these parameters only affect settling time slightly.

Berthod and Schimitt [1993] showed a direct relationship between stationary phase retention and density difference (lower than 0.35 $g.mL^{-1}$), and concluded that it is the density difference, and not viscosity, that is the most influential parameter that affects retention. A higher density difference showed better retention.

Fedetov and Thiébaut [1998] have showed that all these parameters, especially interfacial tension strongly affect the stationary phase retention. Moderate values of interfacial tension (9-14 $dyn.cm^{-1}$) are most favourable. Retention was also increased when using systems with density differences in the range from 0.15 to 0.25 $g.mL^{-1}$, but was independent on density differences from 0.25 to 0.3 $g.mL^{-1}$. Viscosity differences can also affect the retention. Low viscosity differences (<0.1 cP) leads to a significant decrease in the stationary phase retention. The retention increases for values of viscosity between 0.7 and 1.7 cP and then decreases again (after 1.7 cP). Ito and Conway [1984] used systems with viscosities in the range of 0.7 to 1.5 cP which is the region where Fedetov and Thiébaut [1998] saw an improvement in retention. Fedetov and Thiébaut [1998] also noted that the higher the rotation speed, the lower the dependence of the stationary phase retention on the physico-chemical parameters investigated.

1.9.2 Operating variables

Of the operating variable parameters, it is usually the flow rate and rotational speed that is changed to improve stationary phase retention and resolution. Parameters such as the choice of mobile phase (upper or lower phase), mobile phase direction of pumped flow (head to tail or tail to head) and direction of rotation (clockwise or anticlockwise) are usually known beforehand due to the available knowledge of the hydrodynamics of CCC for organic-aqueous systems. There have been a number of studies involving aqueous-aqueous two phase systems for the separations of proteins that examined flow rates and revolution speeds on retention and resolution using a

variety of CPC machinery [Matsuda *et al.*, 1998; Shinomiya *et al.*, 1993; Lei and Hsu, 1992; Shibusawa and Ito, 1991; Foucault and Nakanishi, 1990]. All experiments indicated that the retention of the stationary phase increased with decreasing flow rates and increasing rotational speeds. Shinomiya *et al.* [1993] was able to obtain retentions of over 50 % using the lowest flow rate (0.5 $ml.min^{-1}$) for PEG-phosphate systems. The stationary phase retention also had a direct effect on the resolution of the eluting protein. A higher retention gave higher resolution. Chromatographic resolution (R_s) is defined as the peak separation (t_{R2}-t_{R1}) divided by the average base width (W_b) which is estimated by drawing tangents to the peak inflection points and extrapolating these to the baseline: $R_s = 2(t_{R2}-t_{R1})/(W_{b2} + W_{b1})$. In this equation t_R represents the peak retention time. Both the peak retention time (t_E) and average peak width (W_b) decreased when the flow rate was increased and rotational speed decreased. This was also seen for organic-aqueous phase systems [Sutherland *et al.*, 2001a; Wang-Fan *et al.*, 2001; Matsuda *et al.*, 1998; Menet *et al.*, 1992]. However, if the rotational is increased beyond a certain speed, a reduction in retention can occur. This is probably due to emulsification caused by excessive mixing of the two phases and is more common in aqueous-aqueous two phase systems which have lower interfacial tensions [Shinomiya *et al.*, 1993].

Process temperature was also seen to affect retention [Maryutina *et al.*, 2003; Kendall, 2002, Menet and Thiebaut, 1999] and resolution [Foucault and Nakanishi, 1990]. A higher temperature reduces the viscosities of the two phases, which can increase mixing and settling times, and hence increase mass transfer of a solute between the phases. Ito [1984b] also found that increasing the temperature from 20^0C to 50^0C could halve the settling time of the two phases. This resulted in improved retention of the stationary phase resulting in higher peak resolution, higher partition efficiency due to a reduction in mass transfer resistance, and increased sample loading capacity due to higher solubility. However, further increases in temperature results in the solvent system nearing its plait point and becoming a single phase.

1.9.3 Coil/column parameters

The effect of column volume on retention and resolution has been tested for a range of aqueous-aqueous and organic-aqueous two phase systems. The coil volume is

changed by either changing column length or internal bore diameter. Increasing the column length (by increasing the number of layer around a coil) has shown to increase the retention and hence improve the resolution in CCC for aqueous-aqueous [Shinomiya *et al.*, 2003; Shibusawa *et al.*, 1997; Shibusawa *et al.*, 1995; Shibusawa and Ito, 1991] and organic-aqueous [Matsuda *et al.*, 1998] systems. Increasing internal bore diameter was also shown to have the same effect for aqueous-aqueous [Shibusawa *et al.*, 2000; Shibusawa *et al.*, 1997] and organic-aqueous [Maryutina *et al.*, 2003; Sutherland *et al.*, 2001] two phase systems. A recent study has also shown that retention increased with bore diameter [Sutherland *et al.*, 2003], however this decreased the resolution at low flow rates and increasing rotational speeds due to the ratio of the bulk volume to interfacial area increasing. At high flow, the opposite was true. Additionally increasing both the coil length and internal bore diameter generally gives the best improvement [Shibusawa *et al.*, 1997; Ito *et al.*, 1991].

The effect of coil tube material was shown to have no effect on resolution or retention when PTFE and stainless steel tubes were compared [Maryutina *et al.*, 2003; Sutherland *et al.*, 2001]. This suggested that retention and mixing are more of a function of the hydrodynamics than a consequence of the properties of the tubing material.

The effect of tube geometry on retention was studied using a variety of tubing shapes (standard, long-side down, short-side down and twisted-1.8 turns/10 cm) [Degenhardt *et al.*, 2001]. It was found that a twisted bore resulted in better retention and resolution due to the reduced violent 'sloshing' of the two phases compared to standard tubing thus minimizing longitudinal solute band broadening which reduce partition efficiency. In addition, a twisted tubing results in constant lateral mixing (as opposed to longitudinal mixing) within each phase which improves partition efficiency. Other parameters such as the coil/column type are fixed by the manufacturer.

1.9.4 Rotor parameters

The rotor parameters are usually fixed by the manufacturer and are machine specific. These parameters are not normally examined against retention and resolution.

1.9.5 Chromatographical variables

The column volume effect was previously explained in Section 1.9.3. The only other parameter examined in this group is the effect of sample volume on retention and resolution. A large sample volume tends to reduce the retention of the stationary phase and result in reduced resolution [Matsuda *et al.*, 1998] probably due to increased settling times. However Bhatnagar [Bhatnagar *et al.*, 1989] reported high retention (S_f > 70 %) when a 5 g sample in a solvent mixture with a settling time of about 100 seconds was used. This unusual behaviour was explained as a result of the CPC design used where high S_f values can be achieved.

High sample concentrations were also seen to decrease the retention of stationary phase that in turn lowers the resolution [Du *et al.*, 1998]. The reason put forward for this is that high concentrations of sample alter the properties of the phase system. Thus it is important to measure how high sample concentrations and loadings affect the physical properties of the phase system. Du *et al.* [1998] showed that the sample's concentration and volume did not affect the solvent systems physical properties enough to cause a significant loss of stationary phase retention.

Partition coefficients are variables that relate to the sample being separated and do not significantly affect the CCC operation.

1.10 Other countercurrent chromatography machines

1.10.1 Cross-axis synchronous flow through coil planet centrifuge

This type of CCC machine, described by Ito and co-workers [Ito, 1996] differs from the J-type, as the axis of rotation of the column is perpendicular to the axis of rotation of the rotary shaft. The cross-axis machines are further classified into X and L types and various hybrid designs such as XL, XLL and XLLL according to the position of the column holder on the rotary shaft. For the type X cross-axis machine the column holder revolves around the central axis of the centrifuge and simultaneously rotates about its own axis at the same angular velocity. In doing so, it always maintains the same distance (R) from the central axis. Again the parameter β (r/R) has a major influence on the hydrodynamics of the system.

Cross axis machines have been used to effect many separations using ATPS, both with PEG-salt systems and PEG-dextran. Mainly protein separations have been reported [Shinomiya *et al.*, 2003; Shibusawa and Ito, 2001], but an initial report on the separation of plasmid DNA from RNA, utilizing a 4 % w/w PEG 6000, 5 % w/w dextran system has also been reported [Mandava and Ito, 1988]. The apparatus used was a non-synchronous cross axis design coil planet centrifuge, of the XLLL type. The columns were rotated around their own axis at 5rpm, while the speed of rotation of the column holders around the central shaft was 1000 rpm. The linear flow rate of the mobile phase (PEG) was 30 $m.s^{-1}$. Plasmid DNA eluted immediately after the solvent front, with RNA eluting soon after. Some overlap between the plasmid and RNA peak was seen. No separation of the OC and SC plasmid forms was observed, and the separation of chromosomal DNA from plasmid DNA was not considered.

In the most recent experimental machines, it is possible to shift the column holder laterally along the rotary shaft (Figure 1.16). The degree of lateral shift of the holder has been found to be vital for retention of viscous solvent systems, such as the PEG phase in ATPS. The lateral shift of the column holder is described by $\delta = L/R$ where L is the distance from the mid portion of the rotary shaft to the column and R is the total radius of revolution around the mid shaft. For the original cross-axis model type X; $\delta = 0$, for type XL; $\delta = 1$, for type XLL; $\delta = 2$, for type XLLL; $\delta = 3$ and for type L; $\delta \leqslant \infty$. Use of the cross axis coil planet centrifuge with the column holder shifted laterally along the rotary shaft increases the magnitude of the laterally acting centrifugal field. This is thought to suppress emulsification and enables superior retention of ATPS such as PEG 1000-K_2HPO_4 and PEG 8000-dextran T500 [Shinomiya *et al.*, 2000; Shinomiya *et al.*, 1993] which has been found to be poor in other models such as the J-type and cross-axis type X coil planet centrifuge.

The column in a cross-axis coil planet centrifuge follows a three dimensional path due to the coil rotating in the plane perpendicular to the rotary shaft. The influence of the β value is not as pronounced as for the J-type machine, although the additional variable for the positioning of the column holder along the rotary shaft does influence the centrifugal forces present [Menet and Ito, 1993]. In the X – L positions the

influence of the lateral force is greatly increased compared to the L position, where acceleration is produced mainly perpendicular to the CCC column.

Ito and co-workers [Ito and Conway, 1996] have also reported on the effect of revolution speed and mobile phase flow rate on stationary phase retention using cross-axis coil planet centrifuge with ATPS. The optimum speed of revolution in terms of stationary phase retention will vary with the design of machine and the phase system used but is likely to be in the region of 800 rpm [Shinomiya *et al.*, 1998; Ito and Conway, 1996; Goupy *et al.*, 1995]. For slower revolution speeds it was suggested that the lateral acting centrifugal force is too weak to provide optimal separation of the phases, and above this value retention again decreased presumably due to excessive mixing of the two phases.

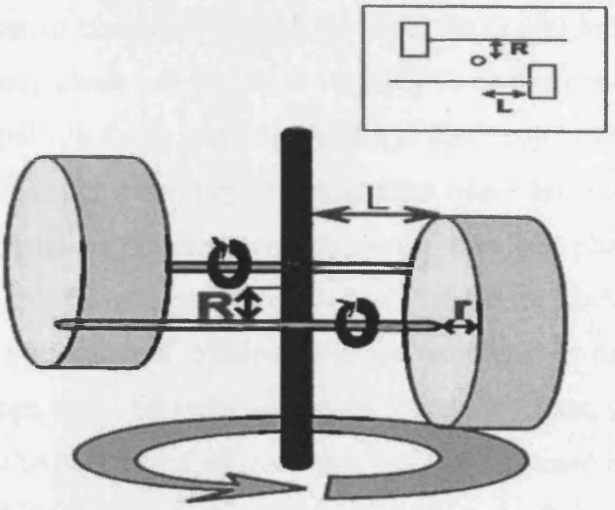

Figure 1.16: Simplified diagram of a type XL cross-axis coil planet centrifuge ($\delta = 1$). The position of the columns in relation to the central axis of revolution (vertical black rod), and the offset of the column and rotary shaft (vertical grey rod) is illustrated. Inset shows a plan view. Reproduced from Kendall [2002]. Not to scale.

1.11 Plasmid DNA separations using CCC and CPC

Ito first reported the use of a nonsynchronous flow-through coil planet centrifuge for the separation of pDNA from RNA [Ito *et al.*, 1983]. A polymer phase system composed of 5% (w/w) dextran 500, 4% (w/w) PEG 6000 and 10mM sodium

phosphate (pH 6.8) was used. The column was first filled with stationary lower phase, and then a sample containing 100 μg DNA of the plasmid pBR 322 was injected. The mobile phase was then pumped from the head end at 8.5 $mL.h^{-1}$ while the apparatus was run at 1000 rpm combined with 5 rpm coil rotation. Results showed that the pDNA had almost entirely partitioned to the upper mobile phase and eluted immediately after the solvent front. A recovery yield of 74% and good separation from the contaminant RNA was achieved. RNA had eluted evenly between the mobile and stationary phases immediately after the pDNA and there was some degree of overlapping, hence reducing the pDNA recovery yield. No protein or chrDNA contamination was considered.

Our laboratory has shown the separation of supercoiled (SC) and open circular (OC) pDNA to be possible using a J-type countercurrent chromatograph [Kendall *et al.*, 2001]. A phase system comprising of 12.5% (w/w) PEG 600 or 16.2% (w/w) PEG 1000 as the stationary phase and 18.5% (w/w) K_2HPO_4 as the mobile phase was used. The column was first filled with stationary phase at 6 $mL.min^{-1}$ in the 'Head' to 'Tail' direction. Once filled with stationary phase, rotation of the bobbin was started in the reverse direction (head-centre, tail-periphery) and the mobile phase was pumped at 0.5 $mL.min^{-1}$. 1 mL of Qiagen purified pDNA (pSVβ, 6.9 kb RNA-free) was injected once equilibrium was achieved. Stationary phase retentions of between 33.2-56.4% were achieved. When PEG 1000 was used as the stationary phase, no DNA had eluted from the column. The bulk of the pDNA was found to be retained in the column when emptied. The SC plasmid was observed in the latest fractions collected (point of sample injection) while the OC plasmid moved a little distance down the tail. It was hypothesized that the high viscosity of PEG 1000 and the large pDNA size had restricted the plasmid back into the mobile salt phase. Another possibility was that the SC DNA was retained at the interface during the phase mixing.

Results using less viscous PEG 600 as the stationary phase showed that the SC form of the plasmid was completely separated from the OC form and had again been retained in the column but had partitioned back to the mobile phase. The OC form was eluted in a peak after 1.1 and 1.29 column volumes. Chromosomal DNA was also visible in the stationary PEG phase near the point of sample injection. Approximately

76% (w/w) of the SC form of the plasmid was recovered in the main SC peak, while the overall recovery of the SC plasmid was 90% (w/w).

Most recently, the use of centrifugal precipitation chromatography (CPC) for the fractionation of protein, RNA and plasmid DNA using cationic surfactant CTAB was achieved [Tomanee *et al.*, 2004]. The system employs a moving concentration gradient of precipitating agent along a channel and solutes of interest undergo repetitive precipitation-dissolution, fractionate at different locations, and elute out from the channel according to their solubility in the precipitating agent solution. Inorganic salts such as NaCl and NH_4Cl were introduced with the cationic surfactant cetyltrimethyl-ammonium bromide (CTAB). The upper and lower channels were completely filled with 0.3% (w/v) CTAB solution. 1mL of clarified lysate containing the 6.9 kb pSVβ plasmid was then injected into the lower channel and the disks were rotated at 1000 rpm. The lysate was washed with ethanol before injection. The upper channel was fed with a decreasing concentration of CTAB solution at a constant flow rate of 1 $mL.min^{-1}$. The lower channel was fed with a solution of 0.7 M NaCl in 5 mM EDTA at 0.06 $mL.min^{-1}$. When CTAB solution with 0.5 M NaCl was used, a satisfactory separation between RNA and pDNA was obtained with about 95.7% and 88.7% of RNA and protein removed respectively from the pDNA fraction (Figure 1.17). The surface charge of the surfactant upon addition of NaCl and NH_4Cl was reduced and weakened the bio molecules/CTAB interactions. This creates a differential solubility between RNA and pDNA. The author does not mention the recovery yield of the pDNA nor does she mention the chromosomal DNA levels in the final solution.

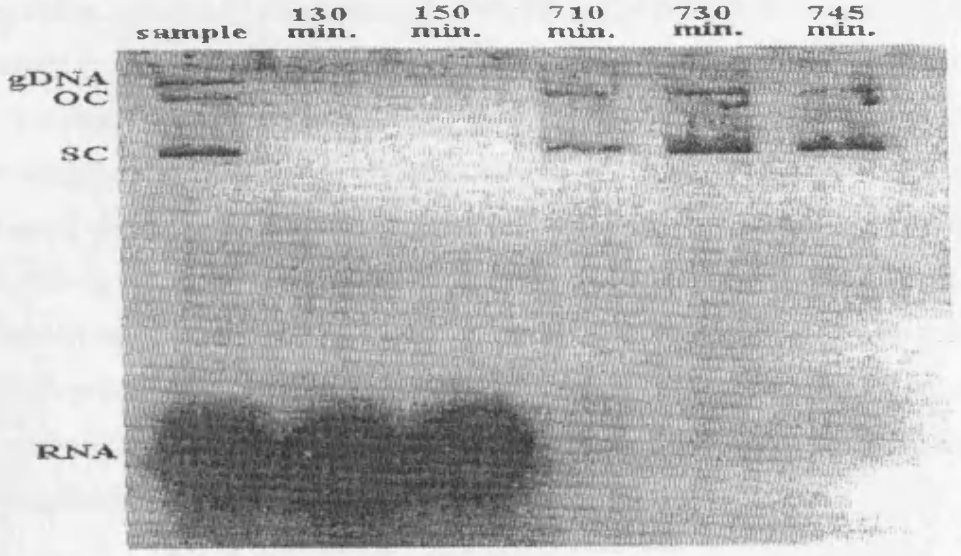

Figure 1.17: Agarose gel electrophoresis of feed and fractions collected from centrifugal precipitation chromatography of *E. coli* clarified lysate using CTAB solution containing 0.5 M NaCl as a precipitating agent. Complete separation of contaminant RNA is shown from pDNA reproduced from Tomanee *et al.* [2004].

1.12 Aims of the project

The aim of this thesis is to develop alternative strategies for the downstream processing of naked pDNA, with the intention of improving upon the efficiency of the purification strategies reported in the literature to date. The selective adsorption of single stranded chromosomal DNA and other cellular contaminants from the double stranded pDNA model product was investigated as a primary purification step, with the aim of increasing the capacity of conventional chromatographic techniques for the purification of pDNA. A novel high-resolution technique utilizing countercurrent chromatography for the separation of plasmid DNA from contaminant RNA and chrDNA was developed. Our laboratory has previous shown that CCC can be used as a final polishing step for the separation of the different forms of pDNA whereas this thesis looks at the use of CCC as a primary purification step. This approach has the potential to circumvent many of the problems associated with conventional purification techniques such as high cost of matrix and low capacity for plasmid DNA, and potential problems due to loading the high viscosity process stream onto a conventional packed column.

The selective removal of chromosomal DNA, RNA and proteins from clarified lysate containing the double stranded pDNA product was examined as a combined recovery and purification step, intended to be placed before the high-resolution chromatography operations. Pre-purification of the sample should increase the capacity of conventional chromatographic techniques for the purification of plasmid DNA, which has been reported to be low [Levy *et al.*, 2000]. Thus initial pre-purification using ATPS was examined. Although there has been some initial studies on pDNA partitioning in ATPS [Ribeiro *et al.*, 2002], the effect of ATPS parameters such as volume ratio, pH effects and settling times on pDNA partitioning and its resulting separation from its contaminates has not been well documented.

The CCC technique has been shown to be extremely versatile in terms of the variety and nature of the solute and feed streams which have been purified [Sutherland *et al.*, 1998; Ito, 1996]. Current gene therapy clinical trials can use plasmid vectors between 2 and 200 kbp, thus the recovery of different sized plasmid, especially larger sized plasmids, needs to be examined.

Before experiments are done using pDNA, the behavior of ATPS in CCC has to be examined, and the hydrodynamics of aqueous-aqueous systems in the J-type CCC, which has never been tested, needs to be extensively studied to find the optimal conditions for pDNA separation. The separation of pDNA from chrDNA, proteins and RNA contaminants using clarified and crude lysates in a J-type CCC device has not been previously described. Thus the major aims of this thesis is to:

- Define the conditions which gives the optimum stationary phase retention of ATPS in J-type CCC devices. The stationary phase retention will be examined using a wide range of phase compositions and CCC operating conditions to define conditions in which the CCC should be operated. Correlations will also be tested for the prediction of retention as a function of CCC parameters for use in studies involving plasmid DNA. This work will be described in Chapter 3.

- Identify optimal ATPS conditions for the recovery and purification of plasmid DNA (Chapter 4) for use in the subsequent CCC runs (Chapter 5). The choice of phase systems will be tested initially before studying the effects of volume ratio, pH, plasmid size and settling times of ATPS on both pDNA partitioning and contaminants. A method incorporating both ATP batch extraction and subsequent separation using CCC will be examined to effectively separate pDNA from its contaminants with different initial buffer selection (for pDNA resuspention) and pumping orientations tested.

- Describe the optimization of CCC by testing different parameters such as the mobile phase flow rate and rotational speeds. The effect of solute loading and operating modes are also examined in order improve the throughput of purified plasmid DNA and this is described in Chapter 6.

Consideration of the forecast made by Sutherland and co-workers regarding the throughputs achievable, and the low cost of operation of CCC suggest that the use of CCC for the high resolution purification of pharmaceutical grade plasmid DNA has the potential to overcome the current constraints imposed by the low capacity, and high cost of solid chromatographic matrices, as used in plasmid purification processes reported to date [Diogo *et al.*, 2005; Ferreira *et al.*, 1999; Varley *et al.*, 1999; Horn *et al.*, 1995].

Chapter 2
Materials and Methods

2.1 Chemicals

All chemicals were obtained from Sigma Aldrich chemical company (Poole, Dorset, UK) and were of analytical grade unless otherwise stated. Deionised water was used for make up of all reagents.

2.2 Plasmids and fermentation conditions

The plasmids used were gWiz [Rock *et al.*, 2003] with 5700 base pairs, pSVβ (obtained from Promega Corp., MA, USA) with 6900 base pairs, pQR150 [Jackson *et al.*, 1995] with 20500 base pairs and p5180 [Rock *et al.*, 2003] with 72000 base pairs. Plasmids gWiz, pSVβ and pQR150 were transformed and propagated in *Escherichia coli* DH5α (Gibco-Life Technologies, MD, USA) while for plasmid p5180, *E. coli* DH10β [Wade-Martins *et al.*, 1999] was used. The *E. coli* DH5α recombinant bacteria gWiz, pSVβ and pQR150 were cultured in Luria Broth media [Sambrook *et al.*, 1989] (containing 5g.L^{-1} bacto yeast extract, 10g.L^{-1} tryptone,, 10g.L^{-1} sodium chloride) and strain harbouring plasmid were grown overnight. Bacterial colonies from master cells stocks in 20 % glycerol were streaked onto the plates using aseptic techniques. The inoculum was prepared by transferring a single colony from the agar plate to a shake flask or universal bottle containing the sterile LB media. The gWiz and PQR150 plasmids were grown overnight in six 2 L shake flasks containing 500 mL LB media (for large scale fermentation) while pSVβ plasmid was grown in 40 mL universal bottles containing 5 mL LB media (for shake flask fermentation). All flasks and bottles contained ampicillin (100 μg.mL^{-1}) and were incubated at 37°C with agitation (300 rpm).

E. coli cell pastes containing gWiz and pQR150 plasmids were obtained from a 450 L fermentation performed as part of an undergraduate pilot plant week (The Advanced Centre for Biochemical Engineering, University College London). Bacteria first grown in baffled shake flasks were used to inoculate a Series 2000 LH 75 L bioreactor (Inceltech, Reading, Berks, UK) containing 50 L of LB media with 0.1

$mL.L^{-1}$ polypropylenglycol and 0.1 $g.L^{-1}$ ampicillin. Bioreactor conditions were: temperature, 37 °C; agitation, 400 rpm; air flow rate, 30 $L.h^{-1}$, pH = 6.95. Bacteria were harvested at a final OD_{600} = 1.6. A volume of 12 L was then used to inoculate 300 L of LB media contained in a 450 L Chemap bioreactor (Chemap AG, Maenndorf, Switzerland). The fermentation conditions were: temperature, 37°C; agitation, 250 rpm; air flow rate, 150 $L.h^{-1}$. The bacteria were grown for 10 h to a final OD_{600} = 2.85 [Levy *et al.*, 2000].

For the pSVβ plasmid, six 2 L shake flasks were prepared each containing 500 mL of sterile LB broth with ampicillin (100 $\mu g.mL^{-1}$). A 5 mL inoculate was added to each flask. The flasks were incubated for 16 hours at 37 °C and 300 rpm.

For the p5180 plasmid, super broth media (containing 20 $g.L^{-1}$ yeast extract, 5 $g.L^{-1}$ NaCl, 32 $g.L^{-1}$ tryptone, 15 $g.L^{-1}$ Agar) was used with kanamycin (15 $\mu g.mL^{-1}$) added. Bacterial colonies from master cells stocks in 20 % glycerol were streaked onto the plates using aseptic techniques. The inoculum was prepared by transferring a single colony from the agar plate to a 40 mL universal bottle holding 5 ml of sterile super broth. The inoculate was placed in a Jalabo-20B water bath where it was incubated at 37 °C and 200 rpm for 8 hours. Six 2 L shake flasks were prepared each containing 500 mL of sterile super broth. 5 mL inocula was added to each flask. The flasks were incubated for 16 hours at 37 °C and 200 rpm.

Bacterial cells from shake flask fermentations (pSVβ and P5180) were harvested using a JA10 Beckman centrifuge (Buckinghamshire, UK) at 6000 rpm for 20 mins. The cell paste was stored initially at -20°C then at -70°C until required.

Bacterial cells from the 450 L fermentation were harvested using a semi-continuous Carr Powerfuge P6 (Carr separations Inc., Franklin, MA, USA) at a flow rate of 30 L. h^{-1} and 20 000 g. The cell paste was double sealed in plastic bags before being stored initially at –20 °C and then at –70 °C for up to 36 months. Agarose gel electrophoresis, as described in Section 2.7.2, of control samples showed no deterioration in the quality of the plasmid over that time.

2.3 Alkaline lysis of *E. coli* cells and lysate clarification

Cells were lysed using a modified alkaline lysis procedure [Birnboim *et al.*, 1979]. Cells were defrosted by leaving out at room temperature and resuspended in TE buffer (10 mM Tris-HCl, 1 mM EDTA, pH= 8) to a concentration of 30 $g.L^{-1}$ cell paste. No RNaseA was added unless otherwise stated (when used, 0.1 $\mu g.mL^{-1}$ RNaseA (Qiagen, West Sussex, UK) was added to the resuspension buffer). Lysis was achieved by addition of an equal volume of 200 mM sodium hydroxide, containing 1 % (w/v) SDS. The solution was mixed gently by inversion and left to stand for 5 minutes at ambient conditions prior to the neutralisation step which involves gentle mixing with pre-chilled 3 M potassium acetate solution at pH 5.5. The final reaction volume was typically 1.5 L. Gentle mixing was achieved by inversion of the reaction vessel following addition of the buffers. Removal of floc and clarification was achieved by centrifugation (10 000 rpm, 4 °C, 30 minutes) followed by filtration through a single sheet of qualitative No. 1 filtration paper (Whatman, Maidstone, Kent, UK). The clarified lysate was stored at 4°C until required. Typically 1.2 L of clarified lysate was recovered. In some experiments when stated, unclarified lysate (no removal of floc by centrifugation or filtration) was used for CCC experiments. The gWiz and pQR150 plasmid concentration of lysates prepared from cell paste from the 450 L fermentation (Section 2.2) was typically 30 $\mu g.mL^{-1}$ and 20 $\mu g.mL^{-1}$ respectively.

2.4 Laboratory scale CCC instrument

The laboratory scale CCC instrument used was a Brunel Labprep (J-type design) (Dynamic Extractions, Uxbridge, U.K). This coil planet centrifuge is shown in Figure 2.1. This device was fitted with two equivalent bobbins, each containing coils prepared from polytetrafluoroethylene (PTFE) tubing of varying diameters. The bobbins accommodating the PTFE coils were labelled as 'Bobbin 7/1' and 'Bobbin 7/2'. Each bobbin consisted of an inner and outer coil, as shown in Figure 2.2. The coil was spirally wound from the centre of the bobbin to its periphery in an anticlockwise manner, forming a multilayered configuration. Once the tubing was wound onto the bobbin, an outer stainless steel sleeve was put in place and the whole internal structure potted together using an epoxy resin, to prevent any lateral movement of the multilayered coils during rotation. The dimensions of the coils are given in Table 2.1.

The flying lead volume for the PTFE coils was 0.35 mL per lead respectively, i.e. 0.7 mL total lead volume. This Brunel CCC device differs from other coil planet centrifuges in the novel design of the flying lead arrangement (Figure 1.10), enabling a higher β value to be generated.

The bobbins were rotated at 600 or 800 rpm in the reverse direction, placing the 'Head' of the coil at the centre of the bobbin. The internal operating temperature of the machine was controlled at 25 ± 1°C with an internal fan and a water-cooled jacket. The stationary and mobile phases, in addition to the sample, were pumped using a Dionex P580 high-pressure isocratic pump (Sunnyvale, CA, USA) at flow rates between 0.5-2 $mL.min^{-1}$. The pump provides a pulse-free flow of the phases and therefore accurate flow rates even at low backpressures. This is of great importance for this investigation as the back-pressure developed and measured (500 – 4000 $kN.m^{-1}$) in CCC is far lower than that encountered in other techniques such as HPLC, and any pulsating flow could influence phase hydrodynamics.

Measurement	Bobbin 7/1		Bobbin 7/2	
	Inner coil	**Outer coil**	**Inner coil**	**Outer coil**
Coil o.d. (mm)	3.13	3.13	3.13	3.13
Coil i.d.(mm)	1.56	1.56	1.56	1.56
Coil length (m)	82.1	47.6	84.5	46.6
Number of loops	162	81	162	81
Coil volume (mL)	162.5	94.3	167.2	92.3
Inner coil radius (r_i) (mm)	75.5	88.2	75.5	88.2
Outer coil radius (r_o) (mm)	88.2	94.6	88.2	94.6
Rotor radius (R) (mm)	110	110	110	110
β ratio range ($r_i/R - r_o/R$)	0.69 – 0.80	0.80 – 0.86	0.69 – 0.80	0.80 – 0.86

Table 2.1: Dimensions of both the inner and outer PTFE coils on bobbins 7/1 and 7/2 together with their respective beta ratio ranges (β).

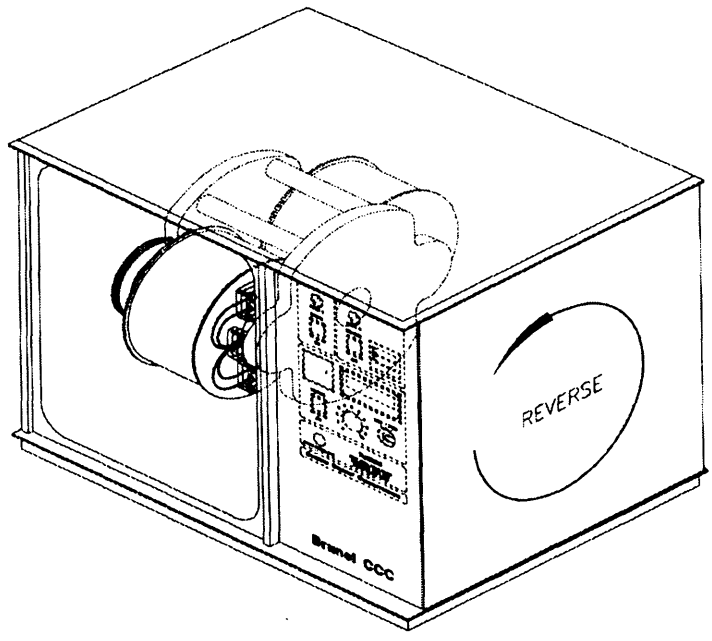

Figure 2.1: The Brunel CCC instrument illustrating the mounting positions of the two bobbins in the rotor housing reproduced from Brunel CCC manual, Brunel Institute of Bioengineering.

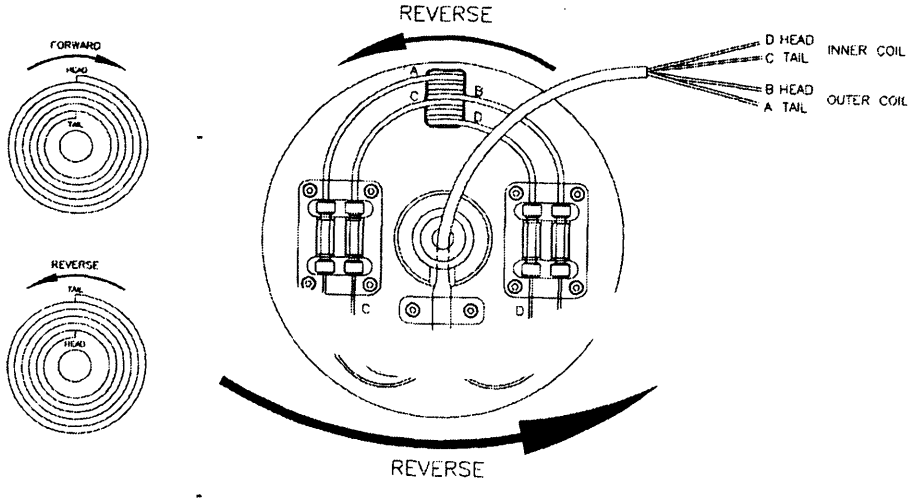

Figure 2.2: Coil winding illustrating the entrance and exit of the two sets of flying lead arrangements reproduced from Brunel CCC manual, Brunel Institute of Bioengineering.

2.5 Aqueous two phase systems (ATPS)

2.5.1 Composition and preparation of aqueous two-phase systems

Polyethylene glycol (PEG) of average molecular weight 200-8000 Daltons and anhydrous K_2HPO_4 were obtained from Sigma Aldrich (Poole, Dorset, UK). ATPS for settling studies were prepared in 20 mL graduated polypropylene centrifuge tubes. In all cases, the biphasic systems were prepared by adding different amounts of PEG and salt in the following order unless otherwise stated: water, salt, PEG and lysate. The amount of lysate was kept constant at 40 % (w/w). Pervious research has found this amount to give the highest plasmid DNA recovery yields in ATPS [Ribeiro *et al.*, 2002]. The phases were then mixed by inversion for 10 seconds, to allow mass transfer to occur and allowed to settle. The upper and lower phase volumes were measured and the volume ratio (V_R) calculated as $\frac{V_L}{V_H}$ where V_L and V_H are volumes of the light and heavy phases respectively. The equilibrium partition coefficients (K) of the various nucleic acids were not estimated due to pDNA quantitatively partitioning only to one of the phases and/or the interface. A number of phase systems were also prepared using different compositions of PEG and phosphate and resulting volume ratio measured. It is noted that changes in the binodial curve (Section 2.5.3) and resulting tie-line length due to changes in PEG-salt compositions were not considered when measuring the final volume ratio.

2.5.2 Quantification of ATPS settling times

Initial screening of effective phase systems (plasmid free) for CCC application was based on measuring the time required after phase mixing (performed by inverting the cylinder 5 times and placing it on a flat table) for two distinct phases to form for a 40g total mass system. The time required for the biphasic mixture to be completely separated into two clear layers in a unit gravitation field is defined as the settling time (t_s) [Conway, 1990]. Settling times were measured for clean ATPS in addition to systems containing lysates (with and without RNaseA treatment).

2.5.3 Construction of binodial phase diagrams

The dependence of phase compositions on the polymer concentrations at given molecular weights of the polymers is graphically displayed in a phase diagram. Binodial curves for a range of phase systems containing different ratios of PEG 8000, 1000, 600, 400, 300 and 200 to K_2HPO_4 were determined. Binodial curves were constructed according to Bamberger *et al.* [1985]. Each starting phase system was made up and the weight of the constituents recorded. 12 mL graduated test tubes were used and the weight of the system is recorded. Deionised water was added in a drop-wise fashion into the tubes containing the phase forming mixtures for several ratios of PEG-K_2HPO_4. After each drop the solution is mixed by shaking thoroughly, and the resultant emulsion formed from the two phases observed. The end of the experiment was reached on the first observation when an emulsion (two-phase) was no longer visible following mixing (cloud point). The cloud point signifies that the solutes in the phase system had been diluted to the critical concentration at which two phases are no longer formed in the system. The total weight of the system at this point is recorded. With knowledge of the concentrations and weight of the starting polymer/salt solutions, and the weight of the system at the cloud point, the final compositions can be determined. This is the first point on the binodial curve. Other points are determined by using different starting compositions for the same PEG molecular weight. Binodial curves of PEG-K_2HPO_4 with additions of lysates (20-40% w/w) and isopropanol (2% w/w) were also constructed by introduction of each into the initial phase forming mixtures.

2.6 CCC setup and operation

2.6.1 Bobbin balancing and rotation

The CCC machine is a dynamic piece of equipment, and in order to ensure both vibration free and reproducible operation, balancing of both bobbins is essential. The manufacturer of the bobbins ensure that all 'flying leads' are correctly labelled, identifying for both the inner and outer coils which is the 'Head' (H) and 'Tail' (T) end. The laboratory scale coils used during this study were helically wound anticlockwise from the bobbins centre to its periphery. It is therefore important to stress the effect of rotational direction on the positioning of the 'Head' and 'Tail'. Sutherland *et al.* [2000a] showed that by rotating the bobbins in the same direction as

they are wound, the 'Head' of the coil will always be situated at the centre of the coil (Figure 2.2). For the CCC device used in this work, when the rotational direction is set to either FORWARD or REVERSE, the coils rotate clockwise and anti-clockwise respectively. In order to position the 'Head' of the coil at the centre of the bobbins, to obtain the highest degree of stationary phase retention [Sutherland *et al.*, 2000a], the coil should be rotated with the rotating switch set to REVERSE.

Both PEG and K_2HPO_4 phases were tested as the stationary phase in CCC experiments. The desired stationary phase was first pumped into the column at a flow rate of 2 $mL.min^{-1}$. Once filled with stationary phase, rotation of the bobbins was started in the 'REVERSE' (anti-clockwise) direction. When a rotational speed of 600 or 800 rpm was reached, the mobile phase was pumped isocratically through the column at a flow rate of between 0.5-2 $mL.min^{-1}$ in the same direction as the stationary phase. Both directions H→T and T→H were tested. A stepwise procedure for the setup and operation of the Brunel Lab-prep machine is given in Table 2.2. The Head and Tail ends can be switched to Tail and Head respectively for steps 1 and 5.

2.6.2 ATPS preparation for use in CCC

1 L of total ATPS was prepared for each CCC experiment. The equilibrated biphasic solvent system was achieved by vigorous mixing and equilibration overnight at room temperature. Prior to any phase pumping, the ATPS was sonicated using a U2800 sonicator (Ultrawave Linited, Cardiff, United Kingdom) for a period of 20 minutes and upper and lower phases were separated.

2.6.3 Sample preparation, injection and fraction collection

In initial experiments, clarified lysate resuspended in TE buffer was injected directly into the CCC device after phase equilibrium. For later experiments, sample preparation for injection first involved preparing 20 mL of the same PEG and salt phase compositions as used for the stationary and mobile phases in the CCC machine. To the ATPS (total: 20 mL, described in Section 2.5.1), 8g of clarified lysate was added and mixed for 10 seconds. The resulting system was left to gravity settle.

Step number	Operation
1	Connect the 'Head' end, outer coil flying lead, labelled as HO of bobbin 7/1, to the outlet of the 'stationary' phase pump.
2	Connect the 'Tail' end, inner coil flying lead on bobbin 7/1, labelled as TI, to the 'Head' end of the inner coil flying lead (HI) on bobbin 7/1.
3	Connect the 'Tail end, inner coil (TI) on bobbin 7/2 to the 'Head' end, inner coil flying lead (HI) on bobbin 7/2.
4	Connect the 'Tail' end, outer coil flying lead (TO) on bobbin 7/2 to the 'Head' end, outer coil flying lead (HO) on bobbin 7/2.
5	The 'Tail' end, outer coil flying lead (TO) on bobbin 7/1 should then be placed in a graduated measuring cylinder and secured to enable the accurate measurement of stationary phase retention.
6	The inlet solvent tubing from the isocratic pump can now be placed into the sonicated phase system, i.e. the chosen stationary phase and secured. Pumping of the solvent at 2 $mL.min^{-1}$ can then be initiated.
7	Once a steady solvent stream is seen eluting from the TO flying lead of bobbin 7/1, indicating the coils are completely filled, stationary phase pumping can be stopped.
8	Using either the same isocratic pump, or a separate one, prime with the corresponding mobile phase, and connect the outlet from that pump to the HO flying lead from bobbin 7/1. Set the required mobile phase flow and start bobbin rotation in the REVERSE direction. Turn on the water circulation ensuring operating temperature is set to 25°C.
9	Increase bobbin rotation up to 600 or 800 rpm as displayed on the tachometer. Ensure the operating temperature of the bobbin housing chamber is at 25°C before continuing.
10	Once at 600 or 800 rpm, ensure that the outlet flying lead TO from bobbin 7/1 is securely connected to the graduated measuring cylinder and that the relative volumes of both the lower mobile and upper stationary phases in the measuring cylinder have been recorded. Simultaneously start the pumping of the mobile phase and a stop watch.
11	At regular time intervals, e.g. 5 minutes, record the new relative volumes of both the upper and lower phases in the measuring cylinder, together with the operating temperature, making adjustments to the circulating cooling water rate as required to maintain the operating temperature at 25°C.
12	Continue to record the relative volumes of the eluting phases from the CCC machine until a constant stationary phase volume is obtained. This now constitutes hydrodynamic phase equilibrium across the whole system and the corresponding degree of stationary phase retention can then be calculated as described in Equations 2.1-2.5.
13	Switch off the mobile phase pump and bobbin rotation. Once bobbin rotation has ceased, reconnect the corresponding head and tail flying leads, enabling only the required coil(s) to be used independently or in series for subsequent experimentation.

Table 2.2: Step-wise procedure for bobbin balancing and determination of S_f in the Brunel J-type countercurrent chromatograph using the outer coil for bobbin 7/1.

Depending on the phase in which the plasmid DNA partitioned to, a defined volume of either lower phase (PEG 600 systems) or upper phase (PEG 300 systems) was then carefully isolated and stored at 4^0C prior to use in CCC experiments. Once hydrodynamic equilibrium had been achieved in the CCC (Section 2.6.4), the phase sample was pumped into the CCC using a Dionex P580 high-pressure isocratic pump (Sunnyvale, CA, USA) at the same flow rate used for the mobile phase flow. Pumping of the mobile phase followed injection of the phase sample. Fraction collection into 10mL screw top plastic vials (VWR International Ltd, Leicestershire, UK) was performed at 2-5 minute intervals depending upon mobile phase flow rate. These were stored at -4^0C for subsequent analysis. A Pharmacia Ultrapsec 2000 (Cambridge, United Kingdom) UV-visible detector was used during laboratory scale studies for identifying the presence of eluting compounds from CCC separations. Absorbances of 260 and 280 nm were used for all CCC experiments. The detector was fitted with an analytical flow cell, enabling mobile phase flow rates of up to 10 mL.min^{-1} to be used.

2.6.4 Experimental method for obtaining S_f versus $\sqrt{F_C}$ plot

The selected stationary phase was prepared and initially pumped into the column as described in Sections 2.6.2 and 2.6.3 respectively. Once completely filled with stationary phase, rotation of the bobbins was started in the 'reverse' (anti-clockwise) direction. When a rotational speed of 600 or 800 rpm had been reached the mobile phase was pumped isocratically through the column at flow rates from 0.5-2 mL.min^{-1}. Eluted stationary phase was collected in a graduated measuring cylinder and used to calculate the proportion, by volume, of stationary phase retained (S_f) once hydrodynamic equilibration of the phases had been achieved (typically after 140 and 240 minutes for the 92.3 mL and 167.2 mL columns respectively at 0.5 mL.min^{-1}). The subsequent calculation of S_f took into account the volume of the inlet and outlet leads as described below [Booth, 2003]:

Let $V_{s\text{-}start}$ and $V_{s\text{-}end}$ correspond to the recorded volumes of the aqueous stationary phase within the graduated measuring cylinder prior to and after hydrodynamic phase equilibrium being achieved. V_e is the volume of stationary phase originally in the coil that has been displaced by the aqueous mobile phase and is equal to $V_{s\text{-}end} - V_{s\text{-}start}$.

This experimental data, together with the knowledge of the volumes of the coil inlet (V_{in}) and outlet (V_{out}) flying leads (Table 2.1) enables the corrected V_e values to be calculated according to:

$$V_{e\text{-}corrected} = V_e - (V_{in} + V_{out}) \qquad \text{(Equation 2.1)}$$

Since the content of the CCC coil at hydrodynamic equilibrium is comprised entirely of the biphasic system in a ratio (S_f) determined by the operating conditions employed, it can therefore be deduced that the total coil volume (V_c) is equal to the sum of the stationary and mobile phase volumes within the coil:

$$V_c = V_s + V_m \qquad \text{(Equation 2.2)}$$

If $V_m = V_e$, with $V_{e\text{-corrected}}$ being equal to the actual volume of stationary phase displaced from the column, Equation 2.2 can be written as:

$$V_c = V_s + V_{e\text{-}corrected} \qquad \text{(Equation 2.3)}$$

By rearranging Equation 2.3 together with the knowledge of V_e from the manufacturer's data as presented in Table 2.1, the volume of the stationary phase can be calculated:

$$V_s = V_c - V_{e\text{-}corrected} \qquad \text{(Equation 2.4)}$$

The stationary phase retention is defined as the fraction of stationary phase (by volume) within the coil and is commonly represented as:

$$S_f = \frac{V_s}{V_c} \times 100 \qquad \text{(Equation 2.5)}$$

After each determination of S_f, the volume of stationary phase retained in the column was pumped out with oxygen-free nitrogen gas (B.O.C., Surrey, UK) and added to the volume of stationary phase eluted to give an estimate of the total column volume. All results were accurate within ± 2 mL of the expected total column volume. Certain experiments were performed in triplicate and the maximum coefficient of variance for the calculation of S_f was 3 %.

2.6.5 Experimental method for obtaining S_f versus ω_N plots

The procedure for obtaining plots of S_f versus ω_N was first described by Ignatova & Sutherland [2001]. The method is similar to the one described in Section 2.6.4 except that the mobile phase flow rate is fixed and the rotational speed is initially set to a maximum value of 850 rpm. When hydrodynamic equilibrium is reached (typically after 140 minutes), the speed is reduced in a step-wise manner until a new equilibrium is achieved. Eluted stationary phase was collected in a graduated measuring cylinder and used to calculate the proportion, by volume, of stationary phase retained (S_f) once hydrodynamic equilibration of the phases had been achieved (Equations 2.1-2.5). After each test, the volume of stationary phase retained in the column was pumped out with oxygen-free nitrogen gas (B.O.C., Surrey, UK) and added to the volume of stationary phase eluted to give an estimate of the total column volume.

2.7 Analytical techniques

2.7.1 Precipitation of nucleic acids by isopropanol precipitation

When stated, isopropanol precipitation was used throughout this work to exchange nucleic acids into a suitable buffer and as a concentration step prior to further analysis. Samples were incubated at room temperature for 10 minutes with 0.7 volumes of isopropanol before the precipitated nucleic acids were pelleted by centrifugation for 25 minutes at 13200 rpm in a 5415R Eppendorf centrifuge (Cambridge, UK). For nucleic acids suspended in salt buffer (lower phase in aqueous two-phase systems), an equal volume of 5M sodium chloride was included in the incubation mixture to facilitate the precipitation of the nucleic acids [Sambrook *et al.*, 1989]. The supernatant was then decanted and the nucleic acid pellet washed with 0.7 volumes of 70% (v/v) ethanol before centrifugation for 30 minutes at 13200 rpm. The supernatant was again decanted, and the samples were air-dried for 10 minutes before being resuspended in the desired volume of the required buffer. Typically samples were resuspended in an equal volume of TE buffer (pH= 8) with the exception of the P5180 plasmid which was typically concentrated by a factor of 5.

2.7.2 Agarose gel electrophoresis conditions

For plasmids gWiz, pSVβ and pQR150, the lysate, upper and lower phases of the initial batch ATPS, and samples collected during CCC were analyzed by electrophoresis. Gels contained 0.8% (w/v) agarose containing 0.05 $\mu g.mL^{-1}$ ethidium bromide with 1 x TAE electrophoresis buffer (0.04 M Tris-acetate, pH 8.0, 1 mM EDTA) and were run for 2 hours at 80 mV. Lysate samples were prepared as described in Section 2.7.1. Samples were mixed with 10-20 μL gel loading buffer (0.25 % w/v bromophenol blue, 40 % w/v sucrose in deionised water). For plasmid P5180 (72 kb), the feed and samples were prepared as described in Section 2.7.1. The samples were then loaded onto a 0.8 % (w/v) agarose gel containing 0.5 $\mu g.mL^{-1}$ ethidium bromide with 0.5 x TBE electrophoresis buffer (0.089 M Tris-borate, pH 8.0, 2 mM EDTA) for 5 hours at 45 mV. A supercoiled DNA ladder was obtained from Sigma Aldrich (Poole, Dorset, UK).

The gels were analyzed and photographed using UVP 5000 Gel Documentation System (Ultra Violet Products Ltd, Cambridge, UK). Typical volumes loaded onto the agarose gels were between 20-40 μL. When necessary, gels were deliberately overloaded to enhance the visualization of contaminant RNA. In the case of fractions obtained from CCC experiments (as described in Section 2.6.3), samples were loaded directly onto the agarose gels for initial analysis due to the large number of fractions obtained from each run.

2.7.3 Plasmid standards

Plasmid standards were prepared using a QIAGEN maxi prep kit (Qiagen, West Sussex, UK) and resuspended in TE buffer (10 mM Tris-HCl, 1 mM EDTA, pH 8.0). Concentrations of ultra-pure plasmid DNA (gWiz, pSVβ and PQR150) solutions in TE were determined by measuring their UV absorbance at 260 nm and 280 nm in a 1 cm path length quartz curvette. Their optical density was measured against TE buffer. An $O.D._{260}$ of 1.0 was taken to be 50 $\mu g.mL^{-1}$ double-stranded DNA [Rock *et al.*, 2003]. The ratio of Abs_{260}/Abs_{280} was calculated to establish DNA purity and was typically 1.8, equivalent to 100% purity.

2.7.4 HPLC analysis for quantitative determination of plasmid DNA

The recovery of total plasmid DNA was quantitatively determined by analytical ion-exchange chromatography on a Q-Sepharose anion exchange column (Amersham Biosciences AB, Uppsala, Sweden) performed with a Dionex (Sunnyvale, CA) HPLC system consisting of a GP40 gradient pump, AS3500 autosampler and AD20 absorbance detector as described by Meacle *et al.* [2004]. All absorbance readings were taken at 260 nm. The column was equilibrated with 0.6 M NaCl, 10 mM Tris-HCl, pH 8. Samples (100 µL) were injected onto the column at 0.3 $mL.min^{-1}$ and eluted over 40 minutes with a linear gradient to 1.0 M NaCl. Elution of clarified lysate and samples from the Q-Sepharose column produced a distinct peak containing the supercoiled and opencircular DNA forms. Concentrations were calculated by comparing with a calibration curve (Figures 9.2 and 9.3, Appendix) of plasmid DNA standards (described in Section 2.7.3). To avoid the interference of RNA in the quantification of plasmid, all the samples were treated with RNaseA ($\approx$100 $\mu g.mL^{-1}$) for 20 minutes prior to HPLC. For CCC purified samples, the presence of RNA was also tested by injecting non-RNaseA treated samples into the HPLC and detecting any peaks that arise before the pDNA peak. Examples of chromatographs in the presence and absence of RNA are shown in the Appendix (Figures 9.4 and 9.5). The maximum coefficient of variance for this assay for the quantification of gWiz and pQR150 plasmids in batch ATP extractions were 10.2 % and 15.5 % respectively, whilst for CCC experiments, the maximum coefficient of variance for the gWiz plasmid using this assay was 2.9 %

2.7.5 Quantification of protein concentration

Protein concentration was measured using the Coomassie Plus Protein Assay Reagent Kit (Pierce Biotechnology, Rockford, IL) according to the manufacturer's protocol. Absorbance was measured at 595nm and concentrations were then calculated by comparing with a calibration curve (Figure 9.1, Appendix) of bovine serum albumin standards. The effects of PEG and salts were accounted for subtracting any signals from blank systems. Lysates were typically diluted by a factor of 5.
The maximum coefficient of variance for this assay for plasmids gWiz and PQR150 in aqueous two-phase systems was 6.5 % and 4.3 % respectively.

2.7.6 Quantification of chromosomal DNA

A modified *Taq*man PCR assay procedure [Vilalta *et al.*, 2002] was used to quantitate *E. coli* chromosomal DNA concentrations in ethanol-precipitated samples. Clarified lysate and CCC fraction samples (as described in Section 2.7.1) were analysed for chromosomal DNA contamination using an ABI PRISM 7700 Sequence Detection System (Applied Biosystems, Foster City, CA, USA). Samples were resuspended in 1M Tris-HCl. Purification of DH5α *E. coli* chromosomal DNA was done with the DNeasy tissue kit according to the manufacturer's protocol (Qiagen, West Sussex, UK) and used to generate standard curves from dilutions ranging from 31-5000 pg (Figure 9.6, Appendix). In order to avoid the interference of double-stranded DNA, samples (10μL) were denatured by heating in a water-bath at 95^0C for 15 minutes followed by cooling on ice for 5 minutes. This step was repeated twice before addition of primers (2.5μL each of oligonucleotide primers 23S-sense (5′ GAA AGG CGC GCG ATA CAG 3′) and 23S-antisense (5′ GTC CGC CCC TAC TCA TCG A 3′)) and SYBR Green mastermix (10 μL, Sigma, Poole, Dorset, UK). Control samples were performed to test the effect of RNaseA on amplification in addition to non-template control samples.

2.7.7 Determination of phase density and viscosity

Densities of PEG and salt phases were determined gravimetrically. The viscosity of each phase was measured using a DV-II viscometer (Brookfield, Stoughton, USA). All physical property measurements were made in triplicate at room temperature (22 ± 0.5^0C). The maximum coefficient of variance in the determination of density and viscosity were 0.6 % and 3.8 % respectively.

2.7.8 Interfacial tension measurements

The interfacial tension of ATPS was measured using a spinning drop tensiometer SITE 04 (Krüss, Hamburg, Germany). The temperature of the tensiometer was controlled at 25 ± 0.5^0C. The heavy salt phase of a pre-equilibrated phase system was loaded into the measuring cylinder, valves opened and measurement chamber flooded. The capillary was then rotated and 5 μL of the upper PEG phase injected by a

microliter syringe through a septum into the rotating capillary. One of the drops that formed was then chosen and the length and diameter of it was measured at three rotation speeds of between 2000-5000 rpm using the built-in microscope. The interfacial tension was then calculated using the Equation:

$$\gamma = \frac{1}{4} r^3 . \Delta \sigma . \omega^2 \qquad \text{(Equation 2.6)}$$

where γ = interfacial tension ($N.m^{-1}$), r = radius (mm), $\Delta\sigma$ = density difference ($kg.m^{-3}$) and ω = rotational speed (rpm). For all measurements, it was ensured that $\frac{L}{D} > 4$ [Chen *et al.*, 2003].

To further understand plasmid partitioning at the interface, the interfacial tension was measured over time for both blank systems and phases which contain lysates in the bottom phase (obtained from batch ATP extraction described in Section 2.6.3). All PEG-phosphate systems consisted of 18 % (w/w) of each component. When lysates were included, the bottom phase (which contains the pDNA from a PEG 600/1000 18% (w/w)-K_2HPO_4 18% (w/w)-40% (w/w) clarified lysate system) was then used as the lower phase in the tensiometer with a clean PEG phase (obtained from a blank PEG 18% (w/w)-K_2HPO_4 18% (w/w) system) as the upper phase.

The maximum coefficient of variance for IT measurement of blank systems using three different rotational speeds were 4.3 % and 2.2 % for PEG 600 and 1000 systems respectively. When lysates were included in the lower phase, the maximum coefficient of variance for interfacial tension measurements were 5.5 % for the gWiz plasmid in a PEG 600 system, 5.8 % for the PQR150 plasmid in a PEG 600 system and 3.1 % for the gWiz plasmid in a PEG 1000 system. PEG 300 systems were not considered due to the difficulty in observing PEG droplets and measuring their diameter accurately.

Chapter 3

Hydrodynamics of PEG-Phosphate Aqueous Two-Phase

3.1 Introduction

For CCC applications involving the separation of biological polymers such as proteins and DNA, the use of organic-aqueous phase systems is not appropriate. In this case, aqueous two-phase systems (ATPS) must be used as they offer gentle, non-toxic environments [Zaslavsky, 1995; Albertsson, 1986; Kula *et al.*, 1982] which promote preservation of biopolymer structure and function as described in Section 1.1. For ATPS, hydrodynamic studies have been previously been performed in non-synchronous CPC [Shinomiya *et al.*, 2003] cross-axis CPC [Shinomiya *et al.*, 1993], horizontal CPC [Shibusawa and Ito, 1991] and eccentric multi-layer CCC [Lei & Hsu, 1992] devices being applied for the separation of model protein mixtures. To date however, there has been no detailed study on the hydrodynamics and phase distribution of ATPS in multilayer J-type CCC devices.

As a basis for subsequent studies on pDNA separations using ATPS, this Chapter therefore described the hydrodynamics and phase distribution of three ATPS in a J-type multilayer CCC device. The ATPS comprised of 18% w/w PEG (average molecular weight ranging from 300-1000 Daltons) and 18% w/w potassium-phosphate. The influence of several operational parameters on stationary phase retention was studied over a wide range of operating conditions including mobile phase flow rate (0.5-2 $ml.min^{-1}$), column volume (92.3 ml or 167.2 ml), rotational speed (600 or 800 rpm), choice of mobile phase (upper or lower) and mobile phase pumping orientation (Head→Tail, or Tail→Head). The specific objectives are to: (i) Define the conditions which give optimum stationary phase retention of ATPS in J-type CCC devices, (ii) Show how S_f values vary as a function of phase composition and CCC operating conditions and (iii) Establish correlations for the prediction of S_f for use in subsequent studies.

Part of this work has already been published as: Al-Marzouqi I, Levy MS and Lye GJ. (2005). Hydrodynamics of PEG-Phosphate Aqueous Two-Phase System in a J-type

Multilayer Countercurrent Chromatograph. J. Liq. Chrom. & Rel. Technol. 28: 1311-1332.

3.1.1 Du plots

Knowledge of the liquid-liquid hydrodynamics in CCC devices at different scales of operation is important if accurate scale-up predictions of the solute elution time are to be achieved. Du and co-workers [Du *et al.*, 1999] suggested a relationship between the percentage stationary phase retention (S_f) and the square root of the mobile phase flow rate (F_c):

$$S_f = A - B\sqrt{F_C} \qquad \text{(Equation 3.1)}$$

Where according to Du, the A parameter indicates the "difference in composition of the phases in any multiphase solvent system" and the B parameter indicates the "difference in the volume ratio of the solvent for the same composition of the solvent system". Using Equation 3.1, only two retention tests are required at different flow rates in order to predict S_f at any other intermediate flow rate. The intercept A on the y-axis is when the mobile phase flow rate is zero and thus the stationary phase retention should theoretically be 100%. Theoretically the coil is full of stationary phase if no mobile phase is flowing through it. Twelve organic-aqueous phase systems had the retention characteristics denoted by Equation 3.1 for reverse phase modes only, and the correlation coefficients varied between R= 0.99293 and 0.99976. The J-type CCC used during these experiments had a rotor radius of 100 mm, a β value range of 0.4-0.78 and was rotated at a speed of 705 rpm using flow rates in the range of 0.8-7.5 $mL.min^{-1}$.The results presented show that the intercept of the vertical axis was close to the 100% value and within experimental error in most cases. The only exception in the J-type CCC device used was for the ethyl acetate-water (1:1) phase system where the equation was $S_f = 132.59 - 58.51\sqrt{F_c}$. A possible reason for this could be due to the low density difference between the phases of only 0.0282 $g.mL^{-1}$.

The gradient of the Du relationship, the B term in Equation 3.1 represents the sensitivity of stationary phase retention to the mobile phase flow rate. The steeper the

gradient, the more quickly stationary phase is lost at higher mobile phase flow rates. As the intercept on the y-axis should always be at S_f = 100% for no mobile phase flow, the gradient term is important for determining how a stationary phase of a solvent system will retain for a given set of operating conditions..

3.1.2 Extended hydrodynamics using Du plots

Extended hydrodynamic studies by Sutherland [2000b], based on the observed correlation between retention and flow [Du *et al.*, 1999] have also shown there to be a linear relationship between S_f and the linear mobile phase velocity (u). Sutherland hypothesised that the u^2 term is related to the Bernoulli kinetic energy term ($\rho u^2/2$) for the mobile phase. The kinetic energy term was plotted against the mobile phase flow for all of Du's twelve phase systems. All the relationships have correlation coefficients (R^2) greater than 0.97 and passes through the vertical axis close to the origin. Sutherland then hypothesised that this relation between the kinetic energy of the mobile phase and the mobile phase flow can be developed further to understand the hydrodynamics in a J-type centrifuge. The slopes of this relationship and of the Du plots (described in Section 3.1.1) will give a good index for comparison between different CCC instruments and may be used to compare their relative performances.

3.1.3 Prediction of S_f as a function of rotational speed

Based on the findings of Du and co-workers (described in Section 3.1.1), Ignatova and Sutherland [2003] were able to accurately predict the relationship between S_f and column rotational speed from the B values of Du plots determined for heptane-ethyl acetate-methanol-water phase systems. This was possible assuming that the coil planet centrifuge acts as a constant pressure pump [Wood, 2002] and the analysis of flow according to the Hagen-Poiseuille equation [Wood *et al.*, 2003a] such that:

$$S_f = A - C/\omega_N \qquad \text{(Equation 3.2)}$$

Where the A parameter is the y-intercept of the initial Du plot, ω_N is the rotational speed of the column (rpm), $C = w B' \sqrt{F}$ and w is the column rotational speed (rpm)

used for the initial Du plot, B' is the gradient obtained from the initial S_f versus $\sqrt{F_C}$ plots at w, and F is the mobile phase flow rate (mL.min^{-1}).

From Equation 3.2 it is seen that only two rotational speeds are needed to predict the stationary phase retention once the value of the Du gradient [Du *et al.*, 1999] is known at any intermediate rotational speed. The 'A' term used was 100 for all phase compositions studied indicating 100% retention of the stationary phase at zero mobile phase flow rate.

Ignatova and Sutherland [2003] also used this data to plot the percentage mobile phase in the coil (V_m) against the reciprocal of rotational speed ($1/\omega_N$). This results in a linear plot which means that retention is proportional to $1/w$ confirming Wood's hypothesis [Wood *et al.*, 2003a; Wood, 2002] that the coil planet centrifuge behaves as a constant pressure pump.

3.1.4 Phase distribution with organic-aqueous systems in J-type CCC devices

Phase distribution in CCC has been extensively studied using organic-aqueous solvent systems by Ito [Ito, 1992; Ito, 1984a; Ito, 1984b] and Sutherland [Sutherland *et al.*, 2000a] as described in Section 1.7.3.4. Ito observed the 'Head' and 'Tail' behaviour of a wide range of solvent systems in a number of horizontal coil planet centrifuge machines (incorporating helix and spiral columns) in order to predict the direction that a given mobile phase should be pumped to obtain the maximum S_f values. He hypothesised that the heavy phase moved towards the 'Tail' (periphery) for hydrophobic phase systems, to the 'Head' (centre) for hydrophilic ones, and could go either way for intermediate phase systems. Sutherland also studied various different phase systems and found that the lower phase prefers the 'Tail' end of the coil when the Tail is at the periphery of the coil planet centrifuge bobbin. Notable exceptions to this general rule were with hydrophilic and intermediate systems, and systems with a low density ratio (<1.15). In these cases, the lower phase was found to travel to the 'Head' end when the head is at the periphery. This was attributed to the Archimedean forces and hydrostatic forces operating in the rotating CCC coil opposing each other. The general hypothesis showed that the Archimedean screw force causes the lower phase to flow towards the 'Tail' end, and the hydrostatic forces causes the lower

phase to flow towards the 'periphery'. When the 'Tail' is at the periphery, both forces will work in the same direction.

3.2 ATPS hydrodynamics in a J-type multilayer CCC

3.2.1 Selection of phase systems and operating variables

Three ATPS were studied as shown in Table 3.1. These systems were chosen as pDNA can be chosen to partition to either the PEG or salt phases depending on the molecular weight of PEG [Ribeiro *et al.*, 2002]. Higher molecular weight PEG were not chosen due to the high viscosity of the PEG phase which can lead to high pressures during the pumping stage, and can also be problematic when emptying the column contents. Other salts (described in Section 4.2) were tested however K_2HPO_4 resulted in the fastest separation time. Table 3.1 also shows the system properties (density, viscosity and interfacial tension) and the settling time, which is considered the major factor in determining if an acceptable level of stationary phase retention (S_f) can be achieved for optimal separation conditions [Conway, 1990].

The following operating variables were tested:

- Mobile phase flow rate to test the linear relationship of Du plots described in Section 3.1.1. Flow rates over 2 $mL.min^{-1}$ were not tested as this leads to excessive stripping of the stationary phase.
- Mobile phase pumping orientation to determine the direction which gives the highest S_f values.
- Rotational speed to test the prediction of stationary phase retention as described in Section 3.1.3. Rotational speeds lower than 500 rpm were not tested as no stationary phase was retained at this speed.
- Column volume as this was shown to have an effect on S_f (Section 1.9.5). In addition, the higher the column volume, the higher the number of mixing and settling stages leading to better separations. Higher column volumes can also be used to increase throughput for plasmid DNA separations.

Kendall [Kendall *et al.*, 2001] has previously reported low S_f values between 33-56 % when using PEG-K_2HPO_4 systems in a J-type CCC. The author pumped the lower salt phase in the 'Head' to 'Tail' direction in the reverse direction (clockwise) where the 'Head' and the 'Tail' ends represent the centre and the periphery of the coil respectively. The reverse pumping direction ('Tail' to 'Head') was not considered as experiments using most organic-aqueous systems in J-type CCC showed this to give lower stationary phase retention [Sutherland *et al.*, 2000a].

.

3.2.2 Determination of S_f values as a function of phase system and CCC operations

S_f values were measured for each of the phase systems shown in Table 3.1 over the operating ranges shown in Table 3.2. The measured values are summarized in Figures 3.1-3.5 in the form of Du plots (Section 3.1.1). Table 3.3 shows the corresponding equations in the form of linear regression and correlation coefficients for the Du plots over the range of parameters studied The interpretation of the results is presented in Sections 3.2.3-3.2.6 with regard to selection of the most appropriate phase systems and associated CCC operating parameters.

Phase and System Physical Properties	PEG 300 (18 % w/w): potassium phosphate (18 % w/w)	PEG 600 (18 % w/w): potassium phosphate (18 % w/w)	PEG 1000 (18 % w/w): potassium phosphate (18 % w/w)
Density Upper phase (ρ_1 – kg.m^{-3})	1000	1020	1030
Density Lower phase (ρ_2 – kg.m^{-3})	1150	1160	1160
Density difference (ρ_2-ρ_1, kg.m^{-3})	150	140	130
Density ratio (ρ_2/ρ_1)	1.15	1.14	1.13
Viscosity Upper phase (η_1 – mPa.s)	5.23	10.73	18.3
Viscosity Lower phase (η_2 – mPa.s)	1.41	2.52	2.14
Viscosity difference (η_2- η_1, mPa.s)	3.82	8.21	16.16
Viscosity ratio (η_2/η_1)	0.27	0.24	0.12
Kinematic viscosity ratio ($\eta_2\rho_1/\rho_2\eta_1$)	0.24	0.21	0.11
Interfacial tension (mN.m^{-1})	<1[19]	1.45	2.76
Settling times (t_s – s)	90	70	51

Table 3.1: Physical properties of the phase systems used in this work. Density, viscosity, interfacial tension and settling times determined as described in Sections 2.7.7, 2.7.7, 2.7.8 and 2.5.2 respectively. All measurements performed at 22°C. Interfacial tension for PEG 300 ATPS taken from [Albertsson, 1986].

Column volume (mL)	Mobile phase flow rates (mL.min^{-1})	Mobile phase pumping orientation	Rotational speed (rpm)
92.3 or 167.2	0.5-2	'Tail' to 'Head' or 'Head' to 'Tail'	500-850

Table 3.2: Range of parameters used to study Du plots of PEG-Potassium phosphate systems.

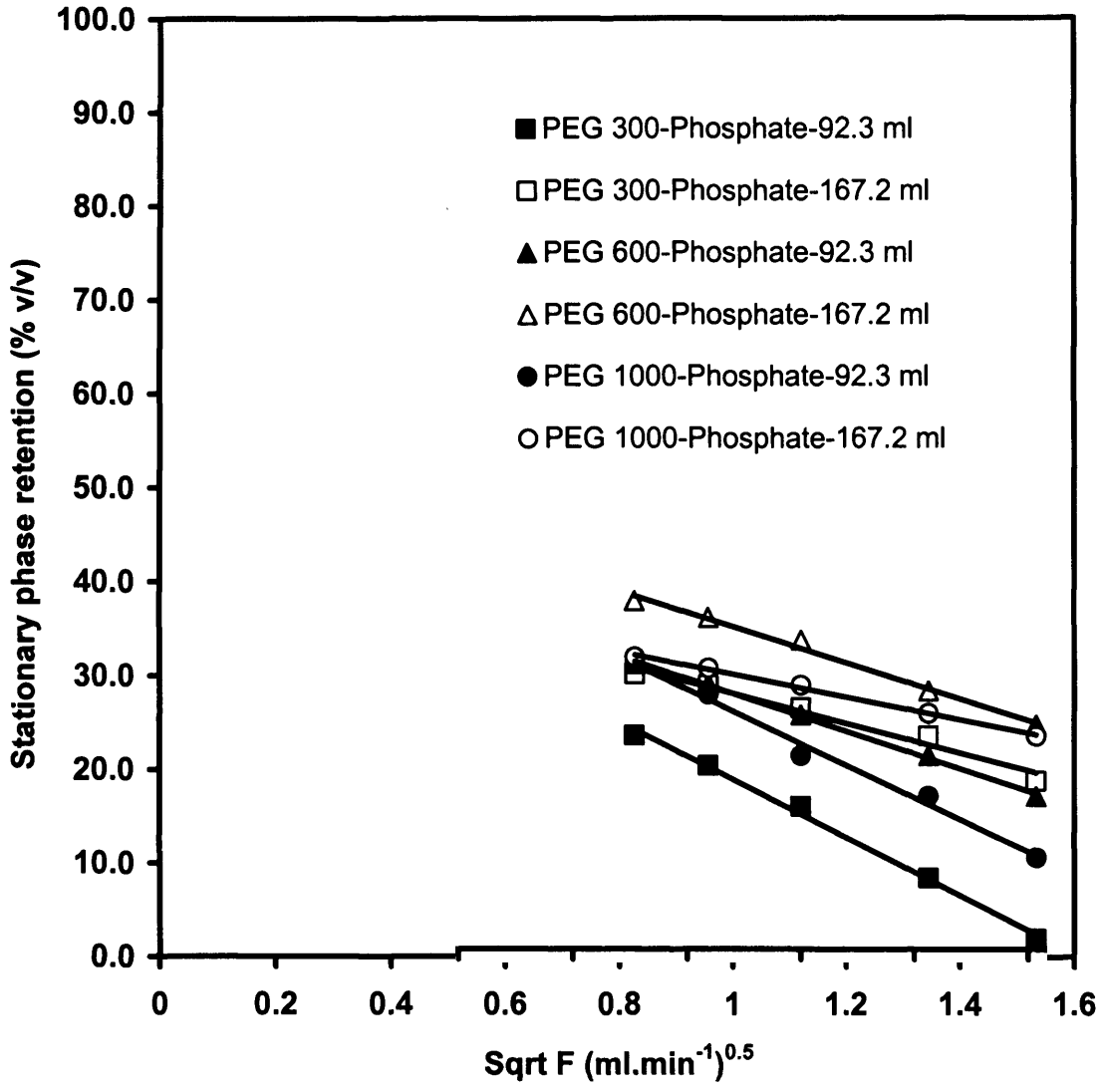

Figure 3.1. Measured stationary phase retention for various PEG molecular weights against square root of mobile phase flow rate (0.5-2.0 mL.min^{-1}) using column volumes of 92.3 mL (closed symbols) and 167.2 mL (open symbols). Rotational speed: 600 rpm. Mobile phase: K_2HPO_4 (18% w/w). Stationary phase: PEG (18% w/w). Direction: HEAD→TAIL. Phase systems prepared and experiments performed as described in Sections 2.6.2 and 2.6.4 respectively. The solid lines are the best fit linear regression as summarized in Table 3.3.

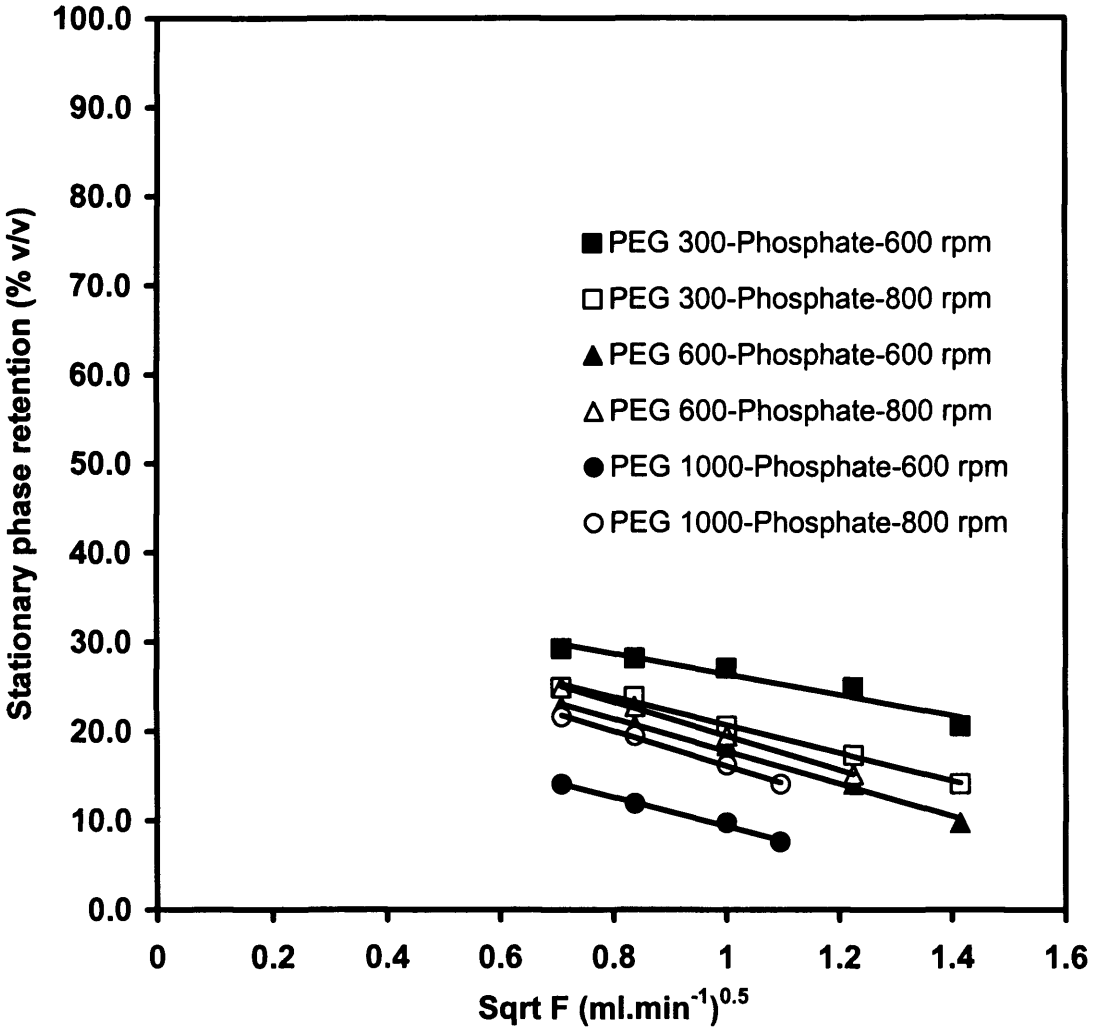

Figure 3.2. Measured stationary phase retention for various PEG molecular weights against square root of mobile phase flow rate (0.5-2.0 mL.min^{-1}) using a column volume of 92.3 mL and rotational speeds of 600 rpm (closed symbols) and 800 rpm (open symbols). Mobile phase: PEG (18% w/w). Stationary phase: K_2HPO_4 (18% w/w). Direction: HEAD→TAIL. Phase systems prepared and experiments performed as described in Sections 2.6.2 and 2.6.4 respectively. The solid lines are the best fit linear regression as summarized in Table 3.3.

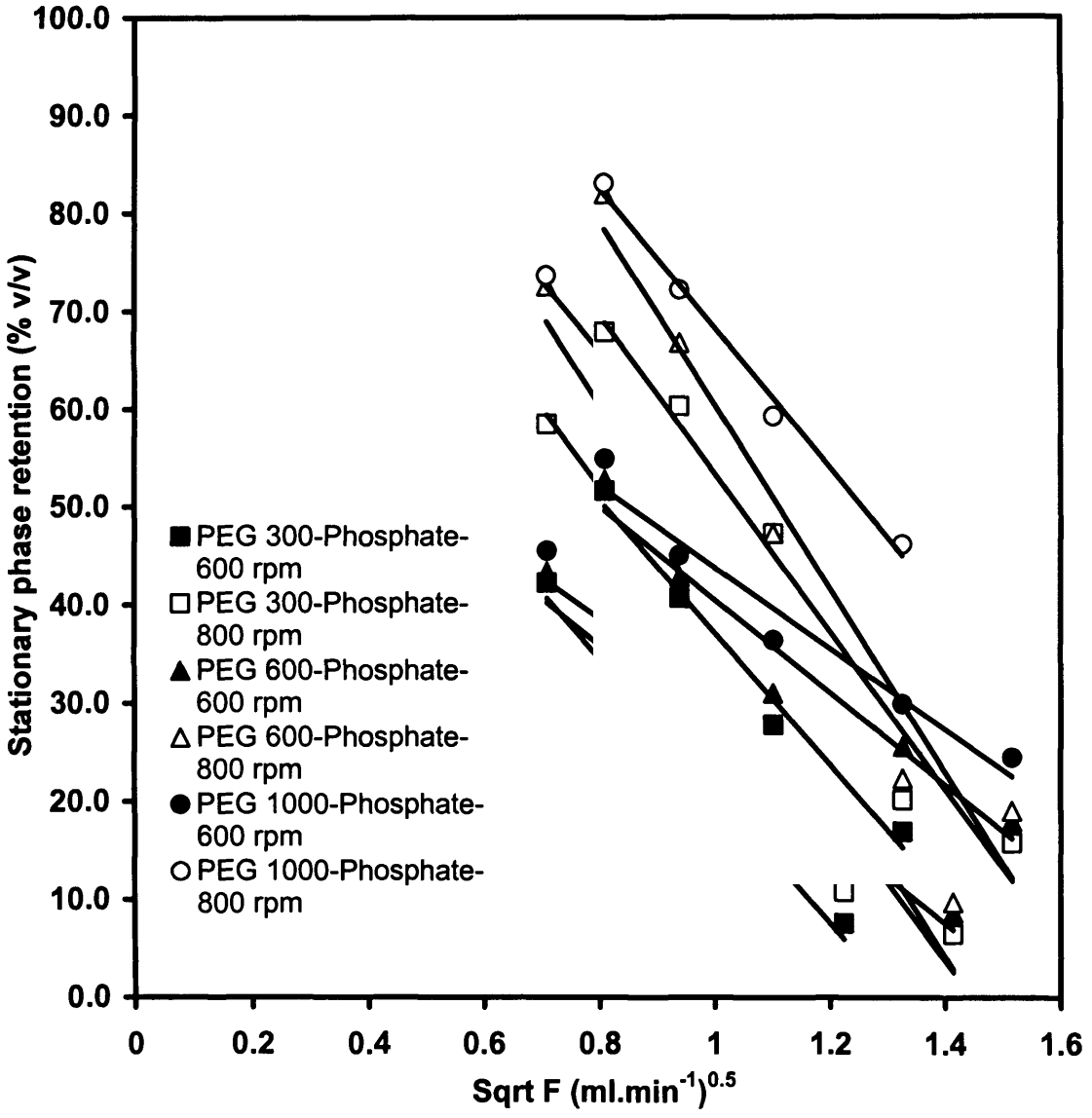

Figure 3.3. Measured stationary phase retention for various PEG molecular weights against square root of mobile phase flow rate (0.5-2.0 mL.min^{-1}) using column volumes of 92.3 mL and rotational speeds of 600 rpm (closed symbols) and 800 rpm (open symbols). Mobile phase: K_2HPO_4 (18% w/w). Stationary phase: PEG (18% w/w). Direction: TAIL→HEAD. Phase systems prepared and experiments performed as described in Sections 2.6.2 and 2.6.4 respectively. The solid lines are the best fit linear regression as summarized in Table 3.3.

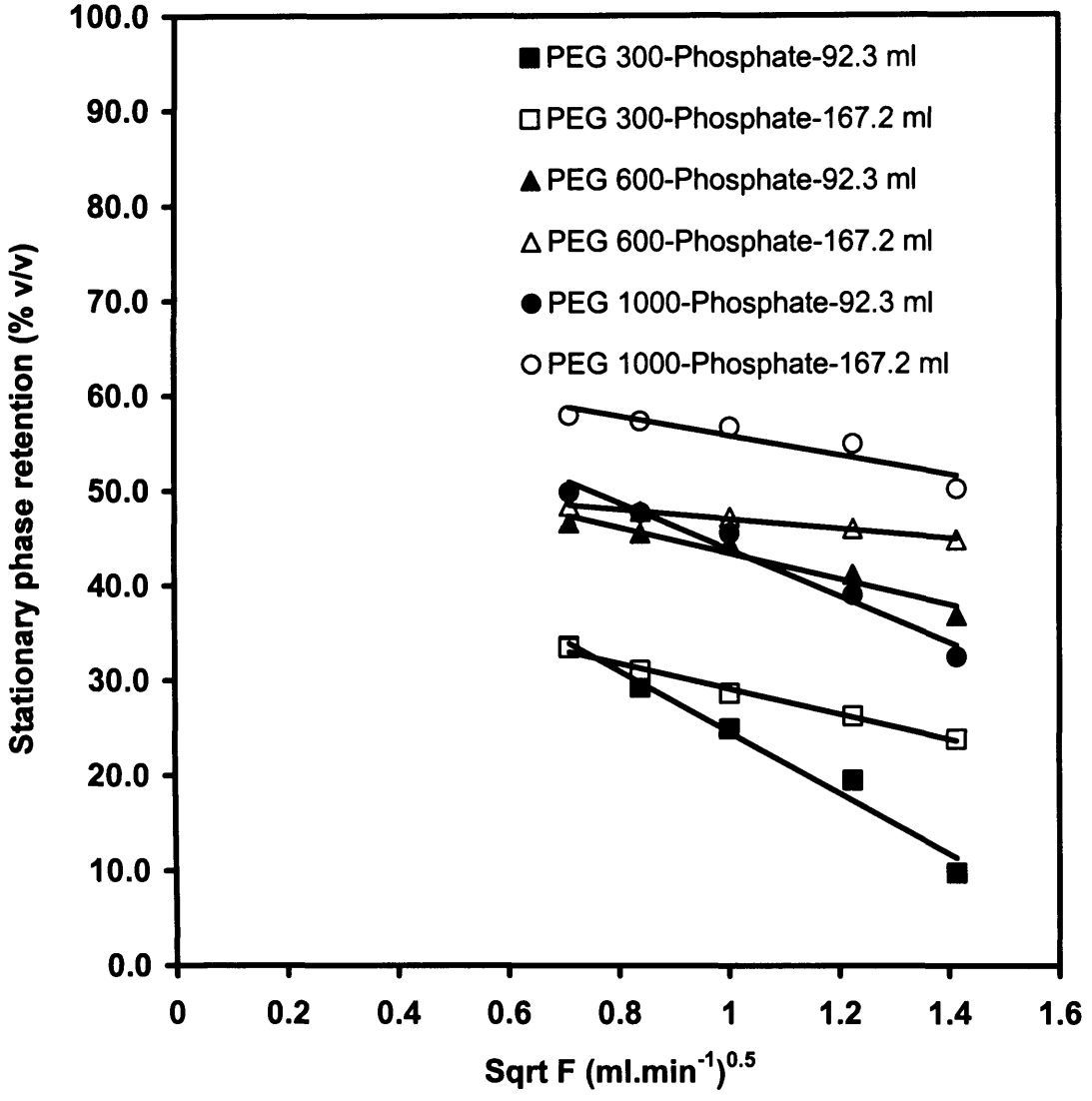

Figure 3.4. Measured stationary phase retention for various PEG molecular weights against square root of mobile phase flow rate (0.5-2.0 mL.min^{-1}) using column volumes of 92.3 mL (closed symbols) and 167.2 mL (open symbols). Rotational speed: 800 rpm. Mobile phase: K_2HPO_4 (18% w/w). Stationary phase: PEG (18% w/w). Direction: HEAD→TAIL. Phase systems prepared and experiments performed as described in Sections 2.6.2 and 2.6.4 respectively. The solid lines are the best fit linear regression as summarized in Table 3.3.

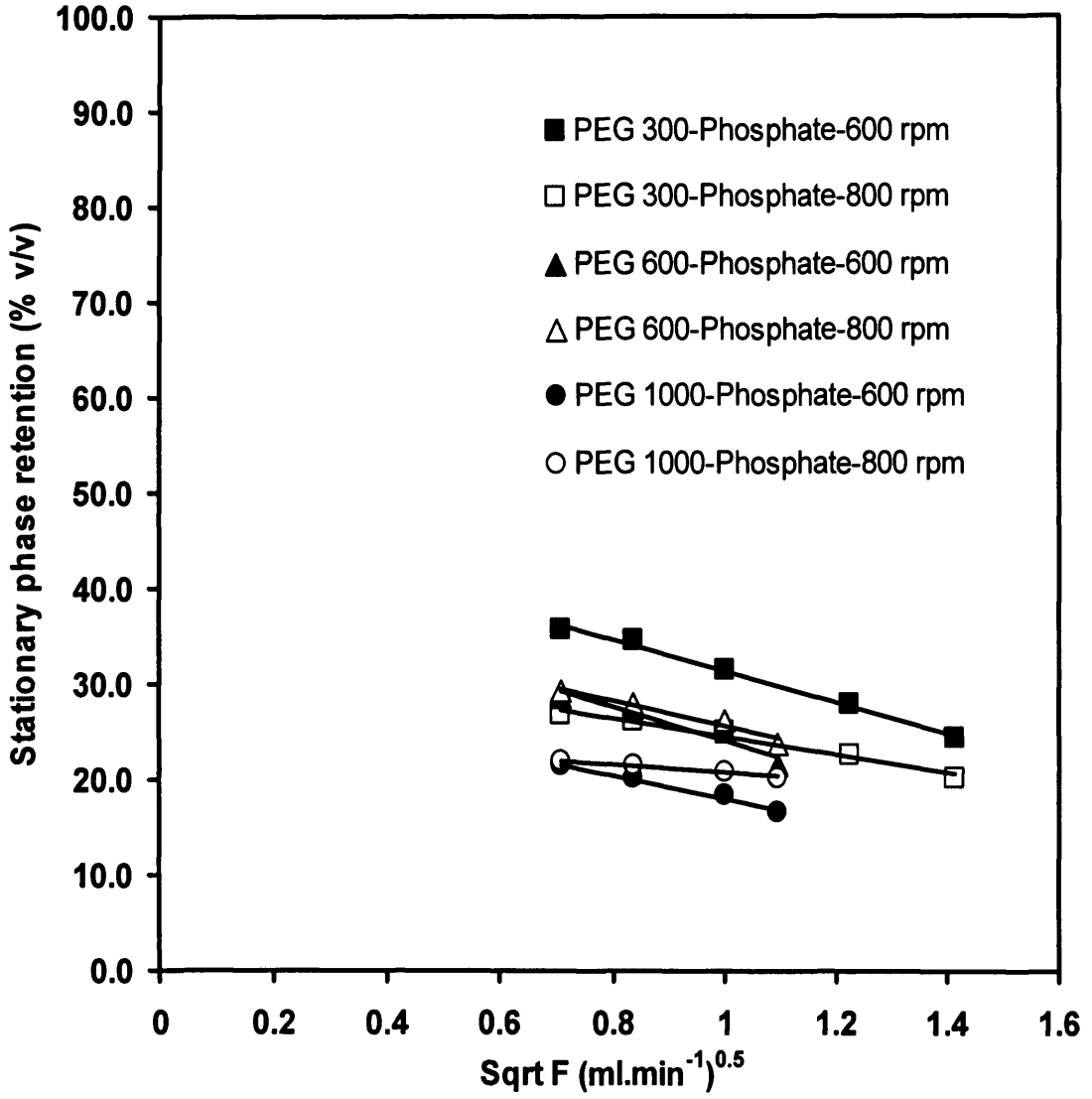

Figure 3.5. Measured stationary phase retention for various PEG molecular weights against square root of mobile phase flow rate (0.5-2.0 mL.min^{-1}) using column volumes of 167.2 mL and rotational speeds of 600 rpm (closed symbols) and 800 rpm (open symbols). Mobile phase: PEG (18% w/w). Stationary phase: K_2HPO_4 (18% w/w). Direction: HEAD→TAIL. Phase systems prepared and experiments performed as described in Sections 2.6.2 and 2.6.4 respectively. The solid lines are the best fit linear regression as summarized in Table 3.3.

3.2.3 Choice of phase system and mobile phase

For the PEG 300 system, a higher S_f was achieved when the upper PEG phase was pumped from Head (centre)→Tail (periphery) at a rotational speed of 600 rpm as opposed to the lower salt phase being pumped in the same direction (compare Figures 3.1 and 3.2). This is the opposite behaviour generally seen with organic-aqueous systems [Sutherland *et al.*, 2000a]. Very low density, high viscosity and low interfacial tension differences exist between the phases used here as indicated in Table 3.1. These result in longer phase settling times compared to organic-aqueous systems where settling times are usually less than 30 seconds [Oka *et al.*, 1991]. The results for the PEG 300 system show similarity to Ito's [Ito, 1992; Ito, 1984a; Ito, 1984b] hydrophilic phase systems (butanol-water) which also have a relatively high viscosity and setting time greater than 30 seconds. The results also show similarity to previous research on hydrophilic and intermediate organic-aqueous systems [Ito, 1992; Ito, 1984a; Ito, 1984b] and heptane-ethyl acetate-methanol-water phase systems with density ratios of less than 1.15 [Sutherland *et al.*, 2000a]. In general, PEG 300 is preferably used as the mobile phase since it results in higher S_f values at higher flow rates and any rotational speed compared to the use of a mobile salt phase (compare Figures 3.2 and 3.3) . This rule only applies to PEG 300 systems.

For the PEG 600 and PEG 1000 systems, using the upper PEG phase as the mobile phase results in lower S_f values, compared to a mobile salt phase due to the high viscosities of the PEG phases. This makes the use of the higher molecular weight PEG phases as a mobile phase undesirable (compare Figures 3.1 and 3.2) and suggests that when operating the J-type CCC devices using either PEG 600 or 1000 systems, it is desirable to use the lower salt phase as the mobile phase.

3.2.4 Effect of mobile phase pumping orientation

The effects of pumping direction of the mobile phase on S_f were examined. Section 1.7.3 showed that the choice of mobile phase pumping direction was an important parameter and greatly affected S_f values. For PEG 300, pumping the upper PEG phase from Tail→Head resulted in no retention (results not shown) which again suggests reversed phase distribution behaviour compared to most organic-aqueous phase

systems [Sutherland *et al.*, 2000a; Ito, 1992]. In addition, pumping the lower salt phase from Tail→Head greatly improves retention for low flow rates (S_f= 42.3 % v/v, Figure 3.3). For PEG 300 systems at lower rotational speeds (600 rpm), pumping the PEG phase as the mobile phase from the Head→Tail direction (Figure 3.2) would be the best system to use since pumping the salt phase from the Tail→Head direction results in a rapid decrease in S_f values with an increase in flow rate (Figure 3.3). These findings are in agreement with those for PEG 1000-phosphate systems used in single-spiral disks [Ito *et al.*, 2003].

Results for PEG 600 and PEG 1000 systems (Figure 3.3) show that the heavy salt phase prefers moving towards the Head (centre) end of the coil. Surprisingly, with these systems very high retentions were achieved, depending on the pumping orientation of the mobile phase, which are comparable to those for organic-aqueous systems [Booth *et al.*, 2003]. In Section 3.2.3, it was recommended to use the salt phase as the mobile phase. Therefore it can be seen that to achieve maximum retention, the lower mobile phase should be pumped in a Tail→Head orientation (Figure 3.3). Pervious research using single-spiral disk J-type devices also yielded the best retention with this pumping orientation [Ito *et al.*, 2003].

Finally, the improvement in retention obtained when pumping the heavy salt phase towards the Head end rather than the Tail end for larger molecular weight PEG systems (600 and 1000) is not as great as for PEG 300 systems. It seems that systems with higher settling times and lower viscosity differences such as PEG 300 systems will have a direct effect on retention, making the choice of whether to pump the mobile lower phase towards the Head or Tail of greater importance.

3.2.5 Effect of rotational speed and column volume

The effects of rotational speed on S_f were studied for the three ATPS described in Table 3.1. An increase in rotational speed from 600 to 800 rpm generally increases S_f, when the upper phase is chosen as the mobile phase due to an increase in the 'g' field [Ignatova and Sutherland, 2003]. When PEG 300 was used as the mobile phase however (Figures 3.2 and 3.5), S_f values were seen to decrease with increasing rotational speeds which could be a result of emulsification [Sibusawa and Ito, 1991].

For all other cases (compare Figures 3.1 and 3.4), an increase in rotational speed increased stationary phase retention, with the highest increases obtained when the lower salt phase was pumped in the Tail→Head direction (Figure 3.3).

The effect of increasing column volume on S_f was also tested and shown to result in an increase in stationary phase retention (compare Figures 3.1 and 3.5) regardless of the choice of mobile phase or pumping direction. An improvement in retention with column volume using longer tube length while keeping the bore size constant using ATPS was previously seen with different CCC devices using aqueous-aqueous systems [Shinomiya *et al.*, 2003; Shibusawa *et al.*, 1997; Shibusawa *et al.*, 1995; Shibusawa and Ito, 1991]. Increasing flow rate when both higher rotational speeds (800 rpm) and column volumes (167.2 ml) were used (compare open symbols in Figure 3.1 and Figure 3.4) did not significantly decrease S_f values to such a great extent in all phase systems. This might indicate that there is a lower dependence of S_f on the phase physico-chemical properties. Higher rotational speeds were previously seen to be less dependant on phase system parameters for organic-aqueous systems [Fedetov and Thiébaut, 1998]

3.2.6 Du plot analysis of S_f data

The relationship between S_f and F_C proposed by Du *et al.* [1999], and described in section 3.1.1 has previously been successfully applied to organic-aqueous systems but has not been extensively tested on aqueous-aqueous phase systems. The regression analysis between $\sqrt{F_C}$ and S_f for the data presented in Figures 3.1-3.5 is summarised in Table 3.3. Certain experiments were performed in triplicate and the maximum coefficient of variance for the calculation of S_f was 3%. Both A and B terms determined from Du plots had a maximum coefficient of variance of 2%. When the mobile phase was pumped in the Head→Tail direction, all the correlation coefficients were found to be greater than 0.96. This indicates that the linear relationship between $\sqrt{F_C}$ and S_f can be applied to PEG-phosphate systems. When the mobile phase was pumped in the Tail→Head direction, the linearity of the curves was limited to S_f values above 20% (Figures 3.6 and 3.3).

The results presented by Du *et al.* [1999] show that the intercept of the vertical axis (A term in Equation 3.1) for most solvent systems tested is close to 100% at zero flow. However, this is not found to be the case for PEG-salt aqueous-aqueous systems (Table 3.3). For PEG 600 and PEG 1000 systems, pumping the lower salt phase from Head→Tail resulted in A values of approximately 50%. When the upper phase was pumped in Head→Tail direction, the A values decreased to 25-40%. The large discrepancy in A terms was not due to the exclusion of the extra coil volume [Wood *et al.*, 2003b] in calculations of the stationary phase retention as addition of this volume to the dead volume did not change S_f significantly (results not shown). Interestingly, when the heavy lower phase is pumped in the Tail→Head direction, the values of A and B increased greatly, with the A value much closer to 100%. Du [Du *et al.*, 1999] states that A indicates the difference in the solvent composition as described in Section 3.1.1. From the results presented here, it can be seen that the A term is instead affected by all parameters tested and most significantly by the mobile phase pumping orientation. A possible explanation for this could be due to the different physical properties of ATPS compared to the solvent systems used previously. At higher rotational speeds (800 rpm), the A values become greater than 100 when the mobile phase is pumped from Tail→Head which is similar to Du's results for ethyl acetate-water (10:10) where the A coefficient is 132.59 [Du *et al.*, 1999] . This system has a small density difference (<40 $kg.m^{-3}$) compared to the other organic-aqueous solvent systems used and is similar to the PEG-phosphate systems used here (Table 3.1). For comparison, the results by other authors [Lei and Hsu, 1992; Shibusawa and Ito, 1991] using aqueous-aqueous phase systems in different CCC designs have been analysed and plotted according to Equation 3.1. The regression analysis for these is presented in Table 3.4. Again these results show A ≠ 100 % indicating that the behaviour is specific to aqueous two-phase systems.

The gradient of the Du relationship, the B term in Equation 3.1, represents the sensitivity of the stationary phase retention to the mobile phase flow rate. The steeper the gradient, the more sensitive the retention is to the mobile phase flow rate. Pumping the lower mobile phase in the Tail→Head results in much higher (negative) B values demonstrating that the mobile phase pumping orientation greatly affects S_f. Higher B values were also obtained for the smaller column volume and lower rotational speed meaning retention is more sensitive to flow rates in these cases. Du

reported that the B term may also indicate the difference in the phase volume ratio [Du *et al.*, 1999]. Tests using different volume ratios (Table 3.6, Figure 3.6) showed that B is indeed affected by volume ratio, however other parameters such as mobile phase pumping direction and rotational speeds were also seen to affect the coefficient. In Figure 3.6, the Du plot was not plotted using linear lines to emphasis the non-linearity of the plots below 20% for systems that used the 'Tail' to 'Head' pumping orientation.

System	Mobile phase	Volume (ml)	Speed (rpm)	Direction	Equation of linear regression	Coefficient (R^2)
PEG 300 (18 % w/w)-potassium phosphate (18 % w/w)						
	Lower	92.3	600	H→T	$S_f = 45.18 - 30.84\sqrt{F_C}$	0.996
	Lower	92.3	800	H→T	$S_f = 56.93 - 32.55\sqrt{F_C}$	0.989
	Upper	92.3	600	H→T	$S_f = 38.08 - 12.07\sqrt{F_C}$	0.988
	Upper	92.3	800	H→T	$S_f = 36.41 - 15.69\sqrt{F_C}$	0.994
	Lower	167.2	600	H→T	$S_f = 41.01 - 15.74\sqrt{F_C}$	0.973
	Lower	167.2	800	H→T	$S_f = 42.28 - 13.15\sqrt{F_C}$	0.999
	Upper	167.2	600	H→T	$S_f = 47.86 - 16.36\sqrt{F_C}$	0.994
	Upper	167.2	800	H→T	$S_f = 33.98 - 9.42\sqrt{F_C}$	0.977
	Lower	92.3	600	T→H	$S_f = 88.12 - 67.09\sqrt{F_C}$	0.982
	Lower	92.3	800	T→H	$S_f = 116.22 - 80.35\sqrt{F_C}$	0.967
PEG 600 (18 % w/w)-potassium phosphate (18% w/w)						
	Lower	92.3	600	H→T	$S_f = 44.68 - 19.90\sqrt{F_C}$	0.998
	Lower	92.3	800	H→T	$S_f = 56.92 - 13.94\sqrt{F_C}$	0.991
	Upper	92.3	600	H→T	$S_f = 35.93 - 18.15\sqrt{F_C}$	0.991
	Upper	92.3	800	H→T	$S_f = 38.47 - 18.99\sqrt{F_C}$	0.999
	Lower	167.2	600	H→T	$S_f = 51.07 - 19.09\sqrt{F_C}$	0.991
	Lower	167.2	800	H→T	$S_f = 52.02 - 5.01\sqrt{F_C}$	0.991
	Upper	167.2	600	H→T	$S_f = 41.10 - 16.98\sqrt{F_C}$	0.969
	Upper	167.2	800	H→T	$S_f = 39.33 - 13.88\sqrt{F_C}$	0.983
	Lower	92.3	600	T→H	$S_f = 73.58 - 47.12\sqrt{F_C}$	0.953
	Lower	92.3	800	T→H	$S_f = 135.03 - 93.48\sqrt{F_C}$	0.956
PEG 1000 (18 % w/w)-potassium phosphate (18% w/w)						
	Lower	92.3	600	H→T	$S_f = 53.27 - 30.91\sqrt{F_C}$	0.984
	Lower	92.3	800	H→T	$S_f = 67.84 - 24.26\sqrt{F_C}$	0.983
	Upper	92.3	600	H→T	$S_f = 35.64 - 16.16\sqrt{F_C}$	0.991
	Upper	92.3	800	H→T	$S_f = 25.54 - 19.52\sqrt{F_C}$	0.997
	Lower	167.2	600	H→T	$S_f = 39.79 - 12.02\sqrt{F_C}$	0.996
	Lower	167.2	800	H→T	$S_f = 65.49 - 10.04\sqrt{F_C}$	0.974
	Upper	167.2	600	H→T	$S_f = 30.17 - 12.03\sqrt{F_C}$	0.979
	Upper	167.2	800	H→T	$S_f = 25.23 - 4.46\sqrt{F_C}$	0.991
	Lower	92.3	600	T→H	$S_f = 71.58 - 41.25\sqrt{F_C}$	0.956
	Lower	92.3	800	T→H	$S_f = 128.76 - 78.03\sqrt{F_C}$	0.991

Table 3.3: Regression analysis between $\sqrt{F_C}$ and S_f of PEG- phosphate systems of the data presented in Figure 3.1-3.5. H-Head, T-Tail.

CCC design	Phase system	β	speed (rpm)	Vol. (ml)	Equation of linear regression	Coefficient (R^2)	Reference
Eccentric multi-layer CCC	PEG 1000 (12.5% w/w)-K_2HPO_4 (12.5% w/w)	0.44	600	430	$S_f = 50.36 - 16.51\sqrt{F_C}$	0.987	Lei & Hsu, 1992
Horizontal CPC	PEG 3400 (10.1 % w/w)-K_2HPO_4 (10.9 % w/w)	0.3	750	250	$S_f = 74.73 - 20.8\sqrt{F_C}$	0.987	Shibusawa & Ito. 1991

Table 3.4: Du plots analysis showing equation of the linear regression and correlation coefficient of previous literature studies using PEG-phosphate aqueous two-phase systems in different CCC machines. The β value is defined as the radial distance (r) between the centre of the coil divided by the radial distance (R) between the centre of the sun gear and the planet gear as described in Section 1.7.2.2.

Volume ratio	Composition (% w/w)	Volume (ml)	Speed (rpm)	Direction	Equation of linear regression	Coefficient (R^2)
PEG 300 -potassium phosphate						
0.3	10/25	92.3	600	T→H	$S_f = 85.97 - 63.08\sqrt{F_C}$	0.863
2.14	30/15	92.3	600	T→H	$S_f = 115.5 - 87.24\sqrt{F_C}$	0.95
PEG 600-potassium phosphate						
0.33	10/25	92.3	600	T→H	$S_f = 88.22 - 58.56\sqrt{F_C}$	0.822
1.71	30/15	92.3	600	T→H	$S_f = 79.19 - 50.48\sqrt{F_C}$	0.847

Table 3.5. Regression analysis between $\sqrt{F_C}$ and S_f of PEG- phosphate systems (Figure 3.6) using different compositions of PEG and potassium phosphate resulting in different volume ratios. Mobile phase: K_2HPO_4. Stationary phase: PEG. Experiments performed as described in Section 2.6.4. H= Head, T= Tail. V_R is calculated as described in Section 2.5.1.

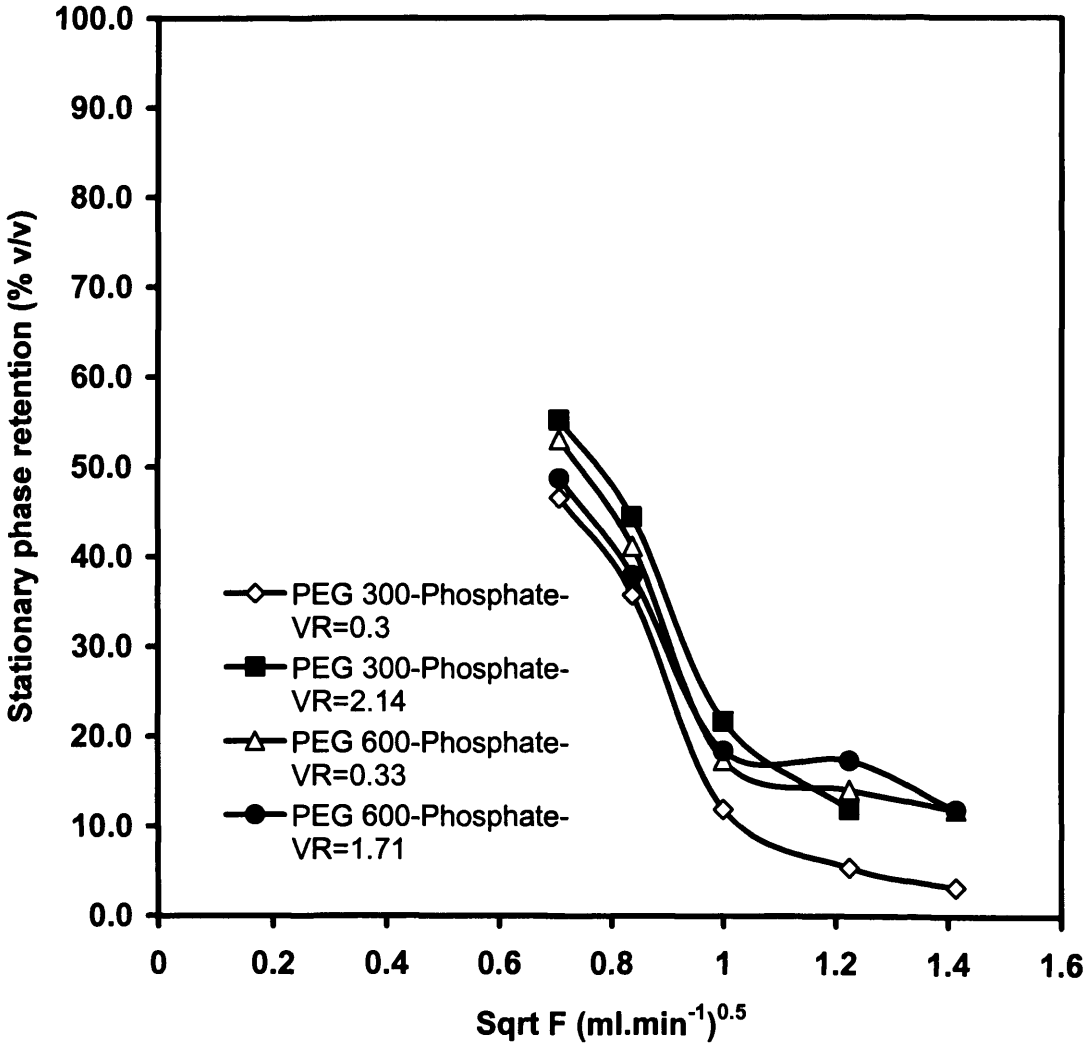

Figure 3.6. Measured stationary phase retention for various PEG molecular weights and phase volume ratios (V_R) against square root of mobile phase flow rate (0.5-2.0 mL.min^{-1}) using a column volume of 92.3 ml. Rotational speed: 600 rpm. Mobile phase: K_2HPO_4. Stationary phase: PEG. Direction: TAIL→HEAD. V_R is calculated as described in Section 2.5.1, while phase systems prepared and experiments performed as described in Sections 2.6.2 and 2.6.4 respectively

3.2.7 Prediction of S_f at different rotational speeds

Sutherland's [2000b] relationship between the stationary phase retention and the linear velocity of the mobile phase as described in Section 3.1.2 will not be considered as the equation relating the mobile phase flow to the kinetic energy term in the Bernoulli's equation is based on the equation of linearity and intercepts of Du plots. Sutherland [2000b] used the same organic-aqueous systems as Du [Du *et al.*, 1999], and the equation is based on the assumption that the y-intercept of Du plots are 100% at zero flow rate, i.e. The stationary phase is fully retained when no mobile phase is pumped through the column. As seen in the pervious section and from Figures 3.1-3.5, the y-intercept (A term) is not 100% for all of the aqueous-aqueous systems used, thus Sutherland's relationship is not applicable.

Equation 3.2 in Section 3.1.3 however shows that the S_f values can be predicted as a function of rotational speed from the information obtained from Du plots. In Equation 3.2, the values A and B are both used, although the authors assume the A term to be 100% as organic-aqueous systems are used. The work presented here using aqueous-aqueous systems showed this equation to be applicable when the A value of 100% was replaced by the actual value determined for the phase systems used as calculated (Figures 3.1-3.5) in Table 3.3. The measured data and the prediction from the S_f versus $\sqrt{F_C}$ plot gave a logarithmic relationship that is in close agreement regardless of the pumping orientation and phase systems. Figure 3.7, for example, shows a plot of S_f versus rotational speed for the PEG 600 system at a fixed flow rate of 0.5 ml.min^{-1}. When Equation 3.2 was used with the A = 100, the theoretical prediction was significantly less than found experimentally (dashed line in Figure 3.7). In contrast, when the A value was taken as 135.03 (as given in Table 3.3) very good agreement was found between experiments and predicted behaviour.

Changing the PEG molecular weight (PEG 300, Figure 3.8) or flow rate (F= 1 mL.min^{-1}, Figure 3.9) also showed a good correlation. It was also seen (results not shown) that when the chosen mobile phase was the salt phase (for PEG 600 systems), better predictions were obtained when the A value chosen from the corresponding Du plots were from higher rotational speeds (800 rpm). In contrast, when the PEG 300 phase was chosen as the mobile phase, better predictions were observed using A

values from lower rotational speeds (600 rpm). It seems that the stationary phase retention obtained has a direct influence on the predictive nature of Equation 3.2 as the best predictions are obtained at the highest stationary phase retentions. Higher S_f values were obtained at higher and lower rotational speeds when the mobile phase was chosen as the salt (for PEG 600 systems) and PEG (PEG 300 systems) phases respectively (as described in Section 3.2.5).

3.2.8 Constant pressure drop theory

The data obtained from Figures 3.1-3.5 were also used to plot (Figures 3.10-3.12) the percentage mobile phase in the coil (V_m) against the reciprocal of rotational speed ($1/w_N$) for different PEG-Salt systems. Wood *et al.*, [2003a] showed that the total pressure drop across a coil is independent of mobile phase flow rate, and that the pressure drop across a coil is constant because the mobile flow rate proportionally increases the effective cross-sectional area occupied by the mobile phase (described in Section 1.8). This results in a linear plot which means that retention is proportional to $1/w$ regardless of the PEG molecular weight used or the pumping orientations confirming Wood's hypothesis that the coil planet centrifuge behaves as a constant pressure pump for systems that use aqueous-aqueous phases. As found with Du plots for aqueous two phase systems (Section 3.2.6), the intercepts obtained from these plots differ with those of organic-aqueous system where y= ∞ at N=0 [Wood *et al.*, 2003a]. The relationships derived from organic-aqueous systems are applicable to such systems although further investigation is needed to understand the difference obtained for the intercepts of aqueous-aqueous systems.

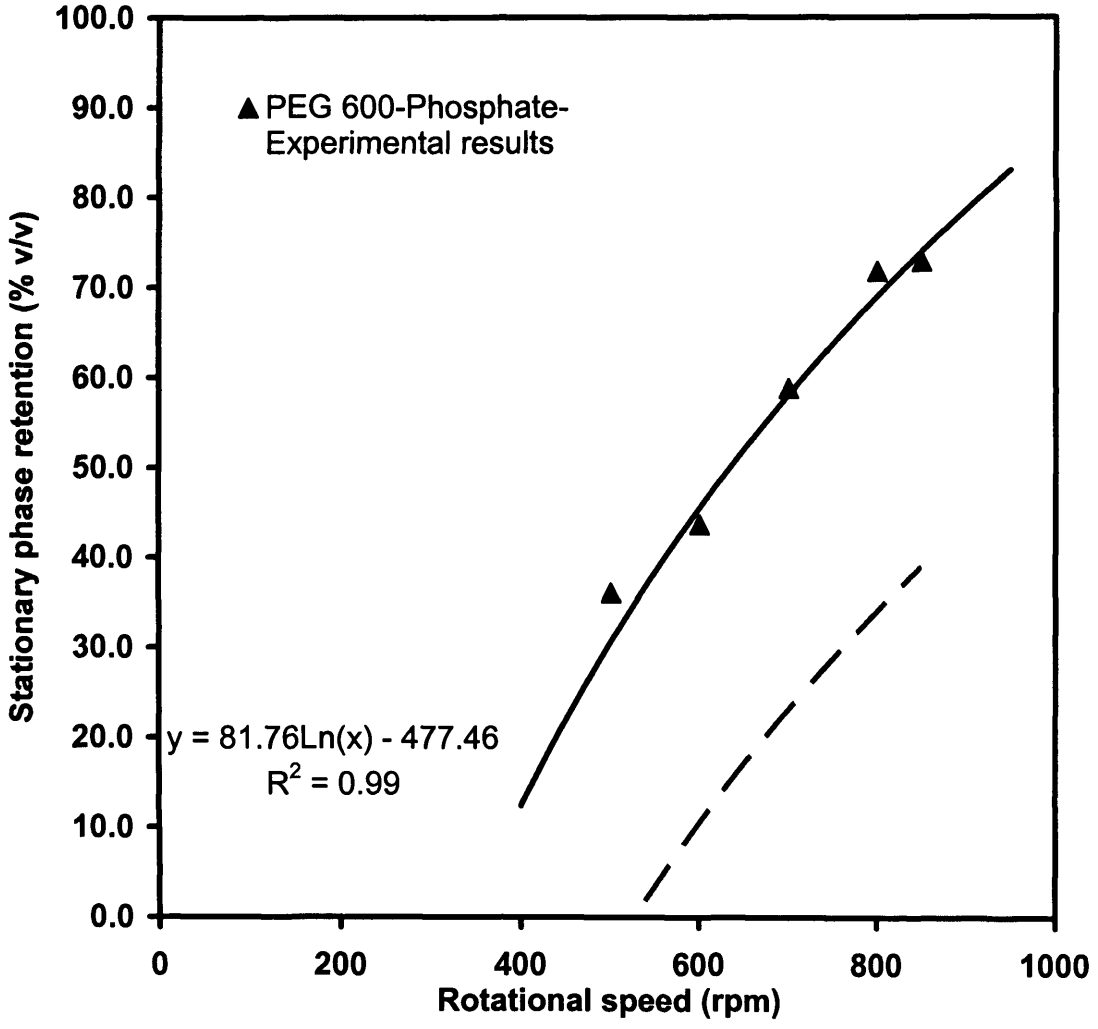

Figure 3.7: Measured and predicted stationary phase retention for a PEG 600 system against rotational speed (500-850 rpm) using a column volume of 92.3 mL. Mobile phase flow rate fixed at 0.5 mL.min^{-1}. Mobile phase: K_2HPO_4 (18% w/w). Stationary phase: PEG 600 (18% w/w). Direction: TAIL→HEAD. Experimental points as described in Section 2.6.5. Solid line predicted as described in Section 3.1.3 with A = 135.03 (from Table 3.3 at 800 rpm rotational speed). Dashed line predicted with A = 100 as proposed by Ignatova and Sutherland [2003].

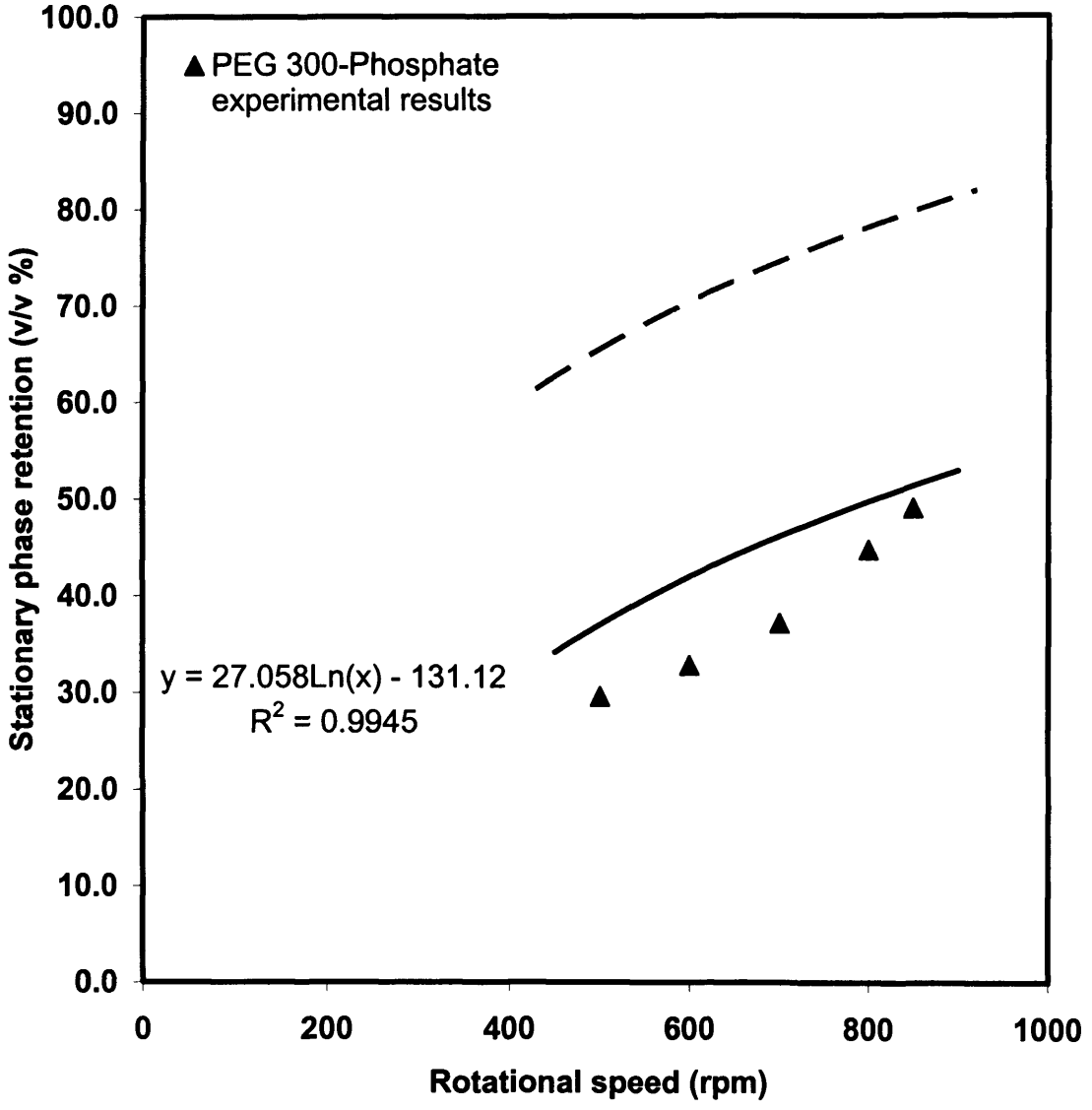

Figure 3.8: Measured and predicted stationary phase retention for a PEG 300 system against rotational speed (500-850 rpm) using a column volumes of 92.3 mL. Mobile phase flow rate fixed at 0.5 mL.min^{-1}. Mobile phase: PEG 300 (18% w/w). Stationary phase: K_2HPO_4 (18% w/w). Direction: HEAD→TAIL. Experimental points as described in Section 2.6.5. Solid line predicted as described in Section 3.1.3 with A = 38.08 (from Table 3.3 at 600 rpm rotational speed). Dashed line predicted with A = 100 as proposed by Ignatova and Sutherland [2003].

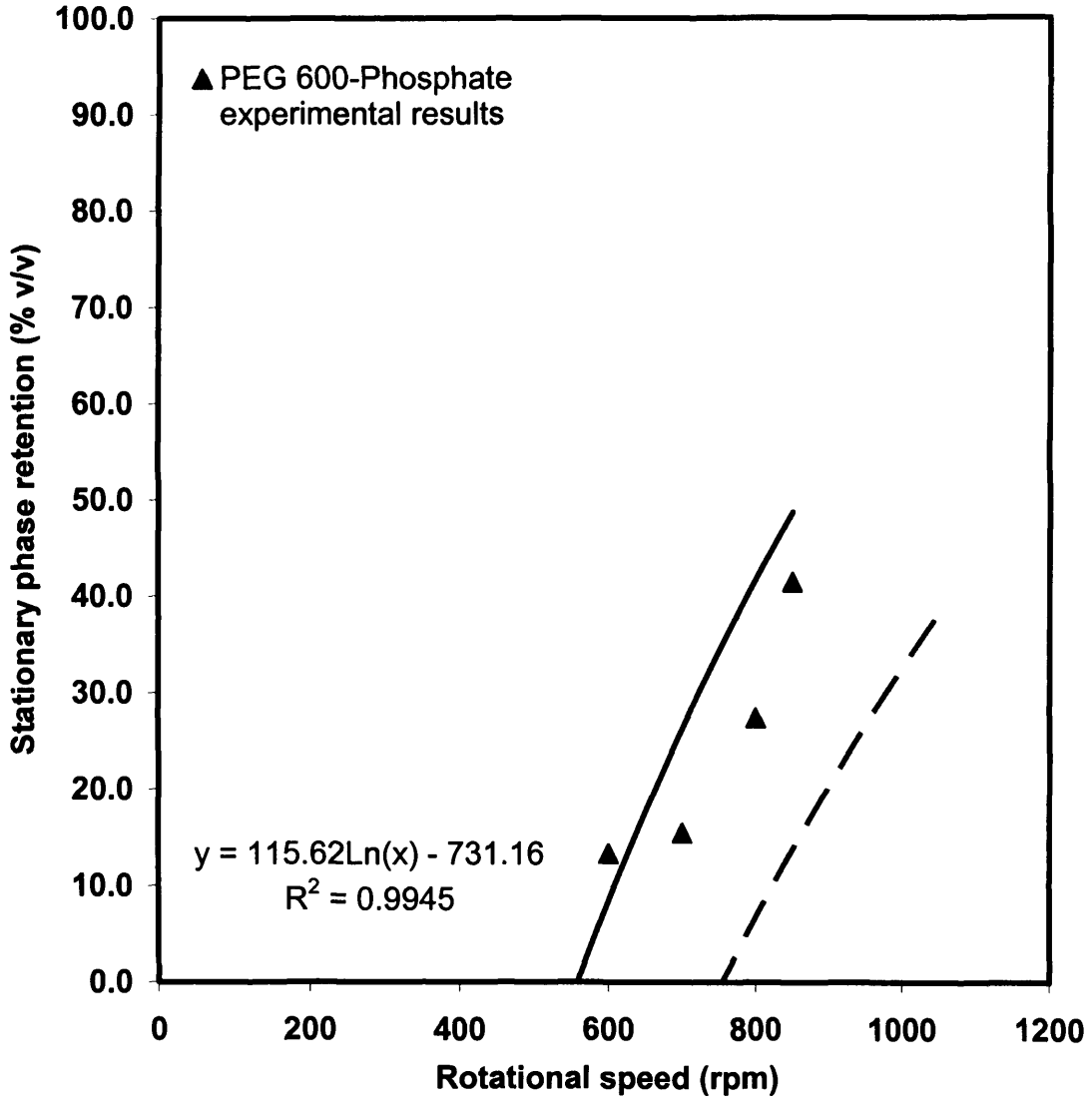

Figure 3.9: Measured and predicted stationary phase retention for a PEG 600 system against rotational speed (500-850 rpm) using a column volume of 92.3 mL. Mobile phase flow rate fixed at 1 mL.min^{-1}. Mobile phase: K_2HPO_4 (18% w/w), Stationary phase: PEG 600 (18% w/w). Direction: TAIL→HEAD. Experimental points as described in Section 2.6.5. Solid line predicted as described in Section 3.1.3 with A = 135.03 (from Table 3.3 at 800 rpm rotational speed). Dashed line predicted with A = 100 as proposed by Ignatova and Sutherland [2003].

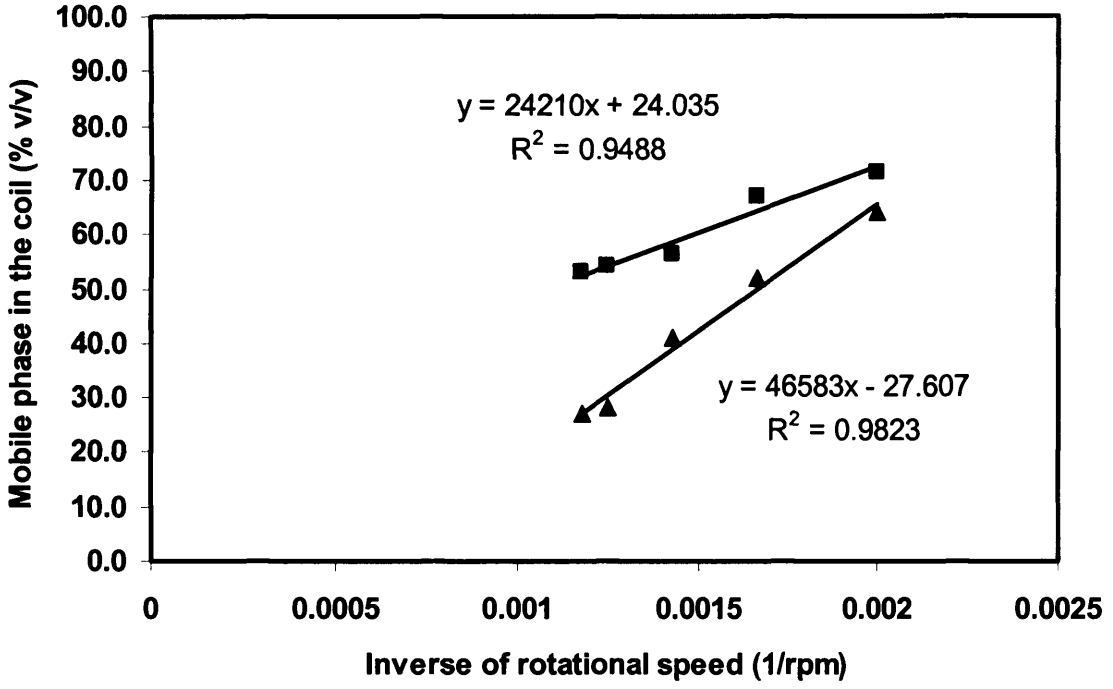

Figure 3.10: Plot of percentage mobile phase in the coil against the inverse of rotational speed for a mobile phase flow rate of 0.5 mL.min^{-1} using a column volume of 92.3 mL. Mobile phase: K_2HPO_4 (18%). Stationary phase: PEG 600 (18%). Direction: (■) HEAD→TAIL, (▲) TAIL→HEAD. The solid lines are the best fit linear regression.

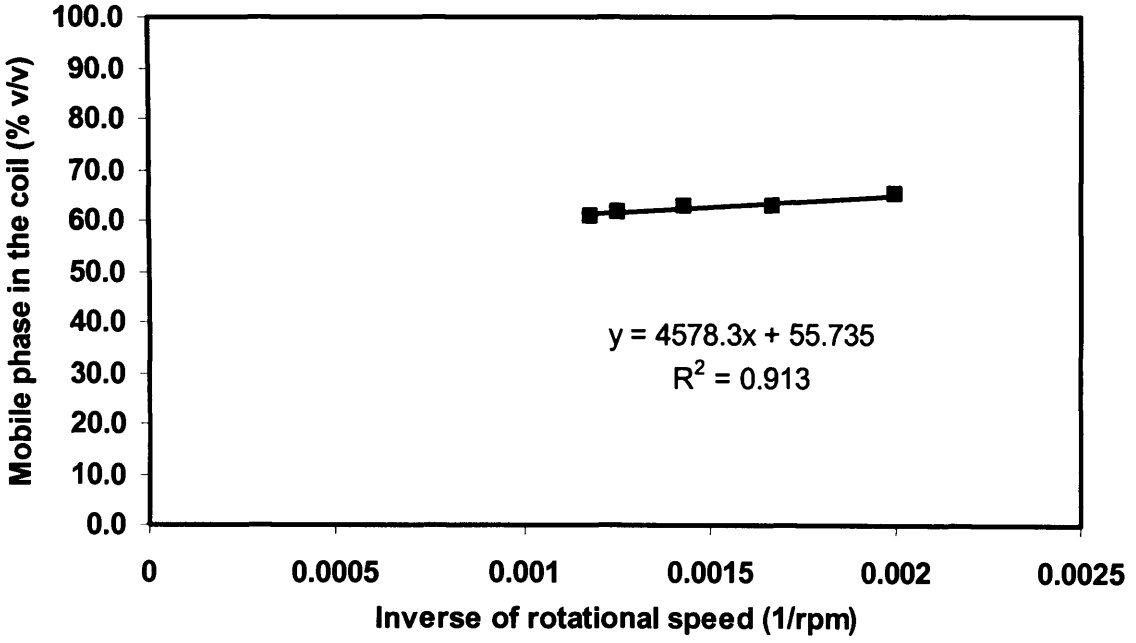

Figure 3.11: Plot of percentage mobile phase in the coil against the inverse of rotational speed for a mobile phase flow rate of 0.5 mL.min^{-1} using a column volume of 92.3 mL. Mobile phase: PEG 600 (18%). Stationary phase: K_2HPO_4 (18%). Direction: (■) HEAD→TAIL. The solid lines are the best fit linear regression.

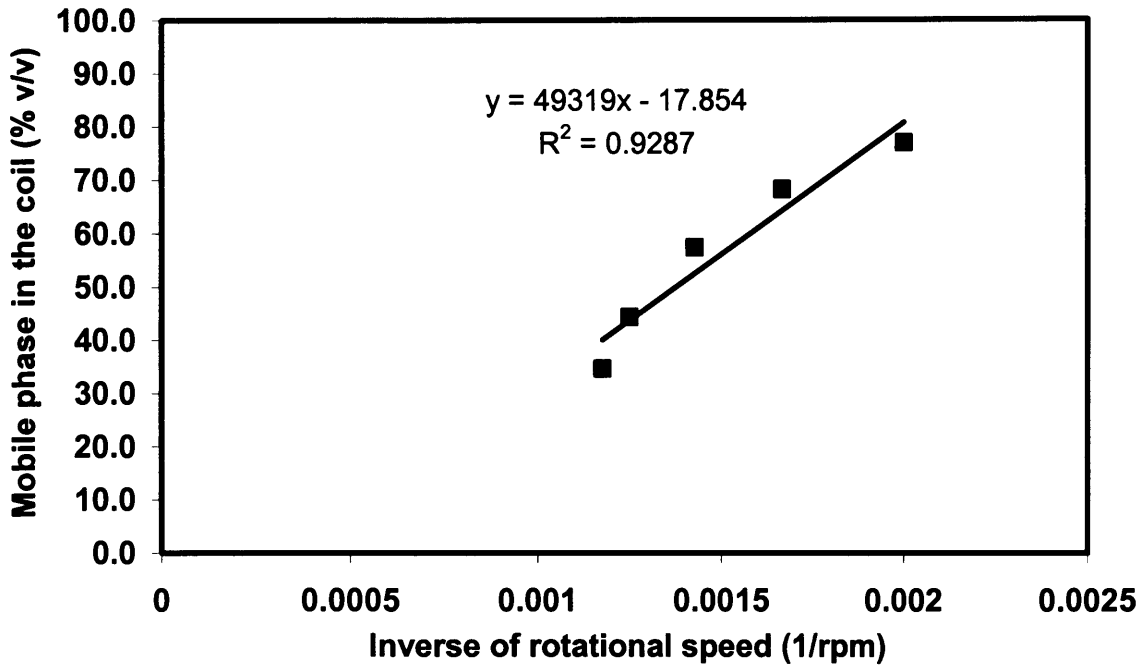

Figure 3.12: Plot of percentage mobile phase in the coil against the inverse of rotational speed for a mobile phase flow rate of 0.5 ml.min^{-1} using a column volume of 92.3 ml. Mobile phase: K_2HPO_4 (18%). Stationary phase: PEG 1000 (18%). Direction: (■) TAIL→HEAD. The solid lines are the best fit linear regression.

3.3 Discussion

As a basis for subsequent studies in the recovery and purification of plasmid DNA by CCC, this chapter has examined some original studies of the hydrodynamics of various PEG-salt aqueous-aqueous two-phase systems in a Brunel J-type countercurrent chromatograph. The initial aim was to define conditions which gave optimum S_f values. To this end, the degree of stationary phase retention, S_f, once a hydrodynamic equilibrium is achieved, is shown to be a function of mobile phase flow rate (0.5-2.0 ml.min^{-1}), coil rotational speed (500-850 rpm), column volume (92.3 and 167.3 ml), choice of mobile phase (PEG or phosphate) and mobile phase pumping direction (Head→Tail or Tail→Head). High S_f values in comparison to previous aqueous-aqueous studies with CCC [Kendall, 2002] were obtained of up to 73.7 % v/v. These high S_f values were obtained when the lower aqueous phase was pumped from Tail (periphery)→Head (centre), opposite to the direction normally recommended for most organic-aqueous systems in J-type CCC machines [Sutherland *et al.*, 2000a]. The second aim was to examine how S_f values vary with phase composition and CCC operating conditions. Three different aqueous two-phase systems (ATPS) were studied comprised of PEG 300-K_2HPO_4, PEG 600- K_2HPO_4 and PEG 1000-K_2HPO_4 having density and viscosity ratios between 1.15-1.13 and 0.27-0.12 respectively. The direction of mobile phase pumping depended on which phase was chosen as the stationary phase. For low MW PEG 300 systems, the highest S_f was achieved by pumping the mobile PEG 300 phase in the Head→Tail direction, while for the PEG 600 and 1000 system, pumping the lower salt phase in the opposite direction gives the highest retention. These conditions are favourable as plasmid DNA partitions preferentially to the PEG phase for PEG 300 systems and to the salt phase for PEG 600 and PEG 1000 ATPS [Ribeiro *et al.*, 2002]. Thus choosing the mobile phase pumping direction that gives the highest S_f values will lead to the plasmid eluting with the mobile phase during the CCC run. The reversed hydrodynamics of these ATPS is believed to be due to the high settling times and low density/high viscosity difference of aqueous-aqueous systems compared to organic-aqueous systems. Higher column volumes and rotational speeds increased S_f values. When both these parameters were increased simultaneously, an increase in flow rate did not reduce S_f values significantly indicating that there is a lower dependence of retention on the physio-chemical properties of the phases. The third aim was to establish

conditions for the prediction of S_f. Du plots of the data showed the essential linear relationship between S_f and $\sqrt{F_c}$ is applicable to aqueous-aqueous systems provided that $S_f > 20\%$. All experiments showed that y intercept $\neq 100\%$ at $F_c = 0$. The retention-rotational speed characteristics of the three phase systems studied could also be successfully predicted from the results of the corresponding Du plots (when A $\neq$ 100 where used) suggesting that the intercepts at zero mobile phase flow rate and rotational speed is due to the property of the aqueous-aqueous systems. The corresponding results also confirmed Wood's hypothesis [Wood *et al.*, 2003a] that as with organic-aqueous systems, the coil planet centrifuge behaves as a constant pressure pump for ATPS.

Thus equations used for the prediction of stationary phase retention as functions of mobile phase flow rate and rotational speed for organic-aqueous systems can be used for aqueous-aqueous systems accurately.

Chapter 4
Quantification and Optimisation of pDNA Recovery and Purification in Batch ATPS

4.1 Introduction

In the previous chapter the hydrodynamics of various ATPS in J-type CCC machines were determined as a basis for performing CCC-based pDNA separations. This chapter will consider the partitioning of pDNA, and related contaminants, in the ATPS studied earlier with a view to defining appropriate conditions for pDNA recovery and purification. Equilibrium solute partitioning in batch studies are performed because they are rapid and use the minimal amount of material given the large number of experimental variables to be investigated. Batch extraction might also probe a useful step to pre-condition the pDNA feed ultimately loaded onto the CCC column.

As described in Section 1.5.1, pervious studies on pDNA partitioning in ATPS have shown that pDNA can be partitioned to either the upper PEG phase or the lower salt phase [Ribeiro *et al.*, 2002]. Parameters already tested for pDNA partitioning include lysate loading, PEG molecular weight selection, tie-line length [Trindade *et al.*, 2005; Ribeiro *et al.*, 2002], plasmid concentration and temperature [Kune, 2002]. Further research is needed to examine the effect of other parameters, most importantly the effect of different compositions of PEG and salt (and hence volume ratios), pH and pDNA size on the partitioning behaviour of pDNA and its contaminants. These tests will help select an appropriate two-phase system for use in subsequent CCC experiments.

The overall aim of this chapter is thus to quantify and optimise pDNA recovery and purification in a batch APTS. Specific objectives are: (i) Quantify and optimise pDNA partitioning (ii) Quantify and optimise partitioning of related contaminants (iii) Define appropriate conditions/phases for subsequent CCC studies. Part of this work is being prepared as a publication: Al-Marzouqi I, Levy MS and Lye GJ. (2006).

Capture and Purification of Plasmid DNA from *Escherichia coli* Cell Lysate using Aqueous-Aqueous Countercurrent Chromatography.

4.2 Initial choice of phase systems and binodial curve construction

The general approach for choosing a suitable phase system for a particular separation is to arbitrarily examine a number of polymer-salt systems which serve to rapidly delineate the partitioning characteristics of the materials of interest [Walter *et al.*, 1985]. A large range of PEG molecular weights (PEG 200, 300, 400, 600, 1000, 8000) and salts (K_2HPO_4 and KH_2PO_4) were initially tested. Binodial curves for the different molecular weights PEGs and K_2HPO_4 are shown in Figure 4.1. Results show that increasing the molecular weight of PEG shifts the binodial curve to the left which agrees with previous literature [Kendall *et al.*, 2002]. It was also seen that when high molecular weight PEG was chosen (PEG 8000), the upper phase become very viscous and increased settling times (t_s) dramatically. PEG 8000 was thus not considered further. Other salts such as $(NH_4)_2HPO_4$, $(NH_4)_2SO_4$, NaH_2PO_4 and Na_2SO_4 were previously tested [Kendall, 2002], however K_2HPO_4 resulted in the fastest separation time. Thus K_2HPO_4 was the only component used for the salt phase. PEG 200 and PEG 400 were not selected as polymers for further studies as PEG 200-phosphate systems was previously shown to co-partition contaminants such as proteins and RNA with the product plasmid DNA, whilst PEG 400-phosphate systems partitioned the majority of the plasmid DNA to the interface [Ribeiro *et al.*, 2002].

The effect of isopropanol to increase interfacial tension, and hence increase stationary phase retention [Kendall *et al.*, 2002] was also tested. Since isopropanol and biological suspensions (clarified lysate) were to be added to the different phase systems, the effect of these on the position of binodial curve was also determined as shown in Figure 4.2 in the case of PEG 600. Figure 4.2 shows that the addition of biological suspensions and isopropanol shifted the binodial curve towards the origin i.e. the binodial curves moves to the left of the clean binodial curve. In general, the presence of complex mixtures of bio-molecules tends to disrupt the equilibrium between PEG, salt, and water and to modify the thermodynamics of the system. This increases the incompatibility between the phase chemicals, and provokes separation at

lower PEG and salt concentrations [Lebreton *et al.*, 2002; Rito-Palomares and Cueto, 2000; Köhler *et al.*, 1989]

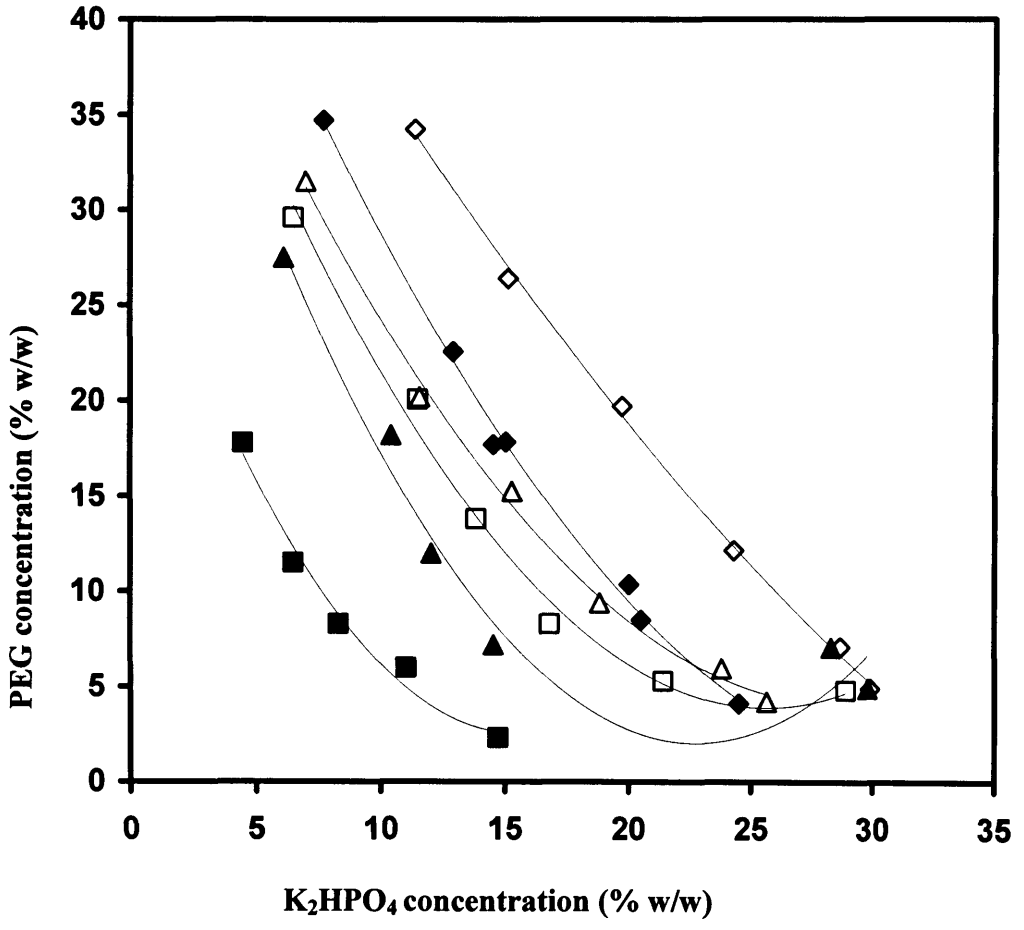

Figure 4.1: Binodial curves for a range of phase systems- PEG 200-K_2HPO_4 (◊); PEG 300-K_2HPO_4 (♦); PEG 400-K_2HPO_4 (Δ); PEG 600-K_2HPO_4 (□); PEG 1000-K_2HPO_4 (▲); PEG 8000-K_2HPO_4 (■). Experiments performed as described in Section 2.5.3.

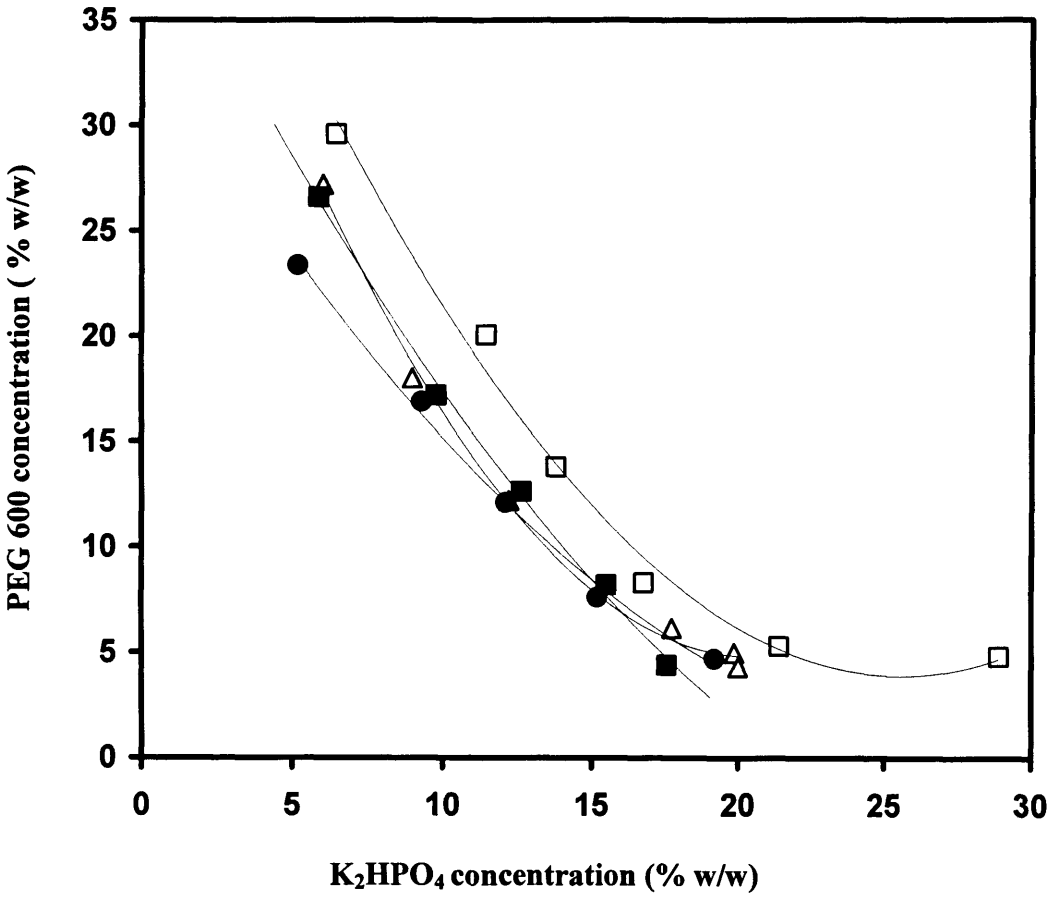

Figure 4.2: Binodial curves for PEG 600-K_2HPO_4 phase systems with various additives: PEG 600-K_2HPO_4 only (□); PEG 600-K_2HPO_4 with 20% (w/w) clarified lysate (■), PEG 600-K_2HPO_4 with 2% (w/w) isopropanol (Δ); PEG 600-K_2HPO_4 with 20% (w/w) clarified lysate and 2% (w/w) isopropanol (•). Experiments performed as described in Section 2.5.3.

4.3 Optimisation of ATPS for pDNA partitioning

The partitioning of plasmid DNA and related contaminants found in *E. coli* lysates (such as RNA, chrDNA and proteins) is complex and is influenced by a large number of factors. Along with the PEG molecular weight, the volume ratio, pH and plasmid size can all affect pDNA partitioning and so these were examined in order to identify suitable systems to be used for subsequent countercurrent chromatography experiments.

4.3.1 Effect of volume ratio

The effects of temperature, lysate loading and pDNA concentration on plasmid partitioning in ATPS have been previously tested [Ribeiro *et al.*, 2002; Kune, 2002], however no detailed study on how the volume ratio influences pDNA partitioning has been reported. As the composition of the phase systems used in CCC will have a direct effect on the partitioning of pDNA and its contaminants, different volume ratios of PEG-phosphate systems were tested in order to maximize the recovery of pDNA and minimize the co-partitioning of contaminants in either one of the phases. The effects of volume ratio on three different molecular weight PEG systems (PEG 300, 600 and 1000) were tested with plasmid DH5α -gWiz (5.7 kb). The pH of these systems were not manipulated. The amount of lysate added was kept constant at 40% (w/w) as this was found to be optimal for pDNA partitioning [Ribeiro *et al.*, 2002] and for reducing the co-partitioning of proteins [Trindade *et al.*, 2005]. All compositions of PEG and salt where chosen as close as possible to the binodial curve as compositions of PEG and salt resulting in the shortest tie-line length was previously shown to increase pDNA yields in ATPS. For this reason specific studies on tie-line lengths are not considered. The results of these experiments are summarised in Table 4.1 and Figure 4.3.

For PEG 300 systems, the plasmid DNA partitioned mainly to the upper PEG phase. One reason for partitioning to the PEG phase could be due to the enthalpic contribution of the ATPS which was seen in the partitioning of proteins [Johansson *et al.*, 1998]. The enthalpic contribution is the sum of all binary interactions between the pDNA and the remaining components in each phase, and the difference in energy of

each phase due to unlike enthalpic interactions between all phase components other than the pDNA. The dependence of partitioning on the self energies of the PEG and salt phases arises because addition of lysate into a phase requires the breaking of interactions between the components of the phase to create a cavity into which the pDNA fits. The complexity of understanding plasmid partitioning arises since protein, RNA and chromosomal DNA also compete to fit into the created cavities [Ribeiro *et al.*, 2002]. In PEG 300-phosphate systems, the PEG phase has a higher self energy because it contains significant concentrations of PEG and potassium phosphate, which strongly repel. pDNA will favour partitioning into the phase with the highest self energy, i.e. the PEG phase. Protein and RNA (Table 4.1 and Figure 4.3) were also seen to co-partition to the PEG 300 phase.

Another factor than can affect pDNA partitioning is the solute characteristics and type of interactions it can establish within the components of each phase. Albertsson [1986] developed a general relationship between the partition coefficient of a charged biomolecule (K) and the electrostatic potential difference $\Delta\psi$:

$$\text{In K} = \text{In K}_0 + \frac{z_b F}{RT}\Delta\Psi \qquad \text{(Equation 4.1)}$$

Where F is Faraday's constant, R is the ideal gas law constant, T is the absolute temperature, z_b is the charge of the biomolecule and K_0 is the partition coefficient of the biomolecule when $\Delta\psi = 0$ and $z_b = 0$. The partition of a charged molecule is influenced by the unequal distribution of ions due to different affinities for the phases which generates an electrical potential between the phases [Johansson *et al.*, 1998]. The magnitude and sign of $\Delta\psi$ are determined by the partitioning behaviour of ions of the majority salt in the system. For PEG 300-salt systems, the phase-forming salt will therefore determine $\Delta\psi$. In systems with K_2HPO_4 as used here, $\Delta\psi$ is positive, thus the partitioning of negatively charged pDNA into the PEG-rich top phase is favoured.

The results for pDNA partitioning in PEG 300 systems at various phase volume ratios show that for the 5.7kb plasmid, the volume ratios have a profound effect on plasmid recovery i.e. when the plasmid partitions to the top phase (Table 4.1). Purification factors of plasmid DNA relative to protein in the plasmid rich phase are defined as the

ratio of the recovery of plasmid DNA to protein. At low volume ratios (V_R<0.6), the plasmid was seen to completely partition to the interface with some RNA partitioning to the PEG 300 phase (Lanes 5 and 6, Figure 4.3). When the volume ratio is increased, it is possible that the electropotential of the system increases (due to larger volumes of PEG available), allowing the negatively charged pDNA to partition to the more positive PEG-rich phase. Some pDNA was found to partition to the bottom salt phase for 1<V_R<2.2, although at higher volume ratios (V_R>5) none was seen in the salt phase. RNA partitioned in a similar manner as pDNA although no significant increase in RNA concentration was seen with increased volume ratios (Figure 4.3). Proteins in these systems partitioned to both phases and to the top phase to a higher extent. Increases in the volume ratio reduced the concentration of protein in the top phase (Tables 4.1) although the overall protein recovery yield to the PEG phase does not change significantly when V_R>1. The influence of volume ratio on the distribution of pure protein [Huddleston *et al.* 1994] and intracellular protein [Flanagan *et al.* 1991] has previously been reported. Thus it would appear beneficial to use high volume ratios when dealing with low molecular weight PEG ATPS due to the higher pDNA recovery yields and purification factors.

For PEG 600 and 1000 systems, the plasmid partitioned to the lower salt phase. There are a number of reasons for the reversed preference of the pDNA into the salt phase compared to PEG 300 systems. One possible factor is due to the entropic contribution of such systems [Johansson *et al.*, 1998]. The entropic effects on partitioning are significantly large in PEG-salt system, where the PEG component is effectively localized in one phase, causing the number density of PEG to be considerably lower than in the conjugate water-rich salt phase. This creates a strong entropic driving force for pDNA partitioning to the polymer-free phase as that phase can accommodate the solute in more ways due to the higher number density. It seems that an increase in PEG molecular weight either increased or reduced the number density of the salt phase and PEG phase respectively, thus driving the pDNA towards the salt phase. The effect of polymer molecular weight on protein partitioning in a PEG-dextran system on entropic effects was previously seen [Johansson *et al.*, 1998] although in this case, the partitioning was to the upper PEG phase.

System	Volume ratio (V_R)	Phase	Total plasmid ($\mu g.mL^{-1}$)	Plasmid Recovery yield (%)	Protein ($\mu g.mL^{-1}$)	PF pDNA relative to Protein
E.coli Lysate	-		24	-	92	-
PEG 300	0.6	T	0	0	111	0
		B	0	0	32	
	1.0	T	7	30	51	0.5
		B	5	21	33	0.6
	2.2	T	7	40	35	0.7
		B	5	15	44	0.5
	5.1	T	8	58	32	1.0
		B	0	0	53	0
PEG 600	0.8	T	0	0	61	-
		B	19	60	0	(a)
	1.3	T	0	0	50	-
		B	20	63	0	(a)
	3	T	0	0	21	-
		B	33	69	0	(a)
	3.8	T	0	0	29	-
		B	37	70	0	(a)
PEG 1000	0.4	T	0	0	27	-
		B	18	63	0	(a)
	1.0	T	0	0	32	-
		B	16	69	0	(a)
	1.2	T	0	0	6	-
		B	23	91	0	(a)
	4.6	T	0	0	1	-
		B	55	92	0	(a)

(a) Purification factors correspond to an infinite value as proteins were below a detectable level in the bottom phase.

Table 4.1: Concentrations and recovery yields of plasmid DNA (gWiz - 5.7 kb) and proteins from a cell lysate after extraction with various ATPS of different volume ratios. T - top phase; B - bottom phase. Purification factors of plasmid (in PEG-rich phase for PEG 300 systems and salt-rich phase for PEG 600 and 1000 systems) relative to total protein are also given. The pH was not controlled and the maximum pH difference measured between the two phases was 0.67, 0.46 and 0.7 for PEG 300, PEG 600 and PEG 1000 systems respectively. Plasmid DNA and protein measurements were performed as described in Sections 2.7.4 and 2.7.5 respectively. Purification factors of plasmid DNA relative to protein is defined as the ratio of the plasmid DNA recovered to protein recovered in the plasmid-rich phase. Plasmid recovery yields defined as the ratio of mass of pDNA in the plasmid-rich phase to the initial mass of pDNA in the lysate.

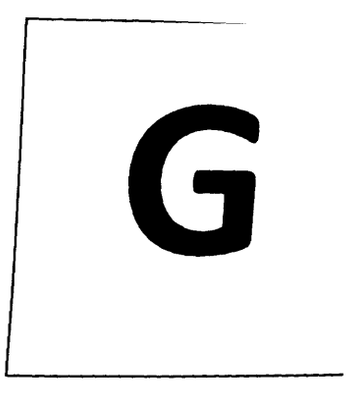
G

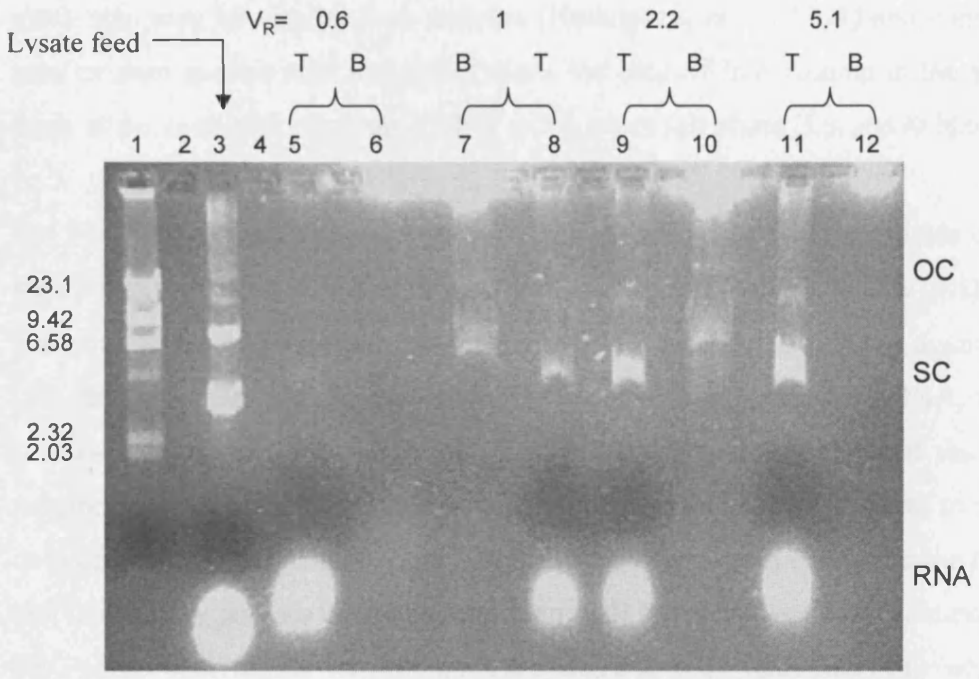

Figure 4.3: Agarose gel analysis of plasmid (gWiz - 5.7 kb) and RNA partitioning in ATPS with 40% (w/w) clarified lysate using different volume ratios of PEG 300 and K_2HPO_4. V_R - volume ratio of ATPS. T - top phase. B - bottom phase. Lane 1: Lambda DNA/HindIII marker (200 ng); Lane 2: Blank; Lane 3: Clarified lysate (24 µg.mL^{-1} pDNA); Lane 4: Blank; Lanes 5 and 6: Top and bottom phases respectively for V_R = 0.6, 10% (w/w) PEG 300-25% (w/w) K_2HPO_4; Lane 7 and 8: Bottom and top phases respectively for V_R = 1, 18% (w/w) PEG 300-18% (w/w) K_2HPO_4; Lanes 9 and 10: Top and bottom phases respectively for V_R = 2.2, 25% (w/w) PEG 300-12.5% (w/w) K_2HPO_4; Lanes 11 and 12: Top and bottom phases respectively for V_R = 5.1, 30% (w/w) PEG 300-10% (w/w) K_2HPO_4. 30µL of indicated phase loaded. Non-labelled tracks indicate blanks. Migration of OC and SC forms of plasmid DNA differ slightly due to the effects of PEG and salts. Experiments were performed as described in Section 2.7.2

Another important factor of pDNA partitioning to the salt phase is due to large interfering polymer molecules that exist in high molecular weight PEG systems. It is known that in systems where polymer length is large, individual polymer molecules interfere with one another effectively producing a polymer solution network whose mesh size may be smaller than proteins [Huddleston *et al.*, 1991] and consequently smaller than nucleic acid molecules. Thus the lack of free volume in the top phase leads to the exclusion of plasmid DNA to the lower salt phase [Lis and Schleif, 1975].

For PEG 600 systems, the volume ratio did not affect the recovery yields of pDNA significantly although higher concentrations were obtained (Table 4.1) with a reduction in the bottom phase volume (i.e. higher volume ratio). RNA again behaves in a similar manner, due to its similar physio chemical properties to pDNA, and RNA increased for higher volume ratios (Figure 4.4). Thus it is concluded that using a volume ratio of around unity would be more beneficial for such systems to minimise co-partitioning of the contaminant RNA. Proteins partitioned entirely to the top phase and interface regardless of the volume ratio with lower concentrations obtained in the PEG phase when higher volume ratios are used due to the increased PEG volume. The systems studied here are advantageous over the PEG 600- $(NH_4)_2SO_4$ system which showed protein co-partitioning with the pDNA to the salt phase for V_R>3 [Trindade *et al.*, 2005]. The recovery yields of proteins to the PEG 600 phase was constant regardless of the volume ratio used.

PEG 1000 systems showed similar trends (results not shown) to PEG 600 and higher plasmid yields were obtained possibly due to the increase in the excluded volume of the longer PEG polymer chain [Albertsson, 1986], increased hydrophobicity of high molecular weight of PEG [Forciniti *et al.* 1991] and increased (more negative) electrostatic potential, perhaps because the phosphate ion is more strongly rejected by the higher molecular weight PEG [Bamberger *et al.*, 1985]. RNA was found to co-partition with the pDNA to a greater extent than in PEG 600 systems, thus these systems were not selected for use in subsequent CCC experiments. In addition, the high viscosity of PEG 1000 systems can also be problematic due to the high pressures that results when using this phase in the CCC machine. As with PEG 600 systems, proteins partitioned to the PEG phase and interface, although protein recovery yields to the PEG 1000 phase decreased significantly as volume ratio increases with almost

98% recovery at the interface when higher volume ratios were used (V_R>4). Thus for PEG 1000 systems, it seems that the protein partitioning preference shifts from the PEG phase to the interface when higher volumes of PEG are available. The partitioning of protein to the PEG phase decreases when the molecular weight of PEG is increased from 300 to 600 to 1000, behaving as if it is more attracted by smaller polymer molecules [Albertsson, 1985].

Chromosomal DNA was not analysed at this stage but can be seen (near the loading well) to partition to the same phase as the plasmid DNA and RNA for all PEG molecular weights. It is expected that a significant amount of chrDNA will be retained at the interface due to its large size compared with pDNA (around 1000 times larger). Although endotoxin levels were not measured for this research, some endotoxin is expected to co-partition to the lower salt phase but recent research has shown levels to be reduced by almost 70% after a single batch aqueous two-phase separation using 34 % (w/w) PEG 600-9 % (w/w) $(NH_4)_2SO_4$ with 20% (w/w) lysate loading [Trindade *et al.*, 2005].

4.3.2 Effect of pH changes on partitioning

Johansson [1970] and then Albertsson [1986] explored protein partitioning dependence on high salt concentration in PEG/dextran systems. Recent results on protein partitioning in ATPS as a function of pH changes have been reported [Balasubramaniam *et al.*, 2002; Simonet *et al.*, 2000; Marcos *et al.*, 1999; Han and Lee, 1997; Asenjo *et al.*, 1994]. The effect of pH changes on pDNA partitioning was examined here using different K_2HPO_4: KH_2PO_4 ratios at a constant ionic strength. A higher pH (K_2HPO_4 > KH_2PO_4) system resulted in an increase of plasmid partitioning to the upper phase when PEG 300 systems were used (Figure 4.5). For PEG 600 and 1000 systems, pDNA still partitioned to the bottom phase but to a lesser extent when using higher pH, due to the accumulation of pDNA at the interface. In addition, RNA followed the same trend as DNA in those phases (Figure 4.6).

The pH effect on pDNA partitioning can be a result of many factors and can be understood from pH effects on protein partitioning. It is a fact that in nucleic acids, phosphate is found as a diester linked to two carbon atoms of adjacent ribose sugars.

The pK_a for dissociation of single –OH proton is about 3. When pH > pK_a, each phosphate residue of the DNA/RNA is dissociated and carries a negative charge. It was previously seen with proteins that increases in pH leads to more negatively charged biomoleucles [Asenjo *et al.*, 1994]. Generally, the phosphate ions in ATPS shifts to the lower phase (i.e. salt phase) which has a higher density, and the lower phase then has a greater negative charge than the upper phase (i.e. PEG phase). This unequal distribution of phosphate ions, along with the requirement of electoneutrality in the phases leads to an electrochemical potential difference to exist between the top (PEG-rich) and bottom (Salt-rich) phase. As the ratio of K_2HPO_4 to KH_2PO_4 changes, so does the electrostatic potential $\Delta\psi$ (Equation 4.1). The positive electrochemical potential of the system coupled with the increased negative charge of the pDNA can lead to an increase in the partition coefficient.

In PEG 600 and 1000 systems, the large interfering polymer, and the entropic contribution (Section 4.3.1) of PEG 600 and 1000 systems can prevent pDNA from partitioning to the PEG phase. This results in the transfer of some pDNA from the bottom phase to the interface (rather than the PEG phase) when the pH is increased. For PEG 300 systems, this leads to an increase in partitioning of pDNA to the PEG phase as the enthalpic contribution of PEG 300 systems already makes the PEG phase the preferred phase (Section 4.3.1). Another possible explanation of the decreased affinity for the lower phase with pH increases is also due to an increase of the salting-out effect in the lower (salt phase) or an increase in hydrophobic interactions between DNA/RNA and PEG in the upper phase [Marcos *et al.*, 1999]. The salting-out effect increases at higher pH values and leads to the pDNA being precipitated (for systems that partition preferentially to the bottom phase). In addition, the PEG-pDNA interactions increase at higher pH values and increases plasmids partitioning to the top phase. As no pDNA was detected in the top phase (Figure 4.6) for PEG 600 and 1000 systems, pH increases led to plasmid loses at the interface.

In general, it was seen that the influence on pH changes was greater for RNA partitioning than for pDNA. This is because RNA is present at a range of molecular weights. RNA can be seen in the top phase to a much greater extent than DNA as low molecular weight RNA behaves like a typical soluble substance partitioning to both the top and bottom phases (Figures 4.4 and 4.6) [Kimura and Kobayashi., 1996]. In

addition, high molecular weight RNA is more easily accumulated at the interface than the DNA (due to its wider surface area), thus more RNA is lost at the interface when the pH was increased [Kimura, 2000], behaving like a particle. A combination of high and low molecular weight RNA partitions to the top, bottom and interface. It is noted that due to RNA being single stranded, it could be easier for it to form hydrophobic interactions in the PEG phase and is more strongly influenced by salting-out effects at the different pH systems used.

From initial analysis of agarose gels, a higher pH seems preferred even though it means less pDNA in the bottom phase of the PEG 600 and 1000 systems. This is because most of the RNA co-partitioned with the pDNA to the lower phases, making it undesirable. The reduction in the RNA partitioning with the DNA is considered more important than the minor losses in pDNA yield which resulted from using higher pH ATPS (K_2HPO_4 as the only salt phase). PEG 1000 systems showed similar results. For PEG 300 and 600, RNA partitions with the DNA to a lesser extent than for PEG 1000 (results not shown) as most of it is lost to the interface. In addition, it was also observed that the solubility of the salt became an issue as the concentration of KH_2PO_4 was increased. This may lead to problems when emptying the CCC column. Addition of monobasic potassium phosphate (KH_2PO_4) also increased the settling time (t_s) which is undesirable due to the importance in maintaining an acceptable level of stationary phase retention [Conway, 1990]. This increase in settling time was also observed when lactic acid dehydrogenase was purified by changing the concentration of monobasic potassium phosphate using CCC [Sibusawa *et al.*, 2002].

The increase in the amount of di-basic K_2HPO_4 (and thus increase in pH) shifted the binodial curve towards the origin (Figure 4.7) i.e. to the left of the clean binodial curve, which is preferred since less phase forming chemicals are needed to produce a two-phase system. This is due to the rejection of anions by PEG and results in the proportion of these ions in phosphate to change significantly. The critical points of ATPS will shift to higher values of total phosphate concentration with decreasing pH values [Huddleston *et al.*, 1991]. This confirmed pervious results using different ATPS [Lei *et al.*, 1990].

Consequently ATPS selected for subsequent CCC runs only consisted of K_2HPO_4 as the salt phase due to the reduced co-partitioning of RNA, lower settling times, lower amount of phase-forming chemicals needed to produce a two-phase system and the low solubility of KH_2PO_4.

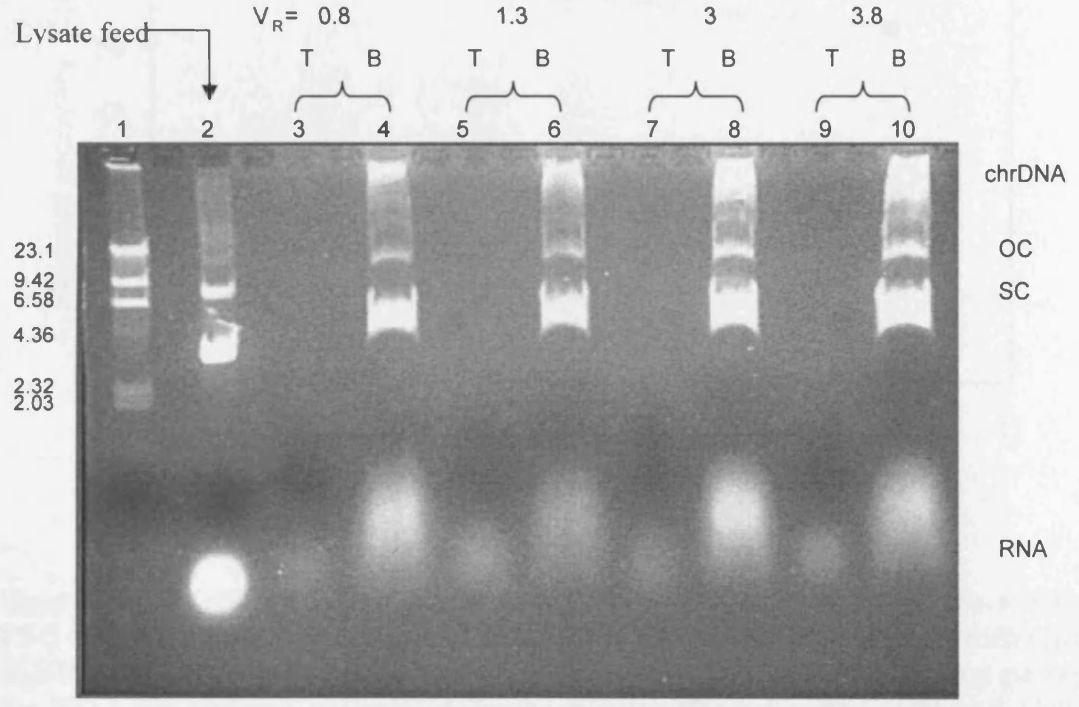

Figure 4.4: Agarose gel analysis of plasmid (gWiz - 5.7 kb) and RNA partitioning in ATPS with 40% (w/w) clarified lysate using different volume ratios of PEG 600 and K_2HPO_4. V_R - volume ratio of ATPS. T - top phase. B - bottom phase. Lane 1: Lambda DNA/HindIII marker (200 ng); Lane 2: Clarified lysate (24 µg.mL^{-1} Lanes 3 and 4: Top and bottom phases respectively for V_R= 0.78, 12.5% (w/w) PEG 600-18% (w/w) K_2HPO_4; Lane 5 and 6: Top and bottom phases respectively for V_R= 1.33, 18% (w/w) PEG 600-18% (w/w) K_2HPO_4; Lanes 7 and 8: Top and bottom phases respectively for V_R= 3, 20% (w/w) PEG 600-12.5% (w/w) K_2HPO_4; Lanes 9 and 10: Top and bottom phases respectively for V_R= 3.78, 25% (w/w) PEG 600-10% (w/w) K_2HPO_4. 30µL of indicated phase loaded. Non-labelled tracks indicate blanks. Migration of OC and SC forms of plasmid DNA differ slightly due to the effects of PEG and salts. Experiments were performed as described in Section 2.7.2

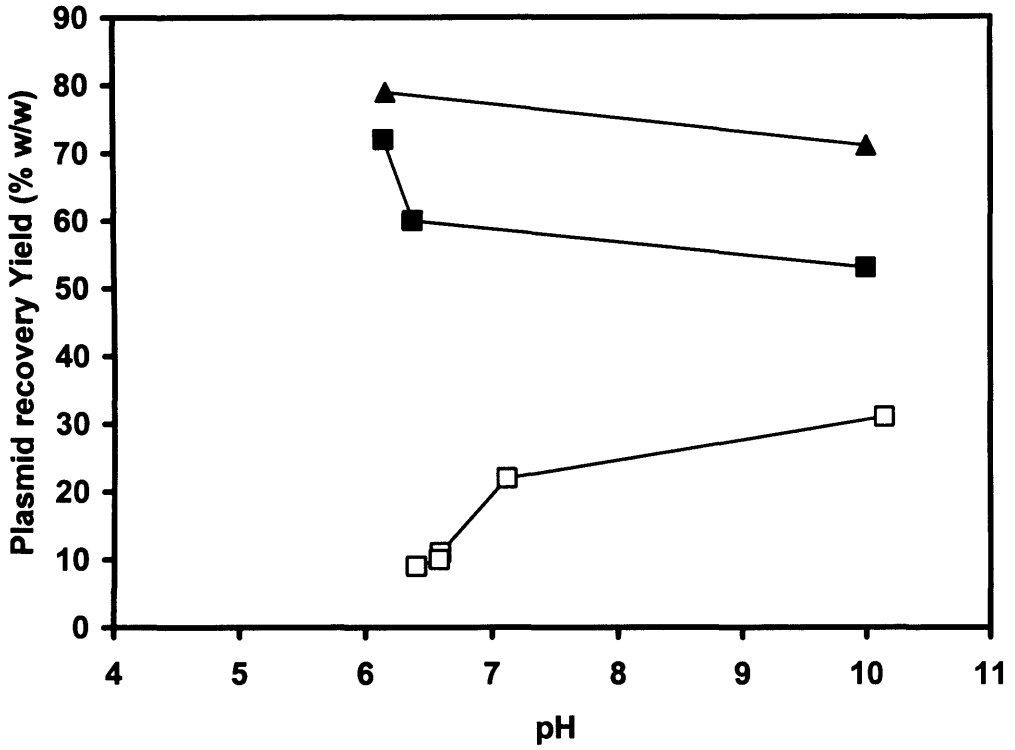

Figure 4.5: Effects on pDNA partitioning using 40 % w/w clarified lysate with PEG 300 (□), PEG 600 (■) and PEG 1000 (▲) phase systems with different K_2HPO_4: KH_2PO_4 ratios. The recovery yield represents pDNA in the top phase for PEG 300 systems and pDNA in the bottom phase for PEG 600 and 1000 systems. Partition coefficients were not calculated since most of the pDNA partitioning to one or other of the bulk phases and/or the interface.
The following ratios of PEG:K_2HPO_4:KH_2PO_4 were used:
PEG 300 ATPS: 18:18:0 (pH = 10.1); 10:25:1 (pH = 7.12); 20:20:2 (pH = 6.59); 20:18:2 (pH = 6.58); 20:18:5 (pH= 6.4).
PEG 600 ATPS: 12.5:18:0 (pH = 10); 18:15:3 (pH = 6.4); 18:13:5 (pH = 6.2).
PEG 1000 ATPS: 18:18:0 (pH = 10); 18:12:6 (pH = 6.2).
All experiments were performed as described in Section 2.5.1 with initial pDNA concentration of 30 $\mu g.mL^{-1}$. Plasmid DNA and protein measurements were performed as described in Sections 2.7.4 and 2.7.5 respectively.

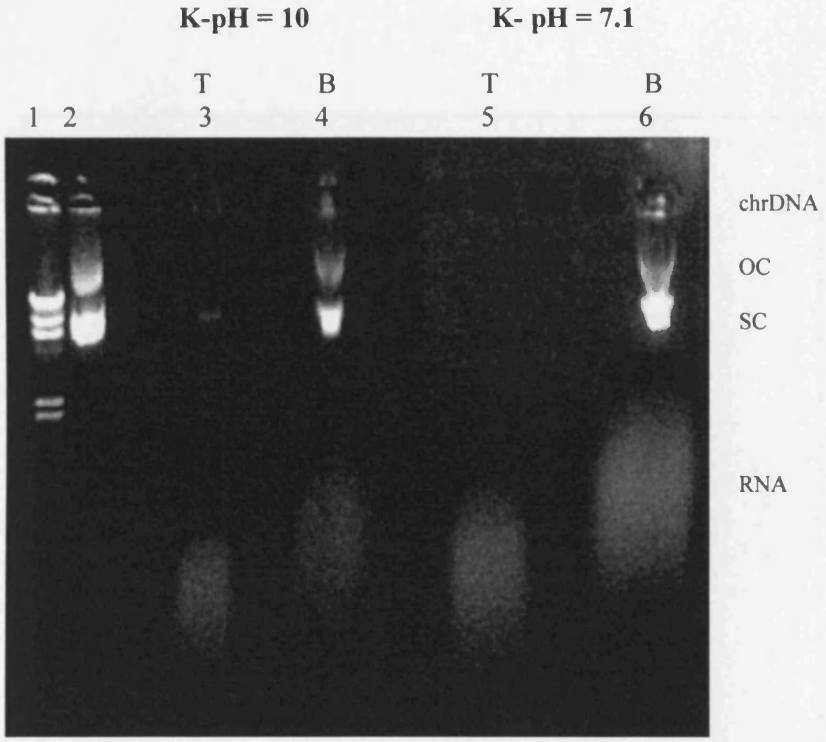

Figure 4.6: Agarose gel analysis of pDNA and RNA partitioning in ATPS with 40% (w/w) clarified lysate using a system of 12.5 % (w/w) PEG 600 and 18 % (w/w) total salt K_2HPO_4:KH_2PO_4. T - top phase. B - bottom phase Lane 1: Lambda DNA/*Hind*III marker (400 ng); Lane 2: Qiagen purified DH5α-gWiz RNA-free; Lane 3 and 4: Top and bottom phase respectively at pH = 10 (K_2HPO_4:KH_2PO_4 = 100:0); Lanes 5 and 6: Top and bottom phase respectively at pH = 7.1 (K_2HPO_4:KH_2PO_4 = 10:7). 10µL of indicated phase loaded. Non-labelled tracks indicate blanks. Migration of OC and SC forms of plasmid DNA differ slightly due to the effects of PEG and salts. Experiments were performed as described in Section 2.7.2 using TBE buffer.

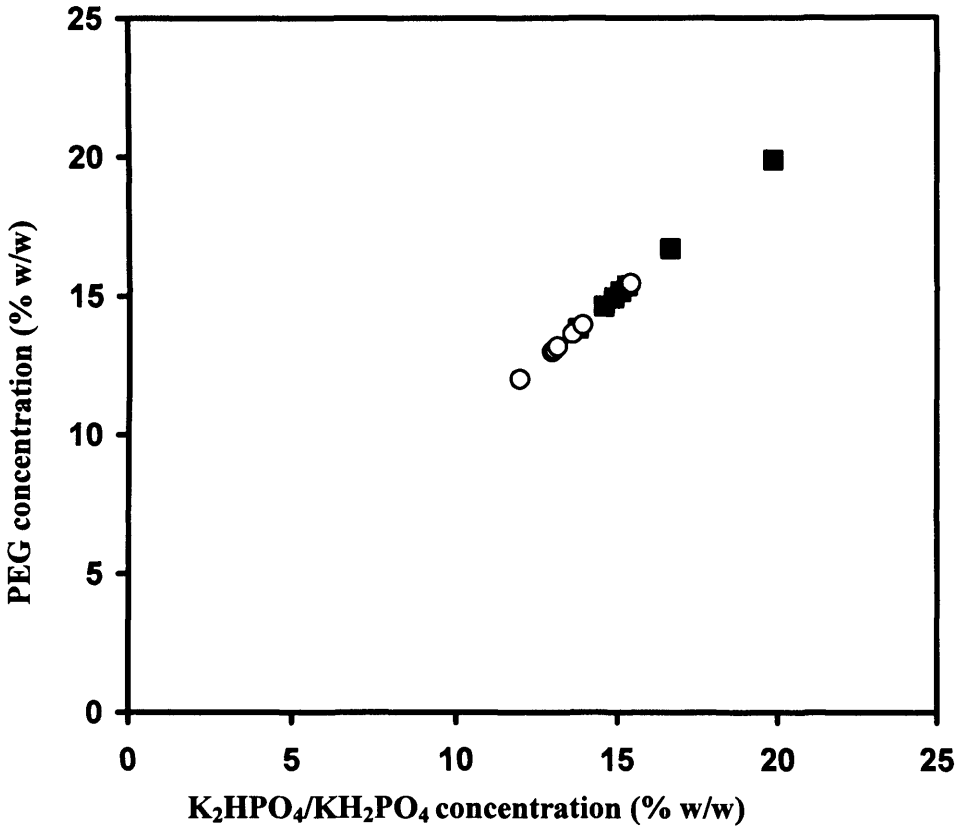

Figure 4.7: Binodial points constructed for PEG 600 and PEG 1000, and different ratios of K_2HPO_4-KH_2PO_4. All points started with a composition of PEG 25% (w/w)- Salt 25% (w/w) with no lysate. For both systems, points furthest from the origin represent the lowest pH (highest KH_2PO_4 concentration). For PEG 600 systems (■), points nearest to the origin moving away represent pH (K_2HPO_4:KH_2PO_4 ratio): 10 (100:0), 7.6 (25:7), 7.4 (18:7), 7.1 (10:7), 6.6 (7:10), 6.3 (7:18), 6.2 (7:25), 4.5 (0:100). For PEG 1000 systems (○), points nearest to the origin moving away represent pH (K_2HPO_4:KH_2PO_4 ratio: 10 (100:0), 8.6 (25:7), 8.5 (18:7), 7.9 (10:7), 7.3 (7:10), 7.1 (7:18), 6.8 (7:25), 4.8 (0:100). Experiments were performed as described in Section 2.5.1.

4.3.3 Effect of plasmid size

The plasmid vectors that today are under gene therapy clinical trails can vary between 2 and 200 kbp in size depending on what target it is developed for [Schleef and Schmidt, 2004]. This requires a robust purification process that can handle plasmid DNA of varying sizes. Three additional plasmids (pSVβ-DH5α: 6.9kb, pQR150-DH5α: 20kb and p5180-DH10β: 72kb) were therefore partitioned in ATPS comprising of PEG-potassium phosphate.

The partitioning behaviour of the 6.9 and 20 kb plasmids was found to be similar to the 5.7 kb plasmid described in Section 4.3.1 and is summarised in Tables 4.2 and 4.3. For PEG 300 systems, pDNA recovery yields increased with volume ratios. At V_R<0.5, no plasmid was recovered in either phase for the 20kb plasmid, while only a 2% (w/w) recovery yield was achieved for the 6.9 kb plasmid, suggesting that at low volume ratios, the electropotential of the system is not high enough to allow significant partitioning of the pDNA into the PEG phase. As with the 5.7 kb plasmid, RNA was seen to partition to the top PEG 300 phase for all volume ratios (Figure 4.8). Higher volume ratios yielded lower protein concentrations in the PEG phase. Figure 4.8 also shows that some chrDNA co-partitioned to the top phase with the pDNA and RNA. On average, the size of chrDNA is around 1000 times that of the plasmid, thus it is expected that a significant proportion of chrDNA is retained at the interface. Protein partitioning in the presence of these larger plasmids was similar to that with the 5.7 kb plasmid described in Section 4.3.1 with partitioning to both phases. Protein concentration decreases in the PEG phase when volume ratio increases, although the overall recovery yields do not change significantly.

For PEG 600 and 1000 systems, the 6.9 and 20 kb plasmid concentrations in the lower salt phase increased with higher volume ratios due to the reduction in the amount of salt phase available. As with the 5.7 kb plasmid, RNA co-partitioned with the pDNA and total RNA partitioning increased with volume ratio. PEG 1000 systems resulted in higher RNA co-partitioning and pDNA recovery yield due to the increased excluded volume of the longer PEG polymer chain [Albertsson, 1986], increased hydrophobicity [Forciniti *et al.* 1991] and increased electrostatic potential [Bamberger *et al.*, 1985]. Again, PEG 1000 systems were not considered due to the viscous nature

of the PEG phase which would be problematic when operated in the CCC. Lower yields for the 6.9 kb plasmids are obtained compared to the 5.7 and 20 kb plasmids (Table 4.2). Initially this was thought to be due to the higher plasmid concentration (137 $\mu g.mL^{-1}$ for 6.9 kb plasmid compared 24 $\mu g.mL^{-1}$ and 19 $\mu g.mL^{-1}$ for the 5.7 and 20 kb plasmids respectively). The effect of concentration effect on pDNA using several volume ratios are shown in Table 4.4. When the plasmid was diluted by a factor of 5, PEG 300 systems showed a significant increase in recovery yields by up to 24% w/w in the top phase. PEG 600 systems showed results to be dependent on volume ratios. No increase in recovery yields was seen when volume ratio of around unity was used, while a reduction of 13% resulted when $V_R > 1$. It is therefore thought that the 6.9 kb plasmid preparation might contain a number of different isoforms which might increase partitioning to the interface when higher concentrations are used. This is especially true for PEG 300 systems which are influenced mainly by electrostatic potential difference. Plasmid partitioning to the salt phase are partly governed by the lack of free volume of the PEG 600 phase and thus a decrease in initial plasmid concentration will mean a reduction in the amount of pDNA recovered in the salt phase. Higher amounts of PEG 600 (higher volume ratios) will increase this effect due to the reduction in volumes of the salt phase. Total plasmid yields have been reported to be affected greatly by an increase in isoforms produced [Kepka *et al.*, 2004b].

Protein partitioning for PEG 600 and 1000 systems is usually to the PEG phase and interface with decreasing concentration for higher volume ratios (as with the 5.7 kb plasmid). Exceptions to this are systems (both PEG 600 and 1000 for the 6.9 kb plasmid, and PEG 1000 for the 20 kb plasmid) with volume ratio of around 1 (Table 4.2 and 4.3) where some protein partitioned to the lower phase. It can be seen from Figure 4.1 that the compositions of PEG and salt used to achieve a volume ratio of 1 (18% w/w each of PEG and salt) are a greater distance from the binodial curve compared to all the other volume ratios that resulted from different PEG and salt compositions, which were selected closer to the binodial curve. This increased the tie-line length (Figure 1.1) which results in increased interfacial tension and increased electrochemical potential between the phases [Bamberger *et al.*, 1985]. This may result in some proteins partitioning to the bottom phase due to the PEG phase exceeding its solubility limit [Trindade *et al.*, 2005], with the maximum recovery

yield of protein in the salt phase found to be 23% w/w for the 6.9 kb plasmid and 7% w/w for the 20 kb plasmid, both using PEG 1000 as the upper phase.
Chromosomal DNA partitioning can only be qualitatively analysed using agarose gels, and can be seen to co-partition to the salt phase with the plasmid with significant amounts removed at the interface.

For the largest plasmid size of 72 kb, the partitioning behaviour was different than from the 5.7, 6.9 and 20 kb plasmids in that interfacial forces were dominant. In these cases 100% of the plasmid was recovered at the interface regardless of the PEG molecular weight or volume ratios. For PEG 300 systems (Figure 4.10), plasmid DNA was not seen in either phase although at V_R= 4.8, some DNA was seen in the top phase suggesting that at much high volume ratios, pDNA can be recovered in the top PEG-rich phase. Such high volume ratios would not be suitable for use in the CCC as the high concentration of PEG needed (leading to higher viscosities) would be problematic due to the high pressures that can result from pumping such phases. RNA can be clearly seen to partition to the PEG phase. For PEG 600 systems (Figure 4.11), no plasmid was seen in either phase, and again, RNA was seen to partition to the salt and PEG phases, further suggesting that RNA behaves like a typical soluble substance. PEG 1000 systems (results not shown) showed similar results with some RNA partitioning to both phases although the majority is retained at the interface along with the pDNA. It seems that interfacial tension is dominant for pDNA partitioning regardless of the PEG molecular weight, whilst RNA behaves like a soluble substance for low MW PEG (PEG 300) with most partitioning to the PEG phase, and similar to a particle when higher molecular weight PEG systems (PEG 1000) with the majority being retained at the interface. Protein partitioning was similar to the smaller sized plasmids and full results are shown in Table 4.5.

System	Volume ratio (V_R)	Phase	Total Plasmid ($\mu g.mL^{-1}$)	Plasmid Recovery yield (%)	Protein ($\mu g.mL^{-1}$)	PF pDNA relative to Protein
E. coli lysate	-		137	-	79	-
PEG 300	0.5	T	0	0	40	-
		B	2	2	31	0.3
	1.0	T	9	6	42	0.8
		B	0	0	37	-
	2.3	T	9	9	27	1.3
		B	0	0	38	-
	3.3	T	13	15	17	2.9
		B	0	0	43	-
PEG 600	0.6	T	0	0	29	-
		B	56	51	0	(a)
	1.0	T	0	0	31	-
		B	50	37	15	13.2
	1.8	T	0	0	8	-
		B	84	46	0	(a)
	3.8	T	0	0	3	-
		B	120	40	0	(a)
PEG 1000	0.5	T	0	0	10	-
		B	56	58	0	(a)
	1.0	T	0	0	22	-
		B	53	39	18	11.2
	1.3	T	0	0	5	-
		B	59	53	0	(a)
	3.9	T	0	0	0	-
		B	193	63	0	(a)

(a) Purification factors correspond to an infinite value as proteins were below a detectable level in the bottom phase.

Table 4.2: Concentrations and recovery yields of plasmid DNA (pSVβ-6.9 kb) and proteins from a cell lysate after extraction with various ATPS of different volume ratios. T - top phase; B - bottom phase. Purification factors of plasmid (in PEG-rich phase for PEG 300 systems and salt-rich phase for PEG 600 and 1000 systems) relative to total protein are also given. The pH was not controlled and the maximum pH difference measured between the two phases was 0.63, 0.71 and 0.9 for PEG 300, PEG 600 and PEG 1000 systems respectively. Plasmid DNA and protein measurements were performed as described in Sections 2.7.4 and 2.7.5 respectively. Purification factors of plasmid DNA relative to protein is defined as the ratio of the plasmid DNA recovered to protein recovered in the plasmid-rich phase. Plasmid recovery yields defined as the ratio of mass of pDNA in the plasmid-rich phase to the initial mass of pDNA in the lysate.

System	Volume ratio (V_R)	Phase	Total Plasmid ($\mu g.mL^{-1}$)	Plasmid Recovery yield (%)	Protein ($\mu g.mL^{-1}$)	PF pDNA relative to Protein
E. coli Lysate	-		19	-	142	-
PEG 300	0.4	T	0	0	155	-
		B	0	0	33	-
	1.2	T	2	14	96	0.1
		B	0	0	26	-
	3.1	T	4	32	74	0.2
		B	3	24	21	0.5
	7.3	T	4	37	61	0.2
		B	0	0	32	-
PEG 600	0.6	T	0	0	108	-
		B	9	62	0	(a)
	1.3	T	0	0	113	-
		B	17	67	0	(a)
	3	T	0	0	64	-
		B	29	75	0	(a)
	4.4	T	0	0	62	-
		B	43	90	0	(a)
PEG 1000	0.4	T	0	0	59	-
		B	15	116	0	(a)
	0.9	T	0	0	55	-
		B	17	94	9	7.0
	1.1	T	0	0	33	-
		B	22	115	0	(a)
	4.7	T	0	0	21	-
		B	43	84	0	(a)

(a) Purification factors correspond to an infinite value as proteins were below a detectable level in the bottom phase.

Table 4.3: Concentrations and recovery yields of plasmid DNA (pQR150 -20 kb) and proteins from a cell lysate after extraction with various ATPS of different volume ratios. T - top phase; B - bottom phase. Purification factors of plasmid (in PEG-rich phase for PEG 300 systems and salt-rich phase for PEG 600 and 1000 systems) relative to total protein are also given. The pH was not controlled and the maximum pH difference measured between the two phases was 0.75, 0.56 and 0.37 for PEG 300, PEG 600 and PEG 1000 systems respectively. Plasmid DNA and protein measurements were performed as described in Sections 2.7.4 and 2.7.5 respectively. Purification factors of plasmid DNA relative to protein is defined as the ratio of the plasmid DNA recovered to protein recovered in the plasmid-rich phase. Plasmid recovery yields defined as the ratio of mass of pDNA in the plasmid-rich phase to the initial mass of pDNA in the lysate.

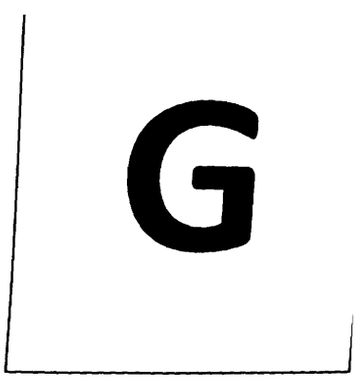
G

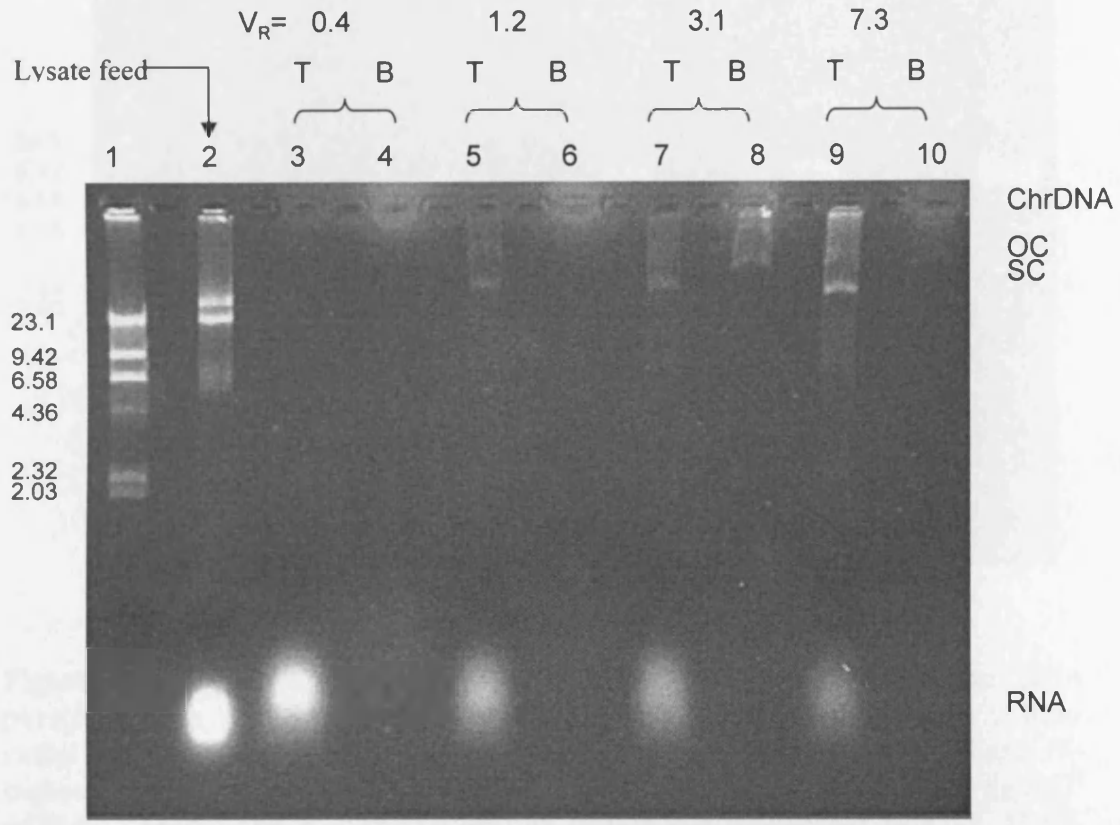

Figure 4.8: Agarose gel analysis of plasmid (pQR150 - 20 kb) and RNA partitioning in ATPS with 40% (w/w) clarified lysate using different volume ratios of PEG 300 and K_2HPO_4. V_R - volume ratio of ATPS. T - top phase. B - bottom phase. Lane 1: DNA ladder; Lane 2: Clarified lysate (19µg.mL^{-1} pDNA); Lanes 3 and 4: Top and bottom phases respectively for V_R= 0.42, 10% (w/w) PEG 300-25% (w/w) K_2HPO_4; Lanes 5 and 6: Top and bottom phases respectively for V_R= 1.16, 18% (w/w) PEG 300-18% (w/w) K_2HPO_4; Lanes 7 and 8: Top and bottom phases respectively for V_R= 3.1, 25% (w/w) PEG 300-12.5% (w/w) K_2HPO_4; Lanes 9 and 10: Top and bottom phases respectively for V_R= 7.3, 30% (w/w) PEG 300-10% (w/w) K_2HPO_4.30% (w/w) PEG 300-10% (w/w) K_2HPO_4. 30µL of indicated phase loaded. Non-labelled tracks indicate blanks. Migration of OC and SC forms of plasmid DNA differ slightly due to the effects of PEG and salts. Experiments were performed as described in Section 2.7.2

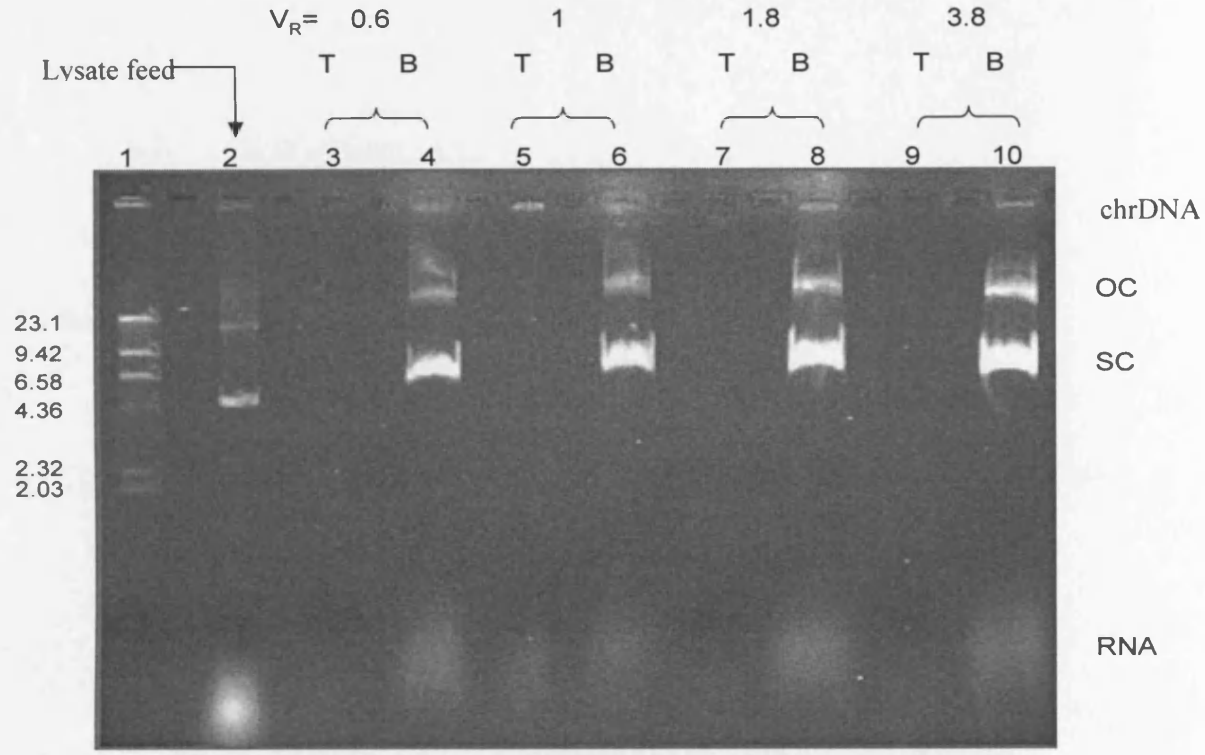

Figure 4.9: Agarose gel analysis of plasmid (pSVβ - 6.9 kb) and RNA partitioning in ATPS with 40% (w/w) clarified lysate using different volume ratios of PEG 600 and K_2HPO_4. V_R - volume ratio of ATPS. T - top phase. B - bottom phase. Lane 1: DNA ladder; Lane 2: Clarified lysate (137 μg.mL^{-1} pDNA); Lanes 3 and 4: Top and bottom phases respectively for V_R= 0.6, 12.5% (w/w) PEG 600-18% (w/w) K_2HPO_4; Lanes 5 and 6: Top and bottom phases respectively for V_R= 1, 18% (w/w) PEG 600-18% (w/w) K_2HPO_4; Lanes 7 and 8: Top and bottom phases respectively for V_R= 1.8, 20% (w/w) PEG 600-12.5% (w/w) K_2HPO_4; Lanes 9 and 10: Top and bottom phases respectively for V_R= 3.8, 25% (w/w) PEG 600-10% (w/w) K_2HPO_4. 30μL of indicated phase loaded. Non-labelled tracks indicate blanks. Migration of OC and SC forms of plasmid DNA differ slightly due to the effects of PEG and salts. Experiments were performed as described in Section 2.7.2

	Plasmid concentration: 137 μg.mL^{-1}				Plasmid concentration: 38 μg.mL^{-1}			
	PEG 300		PEG 600		PEG 300		PEG 600	
Volume ratio (V_R)	1.0	3.25	1	1.83	1.05	3.83	0.85	1.76
pDNA (μg.mL^{-1})	9	13	50	84	10	9	13	15
Recovery Yields (%)	6	15	37	46	27	39	39	32

Table 4.4: Effect of plasmid concentration (pSVβ - 6.9 kb) on partitioning in ATPS using different volume ratios and PEG molecular weight. Total pDNA concentrations were measured using HPLC as described in Section 2.7.4.

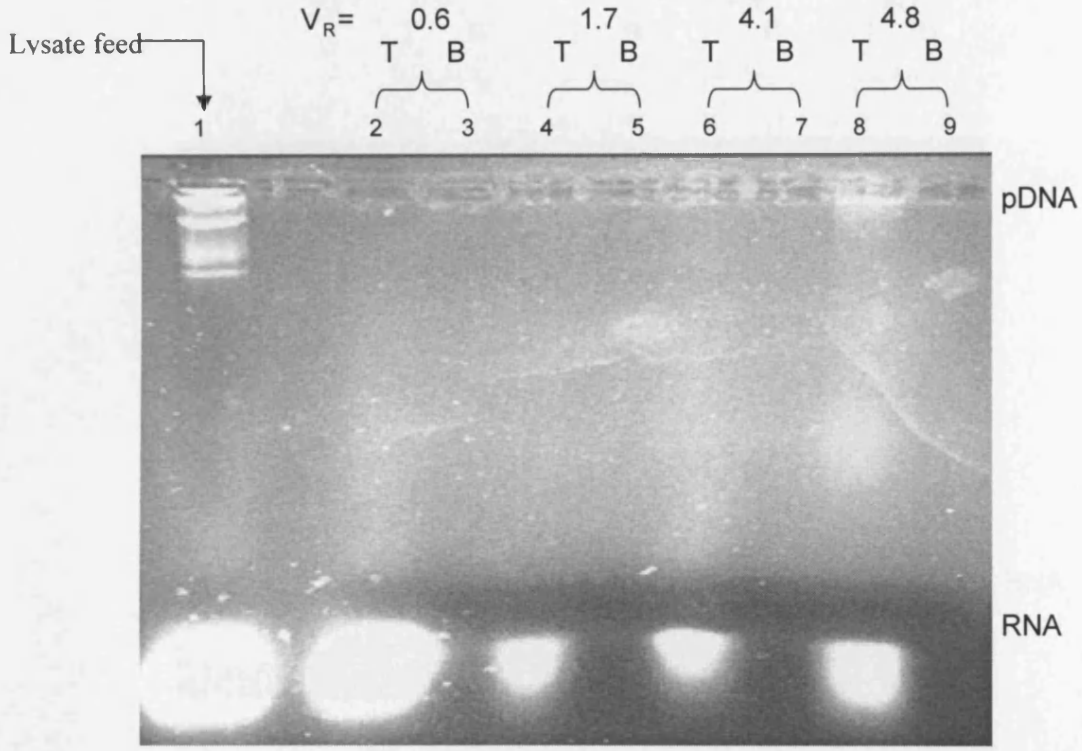

Figure 4.10: Agarose gel analysis of plasmid (p5180 - 72 kb) and RNA partitioning in ATPS with 40% (w/w) clarified lysate using different volume ratios of PEG 300 and K_2HPO_4. V_R - volume ratio of ATPS. T - top phase. B - bottom phase. Lane 1: Clarified lysate; Lanes 2 and 3: Top and bottom phases respectively for V_R= 0.6, 10% (w/w) PEG 300-25% (w/w) K_2HPO_4; Lane 4 and 5: Top and bottom phases respectively for V_R= 1.7, 18% (w/w) PEG 300-18% (w/w) K_2HPO_4; Lanes 6 and 7: Top and bottom phases respectively for V_R= 4.1, 25% (w/w) PEG 300-12.5% (w/w) K_2HPO_4; Lanes 8 and 9: Top and bottom phases respectively for V_R= 4.8, 30% (w/w) PEG 300-10% (w/w) K_2HPO_4. 30µL of indicated phase loaded. Non-labelled tracks indicate blanks. Migration of OC and SC forms of plasmid DNA differ slightly due to the effects of PEG and salts. Wells were overloaded for ease of qualitative analysis. All samples were prepared as described in Sections 2.7.1 and 2.7.2.

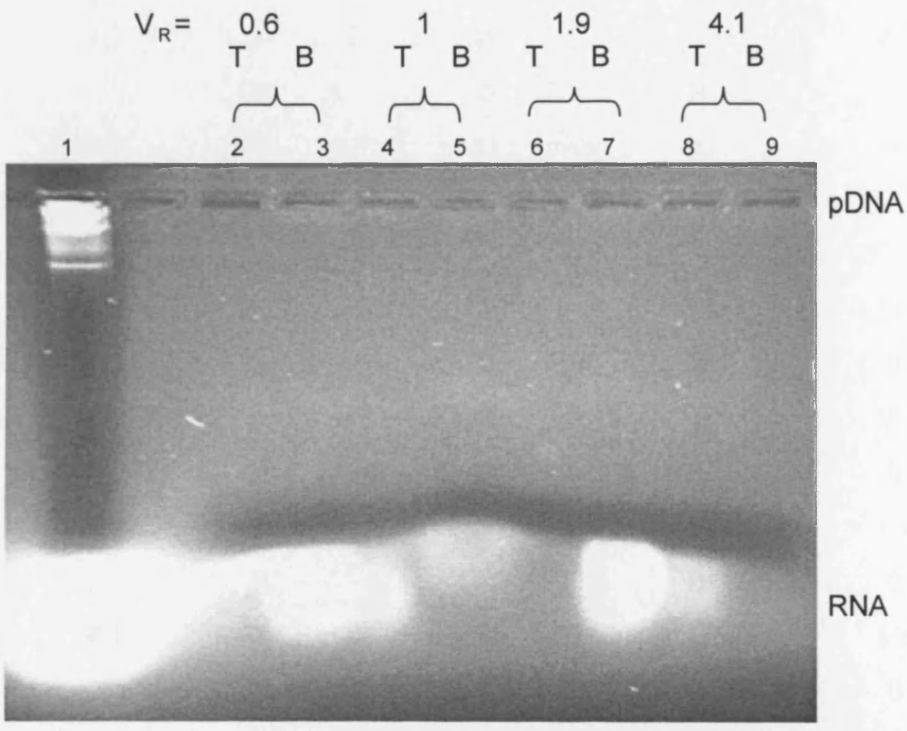

Figure 4.11: Agarose gel analysis of plasmid (P5180 - 72 kb) and RNA partitioning in ATPS with 40% (w/w) clarified lysate using different volume ratios of PEG 600 and K_2HPO_4. V_R - volume ratio of ATPS. T - top phase. B - bottom phase. Lane 1:Clarified lysate; Lanes 2 and 3: Top and bottom phases respectively for V_R= 0.6, 12.5% (w/w) PEG 600- 18% (w/w) K_2HPO_4; Lanes 4 and 5: Top and bottom phases respectively for V_R= 1, 18% (w/w) PEG 600- 18% (w/w) K_2HPO_4; Lanes 6 and 7 : Top and bottom phases respectively for V_R= 1.9, 20% (w/w) PEG 600- 12.5% (w/w) K_2HPO_4; Lanes 8 and 9: Top and bottom phases respectively for V_R= 4.1, 25% (w/w) PEG 600-10% (w/w) K_2HPO_4. 30µL of indicated phase loaded. Non-labelled tracks indicate blanks. Migration of OC and SC forms of plasmid DNA differ slightly due to the effects of PEG and salts. Wells were overloaded for ease of qualitative analysis. All samples were prepared as described in Sections 2.7.1 and 2.7.2.

	V_R	Protein concentration $\mu g.mL^{-1}$		Protein reduction (%)	
PEG 300	0.6	T	132	T	93
		B	7	B	8
	1.7	T	47	T	57
		B	0	B	0
	4.1	T	49	T	82
		B	0	B	0
	4.8	T	31	T	64
		B	0	B	0
PEG 600	0.6	T	123	T	96
		B	0	B	0
	1.0	T	95	T	97
		B	0	B	0
	1.9	T	46	T	63
		B	0	B	0
	4.1	T	59	T	98
		B	0	B	0
PEG 1000	0.4	T	48	T	29
		B	0	B	0
	1	T	83	T	83
		B	0	B	0
	1.4	T	31	T	38
		B	0	B	0
	4.1	T	24	T	41
		B	16	B	6

Table 4.5: Concentrations and recovery yields of protein from *E. coli* lysate containing plasmid P5180 – 72 kb after extraction with various ATPS of different volume ratios. T - Top phase; B - Bottom phase. The pH was not controlled and the maximum pH difference measured between the two phases was 0.52. Protein measurements were performed as described in Section 2.7.5.

4.4 Settling times and choice of phase systems for CCC experiments

It is generally desirable to choose phase systems close to the binodial curve, as the interfacial tension increases with higher polymer concentrations, and more extreme partitioning behaviour has been reported for proteins at higher polymer concentrations [Walter *et al.*, 1985]. It has also been shown that higher pDNA yields were obtained in ATPS by using polymer concentrations closest to the binodial curve (shortest tie-line length) [Trindade *et al.*, 2005]. However, as a result of the vigorous mixing present during the operation of the J-type CCC machine, the speed with which the phases systems settles (t_s) is also considered a major factor in determining if an acceptable level of stationary phase retention (S_f) can be achieved for optimal conditions [Conway *et al.*, 1990]. Thus a low settling time (preferably < 60 seconds, ideally < 20 seconds) is generally considered of paramount importance

It can been seen from Table 4.6 that systems further from the binodial curve give shorter settling times, thus it is necessary to compromise and choose a system located further from the origin of the phase diagram. Higher volume ratios resulted in an increase in settling times. PEG 600 systems have higher settling times compared to PEG 1000 due to its lower interfacial tension. In general, RNA-free lysates (Table 4.6) increased the settling times of clean ATPS (Table 3.2, Chapter 3) by around 20-30 seconds. The presence of lysates containing RNA increased the settling times of the ATPS even further, possibly due to the accumulation of RNA at the interface. Agarose gel analysis identified that the increased accumulation at the interface was found to be mostly RNA due to its higher surface area compared to pDNA. It is known that aqueous-aqueous systems usually have much higher settling times compared to organic-aqueous systems and results in Chapter 3 have shown that high stationary phase retention values could be obtained for aqueous-aqueous systems in the J-type machine depending on the choice of mobile phase and pumping direction. Thus ATPS were finally chosen on the basis of obtaining high recovery yields of plasmids and low co-partitioning of contaminants rather than on low settling times.

4.5 Discussion

It was seen that ATPS can be influenced by all the parameters examined in this chapter: Volume ratios, PEG molecular weight, pH and plasmid sizes. For PEG 600

systems, the volume ratio did not affect the recovery yields of pDNA significantly although higher concentrations were obtained with a reduction in the bottom phase volume (i.e. higher volume ratio). RNA co-partitions in a similar manner but higher amounts were observed qualitatively when higher volume ratios were used. Volume ratios of around unity (resulting in pDNA recovery yield of around 63% w/w) would appear beneficial to use for such systems to minimise co-partitioning of the contaminant RNA. Proteins partitioned entirely to the top phase and interface regardless of the volume ratio. It was also seen that recovery yields of 100% w/w can be achieved when using higher volume ratios for PEG 1000 systems. However these systems allowed a large amount of RNA to co-partition with the plasmid and were thus not considered for use in subsequent CCC studies.

For PEG 300 systems, where the plasmid partition to the upper PEG phase, the highest recovery yield achieved was 58% w/w. Plasmid partitioning in these systems increased with volume ratios, whilst qualitative analysis of RNA showed no significant increases. Protein concentrations also reduced with volume ratio and thus, it would appear beneficial to use high volume ratios when dealing with low molecular weight PEG ATPS due to the higher pDNA recovery yields and purification factors. In all cases, plasmids were seen to partition to a bulk phase and the interface.

Plasmid sizes of 5.7 and 20 kb showed similar partitioning behaviour with larger plasmids of 72 kb being dominated by interfacial tension with 100% recovery at the interface.

Higher pDNA recovery yields were obtained when using a low pH value in PEG 600 and 1000 systems. However, due to the fact that RNA co-partitioning increased significantly with lower pH values, the pH value of systems were not manipulated with only the di-basic form of potassium phosphate being used as the lower phase. This is in contrast to PEG 300 systems were the pDNA recovery yields increased with pH values.

Plasmid DNA partitioning behaviour in this chapter was explained from previous studies performed mainly by Albertsson [1986] and Johansson *et al.* [1998], and include partitioning preferences due to electrochemical potential, enthalpic/entropic contributions and PEG polymer structure. A series of experiments is performed in Chapter 5 to further clarify the pDNA partitioning behaviour in ATPS.

Although chrDNA and endotoxin analysis were not done at this stage, it is expected that both will be significantly removed at the interface with some co-partitioning with pDNA [Trindade *et al.*, 2005].

This chapter was able to quantify and optimise pDNA partitioning in ATPS by testing a range of parameters. Equally important, the partitioning of related contaminants, notably RNA and proteins, were also successfully reduced by optimising the ATPS. Volume ratios can be selected accordingly in order to significantly reduce the co-partitioning of contaminants with the pDNA. Finally, this chapter was able to define appropriate conditions and phases for subsequent CCC studies which are performed in Chapter 5.

PEG 300 (with 40 % w/w lysate RNA-free)

PEG 300	K_2HPO_4	t_S , s	V_R
10	25	83	0.4
16.2	18	92	1.3
18	18	110	1
25	12.5	175	1.4
35	10	209	4.6

PEG 300 (with 40 % w/w lysate includes RNA)

PEG 300	K_2HPO_4	t_S, s	V_R
10	25	148	0.4
16.2	18	162	1.1
18	18	180	1.1
25	12.5	326	-
35	10	290	9.5

PEG 600 (with 40 % w/w lysate RNA-free)

PEG 600	K_2HPO_4	t_S, s	V_R
12.5	18	87	0.6
18	18	101	1
20	12.5	136	1.6
25	10	150	3.8

PEG 600 (with 40 % w/w lysate includes RNA)

PEG 600	K_2HPO_4	t_S, s	V_R
12.5	18	150	0.6
18	18	172	1
20	12.5	258	1.8
25	10	277	3.8

PEG 1000 (with 40 % w/w lysate RNA-free)

PEG 1000	K_2HPO_4	t_S, s	V_R
10	16	99	0.4
18	18	80	1
18	12.5	130	1.2
25	7.5	161	4.6

PEG 1000 (with 40 % w/w lysate includes RNA)

PEG 1000	K_2HPO_4	t_S, s	V_R
10	16	136	0.4
18	18	120	1
18	12.5	172	1.2
25	8.5	198	4.6

Table 4.6: Phase settling times (t_s) as a function of phase volume ratio (V_R) for various PEG molecular weights. Systems consisted of PEG 300, PEG 600 or PEG 1000 and K_2HPO_4 with 40 % (w/w) clarified lysate (RNA-free lysate includes the addition of RNaseA). Experiments performed as described in Sections 2.5.1 and 2.5.2.

Chapter 5

Plasmid DNA Recovery and Purification in a J-Type CCC machine

5.1 Introduction

This chapter studies pDNA recovery and purification in J-type CCC using results obtained from the selection of CCC operating conditions (Chapter 3) and optimum ATPS studies for pDNA recovery and purification (Chapter 4).

Our laboratory has shown the separation of supercoiled (SC) and open circular (OC) pDNA from a Qiagen purified sample (RNA-free) to be possible using a J-type countercurrent chromatograph [Kendall *et al.*, 2001]. Results using PEG 600 as the stationary phase showed that the SC form of the plasmid was completely separated from the OC form and had been retained in the column but had partitioned back to the mobile phase. Approximately 76% (w/w) of the SC form of the plasmid was recovered in the main SC peak, while the overall recovery of the SC plasmid was 90% (w/w). The use of centrifugal precipitation chromatography (CPC) was also performed for the fractionation of protein, RNA and plasmid DNA using cationic surfactant CTAB [Tomanee *et al.*, 2004]. A satisfactory separation between RNA and pDNA was obtained with about 95.7% (w/w) and 88.7% (w/w) of RNA and protein removed respectively from the pDNA fraction. The author does not mention the recovery yield of the pDNA nor does she mention the chromosomal DNA levels in the final solution.

The aim of this chapter is to perform initial experiments using ATPS in a J-type CCC for the purification and recovery of pDNA. The specific objectives are: (i) Identify suitable operating procedures for use of ATPS in the CCC. (ii) Quantify recovery yields of pDNA. (ii) Quantify partitioning of related contaminants. (iii) Further understand pDNA partitioning in APTS. (iv) Define appropriate conditions/phases for subsequent CCC optimisation studies. Part of this work is being prepared as a publication: Al-Marzouqi I, Levy MS and Lye GJ. (2006). Capture and Purification of Plasmid DNA from *Escherichia coli* Cell Lysate using Aqueous-Aqueous Countercurrent Chromatography.

5.2 Initial results on CCC fractionation of plasmid DNA

5.2.1 Sample loading in TE buffer

Preliminary experiments using a 5 mL injection of clarified lysate (in TE buffer which is the resuspension buffer in alkaline lysis) into the column (92.3 mL) after hydrodynamic equilibrium (S_f = 43.3 % v/v) for a PEG 600 (18% w/w)-K_2HPO_4 (18% w/w) system (with lower salt phase pumped from Tail→Head) showed no satisfactory separation of RNA and plasmid DNA (Figure 5.1). A peak contained both RNA and pDNA (Figure 5.2) eluted just before the solvent front emerges (CV = 0.97). The poor separation of the DNA from RNA is probably because of the insertion of a significant volume of TE buffer, in addition to the large amount of impurities in the lysate which disturbs the hydrodynamics of the CCC column and results in excessive stripping of the stationary PEG phase. After CV= 1.09, no PEG phase remained in the column and the final pDNA recovery yield was 40% w/w. No plasmid DNA or RNA was found to be retained in the column when it was emptied.

5.2.2 Sample loading after initial batch partitioning

With the intention of overcoming this disruption to the hydrodynamic equilibrium with TE buffer, the lysate was first partitioned in a batch extraction using ATPS (20g total system with 40% w/w lysate) with the same initial composition as the bulk CCC phases, and was then separated and used for sample injection into the CCC machine. This batch partitioning step exchanges the initial TE buffer for the mobile phase used in CCC, and provides a preliminary purification reducing the amount of contaminant RNA, proteins and chromosomal DNA loaded. For PEG 600 systems, the salt phase was injected into the CCC, while for PEG 300 systems, PEG phase was injected. The systems used were based on the best results obtained from Section 4.3 where volume ratios and pH effects on plasmid DNA were tested.

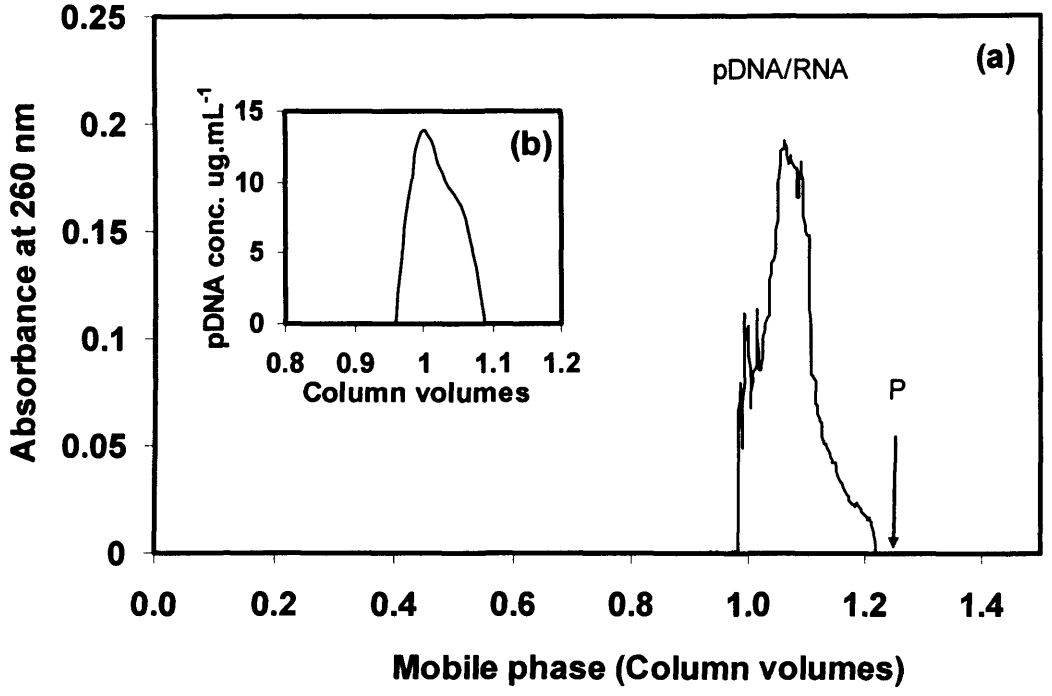

Figure 5.1: (a) CCC chromatogram of plasmid DNA (5.7 kb) and RNA separation using a phase system comprised of 18% (w/w) PEG 600 (stationary phase) and 18% (w/w) K_2HPO_4 (mobile phase) at 600 rpm and a mobile phase flow rate of 0.5 mL.min^{-1} (S_f= 43.3 % v/v). Mobile phase pumped from TAIL→ HEAD. *P* is the point at which rotation is stopped and column contents are pumped out. Feed prepared as described in Section 2.3 and contained 28 µg.mL^{-1} pDNA. Retention time of plasmid DNA/RNA was 1.06 column volumes. (b) pDNA concentration analysed by HPLC as described in Section 2.7.4.

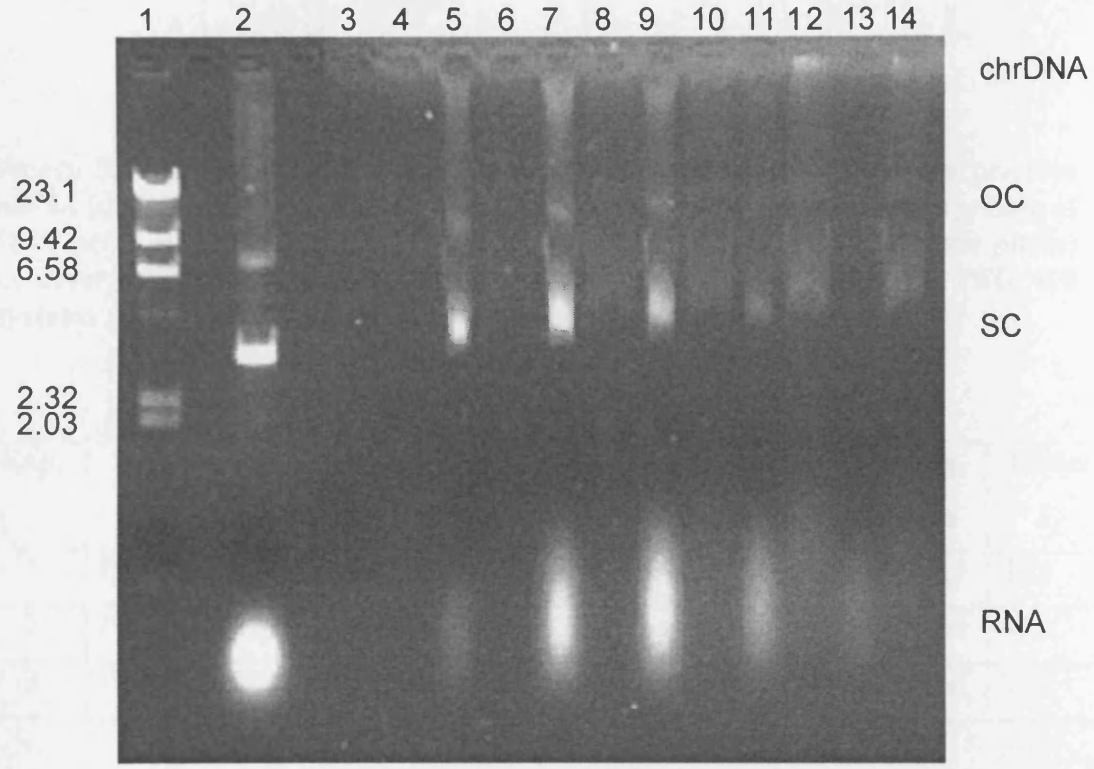

Figure 5.2: Agarose gel analysis of lysate feed and selected fractions collected during the CCC run shown in Figure 5.1. Lane 1: DNA ladder; Lane 2: Clarified lysate- feed (28 µg.mL^{-1} pDNA); Lanes 3, 5, 7, 9, 11 and 13 are top phase (stripped stationary PEG phase) fractions eluted after 0.96, 0.98, 1.00, 1.03, 1.06 and 1.09 column volumes respectively; Lanes 4, 6, 8, 10, 12 and 14 are bottom phase fractions eluted after 0.96, 0.98, 1.00, 1.03, 1.06 and 1.09 column volumes respectively. 30µL of indicated phase loaded. Non-labelled tracks indicate blanks. Migration of OC and SC forms of plasmid DNA differ slightly due to the effects of PEG and salts. Experiments were performed as described in Section 2.7.2.

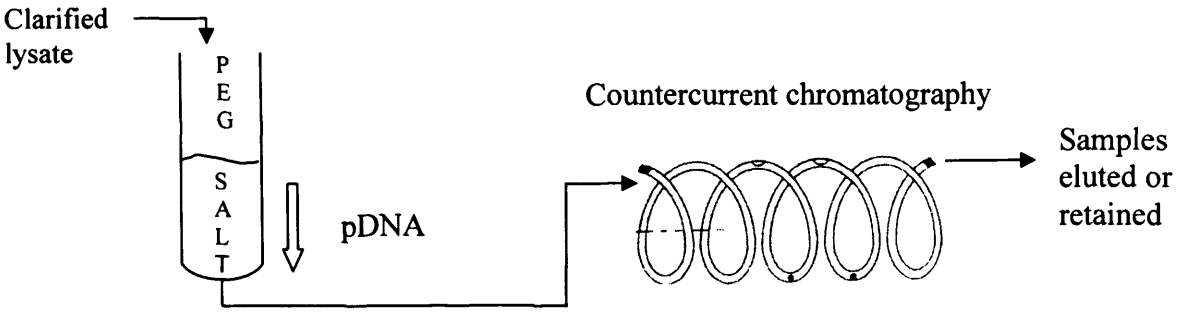

Figure 5.3: Procedure for lysate pre-purification and buffer exchange prior to pDNA loading onto the CCC column illustrated for a lysate system comprising of 18% (w/w) PEG 600 (stationary phase) and 18% (w/w) K_2HPO_4 (mobile phase) as described in Section 2.6.2. The diagram shows the procedure for PEG 600 systems where the DNA partitions to the bottom K_2HPO_4 phase.

Exp.	Phase system	V_R	Mobile phase	Pumping Direction	Initial S_f	Final S_f
1	PEG 600 (18%) - K_2HPO_4 (18%)	1.3	Lower salt	Head→Tail	30.3	18.4
2	PEG 600 (18%) - K_2HPO_4 (18%)	1.3	Lower salt	Tail→Head	43.3	23.8
3	PEG 300 (30%) - K_2HPO_4 (10%)	4.8	Upper PEG	Head→Tail	35.8	35.1

Table 5.1: Initial ATP systems and operating modes chosen for CCC runs with plasmid DH5α-gWiz (5.7 kb). V_R denotes phase volume ratio.

A number of experiments were performed using the batch pre-purification ATPS as shown in Table 5.1. Figure 5.4 shows the resulting chromatograph for a PEG 600 (18% w/w)-K_2HPO_4 (18% w/w) phase system with the salt phase being pumped from Head→Tail (Exp 1, Table 5.1). The batch step ATPS had initially reduced the RNA contaminant (see Figure 5.5, Lane 4) and no protein was detected in the lower salt phase with 56% w/w of pDNA recovered (Table 5.2). 5 ml of the salt phase was then loaded onto the equilibrated column at a mobile phase flow rate of 0.5 $mL.min^{-1}$. A peak was seen after 1.16 column volumes with the fractions eluting comprising primarily the mobile salt phase plus some stripped PEG phase. Gel electrophoresis of both these phases showed the peak contained RNA which eluted in the stripped PEG phase (Figure 5.5). This was surprising as the RNA was shown earlier to partition

mainly to the salt phase in batch ATPS (Section 4.3). A second peak was seen once the column rotation was stopped and the stationary phase pumped out with nitrogen. The majority of the plasmid DNA was found to have been retained within the column. The plasmid DNA was collected in the latest fractions (head end), corresponding to positions close of the point of sample injection and was also present in the PEG phase. No RNA, protein or chrDNA was detected in the pDNA fractions, with off-line HPLC analysis showing recovery yields of 96% (w/w) of the injected pDNA. The overall 2-step process recovery yield including the initial batch partition was 54% (w/w). The total species mass balances are given in Table 5.2.

Although the pDNA and RNA were expected to elute with the salt mobile phase, the main reasons for this is likely to be the high viscosity of the stationary PEG phase, which coupled with the large dynamic volume of DNA molecules [Ito *et al.,* 1998] may limit the mass transfer of the DNA out of the stationary phase during the multiple partitioning steps in CCC. In addition, high interfacial areas between ATPS are expected (due to the low interfacial tension) between the phases [Hatti-Kaul, 1999] which coupled with the large interface present within the coil due to high rotation and mixing, could also result in retention of the plasmid in the PEG phase. The collapse of DNA in PEG solutions can also influence the partitioning. PEG concentrations are relatively low due to the low initial S_f and some degree of PEG stripping that occurs (reducing the initial S_f = 30.3% v/v to 18.4% v/v at end of run). At these lowered PEG concentrations, the flexible polymer chains of PEG can penetrate inside the pDNA which adopts a coil conformation, and a region of compatibility exists between the PEG and pDNA [Vasilevskaya *et al.* 1995]. Compared to batch ATPS where a higher concentration of PEG is available and constant, the solvent quality of PEG for DNA is poor and the effective attraction between the DNA segments in the macromolecule increases with segregation between the DNA chains and the PEG molecules. The DNA thus adopts a compact globular structure leaving the DNA in the salt phase [Vasilevskaya *et al.*, 1995].

In order to further understand the reasons for the observed pDNA partition to the PEG phase during the run, further experiments were performed to examine whether pDNA partitioning was influenced by the presence of the initial buffer that the pDNA was resuspended in or due to the low PEG concentration (resulting in very low

volume ratios) that exist at the end of the run (shown in Section 5.2.3). Previous experiments using small volumes (1mL) of pure DNA (RNA free) samples in J-type CCC machine showed similar results [Kendall *et al.*, 2001]. The initial batch APT extraction proven to be successful in reducing the disturbance on the hydrodynamic equilibrium and also in removing a significant proportion on RNA, chrDNA and proteins prior to CCC experiments. Thus all subsequent CCC runs will adopt this approach using the appropriate phase system.

Exp.	Phase/Sample	Total plasmid ($\mu g.mL^{-1}$)	pDNA Recovery yield (%)	Protein ($\mu g.mL^{-1}$)	Genomic DNA ($\mu g.mL^{-1}$)
1	Lysate	26	-	80	3
	Batch ATP -Top phase	-	-	32	-
	Batch ATP -Bottom phase	16	56	BDL	-
	CCC fraction	7	54 (total) 96 (injected)	BDL	BDL
2	Lysate	22	-	82	2.5
	Batch ATP -Top phase	-	-	45	-
	Batch ATP -Bottom phase	17	55	BDL	-
	CCC fraction	6	45 (total) 80 (injected)	BDL	BDL
3	Lysate	31		73	3.6
	Batch ATP -Top phase	7	42	29	-
	Batch ATP -Bottom phase	-	-	20	-
	CCC fraction	6	41 (total) 97 (injected)	BDL	BDL

Table 5.2: Concentrations of plasmid DNA, protein and chromosomal DNA in the lysate and after the combined batch extraction –CCC process. Total plasmid DNA concentrations were measured by HPLC as described in Section 2.7.4. Protein concentration were measured as described in Section 2.7.5. chrDNA concentrations were measured as described in Section 2.7.6. BDL: Below detectable limit.

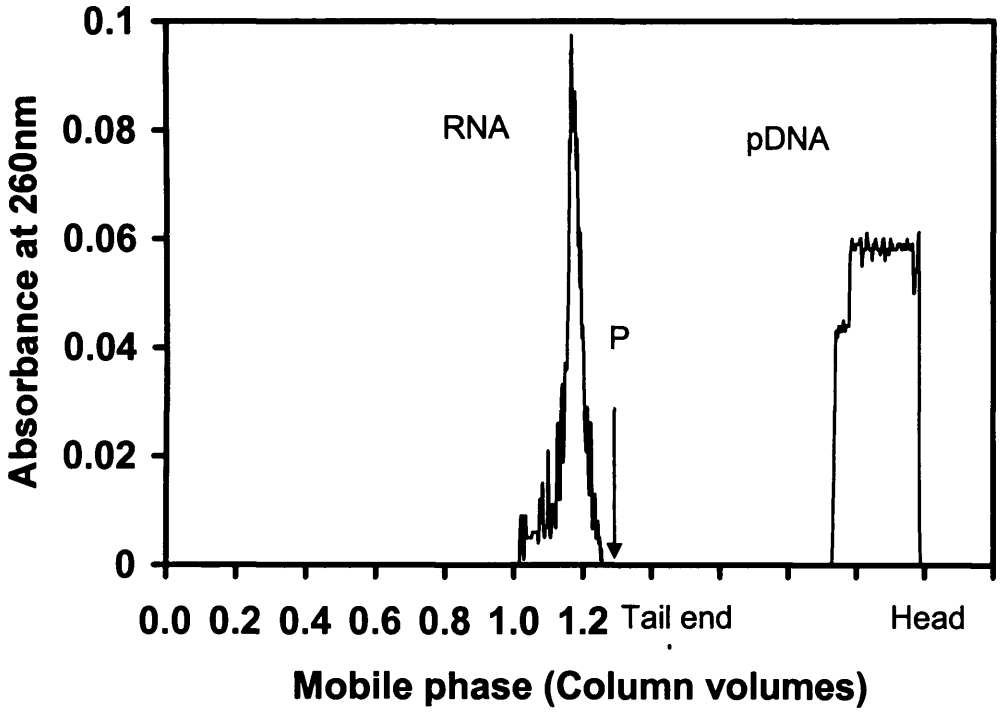

Figure 5.4: CCC chromatogram of plasmid DNA (5.7 kb) and RNA separation using a phase system comprised of 18% (w/w) PEG 600 (stationary phase) and 18% (w/w) K_2HPO_4 (mobile phase) at 600 rpm and a mobile phase flow rate of 0.5 mL.min^{-1} (S_f= 30.3% v/v). Mobile phase pumped from HEAD→TAIL. *P* is the point at which rotation is stopped and column contents are pumped out. Feed prepared as described in Section 2.6.3 and contained 26 µg.mL^{-1} pDNA. Retention time of RNA was 1.16 CV.

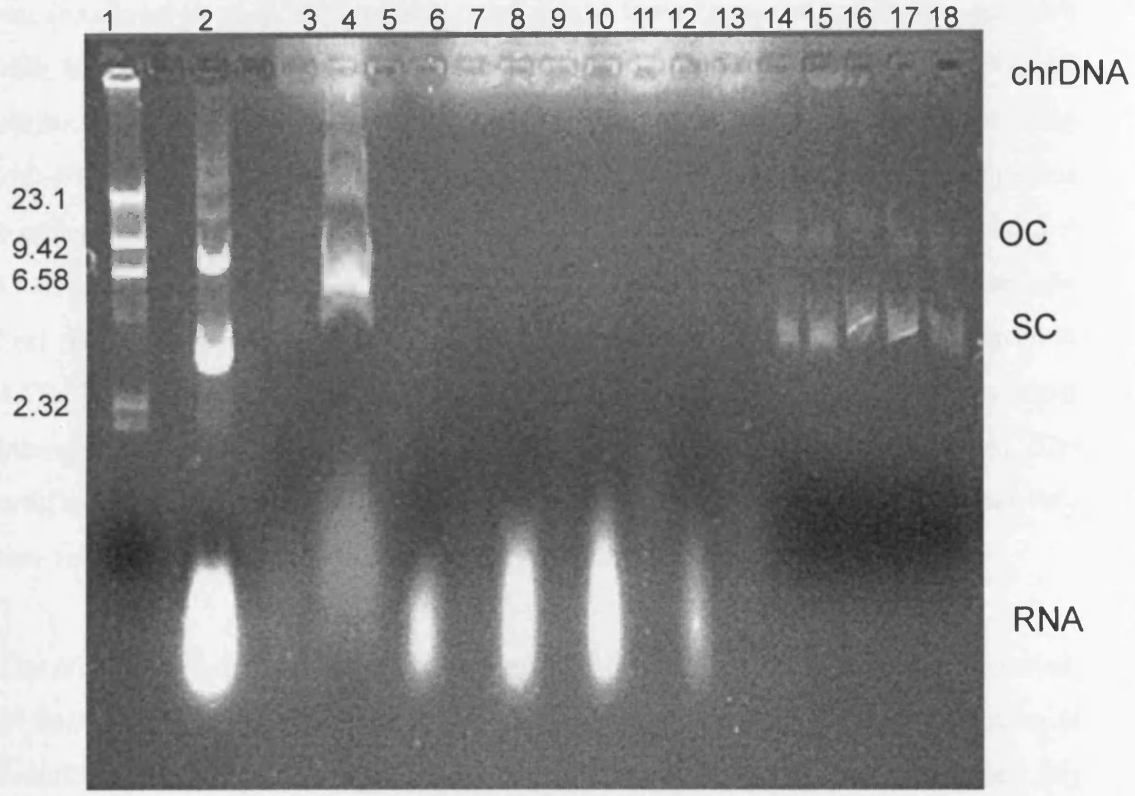

Figure 5.5: Agarose gel analysis of lysate feed and selected fractions collected during the initial batch ATP extraction and CCC run shown in Figure 5.4. Lane 1: DNA ladder; Lane 2: Clarified lysate (26 µg.mL^{-1} pDNA); Lane 3: Top phase of batch ATP extraction; Lane 4: Bottom phase of batch ATP extraction-CCC feed; Lanes 6, 8, 10 and 12 are top phase (stripped stationary PEG phase) fractions eluted after 1.14, 1.16, 1.17 and 1.19 column volumes respectively; Lanes 7, 9, 11 and 13 are bottom phase fractions eluted after 1.14, 1.16, 1.17 and 1.19 column volumes respectively; Lanes 14, 15, 16, 17 and 18 are fractions collected during pump out of the coil at 88, 89, 90, 92 and 95% (v/v) of column eluted. 30µL of indicated phase loaded. Non-labelled tracks indicate blanks. Migration of OC and SC forms of plasmid DNA differ slightly due to the effects of PEG and salts. Experiments were performed as described in Section 2.7.2

5.2.3 Effects of initial buffer selection and low volume ratios on pDNA partitioning

Initially, it was thought that the low PEG concentrations remaining at the end of the run (resulting in very low volume ratio) might have caused the pDNA to partition back to the PEG phase. Lysate suspended in TE buffer (Exp. a, Figure 5.6) showed partitioning of pDNA and RNA to the salt phase for PEG 600 systems when using low PEG and high salt contents comparable to the stationary and mobile phases compositions remaining at the end of the CCC run described in Figure 5.4 (final S_f= 18.4% v/v). In addition, an ATPS was tested in which the lysate (in TE buffer) was first resuspended in 4.5% (w/w) PEG 600 and then added to an ATPS comprised to 4.5% (w/w) PEG 600 and 25% (w/w) salt. This was done to test if the initial interaction of PEG with pDNA might affect partitioning (Exp. b, Figure 5.6). The results again showed that pDNA and RNA partitioned to the salt phase and that very low volume ratios did not affect plasmid partitioning in such systems.

The order in which the different components of the ATPS were added was also tested. In Section 4.3, ATP experiments used the following order during phase formation as described in Section 2.5.1: Water→Salt→PEG→Lysate. The lysate was added last once the two phases had clearly formed. Experiments in which the lysate was mixed with either PEG or salt initially were performed as follows: Lysate (40% w/w)→Salt (18% w/w)→Water→PEG 600 (18% w/w; Exp. c in Fig. 5.6) and Lysate (40% w/w)→PEG 600 (18% w/w)→Water→Salt (18% w/w; Exp d in Fig. 5.6). Agarose gel electrophoresis results showed that initial mixing of the lysate to PEG or salt again did not affect the partitioning of pDNA or RNA which was always to the bottom salt phase (Figure 5.8).

Finally, experiments were performed to see if pDNA resuspended first in a ATPS might affect partitioning in a subsequent ATPS. 2.5 mL of the bottom salt phase (Exp. a, Figure 5.7) of a system comprised 18% (w/w) PEG 600 and 18% (w/w) K_2HPO_4 with 40% lysate (w/w) in TE buffer where the pDNA and RNA partition to the bottom phase (same as CCC feed in Section 5.2.2) was injected into a batch ATPS with low PEG (4.5% w/w) and high salt (25% w/w). These compositions are comparable to the stationary and mobile phases remaining at the end of the CCC run

described in Section 5.2.2 (Exp b, Figure 5.7). Results showed the pDNA and RNA to partition back to the PEG 600 phase (Lanes 7-10, Figure 5.8) confirming what was observed in the CCC experiments. A white precipitate was seen in the top PEG phase for experiment (b) - Figure 5.7 probably due to the increased salting-out of pDNA/RNA at this high salt concentration which diminishes the interactions between the pDNA/RNA and water in the lower phase. The recovery yields obtained from the first ATPS was 52% (w/w) whilst the second APTS only resulted in a recovery yield of 12% (w/w) with most of the pDNA being lost at the interface. Some pDNA can be seen in the bottom phase but was found to be below detectable limits when analysed by HPLC. It is interesting to note that even after two ATP extractions, RNA can clearly be seen to co-partition with the pDNA.

It can thus be concluded that the change in partitioning preference of pDNA is due to the plasmid being in the salt phase initially. Subsequent partitioning to the PEG phase might be due to a change in the pDNA structure [Vasilevskaya *et al.* 1995], a change in the electrostatic potential difference $\Delta\psi$ (due to the plasmid's charge being more negative or lower ionic strength of the system) [Albertsson, 1986], enthalpic contributions due to the higher self energy of the PEG phase [Johansson *et al.*, 1998] or increased salting-out effects in the lower phase. The effect of lowered interfacial tension might also be a reason and is explained in Section 6.8. Whatever the explanation, the results of these batch ATP extractions demonstrate the need for the CCC step in which much higher recovery yields and purer pDNA is obtained with minimal RNA contamination

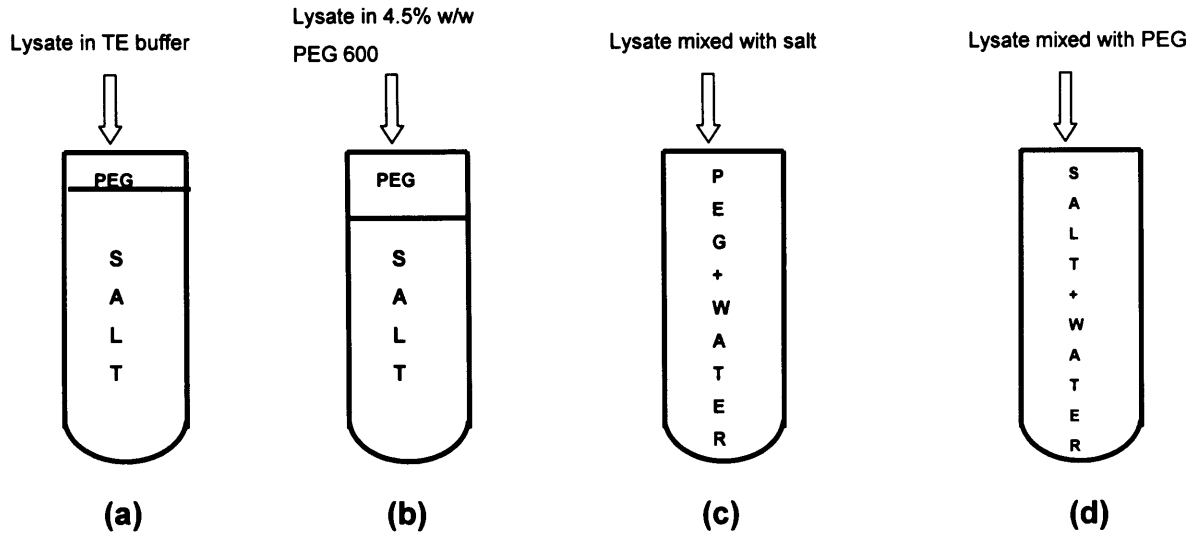

Figure 5.6: Experiments performed to test the effect of very low volume ratios and order of component addition to the ATPS. (a) ATPS comprised of 4.5% (w/w) PEG 600 and 25% (w/w) K_2HPO_4 with 40% (w/w) addition of clarified lysate in TE buffer, V_R= 0.25 (b) ATPS comprised of 4.5% (w/w) PEG 600 and 25% (w/w) K_2HPO_4 with 40% (w/w) addition of clarified lysate in TE buffer mixed initially with 4.5% (w/w) PEG 600, V_R= 0.38 (c) ATPS comprised of 18% (w/w) PEG 600 and 18% (w/w) K_2HPO_4 with 40% (w/w) clarified lysate added in the following order: Lysate→Salt →Water→PEG 600. The lysate and salt were mixed for 30 minutes before adding water and PEG. (d) ATPS comprised of 18% (w/w) PEG 600 and 18% (w/w) K_2HPO_4 with 40% (w/w) clarified lysate added in the following order: Lysate→PEG→Water→Salt. The lysate and PEG were mixed for 30 minutes before adding the water and salt.

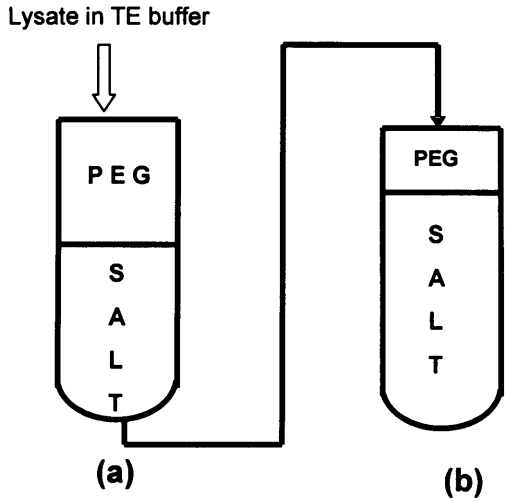

Figure 5.7: (a) ATPS comprised of 18% (w/w) PEG 600 and 18% (w/w) K_2HPO_4 with 40% (w/w) addition of clarified lysate in TE buffer. (b) ATPS comprised of 4.5% (w/w) PEG 600 and 25% (w/w) K_2HPO_4 with 2.5 mL addition of the lower salt phase from experiment (a).

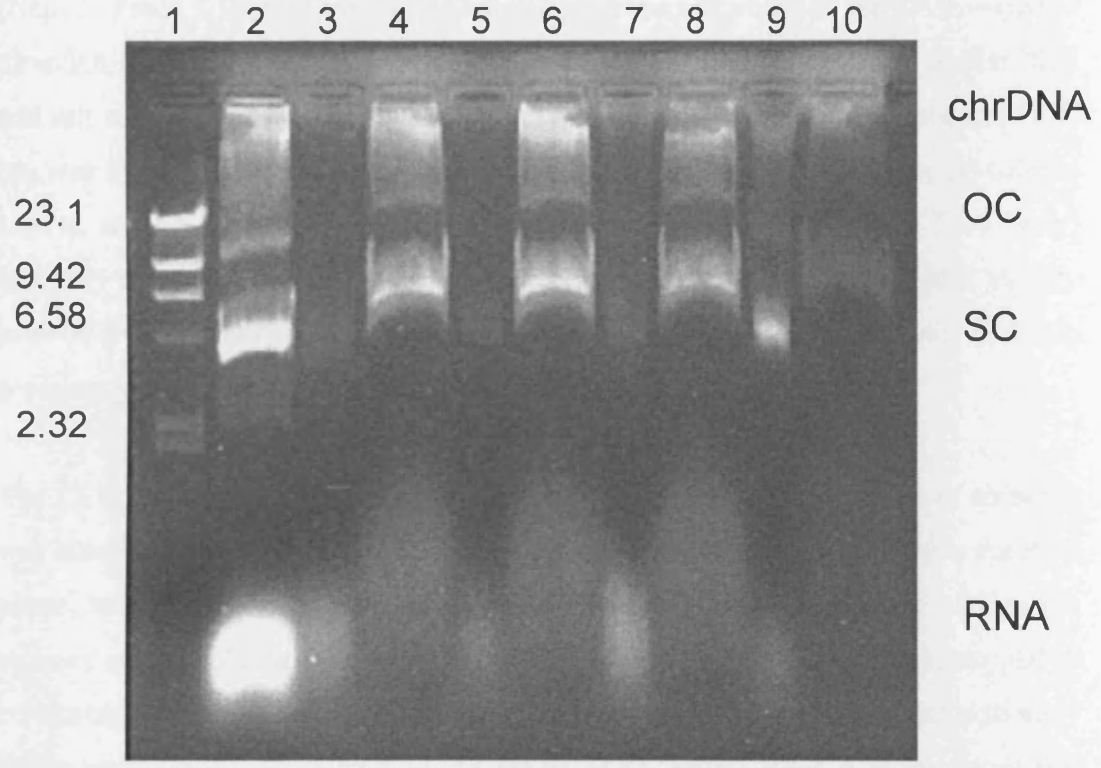

Figure 5.8: Agarose gel analysis of plasmid (gWiz-5.7 kb) and RNA partitioning in ATPS for samples described in Figures 5.6 and 5.7. Lane 1: DNA ladder; Lane 2: Clarified lysate; Lanes 3 and 4: Top and bottom phases respectively for experiment (c) described in Figure 5.6, V_R= 1.13; Lanes 5 and 6: Top and bottom phases respectively for experiment (d) described in Figure 5.6, V_R= 1.4; Lanes 7 and 8: Top and bottom phases respectively for experiment (a) described in Figure 5.7, V_R= 1.13; Lanes 9 and 10: Top and bottom phases respectively for experiment (b) described in Figure 5.7, V_R= 0.23. Initial lysate concentration 26 $\mu g.mL^{-1}$ pDNA. Recovery of pDNA in the lower salt phase of experiment (a)- Figure 5.7 was 52% (w/w) whilst the total recovery yield for experiment (b)- Figure 5.7 was 12% (w/w) in the upper PEG phase when measured using off-line HPLC as described in Section 2.7.4. 30µL of indicated phase loaded. Non-labelled tracks indicate blanks. Migration of OC and SC forms of plasmid DNA differ slightly due to the effects of PEG and salts. Experiments were performed as described in Section 2.7.2.

5.2.4 CCC fractionations carried out in TAIL→HEAD mode

Experiments with the PEG 600 system at a higher initial stationary phase retention (Exp. 2, Table 5.1) were performed by pumping the salt phase in the TAIL→HEAD direction (Figure 3.3, Chapter 3). Again, a batch ATP extraction using similar PEG and salt compositions as the stationary and mobile phase used in the subsequent CCC run was used to minimise disturbance of the hydrodynamic equilibrium in the column and to reduce RNA contaminant. The batch extraction resulted in a 55% (w/w) recovery of pDNA to the bottom phase. Off-line HPLC analysis showed a slightly lower CCC recovery yield (80% w/w) than in Experiment 1, while the overall 2-step recovery yield of pDNA was 45% (w/w) (Table 5.3).

The CCC chromatogram of this run is shown in Figure 5.9. Some degree of stripping was observed, and the RNA and pDNA were again partitioned irreversibly to the PEG phase, with RNA eluting with the stripped PEG (after CV= 1.16) whilst pDNA was retained in the column. The lower recovery yield in this case is due to some pDNA co-eluting with the RNA in the stripped stationary PEG phase. The final stationary phase retention was reduced from 43.3% to 23.8% (w/w). Thus it is concluded that the separation of pDNA from RNA and the resulting recovery yield in such systems might not depend on the initial stationary phase retention. Rather, it might depend on the degree of stripping that results from the movement of the mobile phase through the coil. S_f was reduced by 19.5% (v/v) for the TAIL→HEAD mode compared to 11.9% (v/v) for the HEAD→TAIL mode. Thus the increased loss of the stationary phase resulted in some pDNA being lost with the RNA. The loss of the stationary phase during the run is probably due to the presence of some alkaline-lysis buffers (described in Section 2.3) carried forward to the lower phase (and not due to the pDNA) which disturbed the hydrodynamic equilibrium to some degree, as injection of an identical cell-free volume showed the same amount of stationary phase loss during the run (results not shown). The retention time for the RNA peak was comparable to results obtained by pumping the salt phase in the reverse direction and was 224 minutes (CV= 1.21). Chromosomal DNA analysis (described in section 2.7.6) were below the detectable limit for the CCC fraction retained in the column.

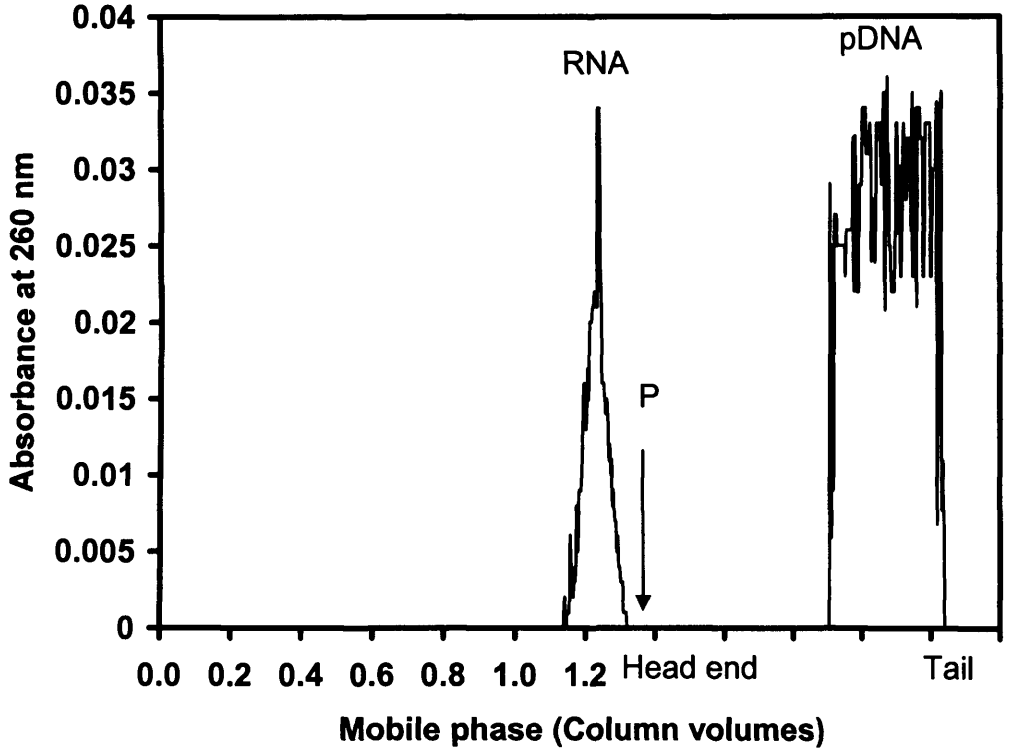

Figure 5.9: CCC chromatogram of plasmid DNA (5.7 kb) and RNA separation using a phase system comprised of 18% (w/w) PEG 600 (stationary phase) and 18% (w/w) K_2HPO_4 (mobile phase) at 600 rpm and a mobile phase flow rate of 0.5 mL.min^{-1} (S_f = 43.3% v/v). Mobile phase pumped from TAIL→HEAD. *P* is the point at which rotation is stopped and column contents are pumped out. Feed prepared as described in Section 2.6.3 and contained 22 µg.mL^{-1} pDNA. Retention time of RNA was 1.21 CV.

5.2.5 CCC fractionations with PEG 300 systems

To avoid the retention of pDNA in the column, one process option would be to operate with a lower molecular weight PEG where the plasmid partitions to the upper PEG phase. In this case, PEG 300 was used as the mobile phase (Exp 3, Table 5.1). Minimal stripping of the stationary salt phase occurred during the PEG elution indicating that a less viscous phase stationary phase might be better suited for CCC operation. From Section 4.3.1, it was recommended to use higher volume ratios for PEG 300 systems in order to obtain higher pDNA recovery yields and reduce protein co-partitioning. A 30% (w/w) PEG 300-10% (w/w) K_2HPO_4 systems was selected for both the initial batch extraction and the subsequent CCC.

The initial batch extraction resulted in the pDNA partitioning to the top PEG phase with a 42% (w/w) recovery yield. Proteins also co-partitioned with pDNA but with a 29% (w/w) reduction compared to the lysate. 5 ml of the top phase was subsequently injected into the CCC column at a mobile phase flow rate of 0.5 $mL.min^{-1}$. The chromatogram (Figure 5.10) shows a large peak eluting between 0.75-1.1 CV with a peak retention time of 161 minutes (CV=0.87). Upon further off-line analysis (Figure 5.11), it was seen that initially RNA was eluted until 0.96 CV followed by pDNA. The CCC recovery yield was 97% (w/w) pDNA as measured by HPLC analysis of the eluted fractions making the overall 2-step recovery yield 41% (w/w) (Table 5.2). No RNA, protein or chrDNA were detected with the eluting pDNA samples from the CCC.

Compared to PEG 600 systems, the pDNA elutes here with the mobile phase as expected due to the lowered viscosity of PEG 300 allowing the more rapid transfer of pDNA back into the mobile phase during the multiple partitioning steps occurring during the CCC run. No pDNA was found to be retained in the column. It is interesting to note that RNA samples were collected as two phases as some stationary salt phase was stripped from the column as the RNA elutes, whereas pDNA samples consisted of only the eluting PEG phase. Thus is seems that it is the stripping of the stationary phase that results in the contaminant RNA being removed whether PEG or salt is used as the stationary phase. This is surprising and may indicate that high S_f values are not critical for ATP pDNA separations compared to small molecule

separations with organic-aqueous systems where high S_f values are normally required for efficient chromatography [Ito & Conway, 1996].

5.3 CCC fractionations using 20 kb plasmid

CCC separations using a larger 20 kb plasmid were also performed using PEG 600 systems. The 20 kb plasmid was found to behave identically to the 5.7 kb plasmid with pDNA again being retained at the point of injection (Figure 5.12) in the PEG phase, while RNA eluted during the run and was found to be in the stripped PEG phase. Recovery yields of 50 % (w/w) and 71% (w/w) were obtained for the bottom batch ATP extraction (V_R=1) and eluted CCC fractions respectively (Table 5.2). The overall pDNA recovery yield for the 2-step process was thus 35% (w/w). The retention time was identical to the 5.7 kb plasmid being pumped in the same direction (CV=1.21).

Contaminant protein and chrDNA in the main pDNA fractions were below the minimum detectable level (using methods described in Section 2.7.5 and 2.7.6 respectively). In addition no RNA was detected in CCC purified samples (Figure 5.13). The lowered recovery in the initial batch ATP extraction compared to experiments with similar volume ratios (Table 4.3) was due to the lower initial concentration of the plasmid and lower volume ratio [Ribeiro *et al.*, 2002]. The lower CCC recovery yield compared to the 5.7 kb plasmid was probably due to some plasmid losses during the gradual stripping of the stationary PEG phase (S_f was reduced from 46.6% to 20.6% v/v). Although the CCC recovery yield in this case was around 25% lower compared to the smaller plasmid, the 20kb plasmid eluted in almost half the volume (5ml) compared to the 5.7kb (11.2 ml) plasmid resulting n a higher volume concentration factor. It can be concluded that CCC is suitable for the purification of pDNA at least upto 20kb in size but that the pDNA recovery yield decreases with size.

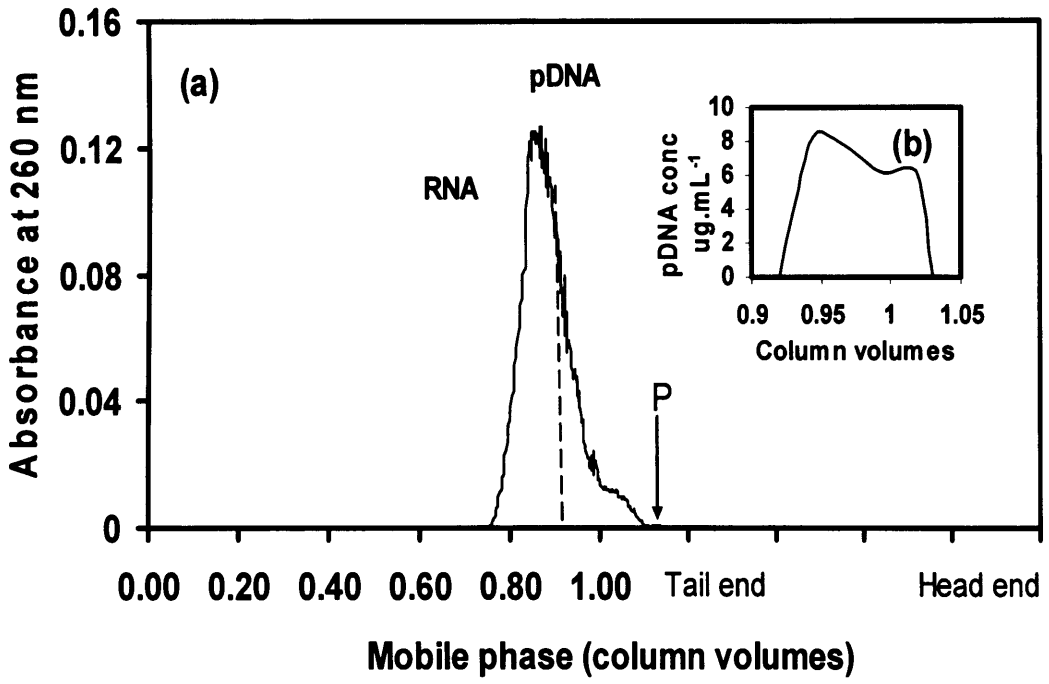

Figure 5.10: (a) CCC chromatogram of plasmid DNA (5.7 kb) and RNA separation using a phase system comprised of 30% (w/w) PEG 300 (mobile phase) and 10% (w/w) K_2HPO_4 (stationary phase) at 600 rpm and a mobile phase flow rate of 0.5 mL.min^{-1} (S_f = 35.8% v/v). Mobile phase pumped from HEAD→TAIL. *P* is the point at which rotation is stopped and column contents are pumped out. Feed prepared as described in Section 2.6.3 and contained 31 µg.mL^{-1} pDNA. Retention time of was 0.87 CV. (b) pDNA concentration (0.96-1.1 CV) analysed by HPLC as described in Section 2.7.4.

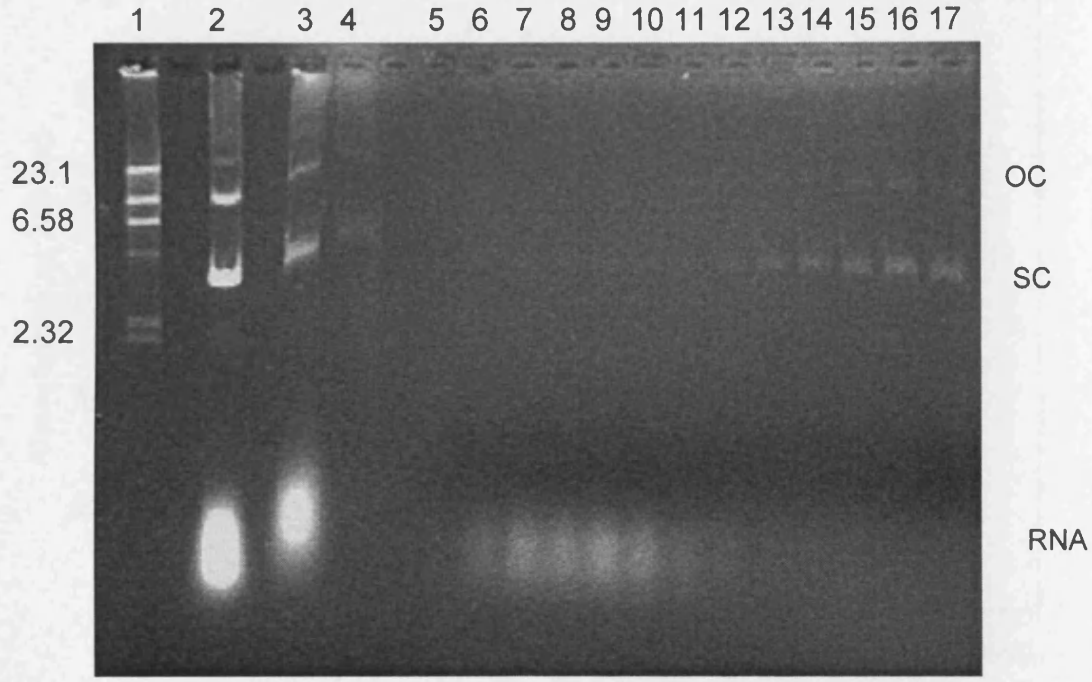

Figure 5.11: Agarose gel analysis of lysate feed and selected fractions collected during the initial batch ATP extraction and CCC run shown in Figure 5.10. Lane 1: DNA ladder; Lane 2: Clarified lysate (31 μg.mL^{-1} pDNA); Lane 3: Top phase of batch ATP extraction- CCC feed; Lane 4: Bottom phase of batch ATP extraction; Lanes 5, 6, 7, 8, 9, 10, 11 and 12 are top phase (mobile PEG phase) fractions eluted after 0.75, 0.78, 0.81, 0.83, 0.85, 0.86, 0.89 and 0.93 column volumes respectively; Lanes 13, 14, 15, 16 and 17 are top phase (mobile PEG phase) fractions eluted after 0.96, 0.98, 0.99, 1 and 1.02 column volumes respectively. 30μL of indicated phase loaded. Non-labelled tracks indicate blanks. Migration of OC and SC forms of plasmid DNA differ slightly due to the effects of PEG and salts. Experiments were performed as described in Section 2.7.2.

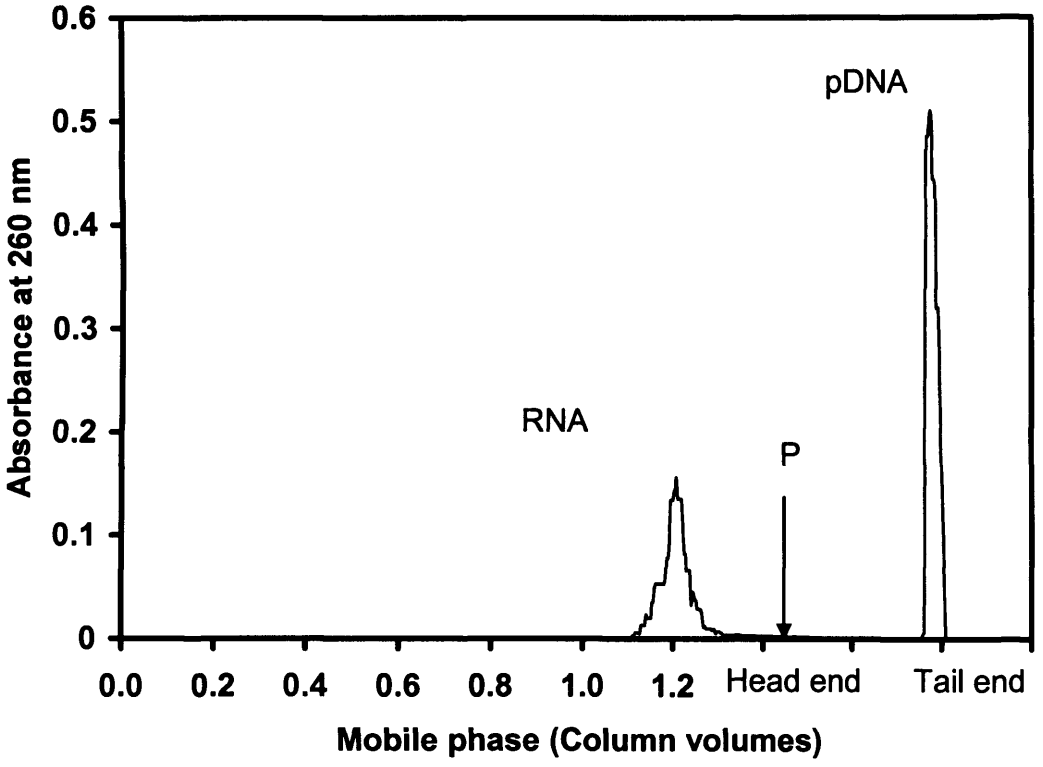

Figure 5.12: CCC chromatogram of plasmid DNA (20 kb) and RNA separation using a phase system comprised of 18% (w/w) PEG 600 (stationary phase) and 18% (w/w) K_2HPO_4 (mobile phase) at 600 rpm and a mobile phase flow rate of 0.5 mL.min^{-1} (S_f = 46.6% v/v). Mobile phase pumped from TAIL→HEAD. *P* is the point at which rotation is stopped and column contents are pumped out. Feed prepared as described in Section 2.6.3 and contained 13 µg.mL^{-1} pDNA. Retention time for RNA was 1.21 CV.

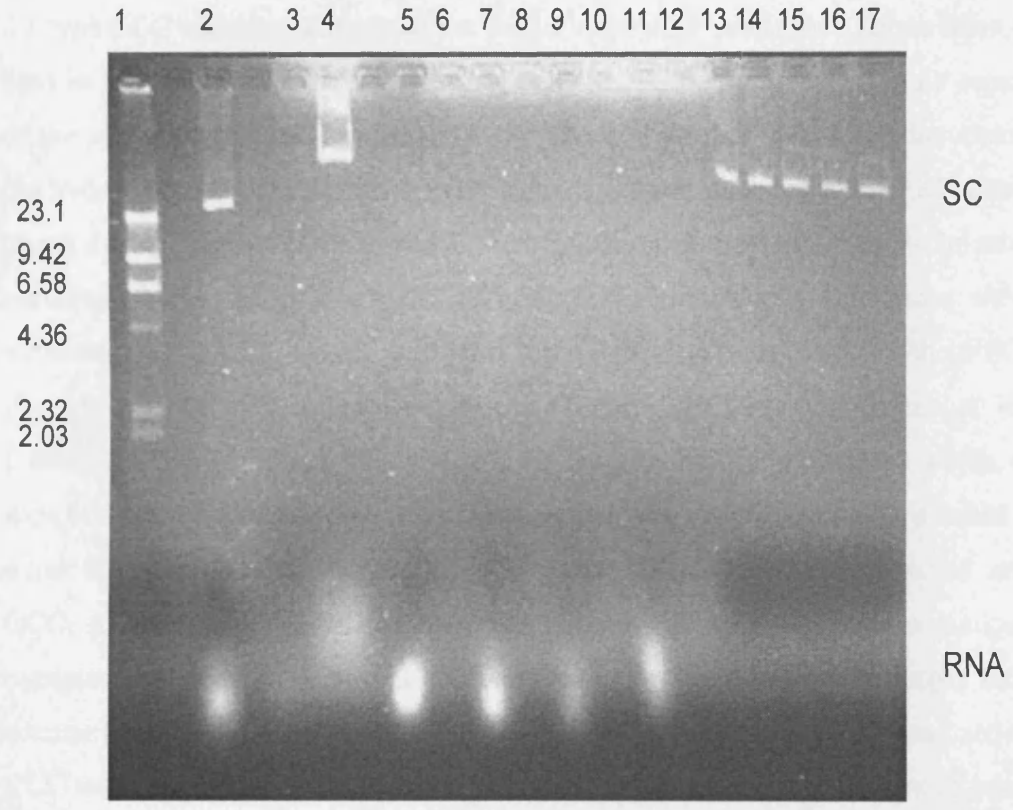

Figure 5.13: Agarose gel analysis of lysate feed and selected fractions collected during the initial batch ATP extraction and CCC run shown in Figure 5.12. Lane 1: DNA ladder; Lane 2: Clarified lysate (13 pDNA $\mu g.mL^{-1}$); Lane 3: Top phase of batch ATP extraction; Lane 4: Bottom phase of batch ATP extraction-CCC feed; Lanes 5, 7, 9 and 11 are top phase (stripped stationary PEG phase) fractions eluted after 1.18, 1.19, 1.21 and 1.22 column volumes respectively; Lanes 6, 8, 10 and 12 are bottom phase fractions eluted after 1.18, 1.19, 1.21 and 1.22 column volumes respectively; Lanes 13, 14, 15, 16 and 17 are fractions collected during pump out of the coil at 94, 96, 97, 99 and 100% (v/v) of column eluted. 30µL of indicated phase loaded. Non-labelled tracks indicate blanks. Migration of OC and SC forms of plasmid DNA differ slightly due to the effects of PEG and salts. Experiments were performed as described in Section 2.7.2.

5.4 Discussion

Initial experiments revealed that separation of pDNA and RNA can be achieved using a J-type CCC machine in conjunction with a batch ATP extraction. Formulation of the feed in buffer in which DNA is readily soluble (TE buffer) resulted in no separation of the pDNA from contaminant RNA (Figures 5.1 and 5.2) due to the disturbance on the hydrodynamic equilibrium which caused excessive stripping of the PEG stationary phase during the run and resulted in zero retention at the end. With the intention of reducing the disturbance on the hydrodynamic equilibrium, the lysate was first extracted in a ATP system with the same initial compositions of the PEG and phosphate to be used in the CCC system (Figure 5.3). This step exchanged the TE buffer for PEG (for PEG 300 systems) or salt (for PEG 600 systems) which would then be selected as the mobile phase during the following CCC run. This initial batch extraction reduced the amount of contaminant RNA and protein injected into the CCC. Although removal of chrDNA was not quantified for the batch extraction, it is expected that there will be a significant reduction due to its much larger size and accumulation at the interface [Ribeiro *et al.*, 2002]. When PEG 600 was used as the CCC stationary phase, pDNA was retained within the column at the point of injection. RNA eluted during the run. Surprisingly, both pDNA and RNA were found to be in the PEG phase even though batch ATPS results suggest that both would partition to the salt phase.

The reversal in partitioning preference could be due to a number of reasons. The high viscosity of the stationary PEG phase, coupled with the large dynamic volume of DNA molecules [Ito *et al.*, 1998] may reduce the mass transfer of the DNA out of the stationary phase during the run. In addition, ATPS result in the formation of high interfacial areas due to their low interfacial tensions [Hatti-Kaul, 1999]. This coupled with the high degree of mixing in the coil due to the high rotational speeds used, could result in the increased retention of the plasmid to the PEG phase. The collapse of pDNA in PEG solutions can also influence the partitioning. At lowered PEG concentrations which were common at the end of CCC runs, the flexible polymer chains of PEG can penetrate inside the pDNA which adopts a coil conformation, and a region of compatibility exists between the PEG and pDNA [Vasilevskaya *et al.* 1995]. Compared to batch ATPS where a higher concentration of PEG is available

and constant, the solvent quality for DNA is poor and the effective attraction between the DNA segments in the macromolecule increases with segregation between the DNA chains and the PEG molecules. The DNA adopts a compact globular structure leaving the DNA in the salt phase [Vasilevskaya *et al.* 1995]. An increase in the salting-out effect (due to high salt concentrations) at the end of the run could also force the pDNA to partition to the PEG phase. It is possible that a combination of the effects mentioned results in the pDNA to change its partitioning preference to the PEG phase.

In initially all CCC runs, the pDNA could only be recovered at the end of the chromatographic run once the column had been pumped out (Figure 5.5) with approximately 96% (w/w) of the pDNA recovered. No chrDNA, protein or RNA was detected with the eluted pDNA indicating an excellent separation had been achieved. With the separation of pDNA from its contaminants, subsequent process could focus on isolating the required supercoiled form of the pDNA and transfer into a buffer suitable for therapeutic use, or a virus removal step.

Lower CCC recovery yields (80 % w/w) were obtained when higher initial stationary phase retentions were used (by reversing the direction of pumping for the mobile phase, Figure 4.19) which suggests that the separation of pDNA from RNA and the resulting recovery yield in such systems does not depend on the initial stationary phase retention, but rather on the degree of stripping that results from the injection of solute and the resulting movement of the mobile phase through the coil. When the lower salt phase was used as the mobile phase for PEG 600 systems, S_f was reduced by 19.5% (v/v) for the TAIL→HEAD mode compared to 11.9% (v/v) for the HEAD→TAIL mode. Thus the increased loss of the stationary phase resulted in some plasmid being lost with the RNA. This may indicate that high S_f values are not critical in aqueous-aqueous systems compared organic-aqueous systems where high S_f values are normally required for efficient chromatography [Ito & Conway, 1996].

Although all PEG 600 ATPS studies showed the plasmid (in TE buffer) to partition to the salt phase, the reversed partitioning to the PEG phase seen during CCC runs was found to be due to the buffer (salt) the pDNA is resuspended in before injection into the CCC (Figures 5.6-5.8). pDNA in TE buffer will preferentially partition to the salt

phase. When a volume of this salt phase was injected into a second ATP system, the pDNA partitioned to the PEG phase. This might be due to a change in the pDNA structure [Vasilevskaya *et al.* 1995] that resulted in the first partitioning step, a change in the electrostatic potential difference $\Delta\psi$ due to the charge on the plasmid being more negative, enthalpic contributions due to the higher self energy of the PEG phase or increased salting-out effects in the lower phase.

When PEG 300 was used as the mobile phase, a single large peak resulted (Figures 5.10 and 5.11) composed firstly of RNA followed by pDNA. A CCC step recovery yield of 97% (w/w) could be achieved with a 41% (w/w) overall recovery yield for the 2-step process. The reduced overall yield is due to the lowered pDNA partitioning in the initial batch ATP extraction. Higher volume ratios were used for this system in order to maximise pDNA recovery from this step (Table 4.1).

CCC experiments using larger plasmids (20 kb) for PEG 600 systems showed identical behaviour to the 5.7 kb with pDNA again being retained at the point of injection (Figure 5.12) in the PEG phase, whilst RNA eluted during the run and was found to be in the stripped PEG phase. Recovery yields of 50 % (w/w) and 71% (w/w) were obtained for the bottom phase batch ATP extraction and the eluted CCC fractions respectively. The overall pDNA recovery yield for the 2-step process was 35% (w/w). No RNA, chrDNA or protein were detected again indicating an excellent separation. The lowered CCC recovery compared to the 5.7 kb plasmid was probably due some plasmid being infinitely retained at the interface inside the CCC due to its larger size and some plasmid losses during the gradual stripping of the stationary PEG. The retention at the interface occurs to a much greater extent in the CCC compared to the batch ATPS due to the high number of mixing and settling steps associated with the CCC. Separation using larger plasmids (72 kb) were not performed as the interfacial tension was shown to be a dominant factor for such systems with 100% of the plasmid being retained at the interface (Chapter 4).

From this study it is evident that the preparation of the feed is also an important factor to be considered when designing a CCC protocol. The introduction of new solutes in the mobile phase has shown to alter the hydrodynamics of the phase system within the column and hence affect the separation. In this case, considerable clearance of the

contaminants through the pre-treatment of the plasmid sample was achieved by an initial batch ATP extraction with the same initial compositions of the PEG and phosphate to be used in the CCC system. Optimization of the batch extraction for initial clearance of contaminants and product yield has been achieved in Chapter 4. This pre-treatment step is crucial for the CCC protocol in terms of achieving the desired resolution and reducing hydrodynamic disturbance.

5.5 Conclusions

This chapter has shown the J-type CCC to be an effective chromatographic step for the purification of pDNA removing contaminant RNA, chrDNA and protein. At present the low capacity of conventional chromatographic matrices (typically ~ 50 μg pDNA mL^{-1} solid matrix) [Diogo *et al.*, 2000; Theodossiou *et al.*, 2000] is prohibitive for the purification of pDNA for therapeutic applications. Several approaches to the separation of pDNA and RNA were observed, and evidence found for the significant depletion of other contaminants, such as chrDNA and protein to levels approaching those likely to be required by the FDA [Marquet *et al.*, 1997].

Up to 30 $\mu g.mL^{-1}$ pDNA was loaded onto the CCC column, however the upper limit for loading was not established. The partitioning of high molecular weight DNA in ATPS has been reported at concentrations of 500 $\mu g.mL^{-1}$ [Walter, 1985]. The cost of the ATPS used in this work is likely to be several orders of magnitude less than the cost of the same volume of conventional solid chromatographic matrix, indicating the CCC is likely to be more cost effective as a high resolution operation for pDNA purification. There is room for improvement for all of the protocols for the purification of pDNA by CCC identified. It has been shown in our laboratory that S_f increases upon scale up with aqueous-organic phase systems [Booth *et al.*, 2002]. Should the same prove to be true for ATPS with minimal stripping during the run, then the resolution achieved through this technique can also be expected to improve upon scale-up.

Despite high loading, pDNA was often recovered in a diffuse peak, the concentration of which was rarely estimated from off-line HPLC be more than 8 $\mu g.mL^{-1}$.Further investigation is required to determine the maximum loading possible. Other studies

carried out in our laboratory indicated that loading of up to 10 mg solute mL^{-1} mobile phase are possible [Booth and Lye, 2001]. This compares very favorably to 40 $\mu g.mL^{-1}$ pDNA loaded onto a solid stationary reversed phase HPLC column [Green *et al.*, 1997], and between 200 and 400 $\mu g.mL^{-1}$ plasmid DNA purified using a 10 ml Mustang Q anion exchange membrane adsorber [Nochumson *et al.*, 2000]. Throughputs of 25 – 50 tonnes per year have been predicted for industrial scale CCC machines [Sutherland *et al.*, 1998] and furthermore the operation of CCC at industrial scale is likely to be considerably less costly than industrial scale HPLC [Sutherland *et al.*, 1998].

The chapter has identified suitable operating procedures for the use of ATP systems in the CCC machine. Recovery yields for pDNA and contaminant levels were quantified, and conditions for subsequent optimization studies have been defined. Having shown that pDNA can be effectively recovered and purified by CCC, Chapter 6 will consider examining different CCC parameters to further improve recovery yields and to increase solute throughputs. Experiments will also be performed in order to avoid the irreversible retention of pDNA in the column for PEG 600 systems.

Chapter 6
Optimisation of pDNA recovery using countercurrent chromatography

6.1 Introduction

In Chapter 5, initial CCC experiments demonstrated the successful removal of contaminant RNA, protein and chrDNA from pDNA. The aim of the work presented in this chapter is to systematically investigate the effects of key process variables such as mobile phase flow rate, rotational speed and solute loading. Unclarified lysates were also used as feed in order to reduce the overall clarification steps required after alkaline lysis. In addition, different operating modes such as the Elution-extraction [Conway, 1990] and dual [Berthod, 2002] modes were performed. There are currently no studies that have addressed the issue of how CCC parameters affect the recovery of pDNA. These are obviously vital issues in relation to eventual process scale applications of CCC.

Experiments in Chapter 3 indicated that the retention of the stationary phase increased with decreasing flow rates and increasing rotational speeds. These parameters have previously been tested in a J-type CCC machine using organic-aqueous systems [Booth, 2003]. There have also been a number of studies using CPC machinery involving aqueous-aqueous two phase systems for the separations of proteins that examined flow rates and revolution speeds on retention and resolution [Matsuda *et al.*, 1998; Shinomiya *et al.*, 1993; Lei and Hsu, 1992; Shibusawa and Ito, 1991; Foucault and Nakanishi, 1990]. These results have shown that the stationary phase retention was found to have a direct effect on the resolution of the eluting protein, where higher retention (due to higher rotational speeds or lowered mobile phase flow rate) gave higher resolution. Experiments using higher solute loading in organic-aqueous systems reduced the resolution due to co-elution of contaminants [Booth *et al.*, 2003].

The overall aim of this chapter is thus to optimise the pDNA recovery for the CCC experiments described in Chapter 5. Specific objectives are: (i) Understand the influence of mobile phase flow rate on pDNA recovery (ii) Understand the influence

of column rotational speed on pDNA recovery (iii) Understand the influence of solute loading on pDNA recovery (iv) Investigate different operating modes in order to allow pDNA to elute with the mobile phase for PEG 600 systems (v) Quantify recovery yields of pDNA using unclarifed lysates (vi) Understand the influence of interfacial tension on pDNA partitioning.

6.2 Effect of mobile phase flow rate

Increasing the mobile phase flow rate has the potential to increase solute throughput. The upper limit to mobile phase flow rate is determined by the hydrodynamics of the system, i.e. excessive stripping at higher flow rates and consequently the decrease in chromatographic resolution. The effect of mobile phase flow rate on pDNA recovery is thus examined using both PEG 300 and PEG 600 systems at flow rates of 1 and 2 $mL.min^{-1}$.

6.2.1 PEG 600-K_2HPO_4 system

The CCC chromatogram obtained at a mobile phase flow rate of 1 $mL.min^{-1}$ is shown in Figure 6.1. The separation performed at a mobile phase flow rate of 0.5 $mL.min^{-1}$ was already presented in Section 5.2.4. Both experiments were performed at a fixed injection volume of 5 mL bottom phase of an initial batch extraction with phases consisting of 18% (w/w) PEG 600-18% (w/w) K_2HPO_4 with 40% (w/w) clarified lysate as described in Section 2.6.3.

Prior to solute injection, phase hydrodynamic equilibrium was achieved as described in Section 2.6.4. The corresponding S_f values are given in Table 6.1. Comparing the chromatograms with a doubling in the mobile phase flow rate to 1 $mL.min^{-1}$, the elution time of the RNA peak dropped to 1.13 CV compared to 1.21 CV when a flow rate of 0.5 $mL.min^{-1}$ was used. In addition, the recovery yield for the CCC step was only slightly reduced to 78% (w/w) whilst the overall 2-step recovery yield of the plasmid was the same 45% (w/w). Again, some pDNA eluted with the RNA in the stripped stationary PEG phase. No RNA was detected with the pDNA retained (results not shown) and subsequently pumped out of the column, and the elution volume was reduced to 9.5 mL compared to 11.2 mL when halving the flow rate.

Although the initial S_f at 1 mL.min^{-1} was around 20% (v/v) lower than for 0.5 mL.min^{-1}, the overall recovery yield of the pDNA did not change. This suggests that very high S_f values are not critical for the separation of RNA from pDNA as the gradual degree of stripping during the run is the deciding factor for RNA removal.

When the flow rate was increased further to 2 mL.min^{-1}, the CCC and overall 2-step process recovery yields were dramatically reduced to 44% and 23% (w/w) respectively (Table 6.1). The chromatogram for this highest flow rate is shown in Figure 6.2. Gel electrophoresis showed that although some RNA was removed in the first peak, a significant amount of RNA was still present with the pDNA retained and later pumped out of the column (Figure 6.3), resulting in a poor separation at this flow rate. Some pDNA also co-eluted with the RNA during the run, leading to higher absorbance readings for the initial RNA peak and lower absorbance readings for the retained plasmid peak compared to Figure 6.1.

The reduction in pDNA yields can be explained by calculating the change in the linear velocity of the mobile phase flow rate. As the proportion of the mobile phase within the CCC coil increases with increasing mobile phase flow rate, due to a reduction in S_f, a non-linear increase in the mobile phase velocity (u, cm.s^{-1}) would be expected. From the knowledge of phase system hydrodynamics in all experiments performed, the linear mobile phase velocity (u) can be calculated according to:

$$u = \frac{4.(F/60)}{\pi.d^2.(\frac{V_m}{V_C})} \qquad \text{(Equation 6.1)}$$

where V_m and V_C correspond to the volume of mobile phase and the system volume (mL) respectively, F corresponds to the mobile phase volumetric flow rate (mL.min^{-1}) and d corresponds to the internal tubing diameter (mm).The units of u are therefore being 'cm.s^{-1}'. Table 6.2 illustrates the changes in linear mobile phase velocity with mobile phase flow rate.

Flow rate ($mL.min^{-1}$)	Initial S_f (% v/v)	Final S_f (% v/v)	CCC recovery yield (% w/w)	Overall 2-step recovery yield (% w/w)
0.5	43.3	23.8	80	45
1	22.8	14.1	78	45
2	8.7	7.6	44	23

Table 6.1: Effect of mobile phase flow rate on stationary phase retention and CCC process yields. Recovery yields determined by analytical HPLC as described in Section 2.7.4.

Flow rate ($mL.min^{-1}$)	V_m (mL)	u ($cm.sec^{-1}$)
0.5	53	0.8
1	73	1.1
2	85	1.9

Table 6.2: Variation in mobile phase linear velocity with mobile phase flow rate. Experiments performed as described in Figures 5.9, 6.1 and 6.2. Determination of the mobile phase volume (V_m) based upon initial S_f values in Table 6.1 and Equations 2.1-2.5. Mobile phase linear velocity calculated using Equation 6.1.

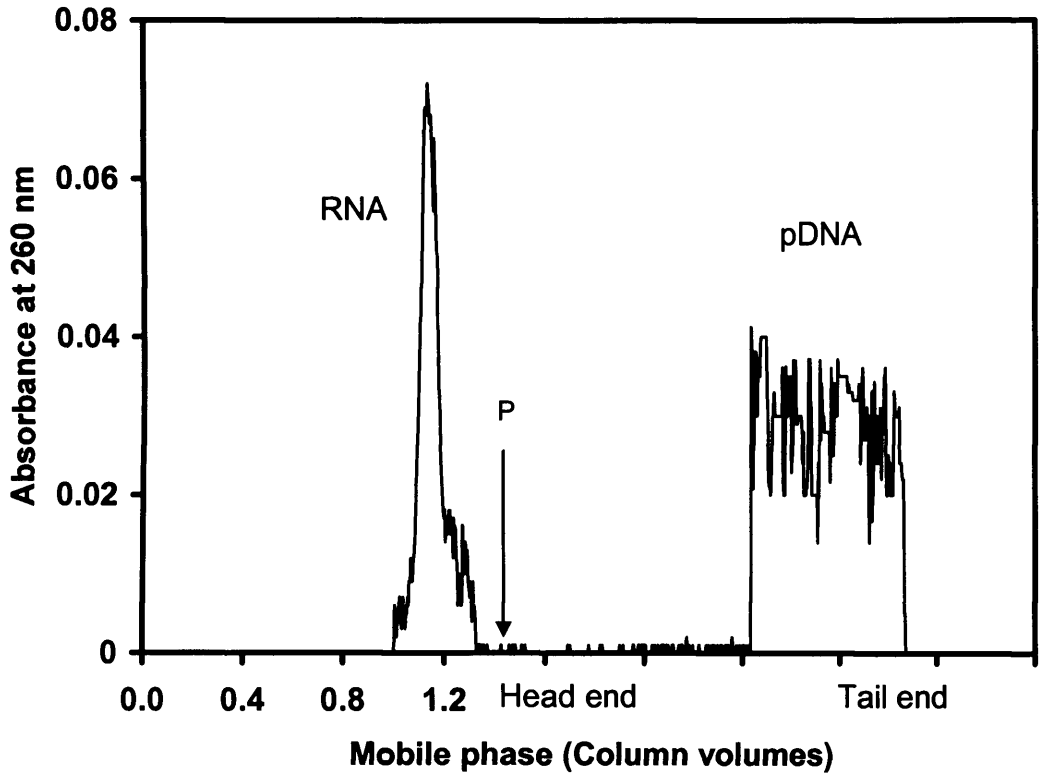

Figure 6.1: CCC chromatogram of plasmid DNA (5.7 kb) and RNA separation using a phase system comprised of 18% (w/w) PEG 600 (stationary phase) and 18% (w/w) K_2HPO_4 (mobile phase) at 600 rpm and a mobile phase flow rate of 1 $mL.min^{-1}$ (S_f= 22.8 % v/v). Mobile phase pumped from TAIL→ HEAD. *P* is the point at which rotation is stopped and column contents are pumped out. Feed prepared as described in Section 2.6.3 and contained 34 $\mu g.mL^{-1}$ pDNA. Retention time for the RNA peak was 1.13 column volumes.

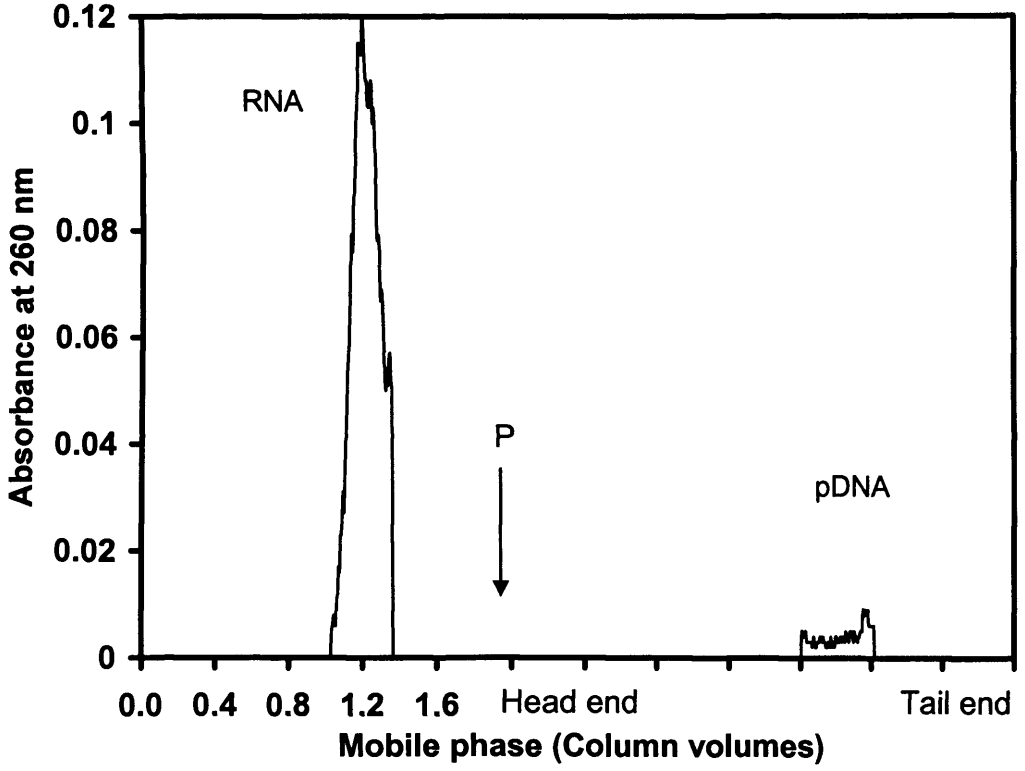

Figure 6.2: CCC chromatogram of plasmid DNA (5.7 kb) and RNA separation using a phase system comprised of 18% (w/w) PEG 600 (stationary phase) and 18% (w/w) K_2HPO_4 (mobile phase) at 600 rpm and a mobile phase flow rate of 2 $mL.min^{-1}$ (S_f= 8.7 % v/v). Mobile phase pumped from TAIL→ HEAD. *P* is the point at which rotation is stopped and column contents are pumped out. Feed prepared as described in Section 2.6.3 and contained 36 $\mu g.mL^{-1}$ pDNA. Retention time for the RNA peak was 1.19 column volumes.

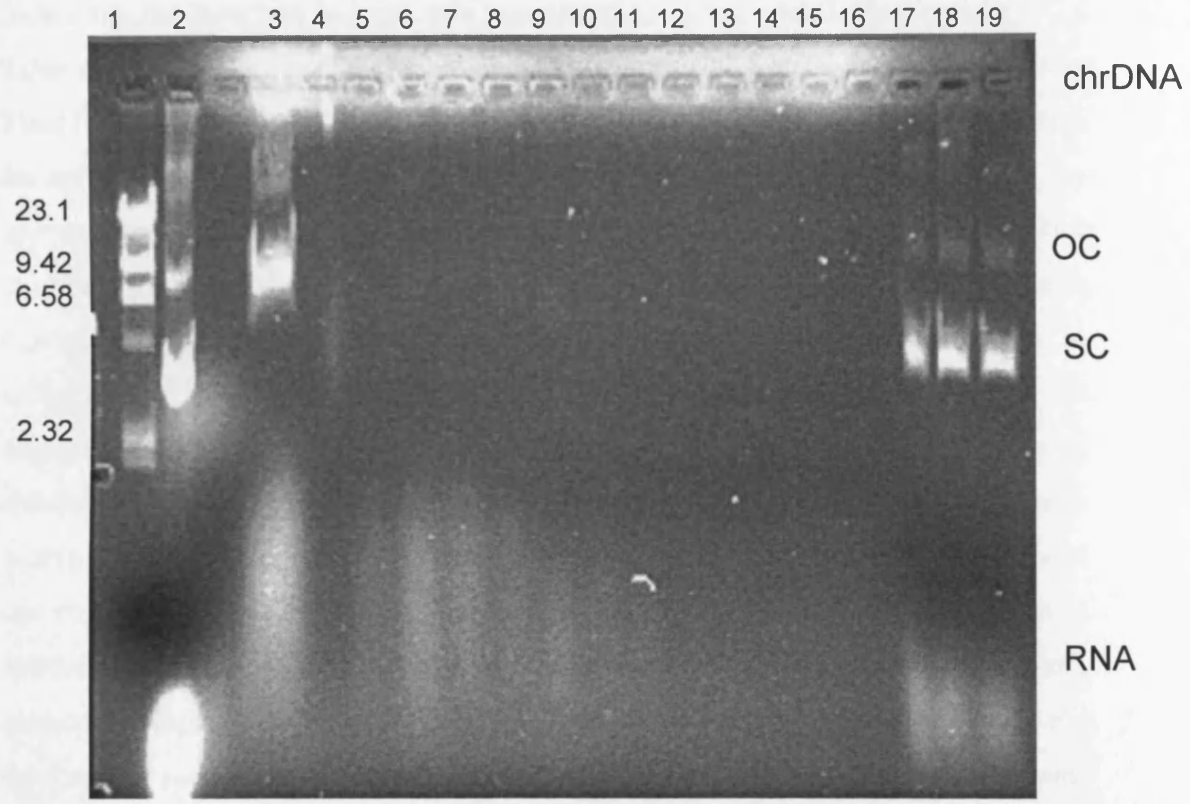

Figure 6.3: Agarose gel analysis of lysate feed and selected fractions collected during the initial batch ATP extraction and CCC run shown in Figure 6.2. Lane 1: DNA ladder; Lane 2: Clarified lysate (36 µg.mL^{-1} pDNA); Lane 3: Bottom phase of batch ATP extraction- CCC feed; Lanes 4, 5, 6, 7, 8, 9, 10, 11, 12, 13, 14, 15 and 16 are top phase (stripped stationary PEG phase) fractions eluted after 0.65, 1.03, 1.11, 1.13, 1.17, 1.19, 1.21, 1.23, 1.28, 1.3, 1.37, 1.39 and 1.45 column volumes respectively; Lanes 17, 18 and 19 are fractions collected during pump out of the coil at 95, 98 and 99% (v/v) of column eluted. 30µL of indicated phase loaded. Non-labelled tracks indicate blanks. Migration of OC and SC forms of pDNA differ slightly due to the effects of PEG and salts. Experiments were performed as described in Section 2.7.2.

In organic-aqueous systems, 'u' only increases by a maximum of ~ 1.9 times even when the flow rate was increased by a factor of 5 due to the high S_f values that can be obtained using such system [Booth, 2003]. From these results, it is apparent that a doubling of mobile phase flow rate to 1 mL.min^{-1} results in a 1.4 times increase in 'u'. Increasing the flow rate to 2 mL.min^{-1} increased the linear mobile flow rate by ~ 2.4 times due to the very low stationary phase retention after hydrodynamic equilibrium. Thus it can be concluded that the linear mobile phase flow rate at 2 mL.min^{-1} is high enough to reduce the CCC step and overall 2-step process recovery yields by approximately half as the available column length for solute distribution to take place is effectively reduced at such low S_f values. The CCC process can be considered as a continuous liquid-liquid distribution process [Conway, 1990] and as such can be subjected to mass transfer investigation. Mass transfer determines the rate of separation, and hence the coil length required to achieve an adequate degree of resolution. Since there is a reduction of 34.6% (v/v) in the available stationary phase within the coil at 2 mL.min^{-1}, correspondingly there is a reduction in the capacity of the stationary phase for the injected solute leading to lower recovery yields. It is interesting to note that higher column efficiencies were obtained at lower S_f values obtained at higher flow rates for organic-aqueous systems [Booth, 2003]. This is not the case for such systems as the resolution of pDNA using aqueous-aqueous systems were determined by the degree of stripping that occurs during the run, and the initial pre-purification and buffer exchange step required for the efficient separation of RNA from pDNA as described in Chapter 5.

6.2.2 PEG 300-K_2HPO_4 system

The effect of mobile flow rate was also tested on PEG 300 systems where the PEG phase was chosen as the mobile phase. A large peak was seen to elute (Figure 6.4) when doubling the flow rate to 1 mL.min^{-1} and gel electrophoresis analysis showed no separation of the pDNA and RNA had occurred. As with pervious experiments using a mobile phase flow rate of 0.5 mL.min^{-1} (Figure 5.10), minimal stripping of the stationary salt phase was seen. The linear velocity, u, increased by a factor of 1.7 times while the initial S_f value was reduced by 14%. Higher flow rates were not tested due to the poor separation and it can be concluded that when using the PEG 300 phase as the mobile phase, the flow rate of such phases should not exceed 0.5 mL.min^{-1} even

though (unlike PEG 600 systems) there is minimal stripping of the stationary salt phase at higher flow rate for such systems (Section 3.2.1).

6.3 Effect of rotational speed

The effect of higher rotational speed (800 rpm) on pDNA purification was tested using a PEG 600-K_2HPO_4 system with the lower salt phase pumped from TAIL→HEAD. Gel electrophoresis of the eluted mobile phase fractions obtained during the run revealed no pDNA or RNA had eluted from the column. Rather, the bulk of the pDNA/RNA was found to have been retained in the PEG phase within the column near the 'Head' end when the coil was pumped out after rotation of the column was halted (Figure 6.5). This was surprising as all previous experiments (Chapter 5) had shown the pDNA being retained in the column at the point of injection (i.e. 'Tail' end in this case) regardless of the pumping direction.

Although the RNA was expected to elute with the stripped PEG phase during the run, the high initial S_f value that was achieved (72.6 %) restricted this and resulted in the majority of RNA to be retained in the column along with the pDNA, even though the S_f value was reduced by 14.1 % during the run. This might suggest that obtaining such high initial S_f values for aqueous two-phase separation of pDNA is not necessary as the RNA/pDNA becomes associated with the large interfacial area generated between the two phases during phase mixing at high rotational speeds. Unlike at low rotational speeds, this mixing allows the pDNA/RNA to travel the distance of the column resulting in them not being retained at the point of injection. By decreasing the intensity of the mixing, less interfacial area should be present in the column and allows the RNA to be eluted with the stripped stationary phase (described in Sections 5.2.2 and 5.2.4). These results show similarity with previous experiments using J-type machines operated at 800 rpm for the separation of open-circular and supercoiled forms of plasmid DNA [Kendall, 2003]. The CCC step and overall 2-step process recovery yields obtained were 89% w/w and 46% w/w respectively.

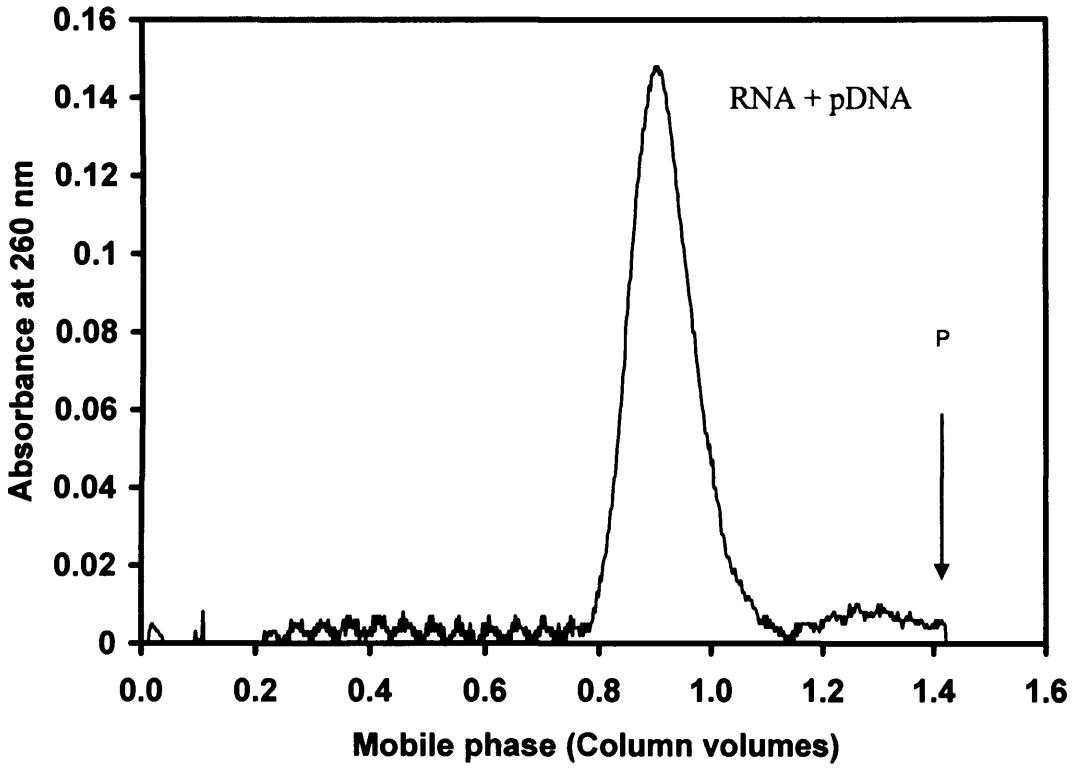

Figure 6.4: CCC chromatogram of plasmid DNA (5.7 kb) and RNA separation using a phase system comprised of 30% (w/w) PEG 300 (mobile phase) and 10% (w/w) K_2HPO_4 (stationary phase) at 600 rpm and a mobile phase flow rate of 1 mL.min^{-1} (S_f = 22.0 % v/v). Mobile phase pumped from HEAD→TAIL. *P* is the point at which rotation is stopped and column contents are pumped out. Feed prepared as described in Section 2.6.3 and contained 34 μg.mL^{-1} pDNA. Retention time for the RNA/DNA peak was 0.89 column volumes.

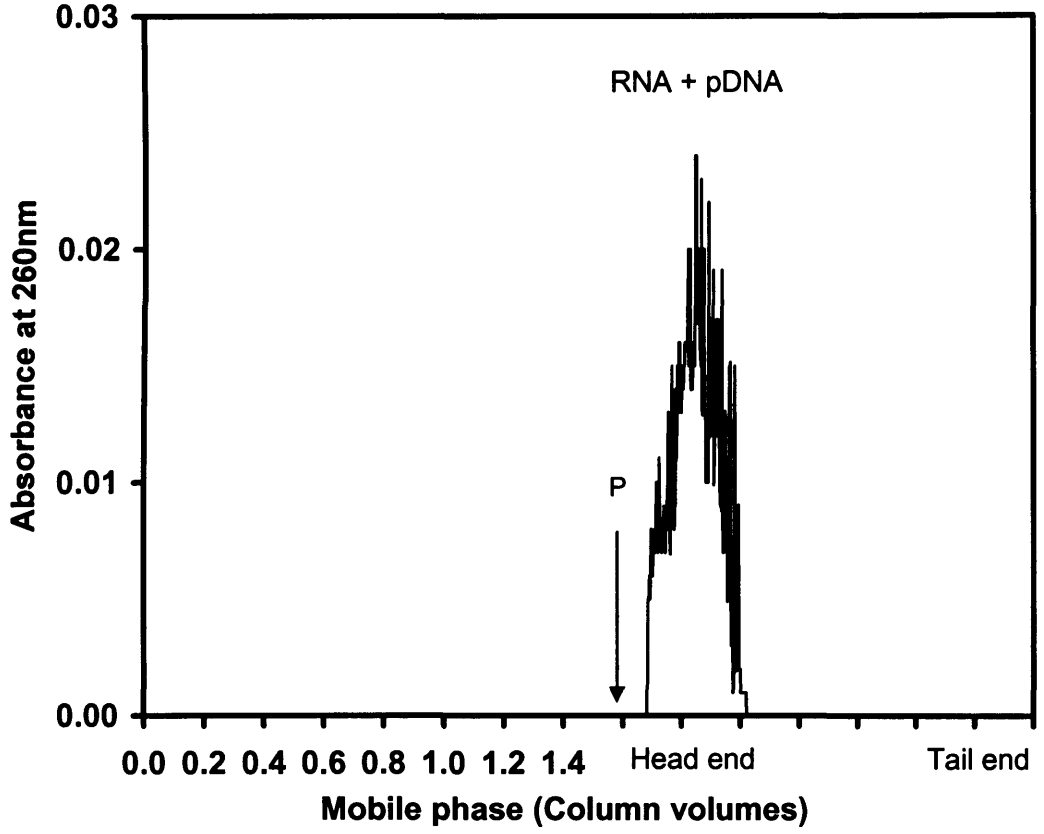

Figure 6.5: CCC chromatogram of plasmid DNA (5.7 kb) and RNA separation using a phase system comprised of 18% (w/w) PEG 600 (stationary phase) and 18% (w/w) K_2HPO_4 (mobile phase) at 800 rpm and a mobile phase flow rate of 0.5 mL.min^{-1} (S_f= 72.6 % v/v). Mobile phase pumped from TAIL→HEAD. *P* is the point at which rotation is stopped and column contents are pumped out. Feed prepared as described in Section 2.6.3 and contained 36 μg.mL^{-1} pDNA.

6.4 Effect of solute loading

A second means of achieving a higher throughput of processed material is to increase the volume of solute injected onto the CCC column. To study this effect, the volume of sample was doubled to 10 mL of the bottom phase from the initial batch extraction (described in Section 2.6.3) while the pDNA concentration was kept the same. In this case, a PEG 600-K_2HPO_4 system was used where the mobile salt phase was pumped from TAIL→HEAD at 0.5 mL.min^{-1} and the column was rotated at 600 rpm. The chromatogram is shown in Figure 6.6.

The results were similar to a 5 mL injection (described in Section 5.2.4) in that the plasmid DNA was found to be in the PEG phase retained in the column whilst the RNA had eluted during the run. Gel electrophoresis showed that some pDNA had co-eluted with the RNA during the run resulting in a lower CCC step recovery yield of 75 % w/w (Figure 6.7). The overall 2-step process recovery yield decreased to 36 % (w/w) compared to 45 % (w/w) using half the injected volume. This was due to the increased disturbance on the hydrodynamic equilibrium of the system which reduced the S_f value by 28.6% (v/v) compared to 19.5% (v/v), meaning increased stripping of the stationary PEG phase and hence pDNA losses during the run. In addition, previous research using organic-aqueous systems has shown that the column efficiency decreases with an increase in sample volume due to the band broadening phenomena in addition to increased fronting and tailing leading to reduced yields [Booth, 2003; Hermans-Lokkerbol *et al.*, 1997]. The volume of fraction in which pDNA was eluted only increased by 2.1 mL (13.3 mL compared to 11.2 mL when halving the injection volume).

No RNA was detected with the pDNA. The fact that the CCC step yield was only reduced by 5 % (w/w) indicates that the maximum solute loading volume was not reached and higher sample volumes can be used for such systems. These results are encouraging as the volume injected equates to a column volume of 11 % suggesting that increasing solute throughput for these systems can be achieved by increasing sample volumes. The effect of doubling sample volume was similar to the effect seen when the mobile phase flow rate was doubled (Section 6.2.1) with both systems giving a final S_f value of 14.1 % (v/v).

The effect of multiple injections was also tested using a PEG 600-K_2HPO_4 system where the mobile salt phase was pumped from TAIL→HEAD at 0.5 mL.min^{-1} and the column was rotated at 600 rpm. An initial 5 mL of lower phase containing plasmid (described in Section 2.6.3) was injected onto the column once hydrodynamic equilibrium was achieved. Based on the results obtained from Sections 5.2.2 and 5.2.4, a further 5 mL of similar feed was injected after a period of 20 minutes. The chromatogram is shown in Figure 6.8.

As with previous experiments, a initial peak was seen containing the majority of the RNA while a second peak was seen after pumping the column contents out, indicating pDNA retained in the column at the point of injection. Agarose gel electrophoresis (Figure 6.9) showed that a significant proportion of pDNA had co-eluted with the RNA in the stripped PEG phase reducing the CCC step recovery yield to 46 % (w/w) indicating reduced purity. RNA was also detected with the plasmid retained in the column and the overall 2-step process yield was only 29 % (w/w). Although the S_f value had decreased by a similar amount (30 % v/v) compared to a 10 mL direct injection discussed previously, it seems that multiple injections are not suitable for use with ATPS. Adding an equal amount of solute disturbs the equilibrium in which RNA is removed by the stripped PEG phase and leads to the majority of the plasmid from the second injection to be removed along with the RNA, as seen with the broadening of the first peak in Figure 6.8. The fact that the CCC step recovery yield was reduced by over half compared with a 10 mL injection suggests that the majority of pDNA retained in this experiment resulted from the first injection. In addition, the disturbance caused to the separation process by injection of the second feed reduces the efficiency of the RNA removal process leading to some RNA being retained in the CCC column resulting in higher absorbance readings for the pDNA peak retained in comparison to Figure 6.6. Thus it likely that in order to increase the solute throughput, doubling the volume of pre-purified feed to 10 mL leads to higher recovery yield and no contamination of the pDNA compared to multiple injections.

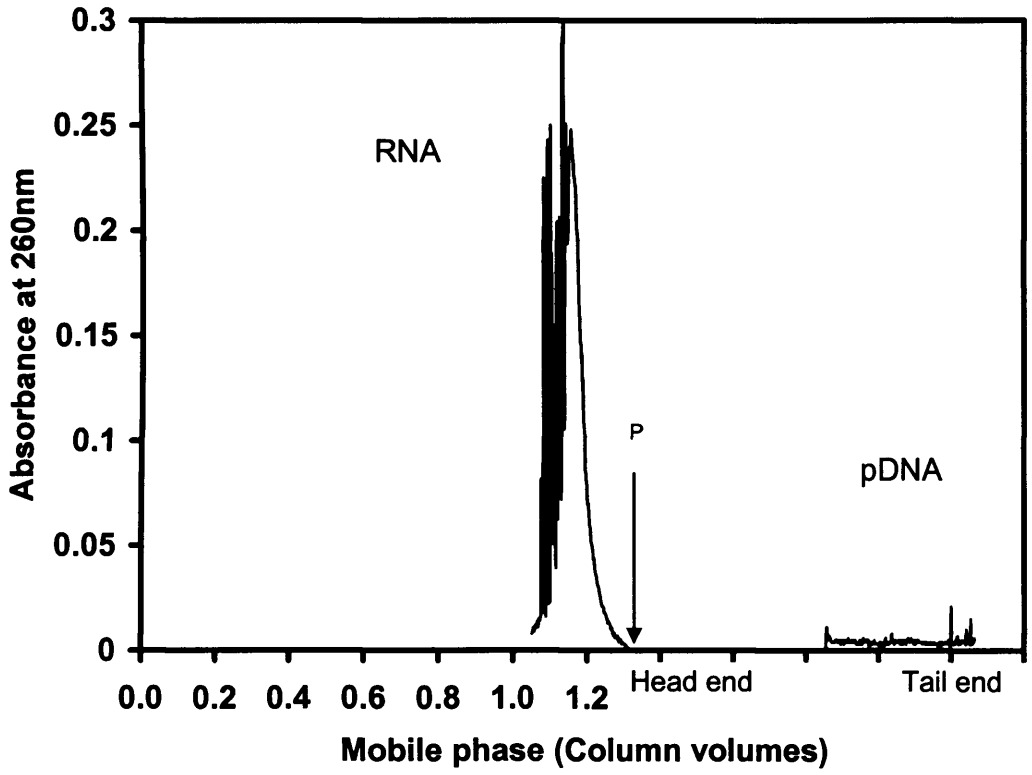

Figure 6.6: CCC chromatogram of plasmid DNA (5.7 kb) and RNA separation using a phase system comprised of 18% (w/w) PEG 600 (stationary phase) and 18% (w/w) K_2HPO_4 (mobile phase) at 600 rpm and a mobile phase flow rate of 0.5 mL.min^{-1} (S_f= 43.3 % v/v) using a 10 mL sample injection volume of bottom phase batch extraction. Mobile phase pumped from TAIL→ HEAD. *P* is the point at which rotation is stopped and column contents are pumped out. Feed prepared as described in Section 2.6.3 and contained 27 µg.mL^{-1} pDNA. Retention time for the RNA peak was 1.16 column volumes.

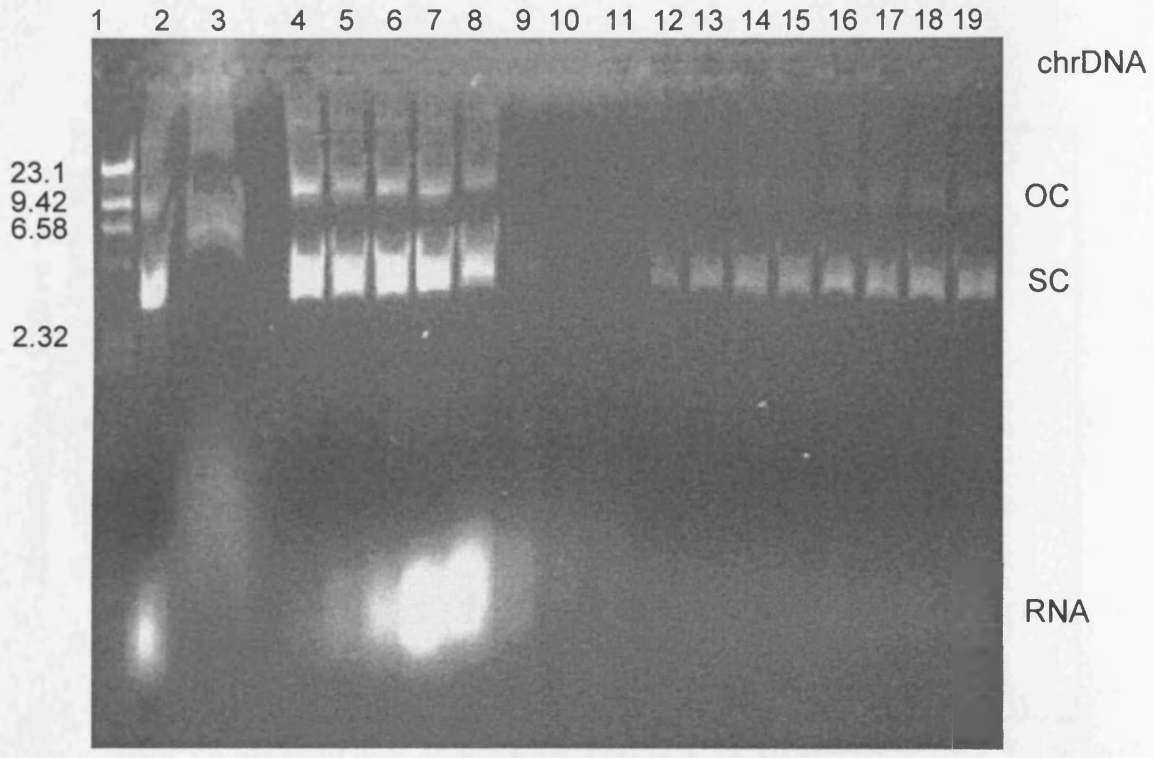

Figure 6.7: Agarose gel analysis of lysate feed and selected fractions collected during the initial batch ATP extraction and CCC run shown in Figure 6.6. Lane 1: DNA ladder; Lane 2: Clarified lysate (27 µg.mL^{-1} pDNA); Lane 3: Bottom phase of batch ATP extraction- CCC feed; Lanes 4, 5, 6, 7, 8, 9, 10 and 11 are top phase (stripped stationary PEG phase) fractions eluted after 1.06, 1.08, 1.12, 1.13, 1.15, 1.18, 1.20 and 1.23 column volumes respectively; Lanes 12, 13, 14, 15, 16, 17, 18 and 19 are fractions collected during pump out of the coil at 85, 86, 88, 90, 92, 94, 96 and 98 % (v/v) of column eluted. 30µL of indicated phase loaded. Non-labelled tracks indicate blanks. Migration of OC and SC forms of pDNA differ slightly due to the effects of PEG and salts. Experiments were performed as described in Section 2.7.2.

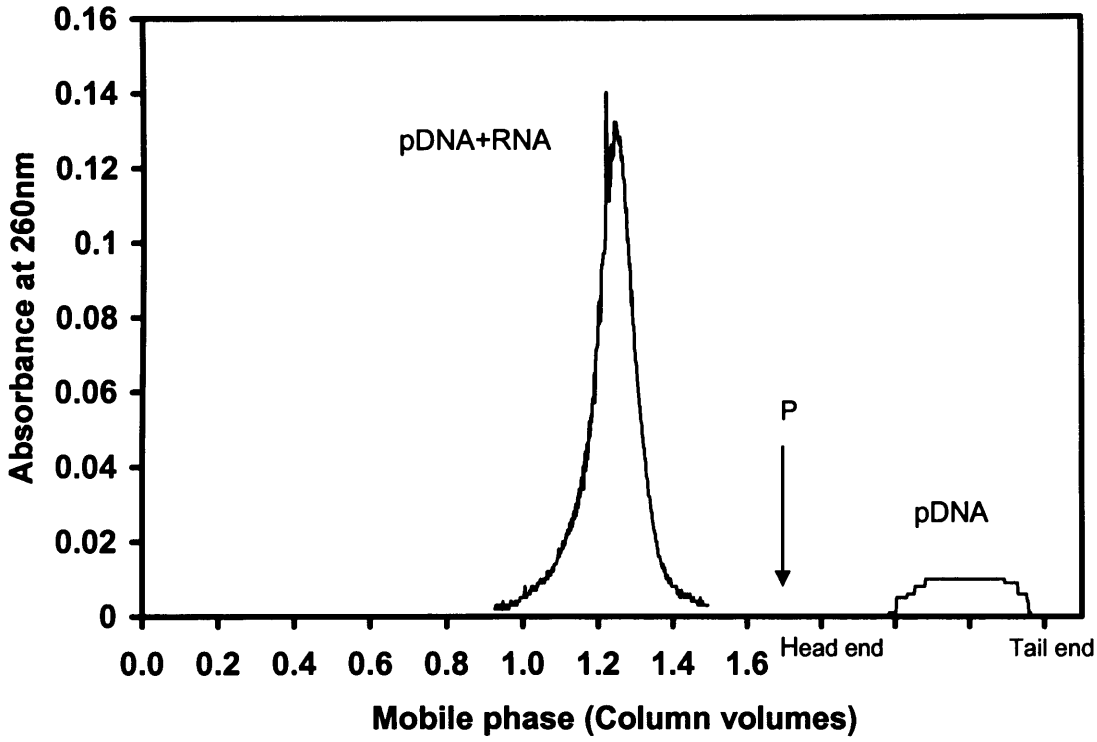

Figure 6.8: CCC chromatogram of plasmid DNA (5.7 kb) and RNA separation using a phase system comprised of 18% (w/w) PEG 600 (stationary phase) and 18% (w/w) K_2HPO_4 (mobile phase) at 600 rpm and a mobile phase flow rate of 0.5 mL.min^{-1} (S_f = 45.5 % v/v) using two multiple injection of 5 mL taken from the bottom phase batch extraction. Mobile phase pumped from TAIL→HEAD. *P* is the point at which rotation is stopped and column contents are pumped out. Feed prepared as described in Section 2.6.3 and contained 28 μg.mL^{-1} pDNA. Retention time for the RNA peak was 1.22 column volumes.

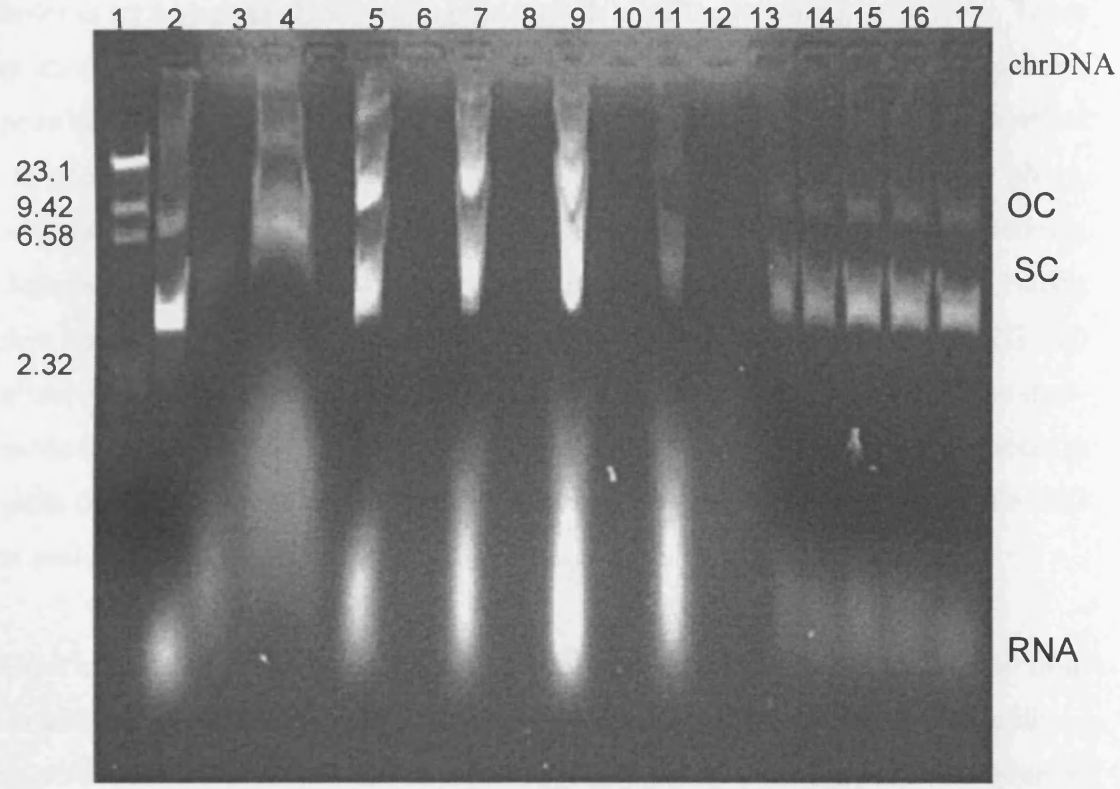

Figure 6.9: Agarose gel analysis of lysate feed and selected fractions collected during the initial batch ATP extraction and CCC run shown in Figure 6.8. Lane 1: DNA ladder; Lane 2: Clarified lysate (28 µg.mL^{-1} pDNA); 3: Top phase of batch ATP extraction. Lane 4: Bottom phase of batch ATP extraction- CCC feed; Lanes 5, 7, 9 and 11 are top phase (stripped stationary PEG phase) fractions eluted after 1.13, 1.15, 1.18 and 1.26 column volumes respectively; Lanes 6, 8, 10 and 12 are bottom phase fractions eluted after 1.13, 1.15, 1.18 and 1.26 column volumes respectively. Lanes 13, 14, 15, 16 and 17 are fractions collected during pump out of the coil at 87, 89, 92, 93 and 97 % (v/v) of column eluted. 30µL of indicated phase loaded. Non-labelled tracks indicate blanks. Migration of OC and SC forms of pDNA differ slightly due to the effects of PEG and salts. Experiments were performed as described in Section 2.7.2.

6.5 Alternative Operating Strategies

6.5.1 Dual-mode method

In order to overcome the infinite retention of pDNA in the CCC column during rotation seen in Section 5.2.2, several unique operational approaches were tested in order to try and elute pDNA during the run while still separating it from RNA. These methods take advantage of the liquid nature of the stationary phase and are not possible in classical chromatography using a solid stationary phase. The first method reverses the role of the phases: the mobile phase will become the stationary phase, and the stationary phase, in which the pDNA is retained in (reversible partitioning described in Section 5.2.2), will become the mobile phase with the intention of eluting this phase. Thus for PEG 600-salt systems, the new mobile phase is the PEG 600 phase while the stationary phase is the salt phase. This approach is called the dual-mode method [Berthod, 2002]. The direction of flow is switched during the process in order to obtain a reasonable level of stationary phase retention. Thus the mobile PEG is switched from H→T.

Once initial hydrodynamic equilibrium has been achieved, 5mL of bottom phase from an initial batch ATP extraction (described in Section 2.6.3) was injected. The addition of pDNA (in salt phase) to the mobile PEG phase greatly disturbed the hydrodynamic and led to the complete stripping of the stationary salt phase after 0.38 CV (from S_f = 22.8 % v/v initially). The majority of RNA was seen to elute at CV= 0.76 while the majority of pDNA eluted at CV= 1 with the mobile PEG phase. This was expected as previous tests (Section 5.2.3) showed the RNA and pDNA to partition back to the PEG phase when introduced into a second ATP system. The chromatogram is shown in Figure 6.10. The noisy baseline after CV= 0.38 was due to elution of the viscous PEG phase due to the complete stripping of the stationary salt phase. Only a 41% (w/w) pDNA recovery for the CCC step (CV=1) was achieved due to some pDNA lost by co-elution with the RNA. The overall recovery yield was 26% (w/w). RNA was also detected in the main pDNA peak (Figure 6.11). Although no plasmid was retained in the column, the introduction of feed in one phase into a column using a different mobile phase is not recommended for aqueous two-phase systems as this leads to excessive stripping of the stationary phase and poor resolution between the

pDNA and RNA. Organic-aqueous systems have higher initial retention values and are less sensitive to the introduction of feed material into the CCC (leading to less stripping during the run) thus making the dual-mode method more applicable to such systems [Berthod, 2002].

6.5.2 Elution-extrusion method

The second alternative operating mode examined was a continuous method called the elution-extrusion mode first proposed by Conway [1990]. As the pDNA is retained by the stationary phase, then the stationary phase itself is used to extrude the entire contents of the column. After a normal elution step, the liquid used as the stationary phase is pumped in the column in the reverse direction to that of the initial mobile phase. In this case, 18% (w/w) PEG 600 was initially used as the stationary phase with 18% (w/w) K_2HPO_4 used as the mobile phase pumped in the TAIL→HEAD direction, achieving the highest S_f value as described in Section 3.2.4. Once hydrodynamic equilibrium had been achieved, the pDNA (prepared as described in Section 2.6.3) was injected at the same flow rate as the mobile phase. All the RNA was initially removed with the stripped PEG phase similar to results seen in Sections 5.2.2 and 5.2.4. The retention time of 225 minutes (CV= 1.21) agrees with similar CCC runs (described in Section 5.2.2). At this point, the rotation of the column continued and the PEG phase is now pumped in the HEAD→TAIL direction. This will eventually push the remaining salt phase out of the column. Since the lower phase will now be the minor phase in the column, relatively little additional fractionation is expected, and the retained solutes will be eluted fairly rapidly.

The chromatogram obtained using this approach is shown in Figure 6.12. The pDNA is seen immediately once the PEG phase starts to elute, further indicating that as with previous experiments (described in Sections 5.2.2 and 5.2.4), it is retained at the point of injection (the Tail end in this case). No RNA was detected with the eluting pDNA (Figure 6.13). A high overall 2- step recovery yield of 58% (w/w) was achieved with a CCC step yield of 93% (w/w). This mode of operation is preferable in that it avoids mixing of the zones, which occurs when the contents are pumped out of the stationary column using nitrogen. The flow rate the mobile PEG can be further increased after the first RNA peak to speed up the elution of pDNA. Previous experiments using this

mode showed that the chromatographic band broadening does not occur inside the column where the solutes partition between the two phase but outside the column when the solutes leave it [Berthod *et al.*, 2005]. Highly retained solutes elute in broader mobile phase peaks than fast eluting solutes. When extruded with the liquid stationary phase, highly retained peaks elute in thin stationary phase peaks provided that the centrifugal field was not modified, leading to higher overall recovery yields [Berthod *et al.*, 2005] as seen here.

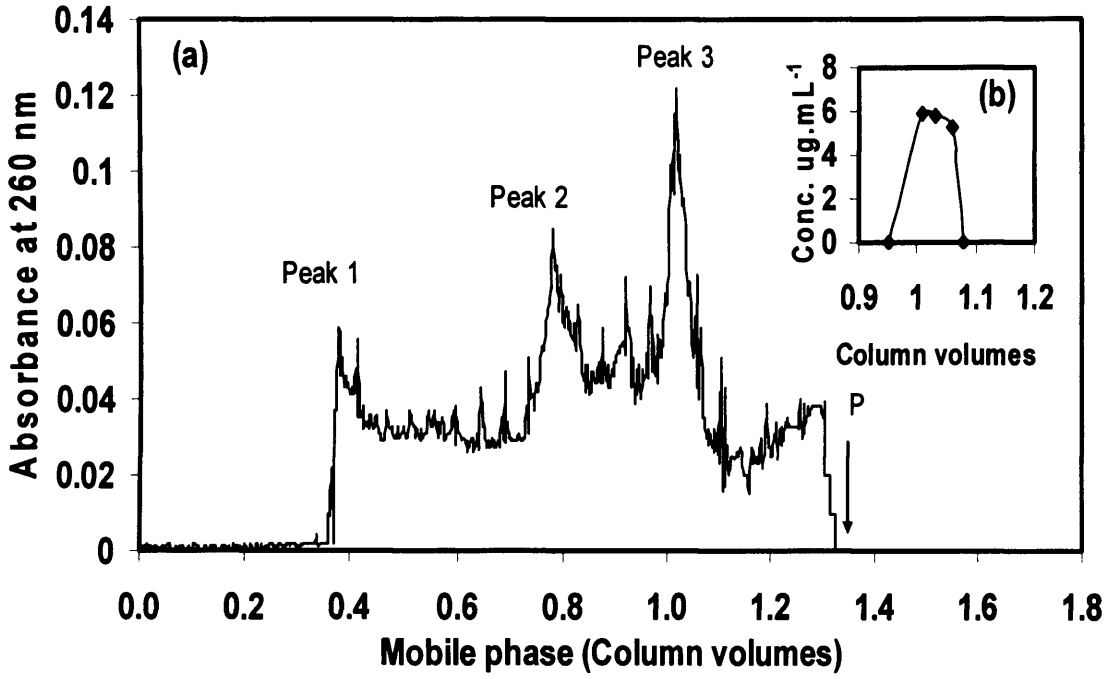

Figure 6.10: (a) CCC chromatogram of plasmid DNA (5.7 kb) and RNA separation using a phase system comprised of 18% (w/w) PEG 600 (mobile phase) and 18% (w/w) K_2HPO_4 (stationary phase) at 600 rpm and a mobile phase flow rate of 0.5 mL.min^{-1} (S_f = 22.8 % v/v). Mobile phase pumped from HEAD→TAIL. *P* is the point at which rotation is stopped and column contents are pumped out. Peak 1 represents the point at which the stationary phase is completely stripped (S_f = 0% v/v). Peak 2 and 3 represents the majority of RNA and pDNA eluting respectively Feed prepared as described in Section 2.6.3 and contained 40 μg.mL^{-1} pDNA. Retention time for the RNA peak was 1.13 CV. (b) pDNA concentration (1.00-1.06 CV) analysed by HPLC as described in Section 2.7.4.

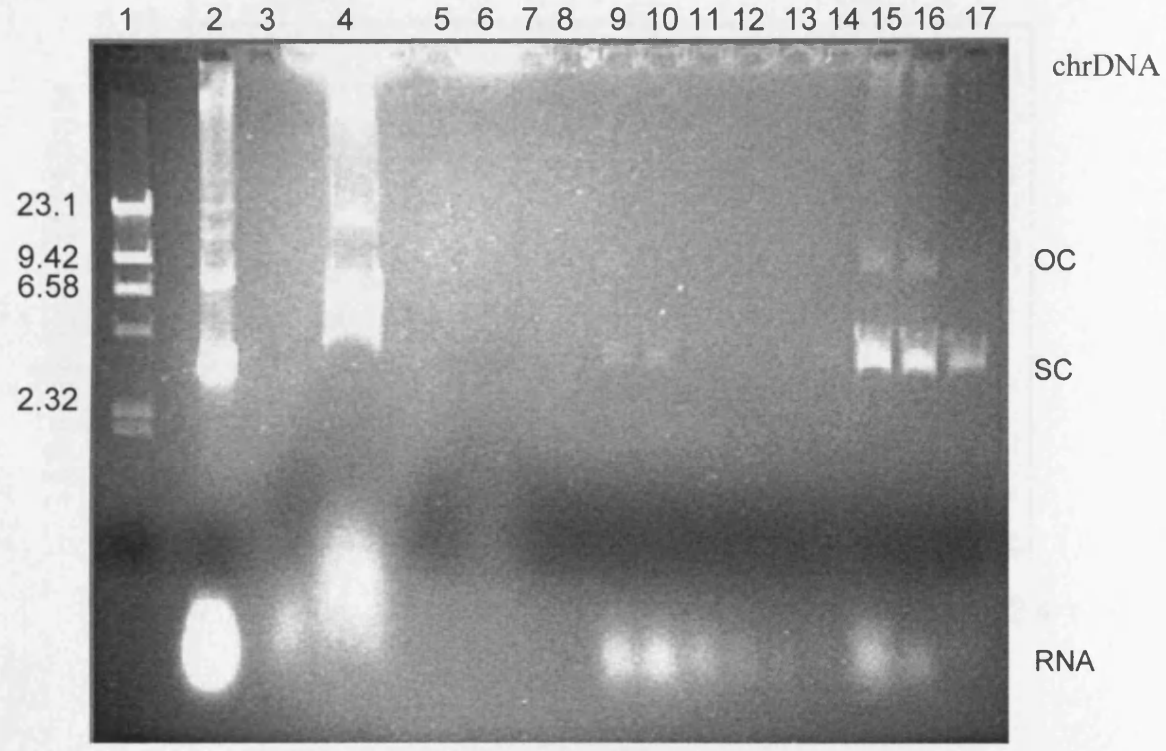

Figure 6.11: Agarose gel analysis of lysate feed and selected fractions collected during the initial batch ATP extraction and CCC run shown in Figure 6.10. Lane 1: DNA ladder; Lane 2: Clarified lysate (40 μg.mL^{-1} pDNA); 3: Top phase of batch ATP extraction. Lane 4: Bottom phase of batch ATP extraction- CCC feed; Lanes 5 and 7: Top phase fractions eluted after 0.35 and 0.38 column volumes respectively; Lanes 6 and 8: Bottom phase (stripped salt phase) fractions eluted after 0.35 and 0.38 column volumes respectively. Lanes 9, 10, 11, 12, 13, 14, 15, 16 and 17 are top phase fractions eluted after 0.76, 0.79, 0.82, 0.85, 0.87, 0.89, 1, 1.03 and 1.06 column volumes respectively. 30μL of indicated phase loaded. Non-labelled tracks indicate blanks. Migration of OC and SC forms of pDNA differ slightly due to the effects of PEG and salts. Experiments were performed as described in Section 2.7.2.

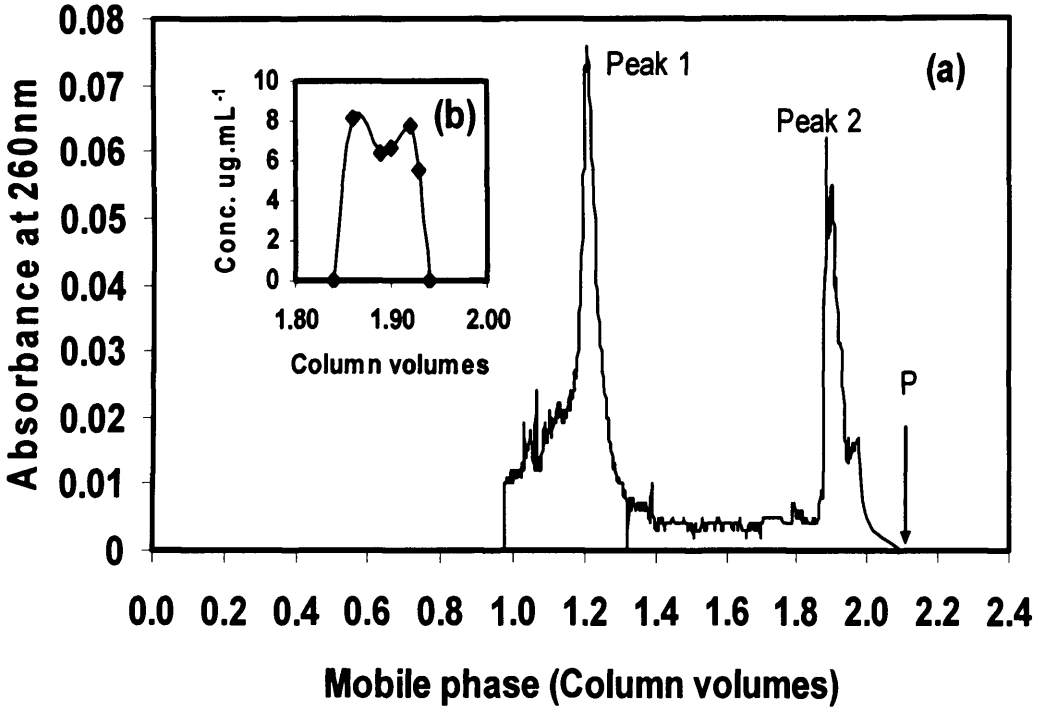

Figure 6.12: (a) CCC chromatogram of plasmid DNA (5.7 kb) and RNA separation using a phase system comprised of 18% (w/w) PEG 600 (stationary phase) and 18% (w/w) K_2HPO_4 (mobile phase) at 600 rpm and a mobile phase flow rate of 0.5 mL.min^{-1} (S_f = 43.3 % v/v). Mobile phase pumped from TAIL→HEAD. After the first peak, PEG 600 is selected as the mobile phase and pumped in the HEAD→TAIL as described in Section 6.5.2. Peak 1 represents the RNA removed with the initial stripped stationary PEG phase. Peak 2 represents the pDNA eluting with the mobile PEG phase. *P* is the point at which rotation is stopped and column contents are pumped out. Feed prepared as described in Section 2.6.3 and contained 30 μg.mL^{-1} pDNA. Retention time for the RNA peak was 1.21 CV. (b) pDNA concentration (1.84-1.93 CV) analysed by HPLC as described in Section 2.7.4.

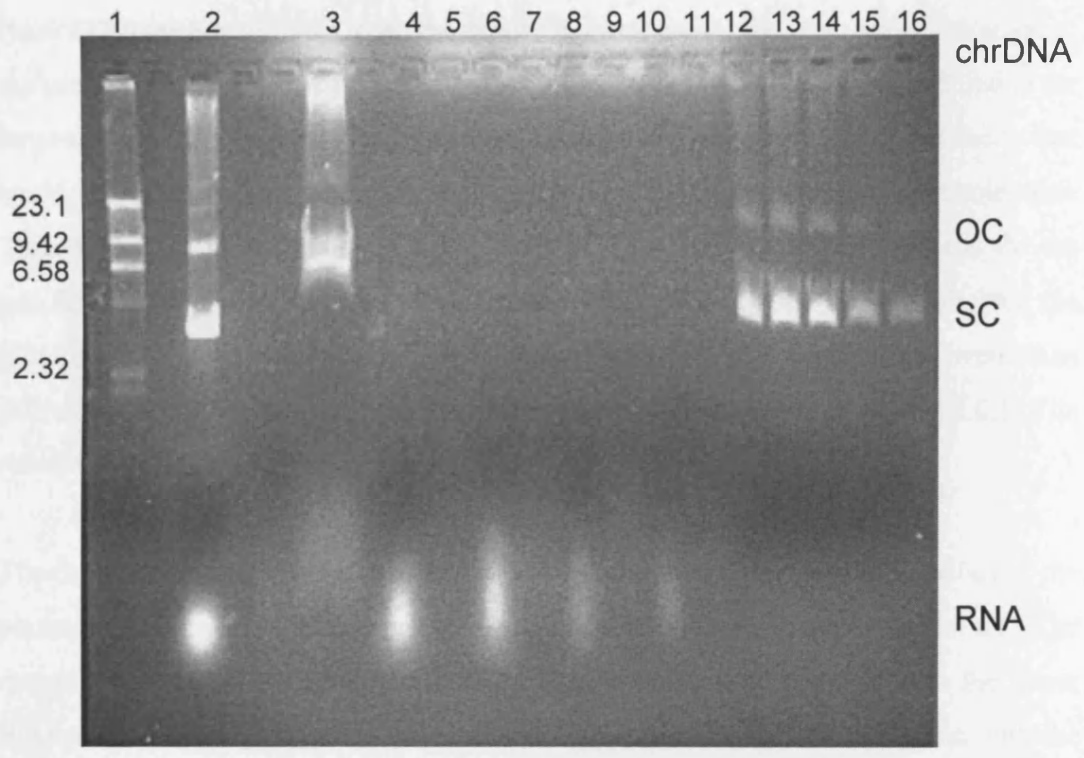

Figure 6.13: Agarose gel analysis of lysate feed and selected fractions collected during the initial batch ATP extraction and CCC run shown in Figure 6.12. Lane 1: DNA ladder; Lane 2: Clarified lysate (30 µg.mL^{-1} pDNA); Lane 3: Bottom phase of batch ATP extraction- CCC feed; Lanes 4, 6, 8 and 10 are stripped PEG phase eluted after 1.18, 1.21, 1.23 and 1.25 column volumes respectively; Lanes 5, 7, 9 and 11 are bottom phase fractions eluted after 1.18, 1.21, 1.23 and 1.25 column volumes respectively. Lanes 12, 13, 14, 15 and 16 are top phase fractions eluted after 1.87, 1.89, 1.9, 1.92 and 1.93 column volumes respectively. 30µL of indicated phase loaded. Non-labelled tracks indicate blanks. Migration of OC and SC forms of pDNA differ slightly due to the effects of PEG and salts. Experiments were performed as described in Section 2.7.2.

6.6 CCC fractionations using unclarified lysates

Following the alkaline-lysis step of the pDNA process (Section 1.3.2), the white precipitate that forms contains cell debris, denatured proteins and nucleic acids with pDNA normally representing only 2% (w/w) of the total nucleic acids in *E. coli* lysates [Ferreira *et al.*, 2000]. At the laboratory and pre-preparative scales, removal of the precipitate is usually by centrifugation. However, centrifugation is not suitable for large-scale production as these machines usually operate with continuous feeds that could shear and consequently break the precipitated material and chrDNA molecules. Thus with the aim of reducing the number of downstream processing steps for the purification of pDNA, the centrifugation and filtration steps that usually followed the alkaline-lysis step (Section 2.3) were not performed. Unclarified lysates were then introduced directly into the batch ATP extraction as described in Section 2.6.3. The resulting chromatogram is shown in Figure 6.14.

The initial ATP batch extraction for the PEG 600 system recovered 66% (w/w) of the plasmid, which agrees with results using clarified lysate shown in Table 4.1. The majority of the precipitate and cell debris were visually seen to partition to the upper PEG phase. Although a small amount of chrDNA is expected to co-partition with the pDNA in the bottom phase when using clarified lysate [Ribeiro *et al.*, 2002], the contamination seen in the PEG phase from gel electrophoresis analysis (Lane 3, Figure 6.15) was due to fragmented chrDNA present in large amounts in the precipitate. During the run, the majority of RNA was removed with the stripped stationary PEG phase with pDNA being retained in the column. The RNA retention time was identical to experiments using clarified lysate (Figure 5.9). The CCC step recovery yield was reduced slightly to 75% (w/w) compared to experiments using clarified lysates (described in Section 4.4.4). This slight reduction was probably due to the lower final S_f value (reduced by around 3% to 21.1% (v/v)) due to the introduction of a cruder sample onto the CCC column. No proteins were detected with the pDNA meaning that the majority of denatured protein present in the precipitate was removed in the initial batch ATP extraction. These results show that the use of unclarified lysates for CCC experiments did greatly not affect the recovery yields of pDNA as the majority of the precipitated material from the lysis step is removed in the initial batch ATP extraction. The importance of this initial extraction step is

further proved not only as a buffer exchange method, but also as a pre-purification step for the reduction of RNA in addition to the removal of precipitated material arising from the alkaline-lysis.

6.7 Measurement of interfacial tension

The interfacial tension between the phases is an important factor influencing the partitioning behavior of pDNA, RNA, proteins and chrDNA since these species usually distribute themselves between the interface and one of the two bulk phases (Section 4.3.1). The degree to which interfacial adsorption will occur increases with increasing interfacial tension because of the decrease in free energy associated with reduced liquid-liquid interfacial area between the phases. To further understand pDNA partitioning in ATPS, interfacial tension measurements were performed using blank ATPS and systems containing lysates to determine the effect of solute partitioning on interfacial tension. In order to mimic conditions of plasmid partitioning in CCC experiments upon injection, the lysate containing plasmids gWiz or PQR150 was first partitioned in a 250mL batch ATPS comprised of PEG 600 or 1000 (18% w/w) and K_2HPO_4 (18% w/w). The bottom phase, where the plasmid partitions to, is then separated and used to fill the measurement chamber (described in Section 2.7.8). A droplet of PEG 600 or 1000 (obtained from a blank 18% w/w PEG-18% w/w K_2HPO_4 system) is then injected into the capillary of the tensiometer to determine the interfacial tension.

The results from these experiments are presented in Table 6.3. An increase in PEG molecular weight increased the interfacial tension measurement and this was previously reported in similar ATPS [Wu *et al.*, 1996]. Interfacial tension decreased when the plasmid is present. This is expected as substances that absorbs at the interface (pDNA, chrDNA and RNA) will generally lower the interfacial tension [Brooks *et al.*, 1985]. When the gWiz (5.7 kb) plasmid was present, the interfacial tension was reduced by around 35% for both the PEG 600 and 1000 systems. For PEG 600 systems there is some variation in the reduced interfacial tension when different sizes of plasmid (5.7 and 20 kb) were examined. Higher plasmid recovery yields were obtained (Section 4.3.1) for PEG 1000 ATPS (compared to PEG 600) despite having a higher interfacial tension. This was due to other factors such as the

increased excluded volume of the PEG polymer chain [Albertsson, 1986] and increased hydrophobicity of PEG 1000 [Forciniti *et al.* 1991] being more dominant in determining plasmid partitioning. The kinetics of pDNA adsorption to the interface was also examined. Interfacial tension did not change over the measured time indicating that the adsorption is very rapid and the solute partitioning to the PEG droplet (described in Section 5.2.3) reaches the saturation limit upon immediate contact with the salt phase due to the large amount of pDNA and other contaminants present in the lower phase used to fill the chamber. This decrease in interfacial tension might explain the partitioning of pDNA and RNA back to the PEG phase once in the salt phase (described in Section 5.2.3). The constant interfacial tension over time might also indicate that the phases do not have a propensity to diffuse into each other [Verma *et al.*, 1998].

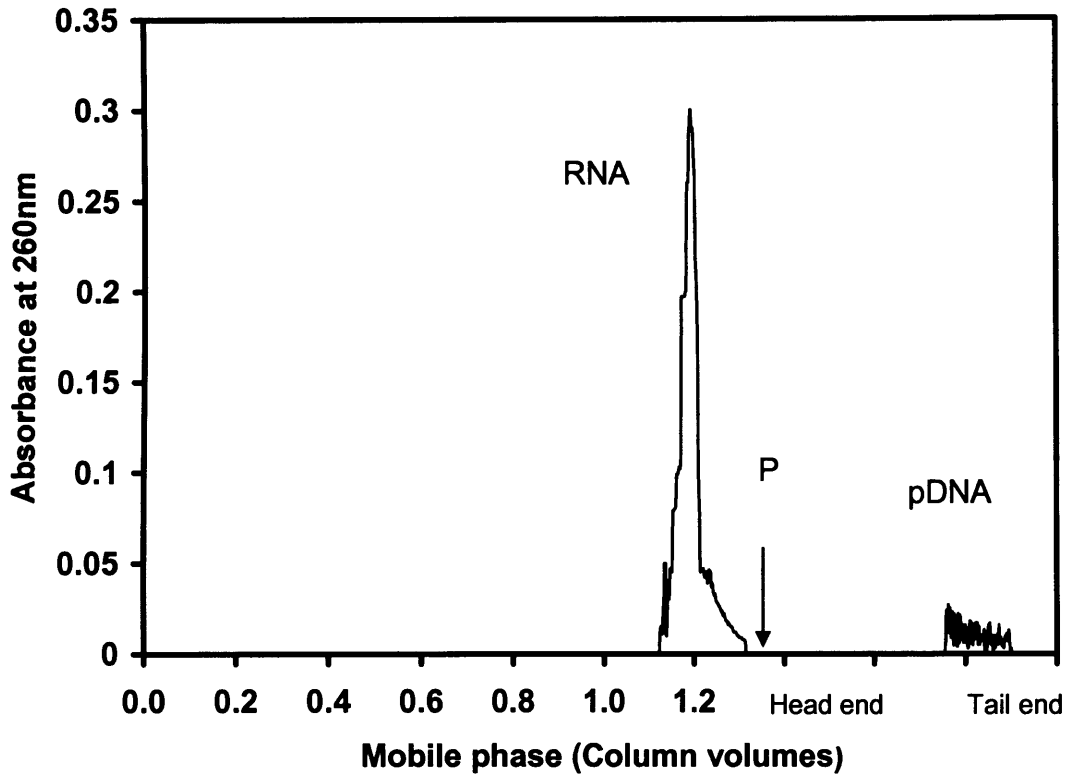

Figure 6.14: CCC chromatogram of plasmid DNA (5.7 kb) and RNA separation using a phase system comprised of 18% (w/w) PEG 600 (stationary phase) and 18% (w/w) K_2HPO_4 (mobile phase) at 600 rpm and a mobile phase flow rate of 0.5 mL.min^{-1} (S_f= 43.3 % v/v). Mobile phase pumped from TAIL→ HEAD. *P* is the point at which rotation is stopped and column contents are pumped out. Feed prepared as described in Section 2.6.3 and contained 32 µg.mL^{-1} pDNA from an unclarified lysate feed. Retention time for the RNA peak was 1.20 column volumes.

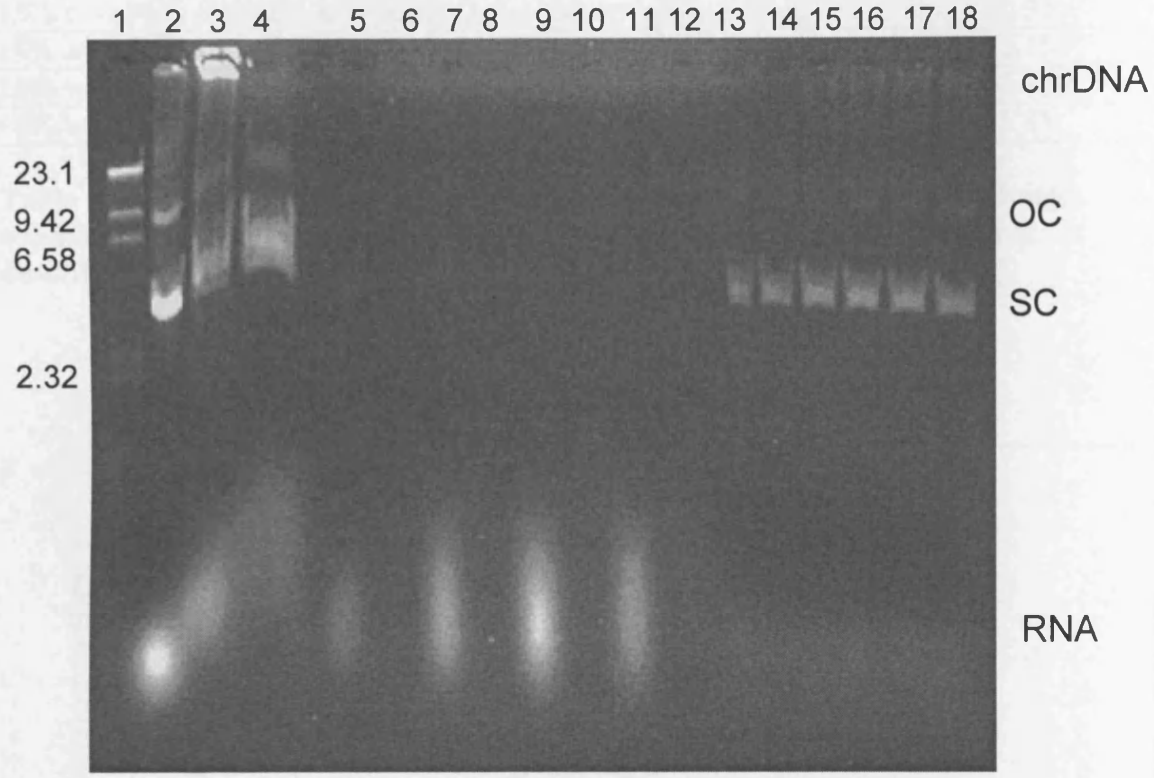

Figure 6.15: Agarose gel analysis of lysate feed and selected fractions collected during the initial batch ATP extraction and CCC run shown in Figure 6.14. Lane 1: DNA ladder; Lane 2: Clarified lysate (32 µg.mL^{-1} pDNA); Lane 3: Top phase of batch ATP extraction. Lane4: Bottom phase of batch ATP extraction- CCC feed; Lanes 5, 7, 9 and 11 are top phase (stripped stationary PEG phase) fractions eluted after 1.15, 1.18, 1.2 and 1.23 column volumes respectively; Lanes 6, 8, 10 and 12 are bottom phase fractions eluted after 1.15, 1.18, 1.2 and 1.23 column volumes respectively; Lanes 13, 14, 15, 16, 17 and 18 are fractions collected during pump out of the coil at 88, 90, 92, 94, 96 and 98% (v/v) of column eluted. 35µL of indicated phase loaded. Migration of OC and SC forms of pDNA differ slightly due to the effects of PEG and salts. Clarified material used (Lane 2) as direct loading of unclarified lysate was unsuitable due to large amounts of contaminants. Experiments were performed as described in Section 2.7.2.

Phase System	Interfacial tension ($mN.m^{-1}$)
18% w/w PEG 600-18% w/w K_2HPO_4	1.45
18% w/w PEG 600-18% w/w K_2HPO_4 inc. lysate (gWiz-5.7 kb)	0.93
18% w/w PEG 600-18% w/w K_2HPO_4 inc. lysate (PQR150-20 kb)	1.15
18% w/w PEG 1000- 18% w/w K_2HPO_4	2.76
18% w/w PEG 1000-18% w/w K_2HPO_4 inc. lysate (gWiz-5.7 kb)	1.83

Table 6.3: Interfacial tension of various ATPS with and without lysates containing a range of plasmid sizes. Interfacial tension was measured as described in Section 2.7.8.

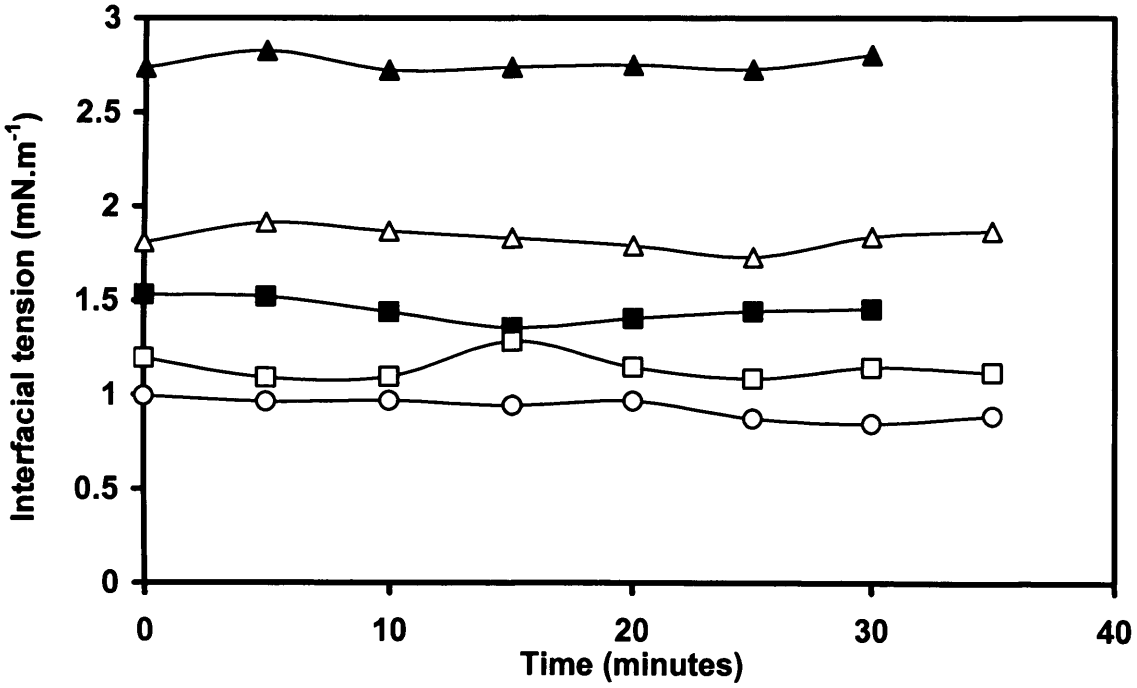

Figure 6.16: Interfacial tension as a function of time for various ATPS: 18% (w/w) PEG 600- 18% w/w K_2HPO_4 (■); 18% (w/w) PEG 600- 18% (w/w) K_2HPO_4 including lysate (gWiz-5.7 kb) (○); 18% (w/w) PEG 600- 18% (w/w) K_2HPO_4 including lysate (PQR150-20 kb) (□); 18% (w/w) PEG 1000- 18% (w/w) K_2HPO_4 (▲); 18% (w/w) PEG 1000- 18% (w/w) K_2HPO_4 including lysate (gWiz-5.7 kb) (Δ). All ATPS were prepared, and interfacial tension measured as described in Section 2.7.8.

6.8 Discussion

For PEG 600 systems, doubling the mobile phase flow rate (Section 6.2) to 1 mL.min^{-1} showed no reduction in the overall recovery yield of pDNA. Equally no RNA was detected with the pumped out pDNA fraction even though the stationary phase retention had been reduced due to the increased flow rate. However, increasing the flow rate from 1 to 2 mL.min^{-1} halved the overall recovery yield of the pDNA. This was due to of pDNA co-eluting with the RNA in the stripped PEG phase and the resulting change in the linear mobile phase flow rate, which increased by ~ 2.4 times due to the very low stationary phase retention (8.7% v/v) after hydrodynamic equilibrium. Thus the available column length for solute distribution to take place is effectively reduced at such retention values and the low S_f value leads to reduction in the capacity of the stationary phase for the injected solute leading to lower recovery yields of plasmid DNA (23% w/w). CCC experiments using organic-aqueous systems achieved higher column efficiencies at higher flow rates due to the high retention values where typical S_f values of around 51% (v/v) were obtained for flow rates of 10 mL.min^{-1} [Booth, 2003]. This was not possible for ATPS due to the large decrease in S_f values that occurred when flow rates were increased (Figure 3.3).

PEG 300 systems showed no separation of pDNA and RNA using higher flow rates even though S_f values were only reduced by 14% (v/v) when doubling the flow rate to 1 mL.min^{-1}. It is concluded that for systems where the plasmid elutes out with the mobile PEG phase, higher flow rates will reduce the solute distribution allowing the majority of pDNA to co-elute with RNA.

Experiments examining increasing column rotational speed to 800 rpm showed no RNA elution during the run. In addition, the majority of RNA/pDNA was found to be present at the opposite end to the point of injection. It is thought that the pDNA/RNA becomes associated with the large interfacial area generated at high rotational speed which allows the solutes to travel the distance of the column rather than being retained at the point of injection. There is no separation of the contaminant RNA and thus higher rotational column speeds are not recommended for pDNA purification using CCC.

The effects of doubling the volume of feed injected showed more promising results with good separation of RNA from pDNA. The overall recovery yields were reduced by 9% (w/w) compared to experiments using half the injected volume. In addition, the volume of the fraction in which the plasmid was eluted only increased by 16% (v/v). This indicates that the maximum solute loading volume was not reached for the system. CCC experiments using multiple injections of feed (5 mL each) were also tested. The results show that the CCC step and overall 2-step process recovery yields were reduced by around 29% and 7% respectively compared to a 10 mL injection, even though in both experiments, S_f values were reduced by the same amount. This was because the second injection disturbed the equilibrium in which the RNA, from the first injection, is removed by the stripped PEG phase and leads to the majority of the plasmid from the second injection being removed along with the RNA. pDNA retained in the column was present with RNA due to the reduced efficiency of the RNA removal process as a result of the second injection. Due to the nature of RNA removal in the CCC, multiple injections are not recommended for use in aqueous two-phase systems.

A number of unique CCC operating modes were tested with the aim of avoiding infinite retention of pDNA in the column thus allowing continuous elution during the run. The dual-mode CCC method proposed by Berthod [2002] (described in Section 6.5.1) was initially tested. The addition of feed using this method greatly disturbed the hydrodynamic and led to the complete stripping of the stationary salt phase after 0.38 CV. Poor separation of RNA from pDNA was seen with only a 26% recovery yield for the process. The introduction of pDNA in salt into the mobile PEG phase is thus not recommended due to the excessive stripping of the stationary phase that occurs. The elution-extrusion method proposed by Conway [1990] and tested by Berthod *et al.* [2005] was also applied (described in Section 6.5.2) and showed very good separation of the pDNA from RNA with an overall 2-step recovery yield of 58%. This is the highest recovery yield achieved in CCC separations so far using the initial batch ATP extraction described in Section 2.6.3. When the pDNA retained in the column is extruded with the liquid stationary phase rather than nitrogen, highly retained peaks elute in thin stationary phase peaks leading to higher overall recovery yields [Berthod *et al.*, 2005]. The use of the PEG phase both as a stationary and mobile phase during the same run can be used to elute the pDNA retained once the RNA is removed in the

normal way with the stripped stationary PEG phase. The overall elution time of the pDNA can be significantly reduced by increasing the flow rate at which the column content is being extruded after removal of RNA. Throughputs of 1.76 $mg.day^{-1}$ purified pDNA can be achieved using this method.

The ability to purify of pDNA when using unclarified lysates in the initial batch extraction was also demonstrated (Section 6.6). RNA was successfully removed with a 49% (w/w) overall 2-step process recovery yield of pDNA. The introduction of a cruder sample reduced the final S_f by only 3% due to the majority of precipitated material partitioning to the upper PEG phase during the initial batch extraction. Although chrDNA contamination was not quantified, it is expected to be completely removed as previous experiments performed (Section 5.2.2) have shown the chrDNA contamination to be below the detectable limit. This further proves the use of CCC as an initial purification method and can be placed immediately after the alkaline-lysis step avoiding the extra centrifugation and filtration steps normally used for the downstream processing of pDNA.

Finally, interfacial tension studies were performed to further understand the reversal in plasmid partitioning once in the salt phase (described in Section 5.2.3). Interfacial tension values were seen to decrease when lysate was present due to pDNA, RNA and other contaminants partitioning to the interface. This reduction in interfacial tension, along with other factors described in Section 5.2.3 might explain the reason plasmid partitioning behaviour reverses from the salt to the PEG phase. No significant change in interfacial tension was seen when plasmids of two sizes (5.7 and 20 kb) were examined, and measurements remained constant with time.

Open-circular and supercoiled forms of the plasmid could not be separated thus further steps should be used to isolate the required supercoiled form of the pDNA for therapeutic applications and transferred into a buffer suitable for therapeutic usage. Alternatively, host cell line/lysis need to be optimised to minimise the generation of OC in the first place. The use of alternate designs for CCC machine (Section 1.10) plus further optimisation of operating conditions and investigation of the wider choice of phase system which may be used with the alternate designs may achieve this. Concentration of the plasmid containing phase of the ATPS by ultrafiltration will

likely improve both the resolution (as less volume is loaded onto the column) and will also increase throughput as more plasmid could be loaded for the maximum volume of sample loaded.

6.9 Conclusions

The results presented in this chapter have shown that efficient separation of pDNA from closely related RNA and other contaminants can still be achieved over a range of operating conditions. The effects of mobile phase flow rate, column rotational speed, solute loading and different modes of CCC operation were examined.

The effect of flow rate on pDNA separation showed that a doubling of mobile phase flow rate up to 1 $mL.min^{-1}$ is possible for ATPS when the plasmid does not usually elute with the RNA i.e. when it is retained in the column, as is the case for PEG 600 systems. In addition doubling the injection volume showed good separation of pDNA from RNA. However the highest recovery yield was obtained when operating the CCC in elusion-extrusion mode where the previously retained pDNA is eluted during the run. The use of unclarified lysates in CCC was also successfully demonstrated and can lead to a reduction in the number of downstream processing steps.

Chapter 7
Discussion and Future work

7.1 Results arising from this study

The overall objective of this research as described in Section 1.12 has been to evaluate CCC as a novel chromatographic technique for the fractionation and recovery of pDNA from its contaminants present after alkaline-lysis. With the industrial scale application of this technology in mind, a number of operational issues were addressed experimentally.

Firstly, due to the lack of any prior knowledge concerning the hydrodynamics of aqueous-aqueous two-phase systems in a J-type CCC, this was examined as described in Chapter 3. Here the ability to attain high S_f values was demonstrated, usually by pumping the mobile phase in the opposite direction to that normally recommended for organic-aqueous systems [Sutherland *et al.*, 2000a]. Values of S_f up to 73.7% v/v were obtained. As with organic-aqueous systems, S_f values were shown to increase with increasing column volumes and rotational speeds, and more importantly, were also predicted successfully as a function of flow rate (Equation 3.1) and rotational speed (Equation 3.2) for the first time using aqueous two-phase systems.

The recovery and purification of pDNA by CCC has been successfully achieved when used in conjunction with an initial batch ATP extraction step (Chapter 5). This initial extraction was used as both a buffer exchange step needed to reduce the disturbance on hydrodynamic equilibrium in the CCC, and to minimise the amount of contaminants present with the pDNA. The optimization of the initial ATP extraction was described in Chapter 4, where the influence of phase volume ratios, PEG molecular weight, pH and plasmid size were examined. Recovery yields of 100% w/w can be achieved when using higher volume ratios and higher molecular weigh PEG; however these systems allowed a large amount of RNA to co-partition with pDNA. Typical ATPS chosen for CCC experiments where the pDNA partitions to the lower salt phase were 18% (w/w) PEG 600-18% (w/w) K_2HPO_4 with a 40% lysate addition giving a volume ratio of around 1. Levels of RNA and proteins were reduced to levels

where these could not be detected using the analytical technology available. For PEG 300 systems, where the plasmid partition to the upper PEG phase, the highest recovery yield achieved was 58% (w/w). In all cases, plasmids were seen to partition to a bulk phase and the interface. Although chrDNA and endotoxin analysis were not done at this stage, it is expected that both will be significantly removed at the interface with some co-partitioning with the pDNA [Trindade *et al.*, 2005]. Plasmid sizes of 5.7 and 20 kb showed similar partitioning behaviour. Larger plasmids of 72 kb were seen to partition entirely to the interface. The ATPS is an efficient purification step in itself and could potentially be used prior to a variety of purification operation such as HIC, tangential-flow adsorption-filtration using nitrocellulose membrane, or countercurrent chromatography as demonstrated in this research. These findings for the batch extraction of pDNA using ATPS are similar to those reported in a number of recent publications [Trindade *et al.*, 2005; Ribeiro *et al.*, 2002]. In this case though, phase systems suitable for subsequent use in the CCC machine were examined.

The best CCC separation (Figure 5.4) achieved overall process recovery yields of 54% w/w (phase system 18% w/w PEG 600-18% w/w K_2HPO_4) with no RNA, protein or chrDNA detected with the pDNA. A summary figure of the 2-step process is shown in Figure 7.1:

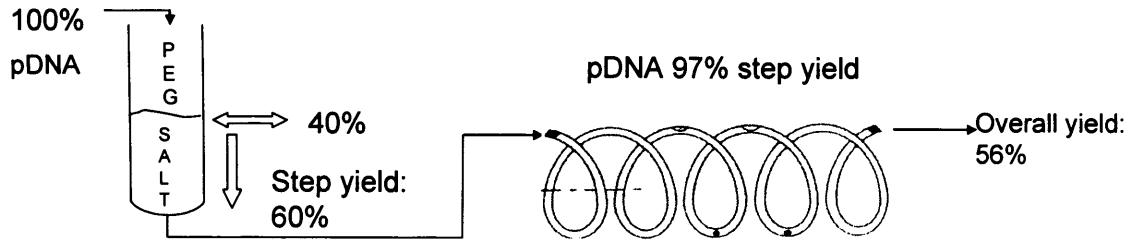

Figure 7.1: Overall 2-step CCC separation as described in Section 5.2.2 and Figure 5.4.

For PEG 600 systems, pDNA was always infinitely retained in the column at the point of injection whilst RNA was removed with the stripped stationary phase PEG. Surprisingly, both pDNA and RNA were found to have partitioned to the PEG phase despite partitioning to the salt phase in initial batch ATP extraction. This reversal in

partitioning preference could be due to a number of reasons including the high viscosity of the stationary PEG phase, coupled with the large dynamic volume of DNA molecules [Ito *et al.*, 1998], the high interfacial contact areas (due to low interfacial tensions) between the two systems [Hatti-Kaul, 1999], the collapse of DNA in PEG solutions [Vasilevskaya *et al.* 1995], an increase in the salting-out effect (due to high salt concentrations) at the end of the run or an reduction in interfacial tension due to some pDNA/RNA being retained at the interface.

Based on the successful fractionation of pDNA from its contaminants, CCC operating variables and modes, as discussed in Chapter 6, were tested with the aim of increasing throughput. This chapter examined for the first time the effect of changing operating parameters for plasmid separations using aqueous two-phase systems. The retention of pDNA in the column can be avoided by operating the CCC in the elution-extrusion mode. Overall process recovery yields as high as 58% (w/w) were achieved due to the plasmid eluting in narrow fractions peaks rather than broader peaks when eluted with nitrogen. The upper loading limit was not established as doubling the injection volume (11% v/v total column volume) did not affect recovery yields or resolution. The ability to purify of pDNA when using unclarified lysates in the initial batch extraction was also demonstrated (Section 6.6). RNA was successfully removed with a 49% (w/w) overall 2-step process recovery yield of pDNA. Thus the 2-step CCC process has the potential to reduce the number of downstream processing steps for the purification of pDNA eliminating the need for the centrifugation and filtration steps that usually followed the alkaline-lysis step. A summary of a potential downstream process is shown in Figure 7.2:

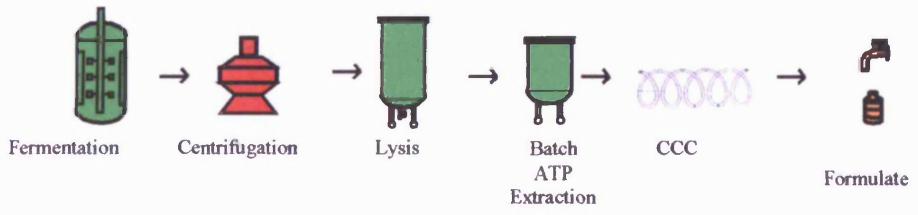

Figure 7.2: Overall downstream of pDNA using unclarified lysate with batch ATP extraction and CCC steps.

7.2 Wider implications of this work

The purification of pDNA from its contaminants achieved through CCC was successful. However the purified product streams have not been fully characterized in terms of endotoxin levels and no separation of the SC and OC form of the plasmid was observed. The low capacity and high cost of conventional chromatography matrices [Green *et al.*, 1997] currently available will continue to drive research into alternative purification strategies such as CCC. The relative cheapness of the phase forming polymer and salt, and potentially high capacity [Booth *et al.*, 2003], combined with low pressure operation and gentle environment of the aqueous two-phase system should make CCC separation of plasmid in this manner an attractive proposition. Table 7.1 shows the purification target achieved using ATPS and CCC.

Purification achieved (target)	**Partitioning using initial batch ATP extraction**	**CCC (following batch ATP extraction)**
Chromosomal DNA# (≤1 % w/w)	Feed: 12 % w/w Purified: Not determined	Feed: Not determined Purified: < 31 pg.μg^{-1}
Protein (undetectable)	Feed: >0.06 mg mL^{-1} Purified: < 0.0025 mg mL^{-1}	Feed: < 0.0025 mg mL^{-1} Purified: Undetectable
RNA (undetectable)	Reduction in RNA co-partitioning with pDNA	Undetectable
Endotoxin (< 0.1 EU μg^{-1} plasmid)	Not determined	Not determined
Yield	52-63 % w/w	80-97 % w/w
Approximate time	~ 30 minutes settling	4-5 hours per cycle 2 hours set up and equilibrium

Table 7.1: Comparison of ATPS and CCC techniques investigated. Target contaminant levels from specification for release of Allovectin-7 pDNA taken from Marquet *et al.* [1997a]. Results based on typical separation using 18% w/w PEG 600-18 % w/w K_2HPO_4 phase systems with volume ratio of approximately 1. Results presented for batch ATP extraction and CCC are described in Sections 4.3.1 and 5.2.2 respectively.

Kendall [2003] previously estimated the cost to purify 480 L lysate (from a 200 L fermentation) using CCC at £7,000 per run. This cost can be reduced by concentrating the plasmid prior to CCC, for example, by ultrafiltration. It is estimated that a 10x increase in the amount of plasmid loaded will reduced the cost to £2,000 per run [Kendall, 2003]. This compares favourably considerably with the estimated £10,000 per run using a conventional ion exchange matrix previously described for pDNA

[Kendall, 2003; Prazeres *et al.*, 1998] Investigation of the possibility of concentration of the plasmid process stream prior to purification by aqueous two-phase partitioning could also improve the cost effectiveness of that operation, as well as reducing the volume to be handled.

The potential for recycling of phase forming chemicals should also be considered. Rito-Palmeres and co-workers [Rito-Palomares *et al.*, 2000] described a continuous mixer extraction system, in which protein from bovine blood was first partitioned to the upper PEG phase, before a back extraction step (at lower PEG concentration) following which PEG was recycled. A similar system could be applied to the purification of plasmid by partitioning in aqueous two-phase systems (the plasmid product being removed in the lower phase following the first extraction, and the back extraction removing contaminants prior to subsequent uses). However, the effect of recycling the polymer on the partitioning behaviour of the nucleic acids, and cost of the recycling operations (i.e. the additional cost of salt phase for back extraction, and cost of operating ultrafiltration for the recovery of salts from biological contaminant species), and the best combination of phase systems to be used must be evaluated [Rito-Palomares *et al.*, 2000].

7.3 Future work

Although the presence of RNA was only detected by visually analysing agarose gels, and in some cases by off-line HPLC, these methods are sufficient according to FDA's recommended assays for assessing the purity, safety and potency of DNA preparations for gene therapy and DNA vaccines [Ferreira *et al.*, 2000]. In addition, endotoxin levels were not measured. A more rigorous determination of purification achieved to quantitatively measure RNA, and an inclusion of endotoxin measurements would be most advantageous for future work on plasmid purification. In addition, the investigation of using affinity ligands, charge polymers and other additives such as urea or various water soluble organic solvents should be considered in greater detail. Different phase forming salts and polymer species in which the plasmid is not retained (due to its reversed partitioning preference) should also be examined.

The exact mechanism behind the purification observed is likely to be important for the optimisation of the batch ATPS. The ability to predict accurately the behaviour of particulates in the phase system and hence rapidly identify an optimal composition for the phase system would be an ideal situation, but to reach such a level of understanding will require a lot of work. At the moment, many of the theories used for protein partitioning [Johansson *et al.*, 1998; Albertsson, 1986] in ATPS are being used to predict plasmid partitioning. The tendency of plasmids and its contaminants to aggregate at the interface of ATPS is a problem that could also be addressed through greater understanding of the interaction between the particulates present and the phase system. This is especially true for larger plasmid sizes were interfacial absorption is dominant.

The proposed generic method development strategy, as shown during the course of this study, did successfully identify a robust phase system and run mode. At the laboratory scale, with the chosen phase system, all studies used for pDNA purification were performed using a nominal coil volume of 93 mL, thus limiting, at any one time, the mass injected onto the coil due to system capacity limitations. To increase product throughput still further, whilst maintaining an acceptable level of product purity, larger coil volumes for plasmid separations should be investigated. Currently, CCC column volumes of up to 10 L are being tested for protein separations using aqueous two-phase systems [Wood, 2005]. Pilot scale studies can also be performed to demonstrate the potential of the technology for scale-up.

The incorporation of aqueous two-phase partitioning with CCC was demonstrated in Chapter 5. However such a purification step (combined with a UF step for concentration of the plasmid) may also be effective as a precursor to hydrophobic interaction chromatography, or in conjunction with a selective adsorption step, such as nitrocellulose adsorption [Kendall *et al.*, 2002]. The potential to adapt the partitioning of nucleic acids in aqueous two-phase system to a continuous mixer – settler system as described by Rito-Palmeres and co-workers [Rito-Palomares *et al.*, 2002] could also be worthy of investigation.

Ideally the CCC step should be operated as a continuous process, with the aim of loading multiple samples to minimize the time and cost of the purification of each

sample. At present stripping of the stationary phase during operation of the CCC machine, and the resultant loss in S_f mean that it is not advisable to load a second sample. Experiments have shown that although a certain level of S_f needs to be achieved initially, very high values comparable to organic-aqueous systems are not required as the removal of contaminant RNA was due to the gradual stripping of the stationary phase. Thus a controlled level of stripping is required to remove the RNA. The disadvantages of the J-type machine for use with ATPS makes the use of such systems for continuous processes virtually impossible. In such a case future work using the J-type machine would be better spent on optimisation of batch runs in terms of resolution between the plasmid and its contaminants and the purification factors achieved.

Although the J-type machine was not designed for use with aqueous two-phase systems, the availability of such a machine at UCL, along with the success separating SC and OC forms of plasmid DNA [Kendall *et al.*, 2001] made the investigation into the use of the J-type machine with ATPS worthwhile. Other designs of CCC machine such as non-synchronous CPC [Shinomiya *et al.*, 2003], cross-axis CPC [Shinomiya *et al.*, 1993; Lei & Hsu, 1992], horizontal CPC [Lei & Hsu, 1992] and eccentric multi-layer CCC [Shibusawa *et al.*, 1991] specifically designed for use with ATPS might reduce the volume the plasmid is retained in. The high laterally acting force field in these machines tends to suppress emulsification at the cost of mixing. This should result in higher retention values, which in turn will result in higher resolution, and reduce batch-processing times. Optimization of the operating conditions using other machinery will be required on many fronts, for example phase system selection, rotational speed and flow rate of the mobile phase.

For the production of biopharmaceuticals, several additional factors will have to be considered for good manufacturing practice in addition to the purification achievable. For instance the parameters under which the machine operates, such as temperature and bobbin rotational speed, will need to be more easily set, and deviations avoided. Limits also need to be set for the variable applicable to CCC, and the performance of the machine between these will need to be validated. Cleaning and sterilization of the column between batches will also be required. These design considerations, and the validation of the cleaning and controls will need to be considered and implemented in

conjunction with the manufacturer of the machine before commercial use will be possible. Currently, there is some work being prepared for the manufacture of disposable CCC coils which would be replaced after each use [Wood, 2005]. This would eliminate problems that might be encountered for the cleaning and sterilization of the columns, and would be particularly useful in multi-product facilities. In addition to the considerations of design, control and purification achieved, removal of residual phase forming chemicals will need to be validated to stringent requirements before the application of this technique is likely to be acceptable to regulatory bodies such as the FDA. However, such exercises must be carried out for each new product, whether the purification process is conventional or novel.

Chapter 8
References

Alberts BM. 1967. Fractionation of nucleic acids by dextran-polyethylene glycol two-phase systems in: Methods in Enzymology, Colowick SP, Kaplan NO (eds.), 12A, 566-581, Academic Press, New York.

Albertsson PA. 1956. Nature. 177, 771.

Albertsson PA. 1986. Partition of cell particles and macromolecules, 3rd edn., Wiley, New York.

Albertsson PA, Cajarville A, Brooks DE, Tjerneld F. 1987. Partition of proteins in aqueous polymer two-phase systems and the effect of molecular weight of the polymer. **Biochim Biophys Acta.** 926, 87-93.

Alstine KK and Veide A. 1999. Two-phase extraction of proteins from cell debris. In: Hatti-Kaul R, editor. Methods in biotechnology, Vol. 11, Aqueous two-phase systems: Methods and protocols. New Jersey: Humana Press. 251-258.

Asenjo JA, Turner RE, Mistry SL, Kaul A. 1994. Separation and purification of recombinant proteins from Escherichia coli with aqueous two-phase systems. **J. Chromatogr. A.** 668 (1): 129-137.

Balasubramaniam D, Wilkinson C, Van Cott K, Zhang C. 2003. Tobacco protein separation by aqueous two-phase extraction. **J. Chromatogr. A.** 989: 119-129.

Bamberger S, Brooks DE, Sharp KA, Van Alstine JM, Webber TJ. 1985. Preparation of phase systems and measurements of their physicochemical properties, in: Walter H, Brooks DE, Fisher D (eds.). Partitioning in aqueous two-phase systems. Theory, methods, uses, and applications to biotechnology. Academic Press Inc., London.

Bergan, D, Galbaith T and Sloane DL. 2000. Gene transfer in vivo by cationic lipids is not significantly affected by levels of supercoiling of a reporter plasmid. **Pharma. Res.** 17(8): 967-973.

Berthod A. 1991. Practical approach to high-speed counter-current chromatography. **J. Chromatogr.** 530: 677-693.

Berthod A and Schmitt N. 1993. Water-organic solvent systems in countercurrent chromatography: Liquid stationary phase retention and solvent polarity. **Talanta.** 15(10): 1489-1498.

Berthod A. 2002. Countercurrent chromatography: The support-free liquid stationary phase. Comprehensive analytical chemistry, vol. 38, Elsevier, Amsterdam.

Berthod A, Hassoun M, Harris G. 2005. Using the liquid nature of the stationary phase: The elution-extrusion method. **J. Liq. Chrom. & Rel. Technol.**, 28 (12-13): 1851-1866.

Bhatnagar M, Oka H, Ito Y. 1989. Improved cross-axis synchronous flow-through coil planet centrifuge for performing counter-current chromatography. II. Studies on retention of stationary phase in short coils and preparative separations in multilayer coils. **J. Chromatogr.** 463: 317-328.

Bibilashvili, R and Savochkina LP. 1971. Distribution of RNA polymerase and its complex with DNA in a diphase dextran-polyethylene glycol system. **Mol. Biol.** (Moscow) 5, 252-258.

Birnboim HC. 1983. A rapid alkaline extraction method for the isolation of plasmid DNA. **Methods Enzymol.** 100, 243-255.

Birnboim HC, Doly J. 1979. A rapid alkaline extraction process for screening the recombinant plasmid DNA. **Nuc. Acids Res.** 7(6), 1513-1521.

Bonilla, PJ, Freytag SO and Lutter LC. 1991. Enhancer-activated plasmid transcription complexes contain constrained supercoiling. **Nuc. Acids Res.** 19(14): 3965-3971.

Booth AJ and Lye GJ. 2001. Optimisation of the fractionation and recovery of polyketide antibiotics by counter-current Chromatography. **J. Liq. Chrom. & Rel. Technol.**, 24: 1841-1861.

Booth AJ, Sutherland IA, Lye GJ. 2003. Modelling the performance of pilot-scale countercurrent chromatography: Scale-up predictions and experimental verification of erythromycin separation. **Biotechnol. Bioeng.** 81 (6): 640-649.

Booth AJ. 2003. Process design and scale-up pf counter-current chromatography for the fractionation and recovery of polyketide antibiotics. Ph.D thesis, University College London, University of London.

Brooks DE, Sharp KA, Fisher D. 1985. Theoretical aspects of partitioning in: Walter H, Brooks DE, Fisher D (eds.). Partitioning in aqueous two-phase systems. Theory, methods, uses, and applications to biotechnology. Academic Press Inc., London.

Brown, WRA, Mee PJ and Shan MH. 2000. Artificial chromosomes: Ideal vectors? **Trends Biotechnol.** 18, 218-223.

Bywater M, Bywater R, Hellman L. 1983. A novel chromatographic procedure for purification of bacterial plasmids. **Anal. Biochem.** 132(1): 219-224.

Brunel Insititute of Bioengineering, Brunel University. 2000. J-Type CCC manual.

Chen, W, Graham C and Ciccarelli RB. 1997. Automated fed batch fermentation with feed back controls based on dissolved oxygen (DO) and pH for production of DNA vaccines. **J. Microb. Technol.** 18: 43-48.

Chen CCV, Elliot JAW, Williams MC. 2003. Investigation of the dependence of inferred interfacial tension on rotation rate in a spinning drop tensiometer. **J. Colliod Interface Sci.** 260: 211-218.

Ciccolini, LAS, Shamlou PA, Titchener-Hooker NJ and Ward JM. 1998. Time course of SDS-alkaline lysis of recombinant bacterial cells for plasmid release. **Biotechnol. Bioeng.** 60(6), 768-770.

Cole KD. 1991. Purification of plasmid and high molecular weight DNA using PEG-salt two-phase extraction. **BioTechniques.** 11: 18-24.

Conway WD and Ito Y. 1984. Phase distribution of liquid-liquid systems in spiral and multilayer helical coils on a centrifugal countercurrent chromatograph. Presented at Pittsburgh Conference, Atlantic City, N.J., U.S.A.

Conway WD. 1990. Counter current chromatography: Apparatus, theory and applications. New York, VCH Publishers.

Crystal, RG. 1995. Transfer of genes to humans: Early lessons and obstacles to success. **Science.** 270: 404-409.

Degenhardt A, Schwarz M, Winterhalter P, Ito Y. 2001. Evaluation of different tubing geometries for high-speed counter-current chromatography. **J. Chromatogr. A.** 922 (1 & 2): 355-358.

Diamond AD and Hsu JT. 1992. Aqueous two-phase systems for biomolecule separations. **Adv Biochem. Eng.** 47: 89-135.

Diogo MM, Queiroz JA and Prazeres DMF. 2005. Chromatography of plasmid DNA. **J. Chromatogr. A.** 1069(1): 3-22.

Diogo MM, Ribeiro S, Queiroz JA, Monteiro GA, Perrin P, Tordo N and Prazeres DMF. 2000. Scale-up of hydrophobic interaction chromatography for the purification of a DNA vaccine against rabies. **Biotechnol. Lett.** 22: 1397-1400.

Du Q, Wu C, Qian G, Wu P. Ito Y. 1999. Relationship between flow rate of the mobile phase and retention of the stationary phase in counter-current chromatography. **J. Chromatogr. A.** 835: 231-235.

Edwardson PAD, Atkinson T, Lowe CR, Small DAP. 1986. A new rapid procedure for the preparation of plasmid DNA. **Anal. Biochem.** 152(2): 215-220.

Elles R and Sutherland IA. 1980. Purification of specific restriction fragments of human deoxyribonucleic acid by using liquid countercurrent chromatography. **Biochem. Soc. Trans.** 8: 173.

Falaschi A and Kornberg A. 1966. Biochemical studies of bacterial sporulation. II. Deoxyribonucleic acid polymerase in spores of Bacillus subtilis. **J. Biol. Chem.** 241,:1478-1482.

Favre J and Petttijohn D. 1967. A method for extracting purified DNA or protein-DNA complexes from *Escherichia coli*. **Europ. J. Biochem.** 3: 33-41.

Fedetov PS and Thiébaut. 1998. Retention of the stationary phase in a coil planet centrifuge: Effects of interfacial tension, density difference and viscosities of liquid phases. **J. Liq. Chrom. & Rel. Technol.**, 21(1&2): 3237-3254.

Fedetov PS, Sutherland IA, Wood P, Spivakov BY. 2003. Retention of solids in rotating coiled columns: The effect of β value and tubing material. **J. Liq. Chrom. & Rel. Technol.**, 26 (9-10): 1649-1657.

Ferreira GNM, Monteiro GA, Prazeres DMF, Cabral JMS. 2000. Downstream processing of plasmid DNA for gene therapy and DNA vaccine applications. **TIBTECH.** 18: 380-388

Ferreira GNM, Cabral JMS, Prazeres DMF. 1999. Development of process flowsheets for the purification of supercoiled plasmids for gene therapy applications. **Biotechnol. Prog.** 15: 725-731.

Ferreira GNM, Cabral JMS, Prazeres DMF. 1998. Purification of supercoild plasmid DNA using chromatographic processes. **J. Molec. Recogn.** 11: 250-251.

Flanagan JA, Huddleston JG, Lyddiatt A. 1991 Application of aqueous two-phase partition in PEG-phosphate system. **Bioseparation.** 2: 43-61.

Forciniti D, Hall CK, Kula MR. 1991. Protein partitioning at the isoelectric point: influence of polymer molecular weight and concentration and protein size. **Biotechnol. Bioeng.** 38: 986-994.

Foucault A and Nakanishi K. 1990. Comparison of several aqueous two phase solvent systems (ATPS) for the fractionation of biopolymers by centrifugal partition chromatography (CPC). **J. Liq. Chromatogr.** 3(12): 2421-2440.

Fox, JL. 1999. Gene therapy safety issues come to the fore. **Nature Biotech.** 17: 1153.

Gaziev AI and Kuzin AM. 1973. The localization of DNA ligase in the chromatin of animal cells. **Eur. J. Biochem.** 37: 7-11.

Goff CG. 1974. Chemical structure of a modification of the *Escherichia coli* ribonucleic acid polymerase α polypeptide induced by the bacteriophage T_4 infection. **J. Biol. Chem.** 249: 6181-6190.

Goupy J, Menet JM, Shinomiya K, Ito Y. 1995. Cross-axis coil planet centrifuge - use of experimental designs to determine the optimal settings. **Mod. Countercurrent Chromatogr.** 593: 47-61.

Green AP, Prior GM, Helveston NM, Taittinger BE, Liu X, Thompson JA. 1997. Preparative purification of supercoiled plasmid DNA for therapeutic applications. **Biopharm**. 10(5): 52-62.

Gustavsson PE, Lemmens R, Nyhammar T, Busson P, Larsson PO. 2004. Purification of plasmid DNA with a new type of anion-exchange beads having a non-charged surface. **J. Chromatogr. A.** 1038: 131-140.

Han JH and Lee CH. 1997. Effects of salts and poly(ethylene glycol)-palmitate on the partitioning of proteins and *Bacillus subtilis* neutral protease in aqueous two-phase systems. **Colloids Surf. Biointerfaces.** 109-116.

Hasan UA, Abai AM, Harper DR, Wren BW and Morrow WJW. 1999. Nucleic acid immunisation: concepts and techniques associated with third generation vaccines. **J. Immunol. Meth.** 229: 1-22.

Hatti-Kaul R. 2000. Aqueous two-phase systems, Methods and protocols. Humana Press Inc., New Jersey, USA.

Hatti-Kaul R. 1999. Aqueous two-phase systems In: Hatti-Kaul R, editor. Methods in biotechnology, Vol. 11, Aqueous two-phase systems: Methods and protocols. New Jersey: Humana Press. p. 1-10.

Hermans-Lokkerbol ACJ, Hoek AC, Verpoorte R. 1997. Preparative separation of bitter acids from hop extracts by centrifugal partition chromatography, **J. Chromatog. A.** 771(1&2): 71-79.

Horn, NA, Meek JA, Budahazi G and Marquet M. 1995. Cancer gene therapy using plasmid DNA - purification of DNA for human clinical trials. **Hum. Gene Ther.** 6(5): 565-573.

Huddleston JG, Wang R, Flanagan JA, O'Brien S, Lyddiatt A. 1994. Variation of protein partition coefficient with volume ratio in poly(ethylene glycol)-salt aqueous two-phase system. **J. Chromatogr. A.** 668: 3-11.

Huddleston JG, Veide A, Kölher K, Flanagan J, Enfors SO, Lydiatt A. 1991. The molecular basis of partitioning in aqueous two-phase systems, **Trends Biotechnol.** 9: 381-388.

Hustedt H, Kroner KH, Kula MR. 1985. Applications of phase partitioning in biotechnology in: Walter H, Brooks DE, Fisher D (eds.): Partitioning in aqueous two-phase systems. Theory, methods, uses, and applications to biotechnology. Academic Press Inc., London, 529-584.

Ignatova SN and Sutherland IA. 2003. A fast, effective method of characterizing new phase systems in CCC. **J. Liq. Chrom. & Rel. Technol.** 2003, 26 (9 & 10), 1551-1564.

Ito Y, Bramblett GT, Bhatnagar R, Huberman M, Leive LL, Cullinane LM, Groves W. 1983. Improved nonsynchronous flow-through coil planet centrifuge without rotating seals: Principle and application. **Sep. Science & Technol.** 18(1): 33-48.

Ito Y. 1984a. Experimental observations of the hydrodynamic behaviour of solvent systems in high speed counter-current chromatography: I. Hydrodynamic distribution of two solvent phases in a helical column subjected to two types of synchronous planetary motion. **J. Chromatogr.** 301: 377-386.

Ito Y. 1984b. Experimental observations of the hydrodynamic behaviour of solvent systems in high speed counter-current chromatography: II. Phase distribution for helical and spiral columns. **J. Chromatogr.** 301: 387-404.

Ito, Y. 1988. Principles and instrumentation of counter-current chromatography. Counter-current chromatography: Theory and practice. NB Madava and Ito, Y. New York and Basel, Marcel Dekker Inc. 44.

Ito Y. 1992. Speculation on the mechanism of unilateral hydrodynamic distribution of two immiscible solvent phases in the rotating coil. **J. Liq. Chromatog.** 15(15&16): 2639-2675.

Ito, Y. 1996. Principle, apparatus, and methodology of high-speed countercurrent chromatography: 3-44. In: eds. Ito, Y. and Conway, W.D. High speed countercurrent chromatography, 132. Chemical analysis series, John Wiley & Sons, New York, U.S.A.

Ito Y, Matsuda K, Ma Y, Qi L. 1998. Toroidal coil counter-current chromatography study of the mass transfer rate of proteins in aqueous-aqueous polymer phase system. **J. Chromatogr. A.** 802: 277-283.

Jackson G, Sherestha S, Ward JM. 1995. Metabolic engineering of the toluene degradation pathway. **J. Cell. Biochem.** S21A CIA, 48.

Johansson H0, Karlström G, Tjerneld F, Haynes CA. 1998. Driving forces for phase separation and partitioning in aqueous two-phase systems. **J. Chromatogr. B.** 718: 3-17.

Johansson G and Andersson M. 1984. Parameters determining affinity partitioning of yeast enzymes using polymer-bound triazine dye ligans. **J. Chromatogr.** 202: 39-51.

Johansson G. 1970. Partition of salts and their effects on partition of proteins in a dextran-poly(ethylene glycol)-water two-phase system. **Biochim. Biophys. Acta.** 221: 387-390.

Kaul A and Asenjo JA. 1994. Partition of soluble proteins from *E. coli* in polyethylene glycol-salt phase systems, in: Pyle (ed.). **Separations for Biotechnology**. 3: 235-241, SCI.

Kaul RH (Ed.). 2000. Aqueous two-phase systems, methods and protocol, Humana Press, Clifton, NJ.

Kendall D, Booth AJ, Levy MS, Lye GJ. 2001. Separation of supercoiled and open-cirular plasmid DNA by liquid-liquid counter-current chromatography. **Biotechnol. Lett.** 23: 613-619.

Kendall D, Lye GJ, Levy MS. 2002. Purification of plasmid DNA by an integrated operation comprising tangential flow and nitrocellulose adsorption. **Biotech. Bioeng.** 78(7): 816-822.

Kendall D. 2002. Novel approaches to the purification of plasmid DNA for therapeutic application. Ph.D thesis, University College London, University of London.

Kepka C, Rhodin J, Lemmens R, Tjerneld F, Gustavsson PE. 2004a. Extraction of plasmid DNA from Escherichia coli cell lysate in a thermoseparating aqueous two-phase system. **J. Chromatogr. A.** 1024: 95-104.

Kepka C, Lemmens, Vasi J, Nyhammar T, Gustavsson PE. 2004b. Integrated process for purification of plasmid DNA using aqueous two-phase systems combined with membrane filtration and lid bead chromatography. **J. Chromatogr. A.** 1057: 115-124.

Kimura K and Kobayashi H. 1996. RNA partitioning accompanied by absorption : high-molecular –mass RNA adsorbed at the interface like a particle. **J. Chromatogr. B.** 680: 213-219.

Kimura K. 2000. Simultaneous accumulation of low-molecular-mass RNA at the interface along with accumulation of high-moelcular-mass RNA on aqueous two-phase system partitioning. **J. Chromatogr. B.** 743: 421-429.

Köhler K, Bonsdorff-Lindeberg LV, Enfors SO. 1989. Influence of distrupted biomass on the partitioning of β-galactosidase fused protein A. **Enzyme Microb. Technol.** 11: 730-735.

Koide, Y, Nagata T, Yoshida A and Uchijima M. 2000. DNA Vaccines. **Jpn. J. Pharmacol.** 83: 167-174.

König CS and Sutherland IA. 2003. An investigation of the influence of the gravity field on the interface of two immiscible liquids- A computational study Comparing prediction with experiment. **J. Liq. Chrom. & Rel. Technol.** 26(9&10): 1521-1535.

Kula MR, Kroner KH, Hustedt H. 1982. Purification of Enzymes by Liquid-Liquid-Extraction. In *Advances in Biochemical Engineering*, 24; Fiechter, A., Eds.; Springer Verlag: Berlin: 73-118.

Kune P. 2002. Process considerations for the recovery of bio-nanoparticulates in polymer-salt aqueous two-phase systems. PhD Thesis, University of Brimingham.

Lahijani R, Hulley G, Soriano G, Horn NA and Marquet M. 1996. High yield production of pBR322-derived plasmids intended for human gene therapy by employing a temperature-controllable point mutation. **Hum. Gene Ther.** 7: 1971-1980.

Lebreton B, Walker SG, Lyddiatt A. 2002. Characterization of aqueous teo-phase partition systems by distribution analysis of radiolabeled analytes (DARA): Application to process definition and control in biorecovery. **Biotechnol. Bioeng.** 77: 329-339.

Lei X, Diamond AD, Hsu JT. 1990. Equilibrium phase behaviour of Poly(ethylene glycol)/Potassium Phosphate/Water two-phase system at 4^0 C. **J. Chem. Eng. Data.** 35: 420-423.

Lei X and Hsu JT. 1992. Separation of proteins using aqueous two-phase systems in eccentric multi-layer coil planet centrifuge. **J. Liq. Chrom. & Rel. Technol.** 15(15& 16): 2801-2817.

Levy MS, Collins IJ, Yim SS, Ward JM, Titchner-Hooker N, Shamlou PA, Dunnill P. 1999. Effect of shear on plasmid DNA in solution. **Bioprocess Eng.** 20: 7-13.

Levy MS, O'Kennedy RD, Ayazi-Shamlou P, Dunnill P. 2000. Biochemical engineering approaches to the challenges of producing pure plasmid DNA. **Trends Biotechnol.** 18: 296-305.

Lodish H, Berk A, Zipursky SL, Matsudaira P, Baltimore D, Darnell J. 2001. Molecular cell biology. 4^{th} Edn, W.H Freeman and Company, New York.

Mahvi, DM, Sheeny MJ and Yang N-S. 1997. DNA cancer vaccines, a gene gun approach. **Immunol. Cell Biol.** 75: 456-460.

Mandava NB and Ito Y. 1988. Countercurrent chromatography. Theory and practice. Marcel Dekker Inc., New York. Chromatographic science series volume 44.

Mao DT, Levin JD, Yu L, Lautamo RMA. 1998. High resolution capillary electrophoretic separation of supercoiled plasmid DNA's and their conformers in dilute hydroxypropylmethy cellulose solutions containing no intercalating agent. **J. Chromatogr. B.** 714: 21-27.

Marcos JC, Fonseca LP, Ramalho MT, Cabral JMS. 1999. Partial purification of penicillin acylase from *Escherichia coli* in poly(ethylene glycol)-sodium citrate aqueous two-phase systems. **J. Chromatogr. B.** 734: 15-22.

Marquet, M, Horn NA and Meek JA. 1997a. Characterization of plasmid DNA vectors for use in human gene therapy. Part 1. **Biopharm.** 10(5): 42-50.

Marquet, M, Horn NA and Meek JA. 1997b. Characterization of plasmid DNA vectors for use in human gene therapy. Part 2. **Biopharm.** 10(6): 40-45.

Marquet, M, Horn NA and Meek JA. 1995. Process development for the manufacture of plasmid DNA vectors for use in gene tharapy. **Biopharm.** 8(7): 26-37.

Maryutina TA, Ignatova SN, Sutherland IA. 2003. Organic phase retention in CCC: Effect of temperature, tubing material, tubing bore, mobile phase flow, and the addition of an extraction agent. **J. Liq. Chrom. & Rel. Technol.** 26 (9 & 10): 1537-1550.

Matsuda K, Matsuda S, Ito I. 1998. Toroidal coil counter-current chromatography: Achievement of high resolution by optimizing flow-rate, rotation speed, sample volume and tube length. **J. Chromatogr. A.** 808(1 & 2): 95-104.

Matthews CK, Van-Holde KE. 1990. Biochemistry. Redwood City, CA, Benjamin/Cumming publishing company.

Meacle FJ, Lander R, Ayazi-Shamlou P, Titchener-Hooker NJ. 2004. Impact of engineering flow conditions on plasmid DNA yield and purity in chemical cell lysis operations. **Biotechnol. Bioeng,** 87 (3): 293-302.

Menet JM, Rolet MC, Thiébaut D, Rosset R, Ito Y. 1992. Fundentental chromatographic parameters in countercurrent chromatography: Influence of the volume of stationary phase and the flow rate. **J. Liq. Chromatogr.** 15(15&16): 2883-2908.

Menet JM and Ito Y. 1993. Studies on a new cross-axis coil planet centrifuge for performing counter-current chromatography: Part II. Path and acceleration of coils and comparison with type J coil planet centrifuge. **J. Chromatogr.** 644: 231-238.

Menet JM and Thiebaut D. 1999. Preparative purification of antibiotics for comparing hydrostatic and hydrodynamic mode counter-current chromatography and preparative high-perfomance liquid chromatography, **J. Chromatogr. A.** 831: 203-216.

Mhashilkar, A, Chada S, Roth JA and Ramesh R. 2001. Gene therapy. Therapeutic approaches and implications. **Biotech. Adv.** 19: 279-297.

Middaugh, CR, Evans RK, Montgomery DL and Casimiro DK. 1998. Analysis of plasmid DNA from a pharmaceutical perspective. **J. Pharm. Sci.** 87(2): 130-146.

Mishima K, Matsuyama K, Ezawa M, Taruta Y, Takarabe S, Nagatani M. 1998. Interfacial tension of aqueous two-phase systems containing poly(ethylene glycol) and dipotassium hydrogenphosphate. **J. Chromatogr. B.** 711: 313-318.

Mistry SL, Kaul A, Merchuk JM, Asenjo JA.1996. Mathematical modelling and computer simulation of aqueous two-phase continuous protein extraction. **J. Chromatogr. A.** 741: 151-163.

Molecular Probes; Pico green dsDNA Quantitation Reagent and Kits, PoortGebouw, Rijnsburgerweg 10, 2333AA Leiden, The Netherlands.

Mountain, A. 2000. Gene therapy: the first decade. **Trends Biotechnol.** 18: 119-128.

Nochumson S, Warner T, Pora H. 2000. Purification of plasmid DNA using a new generation of anion exchange membrane adsorbers. **Bioeurope.** December 11-13, Lake Konstanz, Germany.

Ohlsson R, Hentschel CC, Williams JG. 1978. A rapid method for the isolation of circular DNA using an aqueous two-phase partition system. **Nuc. Acids Res.** 5,:583-590.

Oka F, Oka H, Ito Y. 1991. Systematic search for a suitable two-phase solvent systems for high-speed counter-current chromatography. **J. Chromatogr.** 538: 99-108.

Okazaki T and Kornberg A. 1964. Enzymatic Synthesis of Deoxyribonucleic Acid. XV. Purification and Properties of a Polymerase from Bacillus subtilis, **J. Biol. Chem.** 239: 259.

Petsch D, Anspach FB. 2000. Endotoxin removal from protein solutions. **J. Biotech.** 76: 97-119.

Prather KJ, Sagar S, Murphy J, Chartrain M. 2003. Industrial scale production of plasmid DNA for vaccine and gene therapy: plasmid design, production and purification. **Enz. Microbiol. Technol.** 33: 865-883.

Prazeres, DMF, Ferreira GNM, Monteiro GA, Cooney CL and Cabral JMS. 1999. Large-scale production of pharmacuetical-grade plasmid DNA for gene therapy: Problems and bottlenecks. **Trends Biotechnol.** 17(4): 169-174.

Prazeres, DMF, Schluep T, Cooney CL. 1998. Preparative purification of supercoiled plasmid DNA using anion exchange chromatography. **J. Chromatogr. A.** 806: 31-45.

Qi L, Ma Y, Ito Y, Fales HM. 1998. Isolation and purification of 3-oxo-Delta(5)-steroid from crude E. coli lysate by countercurrent chromatography. **J. Liq. Chromatogr. Rel. Technol.** 21(1 & 2): 83-92.

Rock C, Shamlou PA, Levy SM. 2003. An automated microplate-based method for monitoring DNA strand breaks in plasmids and bacterial artificial chromosomes. **Nuc. Acids Res.** 31,11.

Radding CM. 1966. Regulation of a λ exonuclease. I. Properties of λ exonuclease purified from lysogens of λ_{T11} and wild type. **J. Mol. Biol.** 18: 235-250.

Ribeiro SC, Monteiro GA, Cabral JMS, Prazeres DMF. 2002. Isolation of plasmid DNA from cell lysates by aqueous two-phase systems. **Biotechnol. Bioeng.** 78: 376-384.

Ribeiro SC, Monteiro GA, Martinho G, Cabral JMS, Prazeres DMF. 2000. Quantification of plasmid DNA in aqueous two-phase systems by flurescence analysis. **Biotechnol. Lett.** 22: 1101-1104.

Rito-Palomares M and Cueto L. 2000. Effect of biological suspensions on the position of the binodal curve in aqueous two-phase systems. **J. Chromatogr. B.** 743: 5-12.

Rito-Palomares M, Dale C and Lyddiatt A. 2000. Generic application of aqueous two-phase process for protein recovery from animal blood. **Process Biochem.** 35: 665-673.

Robinson, HL, Ginsberg HS, Davis HL, Johnston SA and Lui MA. 1997. The scientific future of DNA for immunisation. A report from the American Academy of Microbiology, American Academy of Microbiology.

Rubin L and Albertsson PA. 1967. A new method for the isolation of deoxyribonucleic acids from microorganisms. **Biochim. Biophys. Acta.** 134: 37-44..

Saeki S, Kuwahara N, Nakata M, Kaneko M. 1976. Upper and lower critical solution temperatures in poly(ethylene glycol) solutions. **Polymer.** 17: 685-689.

Salabat A. 2001. The influence of salts on the phase compositions in aqueous two phase systems: experiments and predictions. **Fluid Phase Equil.** 489: 187-188.

Sambrook J, Fritsch EF, Maniatis T. 1989. Molecular cloning- a laboratory manual, Cold Spring Harbour Laboratory Press.

Schleef M and Schmidt T. 2004. Animal-free production of ccc-supercoiled plasmids for research and clinical applications. **J. Gene Med.** 6 (1): 45-53.

Schmidt AS, Andrews BA, Asenjo JA. 1996. Correlations for the partition behaviour of proteins in aqueous two-phase systems: Effect of overall protein concentration. **Biotechnol. Bioeng.** 50: 617-626.

Schmidt AS, Ventom AM, Asenjo JA. 1994. Partition and purification of α-amylase in aqueous two-phase systems. **Enzyme Microb. Technol.** 16: 131-142.

Shibusawa Y and Ito Y. 1991. Protein separation with aqueous-aqueous polymer systems by two types of counter-current chromatographs. **J. Chromatogr.** 550: 695-704.

Shibusawa Y, Mugiyama M, Matsumoto U, Ito Y. 1995. Complementary use of counter-current chromatography and hydroxyapatite chromatography for the separation of three main classes of lipoproteins from human serum. **J. Chromatogr. B.** 664 (2): 295-301.

Shibusawa Y, Eriguchi Y, Ito Y. 1997. Purification of lactic acid dehydrogenase from bovine heart crude extract by counter-current chromatography. **J. Chromatogr. B.** 696: 25-31.

Shibusawa Y, Yanagida A, Ito A, Ichihashi K, Shindo H, Ito Y. 2000. High-speed counter-current chromatography of apple procyanidins. **J. Chromatogr. A.** 886 (1 & 2): 65-73.

Shibusawa Y, Naomi Misu, Heisaburo S, Ito Y. 2002. Purification of lactic acid dehydrogenase from crude bovine heart extract by pH-peak focusing counter-current chromatography. **J. Chromatogr. B.** 776(2): 183-189.

Shinomiya K, Menet JM, Fales HM, Ito Y. 1993. Studies on a new cross-axis coil planet centrifuge for performing counter-current chromatography: I. Design of the apparatus, retention of the stationary phase, and efficiency in the separation of proteins with polymer phase systems. **J. Chromatogr.** 644, 215-229.

Shinomiya, K, Kabasawa Y, Ito Y. 1998. Countercurrent chromatographic separation of protein by cross-axis planet centrifuge: Choice of polymer phase systems and revolution speed. **J. Liq. Chrom. & Rel. Technol.** 21(11): 1727-1736.

Shinomiya K, Hirozane S, Kabasawa H, Ito Y. 2000. Protein separation by cross-axis coil planet centrifuge with two different positions of eccentric coil assemblies using polyethylene glycol-dextran solvent system. **J. Liq. Chrom. & Rel. Technol.** 23(7): 1119-1129.

Shinomiya K, Kabasawa, Y, Yanagidaira K, Sasaki H, Muto M, Okada T, Ito Y. 2003. Protein separation by nonchronous coil planet centrifuge with aqueous-aqueous polymer phase systems. **J. Chromatogr. A. 1005: 103-112.**

Shroff, KE, Smith LR, Baine Y and Higgins TJ. 1999. Potential for plasmid DNA as vaccines for the new milennium. **Pharm. Sci. Tech.** 2(5): 205-212.

partitioning preference could be due to a number of reasons including the high viscosity of the stationary PEG phase, coupled with the large dynamic volume of DNA molecules [Ito *et al.*, 1998], the high interfacial contact areas (due to low interfacial tensions) between the two systems [Hatti-Kaul, 1999], the collapse of DNA in PEG solutions [Vasilevskaya *et al.* 1995], an increase in the salting-out effect (due to high salt concentrations) at the end of the run or an reduction in interfacial tension due to some pDNA/RNA being retained at the interface.

Based on the successful fractionation of pDNA from its contaminants, CCC operating variables and modes, as discussed in Chapter 6, were tested with the aim of increasing throughput. This chapter examined for the first time the effect of changing operating parameters for plasmid separations using aqueous two-phase systems. The retention of pDNA in the column can be avoided by operating the CCC in the elution-extrusion mode. Overall process recovery yields as high as 58% (w/w) were achieved due to the plasmid eluting in narrow fractions peaks rather than broader peaks when eluted with nitrogen. The upper loading limit was not established as doubling the injection volume (11% v/v total column volume) did not affect recovery yields or resolution. The ability to purify of pDNA when using unclarified lysates in the initial batch extraction was also demonstrated (Section 6.6). RNA was successfully removed with a 49% (w/w) overall 2-step process recovery yield of pDNA. Thus the 2-step CCC process has the potential to reduce the number of downstream processing steps for the purification of pDNA eliminating the need for the centrifugation and filtration steps that usually followed the alkaline-lysis step. A summary of a potential downstream process is shown in Figure 7.2:

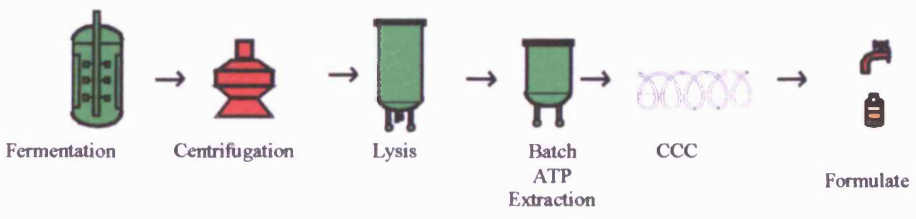

Figure 7.2: Overall downstream of pDNA using unclarified lysate with batch ATP extraction and CCC steps.

Simonet F, Garnier C, Doublier JL. 2000. Partition of protein in the aqueous guar/dextran two-phase system. **Food Hydrocolloids.** 14: 591-600.

Sinden RR. 1994. DNA structure and function. Academic Press Inc., San Diego.

Sinnett D, Richer C, Baccichet A. 1998. Isolation of stable bacterial artificial chromosome DNA using a modified alkaline lysis method. **Biotechniques.** 24: 752-754.

Sparks RB and Elder JH. 1983. A simple and rapid procedure for the purification of plasmid DNA using reverse-phase C18 silica beads. **Anal. Biochem.** 135: 345.

Sutherland IA, Jones S, Heywood-Waddington D.1986. A preliminary study of the hydrodynamics of a range of solvent systems in a single layer coil planet centrifuge. Preparative countercurrent chromatography, No. 1045. Proceedings of the Pittsburgh conference and exposition on analytical chemistry and applied spectroscopy, Altantic City, New Jersey.

Sutherland IA, Heywood-Waddington D, Ito Y. 1987. Counter-current chromatography, Applications to the separation of biopolymers, organelles and cells using wither aqueous-organic or aqueous-aqueous phase systems. **J. Chromatogr.** 384: 197-207.

Sutherland IA, Brown L, Forbes S, Games G, Hawes D, Hostettmann K, McKerrell EH, Marston A, Wheatley D, Wood P. 1998. Countercurrent chromatography (CCC) and its versatile application as an industrial purification & production process. **J. Liq. Chrom. & Rel. Technol.** 21(3): 279-298.

Sutherland IA, Muytjens M, Prins M, Wood, P. 2000a. A new hypothesis on phase distribution in countercurrent chromatography. **J. Liq. Chrom. & Rel. Technol**. 23 (15): 2259-2276.

Sutherland IA. 2000b. Relationship between retention, linear velocity and flow for counter-current chromatography. **J. Chromatogr. A.** 886: 283-287.

Sutherland IA, Booth AJ, Brown L, Kemp B, Kidwell H, Games D, Guillon GG, Hawes D, Hayes M, Janaway L, Lye GJ, Massey P, Preston C, Shering P, Shoulder, T Strawson C, Wood P. 2001. Industrial scale-up of countercurrent chromatography. **J. Liq. Chrom. & Rel. Technol.** 24 (11 & 12): 1533-1553.

Sutherland IA, Hawes D, Van den Heuvel R. 2003. Resolution in CCC: The effect of operating conditions and phase system properties on scale-up. **J. Liq. Chrom. & Rel. Technol.** 26 (9 & 10): 1475-1491.

Theodossiou, I, Olander MA, Sondergaard M, Thomas ORT. 2000. New expanded bed adsorbents for the recovery of DNA. **Biotech. Lett.** 22: 1929-1933.

Thwaites E, Burton SC, Lyddiatt A. 2001. Impact of the physical and topographical characteristics of absorbent soild-phases upon the fluidised bed recovery of plasmid DNA from *Escherichia coli* lysates. **J. Chromatogr. A.** 943: 77-90.

Tomanee P, Hsu JT, Ito Y. 2004. Fractionation of protein, RNA, and plasmid DNA in centrifugal precipitation chromatography using cationic surfactant CTAB containing inorganic salts NaCl and NH_4Cl. **Biotechnol. Bioeng.** 88 (1): 53-59.

Trindade IP, Diogo MM, Prazeres DMF, Marcos JC. 2005. Purification of plasmid DNA vectors by aqueous two-phase extraction and hydrophobic interaction chromatography. **J. Chromatogr. A.** 1082 (2): 176-184.

Varley, DL, Hitchcock AG, Weiss AME, Horler WA, Cowell R, Peddie L, Sharpe GS, Thatcher DR and Hanak JAJ. 1999. Production of plasmid DNA for human gene therapy using modified alkaline cell lysis and expanded bed anion exchange chromatography. **Bioseparation.** 8: 209-217.

Vasilevskaya VV, Khokhlov AR, Matsuzawa Y, Yoshikawa K. 1995. Collapse of single DNA molecule in a poly(ethylene glycol) solutions. **J. Chem. Phys.** 102: 6595-6602.

Verma S, Kumar VV. 1998. Relationship between oil-water interfacial tension and oily soil removal in mixed surfactant systems. **J. Colloid Interface Sci.** 207: 1-10.

Vilalta A, Whitlow V, Martin T. 2002. Real-Time PCR determinations of Escherichia coli genomic DNA concentrations in plasmid preparations. **Anal. Biochem.** 301: 151-153.

Vovis GF and Buttin G. 1970. An ATP-dependent deoxyribonuclease from Diplococcus pneumoniae. I. Partial purification and some biochemical properties. **Biochim. Biophys. Acta.** 224: 29-41.

Wade-Martins R, Frampton J, James MR. 1999. Long-term stability of large insert genomic DNA episomal shuttle vectors in human cells. **Nuc. Acids Res.** 27: 1674-1682.

Walsh CE. 2003. Gene therapy Progress and Prospects: Gene therapy for the hemophilias. **Gene Therapy.** 10: 99̃1003.

Walter H, Brooks DE, Fisher D. 1985. Partitioning in aqueous two-phase systems. Theory, methods, uses, and applications to biotechnology. Academic Press Inc., London.

Wang-Fan W, Küsters E, Mak CP, Wang Y. 2001.Application of coil centrifugal counter-current chromatography to the separation of macrolide antibiotic analogues: III. Effects of flow-rate, mass load and rotation speed on the peak resolution. **J. Chromatogr. A.** 925(1&2): 139-149.

Watson, JD, Gilman M, Witkowski J and Zoller M. 1992. Recombinant DNA. New York, Scientific American Books.

Watson JD and Crick FHC. 1953. Molecular structure of nucleic acids: A structure for deoxyribose nucleic acid. **Nature.** 171: 737-738.

Willard, HF. 1998. Human artificial chromosomes coming into focus. **Nature.** 16: 415-416.

Wood PL, Jaber B, Sutherland IA. 2001. A new hypothesis on the hydrodynamic distribution of the upper and lower phases in CCC. **J. Liq. Chrom. & Rel. Technol.** 24 (11&12): 1629-1654.

Wood PL. 2002. The hydrodynamics of countercurrent chromatography in J-type centrifuges. Burnel University. PhD thesis.

Wood PL, Hawes D, Janaway L, Sutherland IA. 2003a. Stationary phase retention in CCC: Modelling the J-type centrifuge as a constant pressure drop pump. **J. Liq. Chrom. & Rel. Technol.** 26 (9-10): 1373-1396

Wood PL, Hawes D, Janaway L, Sutherland IA. 2003b. Determination of J-type centrifuge extra-coil volume using stationary phase retentions at differing flow rates. **J. Liq. Chrom. & Rel. Technol.** 26 (9-10): 1417-1430.

Wood PL. 2005. Personal Communication. Brunel Institute for Bioengineering, Brunel University, Uxbridge, UB8 3PH, U.K.

Wu YT, Zhu ZQ, Mei LH. 1996. Interfacial tension of poly(ethylene glycol) + salt + water systems. **J. Chem. Eng. Data.** 41: 1032-1035.

Zaslavsky BY. 1995. Aqueous two-phase partitioning, Physical chemistry and bioanalytical applications. Marcel Dekker Inc., New York.

Chapter 9
Appendices

9.1 Calibration curves

This section provides calibration curves for the Coomassie Plus Protein Assay and HPLC assays used for the construction of mass balances.

9.1.1 Protein calibration curve

Presented in Figure 9.1 is a typical calibration curve for protein quantification obtained from bovine serum albumin standards as described in Section 2.7.5.

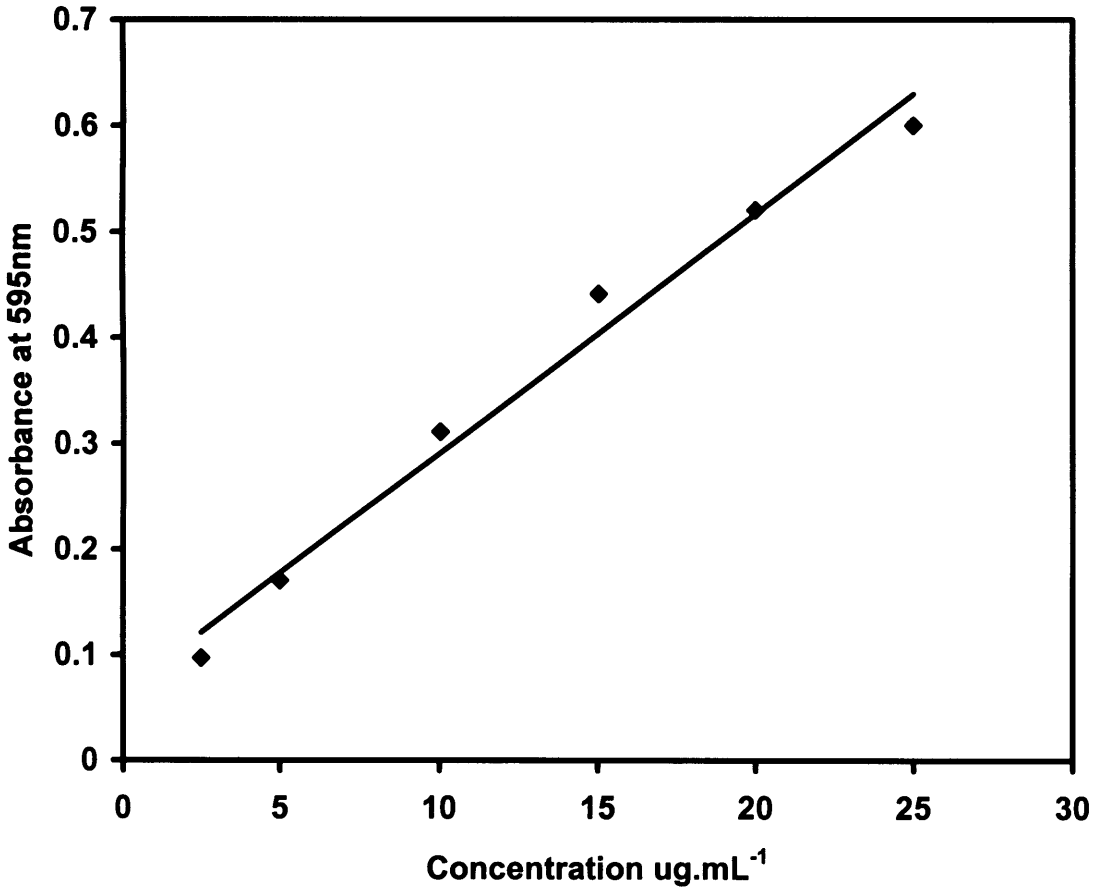

Figure 9.1: Typical calibration curve for quantification of protein using the

Coomassie Plus protein assay as described in Section 2.7.5. Line fitted by linear regression: [Protein] = (Abs-0.0648)/ 0.0226 (R^2 = 0.9831).

9.1.2 HPLC calibration curves

Presented in Figures 9.2 and 9.3 are typical calibration curve for gWiz and PQR150 plasmid DNA as described in Section 2.7.4.

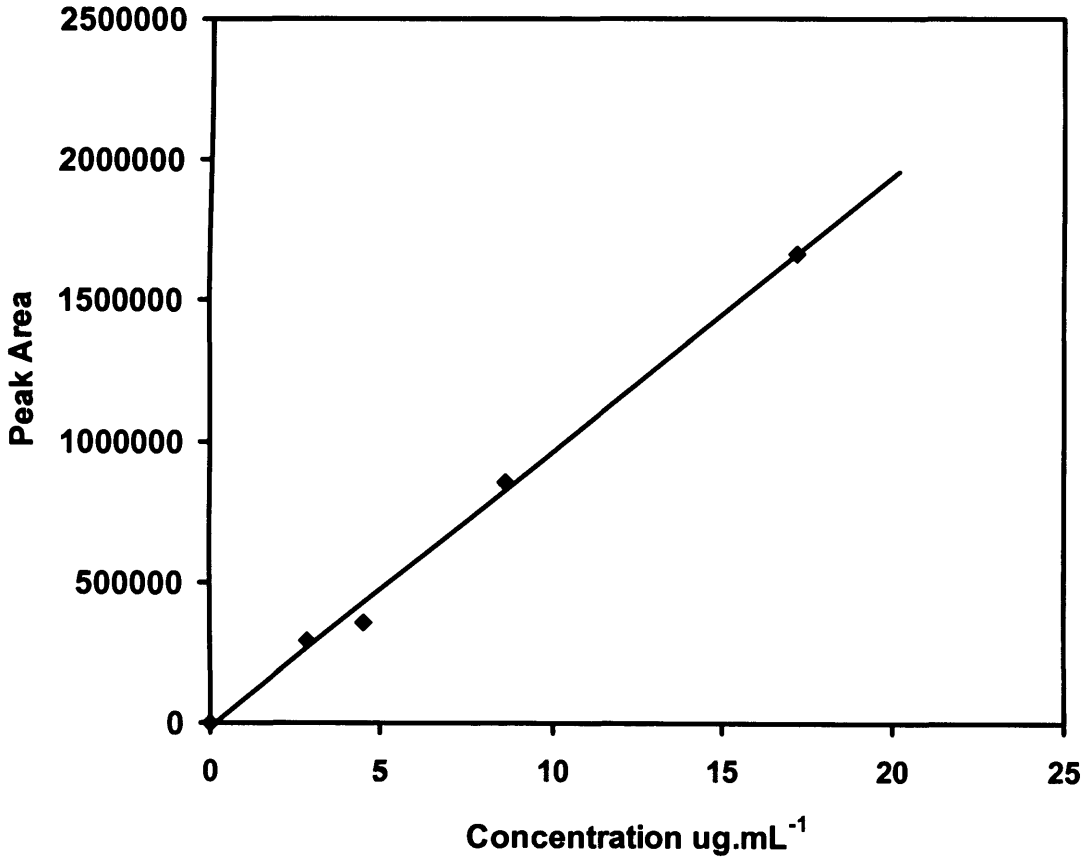

Figure 9.2: Typical calibration curve for quantification of plasmid gWiz using the HLPC assay as described in Section 2.7.4. Line fitted by linear regression: [Plasmid DNA] = (Area + 13451)/ 97712 (R^2 = 0.9961).

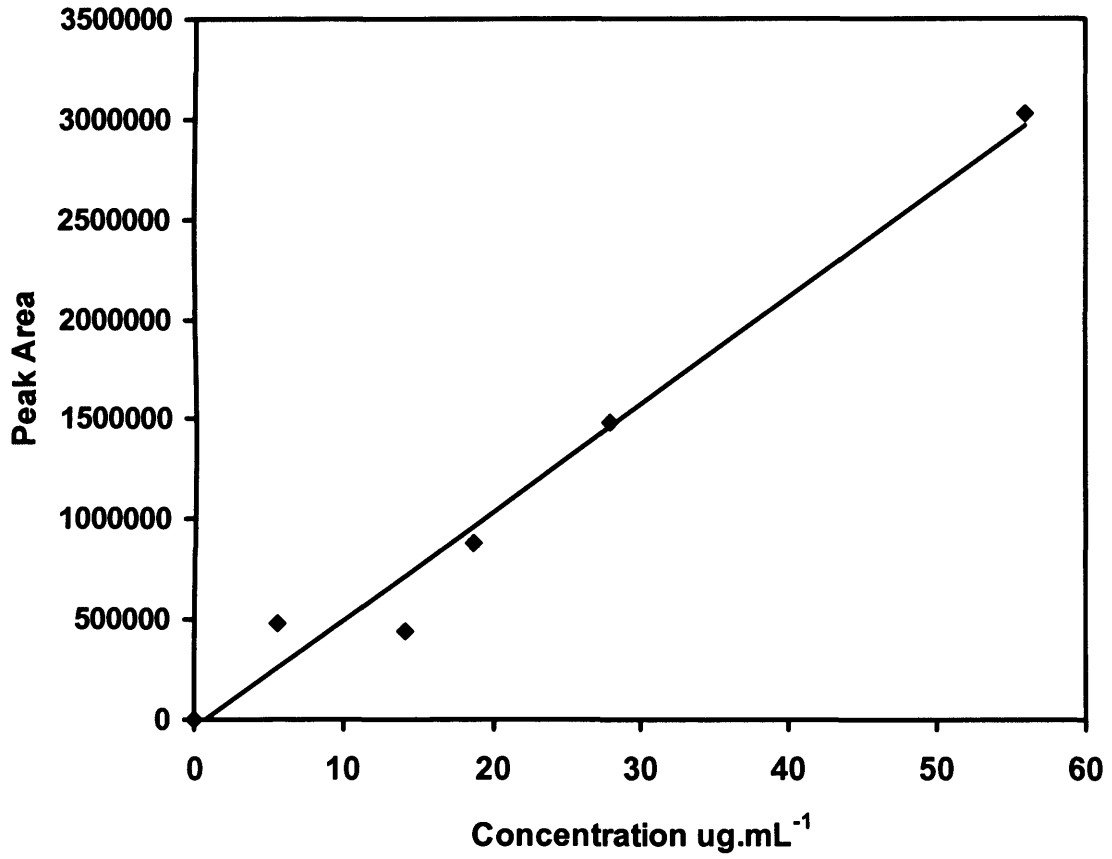

Figure 9.3: Typical calibration curve for quantification of plasmid PQR150 using the HLPC assay as described in Section 2.7.4. Line fitted by linear regression: [Plasmid DNA] = (Area + 43834)/ 53734 (R^2 = 0.9779).

9.1.3 HPLC chromatogram

Presented in Figures 9.4 and 9.5 are typical HPLC traces for gWiz plasmid DNA in the presence and absence of RNA as described in Section 2.7.4.

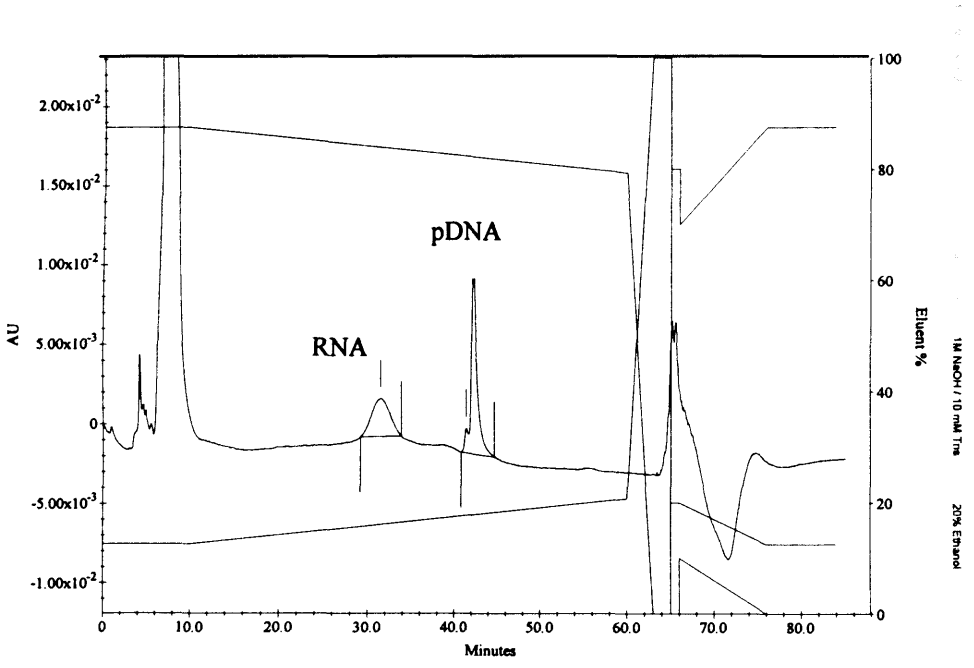

Figure 9.4: Typical HPLC chromatrogram for plasmid gWiz in the presence of RNA (RNaseA free) as described in Section 2.7.4.

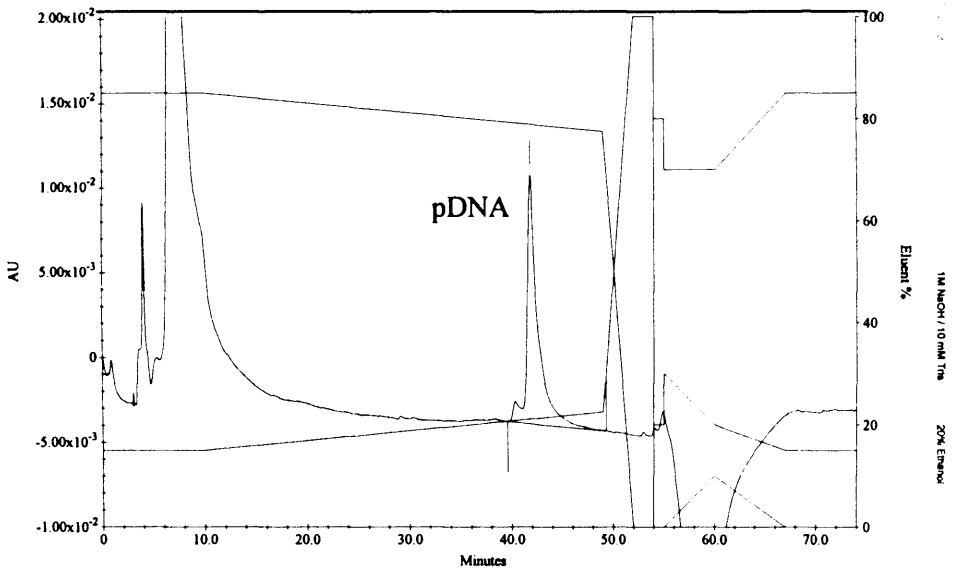

Figure 9.5: Typical HPLC chromatrogram for plasmid gWiz in the absence of RNA (RNaseA treated) as described in Section 2.7.4.

9.1.4 PCR calibration curve

Presented in Figure 9.6 is a typical calibration curve for genomic DNA as described in Section 2.7.6.

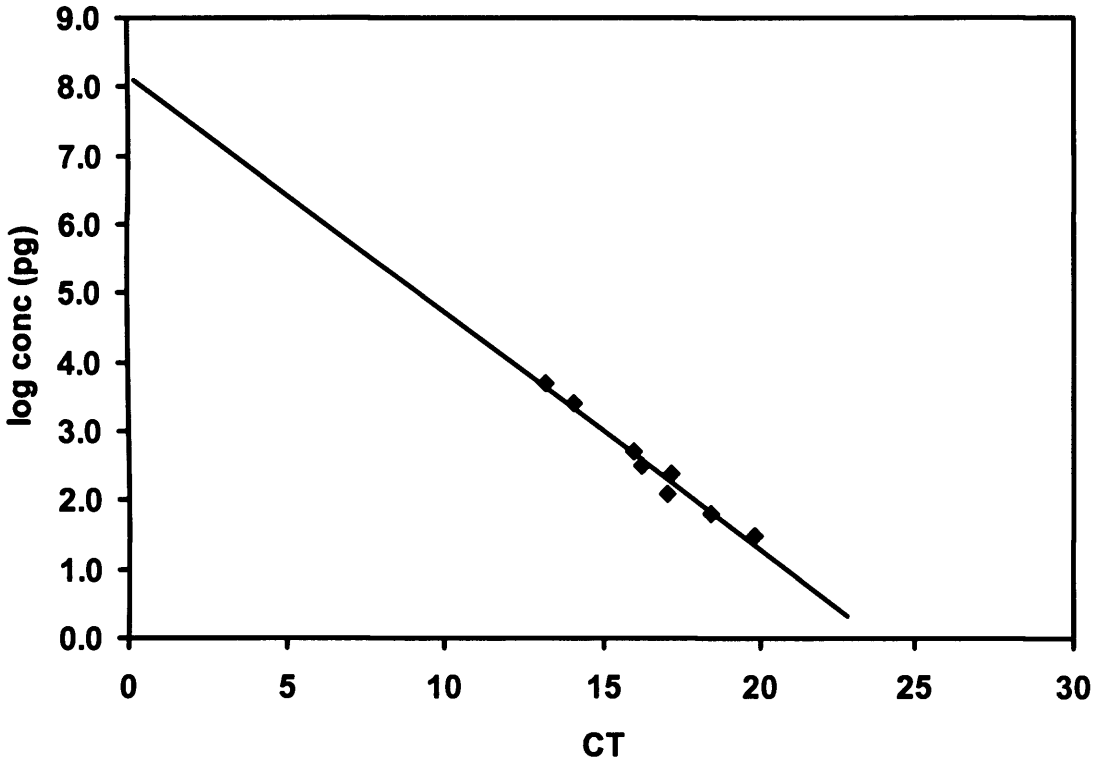

Figure 9.6: Typical calibration curve for quantification of chromosomal DNA using the modified *Taqman* PCR assay as described in Section 2.7.6. Line fitted by linear regression: [Chromosomal DNA] =10^ [(-0.3438 x CT) + 8.1691] (R^2 = 0.9751).